Faculty of Science and Technology
Department of Geosciences

Late Cenozoic development of the mid-Norwegian continental margin – a study of the Naust Formation based on 3D-seismic data

Marius Lundegaard
Master's thesis in Geology, GEO-3900
June 2020

Abstract

The late Cenozoic evolution of the outer continental shelf and slope on the northern part of the mid-Norwegian margin is studied using 3D seismic data. The late Cenozoic stratigraphy is subdivided into four main seismic units: unit A (oldest) to D and correlated to the established stratigraphic framework of the Naust Formation, where the oldest unit in this study correlates to the upper part of Naust unit A. The internal seismic signature of the units and the geomorphology of the unit boundaries form the basis for reconstructing the margin evolution.

Palaeo-troughs and mega-scale glacial lineations (MSGLs) observed on buried shelf horizons suggest that fast-flowing ice streams drained from the Scandinavian mainland, traversed the shelf within Trænadjupet and Sklinnadjupet troughs, and reached the shelf break. Consequently, the palaeo-slope prograded westwards as downslope processes build out the margin. Based on seismic facies and geophysical attributes, the slope sediments were predominantly deposited by debris flows, but turbidity currents have also occurred. Large amount of glacial till was subglacially transported and deposited on the outer shelf and upper slope, before the sediments became unstable and redistributed downslope by gravity driven processes. The sediment distribution of the area suggests that both Trænadjupet and Sklinnadjupet troughs have been active during the glaciations; however, Sklinnadjupet Trough has been the main source of sediment during deposition of Naust A, U, S and T.

Iceberg plough marks on all the buried surfaces testify to free-floating icebergs of sizes capable of eroding the outer shelf and upper slope. The Norwegian Atlantic Current was active during the margin buildout, as suggested by along slope drifting iceberg directions and the presence of the Nyk Drift on the slope.

Acknowledgement

Fem år med studier nærmer seg slutten. Med en klump i halsen og et smil om munnen ser jeg tilbake på en fantastisk studietid ved Universitetet i Tromsø. Studieløpet har bydd på både oppturer og nedturer, noe som har ført til personlig utvikling.

Først og fremst vil jeg rette en spesiell takk til min dyktige hovedveileder, Tom Arne Rydningen. En bedre veileder skal man lete lenge etter. Tusen takk for all veiledning, oppfølging og støttende ord igjennom hele prosessen. Du er dyktig i det du gjør og viser at du bryr deg. Videre vil jeg takke min biveileder, Jan Sverre Laberg, for konstruktive og gode tilbakemeldinger gjennom hele prosessen. En stor takk rettes også til min biveileder, Vidar Kolstad, for engasjement, gode råd og innspill. Til slutt vil jeg takke Schlumberger for akademisk lisens.

Takk til min onkel, Trond Finsland, for hjelp og velvilje til skarpt leserblikk ved korrekturlesing, og takk til medstudent, Arne Hansen, for gode faglige diskusjoner underveis.

Takk til familie, samboer og venner for deres tålmodighet, forståelse og støtte gjennom denne tiden.

Til slutt vil jeg takke alle mine medstudenter. Dere har gjort studietiden til en fantastisk og uforglemmelig tid.

Marius Lundegaard

Tromsø, Juni 2020

Table of Contents

1 Introduction

1.1 Objectives

The glaciation of Fennoscandia led to deposition of the Naust Formation, which underlies the present-day continental shelf and slope offshore mid-Norway (Dahlgren et al., 2002a; Laberg et al., 2005b; Faleide et al., 2008). By analyzing three-dimensional (3-D) seismic, this study describes the middle and upper part of the Naust Formation and the late Cenozoic development of the outer shelf and slope of the Vøring margin.

The main objectives are:

i) Establishing a seismic stratigraphic framework for the Naust Formation and correlate to established framework, in addition to identifying and discussing morphological elements on buried horizons,

ii) Performing a seismic facies analysis of the seismic units, producing attribute maps and discussing depositional processes,

iii) Discussing the depositional environments with respect to the glacial history.

In addition, identifying and shortly describing possible fluid migration pathways and/or other possible shallow gas observations

1.2 Study area

The study area is located in the Norwegian Sea on the northern part of the mid-Norwegian continental margin. It comprises the outermost part of the continental shelf, partially located at Trænadjupet and Trænabanken, and the upper continental slope (Figure 1.1). The study area is covering about 1200 km² where the water depth is ~950 m in the northwestern part.
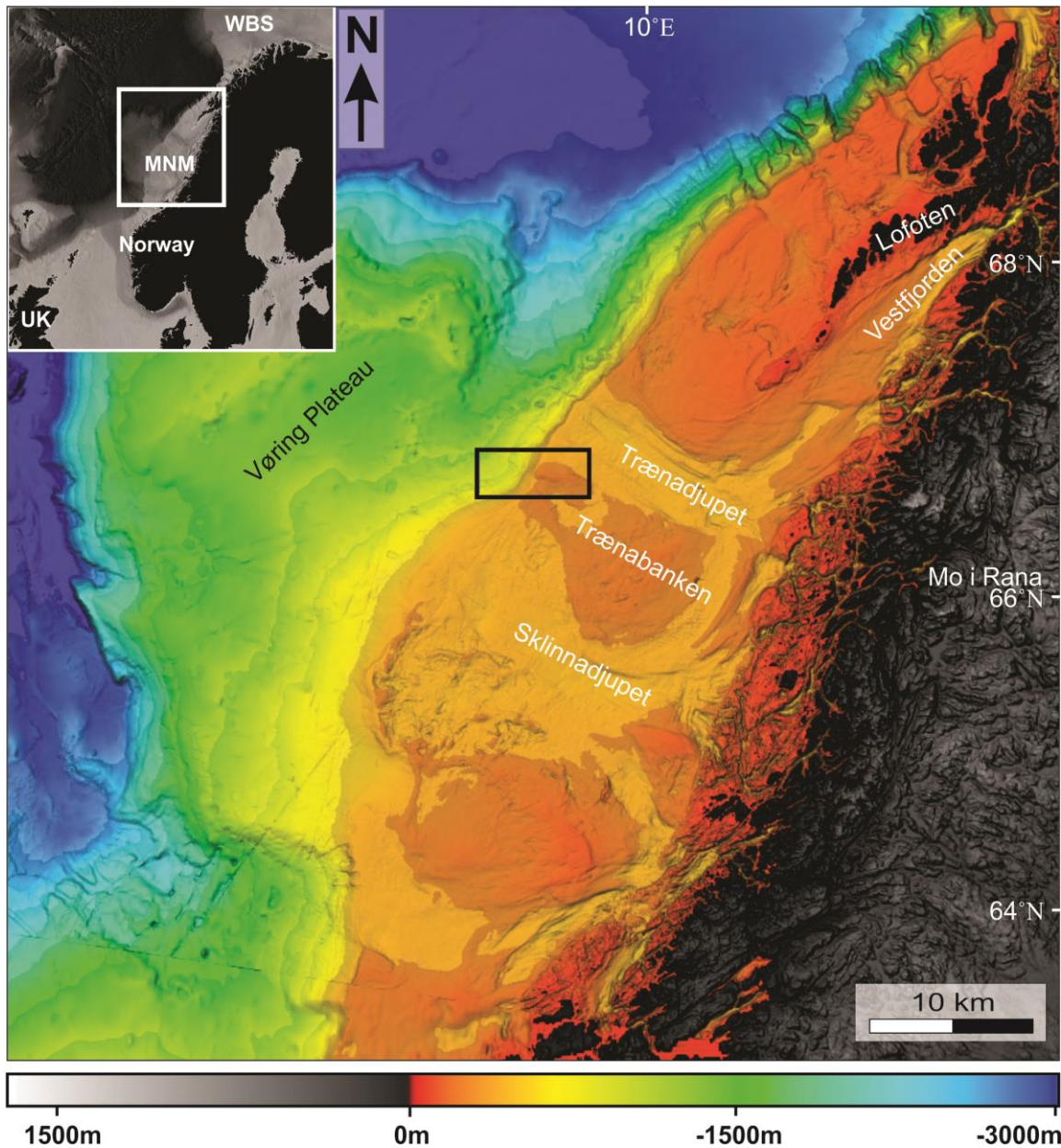

Figure 0.1: Bathymetric map of the northern part of the mid-Norwegian margin with study area indicated as a black rectangle. WBS – West Barents Sea; MNM – mid-Norwegian margin; UK – United Kingdom.

2 Geological background

2.1 Morphology of the mid-Norwegian continental margin

The present-day morphology of the mid-Norwegian continental margin (between 62˚N-69˚30`N) comprises three main provinces with different characteristics, from south to north: the Møre, Vøring, and Lofoten-Vesterålen. Each province is 400-500 km long, separated by the East Jan Mayen Fracture Zone and Bivrost Lineament/Transfer Zone (Figure 2.1) (Blystad et al., 1995; Faleide et al., 2008; Faleide et al., 2015). From south to north, the width of the mid-Norwegian margin ranges from less than 65 km offshore Møre, up to 200 km in the area of Vøring, before narrowing to less than 10 km offshore Lofoten – Vesterålen. Generally, the shallowest water depths and steepest slope gradients occur on the southern and northern part of the margin (Vorren et al., 1998).

The transition zone from the continental shelf into deeper ocean is called the continental slope. The slope of the Møre margin is characterized as a gentle but highly irregular slope leading down to the Møre Basin. Further north, the slope of the Vøring margin has a gradient of 0.58˚ while the continental slope outside the Lofoten islands dips ~5˚(Vorren et al., 1998; Dahlgren et al., 2002a).

Large-scale seabed morphology of the mid-Norwegian continental margin is characterized by cross-cutting divisions of troughs and shallower bank areas (Hjelstuen et al., 2004). From north to south, the margin is comprised of three main troughs known as Trænadjupet, Sklinnadjupet and Suladjupet, as well as five main banks, i.e. Røstbanken, Trænabanken, Sklinnabanken, Haltenbanken and Frøyabanken (Figure 2.1) (Ottesen et al., 2002).

A trough is an elongated depression commonly seen as an offshore continuation of a fjord (Vorren & Mangerud, 2008). The extent and water depth of troughs are varying but the deepest areas on the mid-Norwegian shelf can be found here. Depths are ranging from 150-550 m and troughs are often deepest closest to the coastline. In general, the widest troughs are commonly found on wide shelfs, where troughs on narrow shelfs rarely exceed 20 km widths (Dahlgren et al., 2002a; Vorren & Mangerud, 2008; Ottesen et al., 2009).

Trænadjupet Trough is considered to be a continuation of the NE lying Vestfjorden. It is 150 km long and the width ranges between 40-90 km, where the shelf break area is the widest (Ottesen et al., 2005a).

In between the troughs, several shallow flat-lying areas or banks with a low westward dip can be found. The water depth of these banks are ranging from 50-300 m (Ottesen et al., 2009).

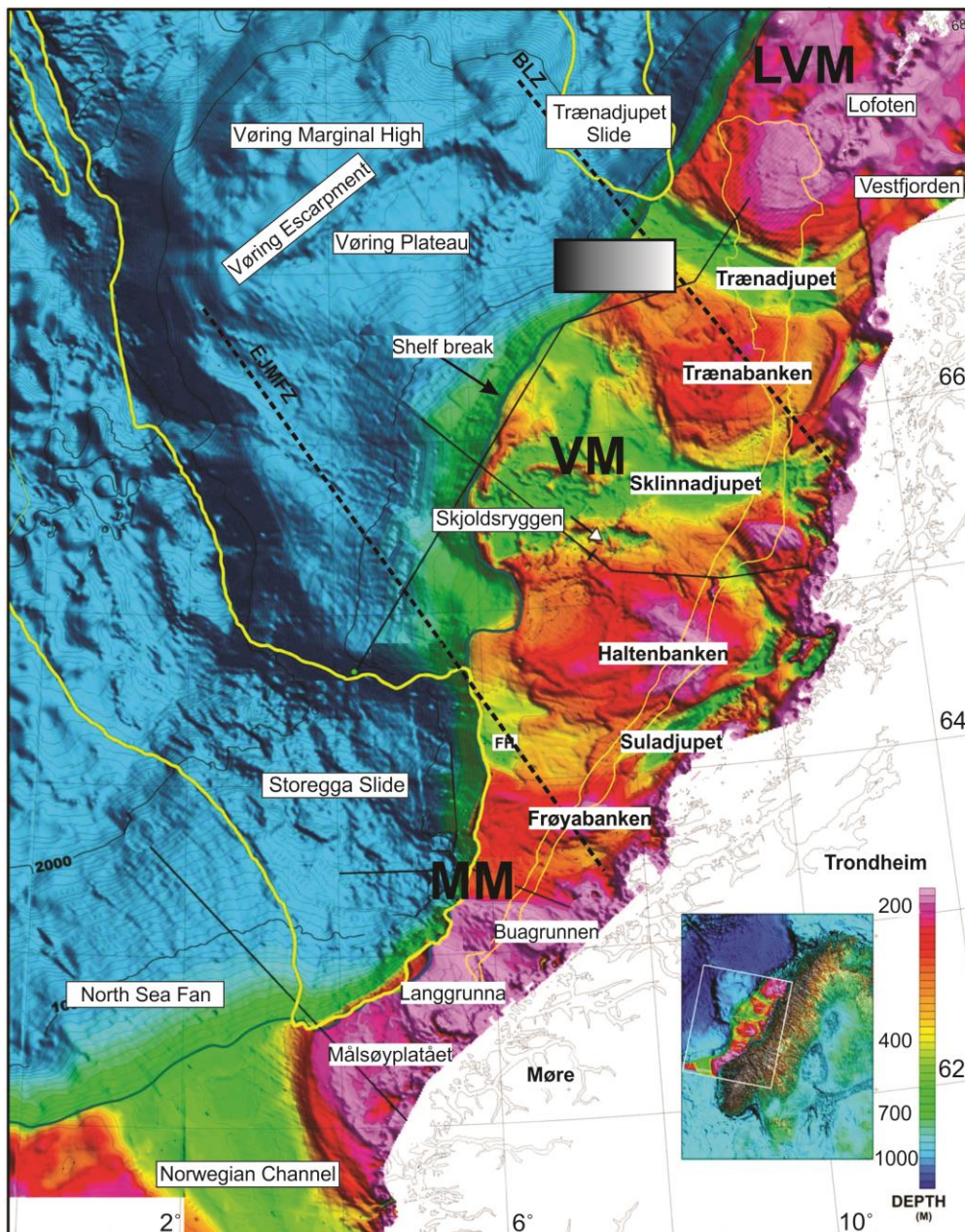*Figure 0.1: Large scale morphology of the mid-Norwegian continental margin with troughs and banks. The study area is indicated by a grey-scaled square on the outermost part of the shelf. The shelf break is indicated by a blue line. MM – Møre margin; VM – Vøring margin; LVM – Lofoten-Vesterålen margin; EJMFZ – East Jan Mayen Fracture Zone; BLZ – Bivrost Lineament Zone. Modified from Rise et al. (2005).*

4

Important structural elements on the Vøring margin are the late Middle Jurassic-Early Cretaceous Trøndelag Platform to the southeast, Halten and Dønna terraces further west and the Late Cretaceous-early Paleogene Vøring Marginal High in the northwest. The 150 km wide Vøring margin was delimited by Fles Fault complex and Utgard High in the east due to reactivation by normal faulting already in the Late Cretaceous (Figure 2.2) (Blystad et al., 1995; Faleide et al., 2008; Faleide et al., 2015).
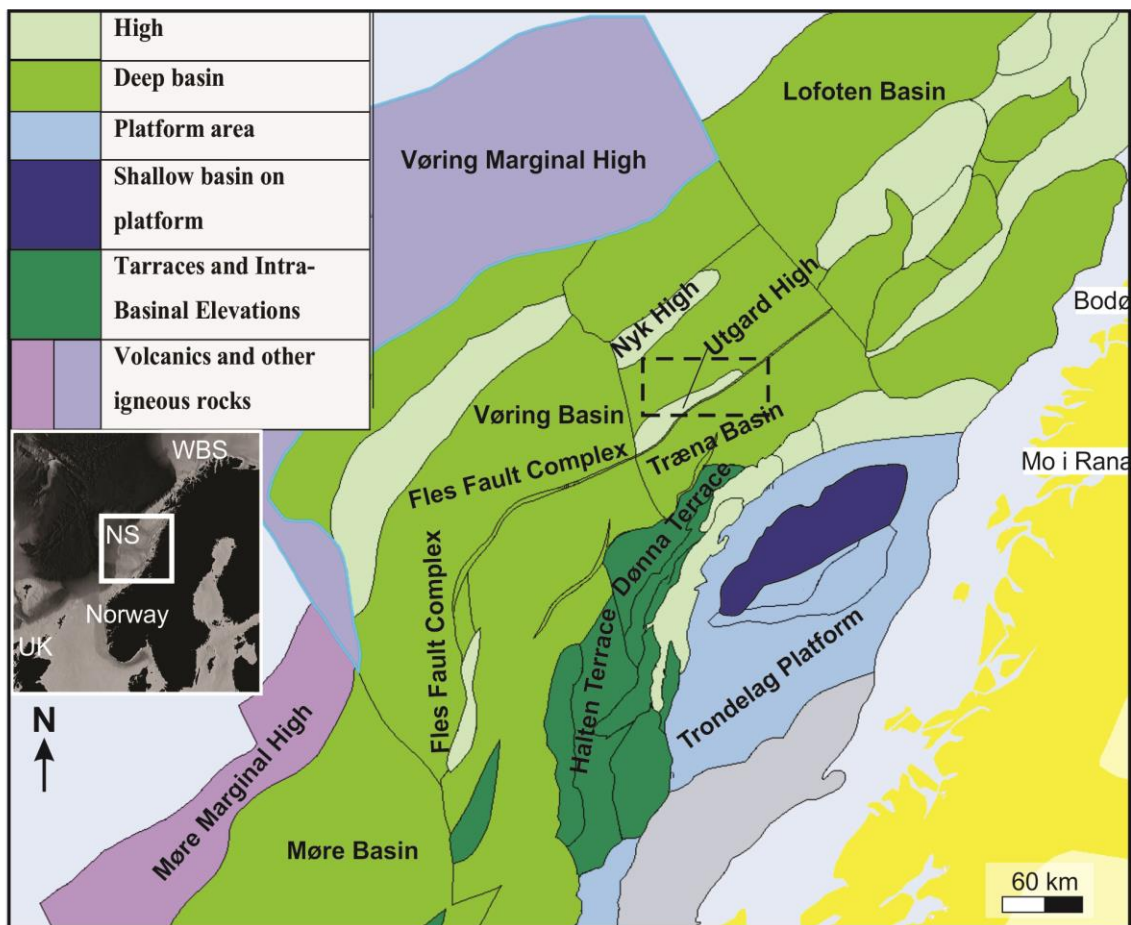

Figure 2.2: Main structural elements on the Vøring margin and some other important structural elements in adjacent areas. The study area is indicated by a black dotted rectangle. WBS – Western Barents Sea; NS – Norwegian Sea; UK – United Kingdom. Modified from NPDfactmaps (n.d).

2.1.1 Slides and trough mouth fans (TMF)

The major slides during late Weichselian and Holocene (i.e. Storegga, Nyk Slide and Trænadjupet Slides) have made their marks on the continental slope (Laberg et al., 2001; Hjelstuen et al., 2004). During the late Weichselian, a large slope failure named Nyk Slide occurred slightly northwest of the study area. Therefore, Nyk Slide scare can be observed in seismics by a basal glide plane running alongside the underlying acoustically laminated unit corresponding to an internal reflection in the Nyk Drift. Further north, the Trænadjupet Slide is located NE of the Trænadjupet mouth, on the continental slope (Figure 2.3). The slide deposits extend from the shelf break, with an average slope gradient of 1.25°, to a depth of 3000 m in the Lofoten Basin. It was probably formed during the mid-Holocene, ca. 4.5-4.8 ka BP (Laberg & Vorren, 2000).

Transverse troughs crossing the mid-Norwegian continental shelf had a substantial sediment transport and therefore sedimentary fans are often observed in front of their mouth (Figure 2.3). Such fans are commonly defined as trough mouth fans (TMF) and can vary in size and shape. TMFs represent some of the largest glacial depositions on the Norwegian territory, i.e. for example the North Sea TMF (Vorren & Laberg, 1997; Vorren & Mangerud, 2008).
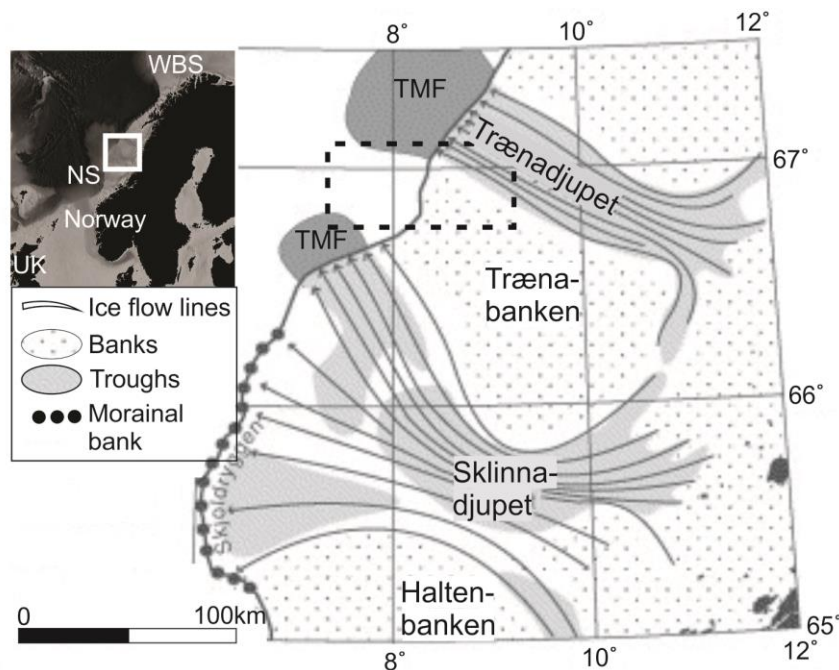

Figure 2.3: Schematic illustration of trough mouth fans building of the upper slope on the Vøring margin during the Late Weichselian. The Study area is indicated by the black dotted rectangle. WBS – West Barents Sea; NS – Norwegian Sea; UK – United Kingdom; TMF – Trough mouth fans. Modified from Dahlgren et al. (2002b)

2.2 Margin development

2.2.1 The Mesozoic development

Already in the Late Jurassic - Early Cretaceous, the tectonic development of the NE Atlantic started. It is believed that this early tectonic movement created the structural framework of the North Atlantic margin. During this episode, the Møre and Vøring basins located off mid-Norway were developed (Figure 2.4). As a consequence of the differential vertical movements which occurred during the evolution of the Vøring Basin, it may be separated into several sub-basins and highs. The Vøring margin went through a higher grade of extension compared to the Lofoten - Vesterålen margin (Faleide et al., 2008).

During the Cretaceous, a deep and narrow epicontinental sea evolved between Laurentia and Fennoscandia (Martinsen & Nøttvedt, 2006). The crust underneath the epicontinental sea represented an extensively weakened continental crust. The Campanian is thought to have been the main brittle rifting period where the rifting caused the formation of detachment structures. These structures uplifted the Cretaceous stratigraphy which resulted in the exposure of Vøring and Lofoten - Vesterålen margin (Faleide et al., 2008; Faleide et al., 2015).
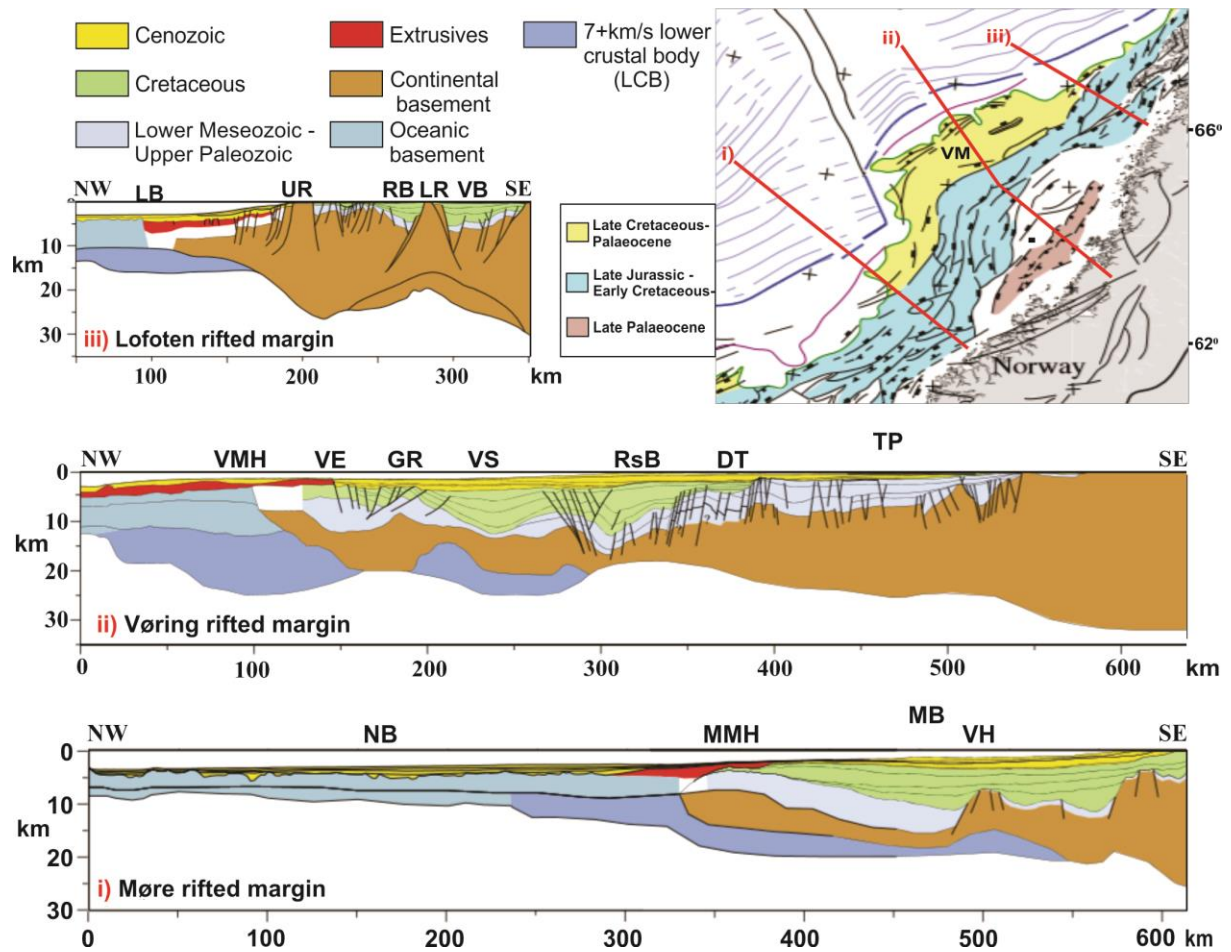
Figure 2.4: Regional structural profiles from south to north across the rifted mid-Norwegian continental margin. The map in the right corner indicates locations of the regional profiles. NB – Norway basin; MMH – Møre Marginal High; VH – Vigra High; MB – Møre Basin; VMH – Vøring Marginal High; VE – Vøring Escarpment; GR – Gjallar Ridge; VS - Vigrid syncline; RsB - Rås Basin; DT- Dønna Terrace; TP – Trøndelag Platform; VF – Vestfjorden Basin; VB – Vestfjorden Basin; LB – Lofoten basin; UR- Utrøst Ridge; RB – Ribban Basin; LR – Lofoten Ridge. Modified from Faleide et al. (2008).

2.2.2 The Cenozoic development

The transition from the Mesozoic to Cenozoic era took place ~65 Ma. The Cenozoic era is characterized by large igneous activity especially near the Mid-Atlantic Ridge. The igneous activity of the mid-Norwegian continental margin continued throughout the Cenozoic and was probably a result of the extension of the lithosphere. The rifting between Greenland and Fennoscandian in the Cenozoic era had great impact on the margins and later on the oceanography in the Atlantic Ocean (Figure 2.5) (Faleide et al., 2008). The Norwegian Sea has developed during several phases with different extension axes through Paleogene and Neogene (Martinsen & Nøttvedt, 2008).

During the Paleogene, the development of the Norwegian Sea was initiated. Prior to the final lithospheric breakup, an epicontinental sea was situated between Greenland and the north-western part of Europe. The major seafloor spreading had until this point been limited to the southern part of the Atlantic Ocean, but in the early Paleogene, this changed. From this point on and throughout the Neogene, the rifting of the NE Atlantic spread gradually towards north (Martinsen & Nøttvedt, 2008). In Paleogene, the Norwegian mainland went through general uplift and sea-level raise. Already in the Paleocene epoch, the Møre and Vøring margins were characterized by relatively deep water conditions (Faleide et al., 2015).

Greenland and Fennoscandia continued to move apart, and eventually new seafloor started to form. The final lithospheric breakup took place around 55 Ma in the transition between Paleocene and Eocene. This was followed by a period of about 3-6 m.y with high igneous activity due to rifting and therefore regional subaerial flood-basalt volcanism (Dahlgren et al., 2002a; Faleide et al., 2008; Faleide et al., 2015).

During the middle Eocene, the mid-Norwegian margin turned into a passive rift margin, characterized by regional low sedimentation and subsidence (Faleide et al., 2008). The muddy sediments deposited at this time corresponds to the Brygge Formation. The subsidence was caused by crustal cooling, sediment loading and compaction of the crust. Later, in the mid-Cenozoic, the margin turned into a compressional regime which is well preserved on the Vøring margin. This transition can be observed as characteristic features like reversed faults, domes or anticlines (Martinsen & Nøttvedt, 2006; Faleide et al., 2015).
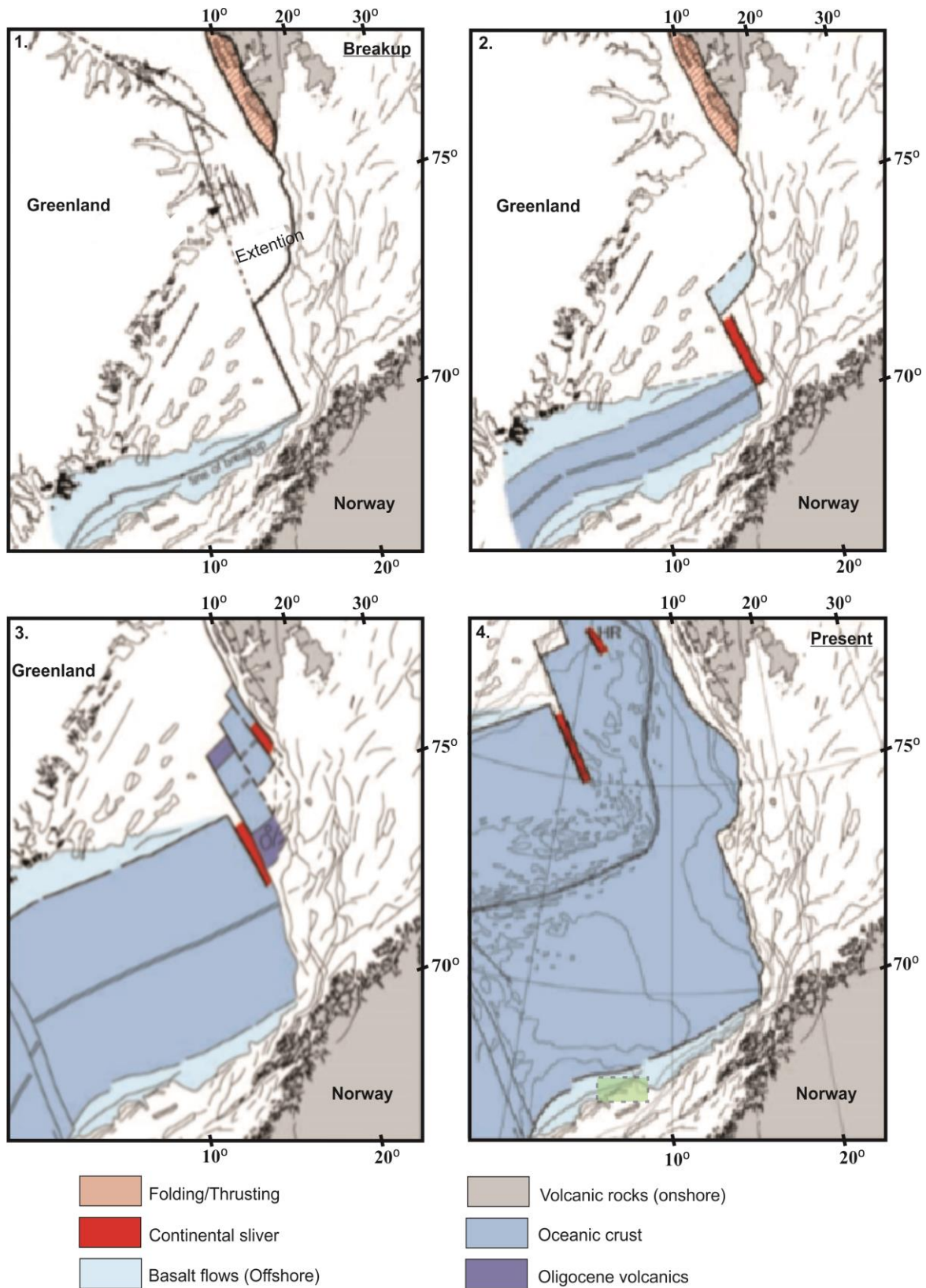
Figure 2.5: Cenozoic rifting evolution of the Norwegian - Greenland Sea from breakup to present situation (1. - 4.). The study area is indicated in stage 4 by a green rectangle. Modified from Faleide et al. (2008).

The ocean circulations in the North Atlantic was influenced by the Miocene development of the Fram Strait between Greenland and Svalbard. Both deep and cold ocean currents circulated from the Arctic Ocean to the North Atlantic and continued southwards. This opening occurred between 20-10 Ma and is often referred to as the North Atlantic-Arctic Gateway (Faleide et al., 2008). In addition, the opening of the Faeroe Conduit in the south and a general subsidence of the Greenland – Scotland Ridge, have all contributed to the formation of contourites along the North Atlantic and the Norwegian-Greenland Sea (Laberg et al., 2005b; Faleide et al., 2008). The Greenland-Scotland Ridge is often referred to as the southern oceanic gateway and the timing of its subsidence has been debated to be ranging from early Oligocene to mid-Miocene (Stoker et al., 2005). The muddy Kai Formation is believed to be deposited during the Miocene (Martinsen & Nøttvedt, 2006).

The Norwegian margin was uplifted in the Neogene and exposed to intense erosion due to glaciation of the Northern hemisphere (Vorren & Mangerud, 2008). During the Miocene age, the main phase of the mid-Cenozoic compressional deformation occurred. The deposition of the deltaic Molo Formation in this epoch may be an indication of a regional moderate uplift of Fennoscandian. An increase in the deposition of contourites from a deep-water environment can also be found during this epoch (Faleide et al., 2015).

Formation of the Neogene mountain ranges, i.e. Pyreneans, Alps and Himalaya prevented free global movement of tropical and polar air masses. The change in ocean and air circulation as well as the change in geographical position of Fennoscandian, turned the humid and warm climate into a gradually colder climate throughout the Neogene (Martinsen & Nøttvedt, 2006).

The passive margin of mid-Norway subsided in the Late Pliocene due to glaciation as well as the progradation of the sedimentary wedge. The wedge is comprised of the Naust Formation (sub-divided into N, A, U, S and T) which started in the late Neogene (Figure 2.6) (Faleide et al., 2008).
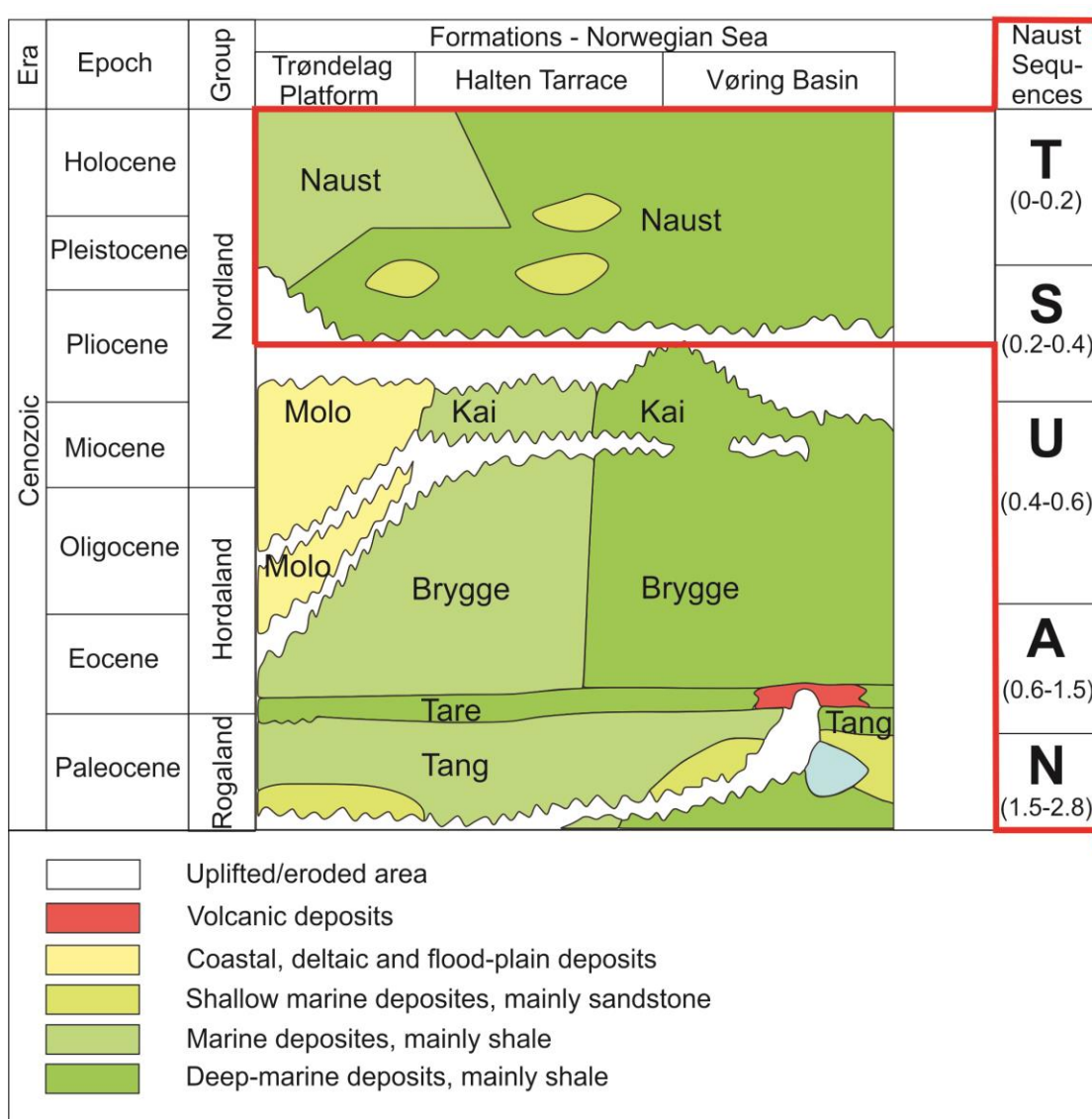
Figure 2.6: Cenozoic lithostratigraphic diagram from the Norwegian Sea with the sequences of the Naust Formation indicated. Modified from Rise et al. (2006) and NPDfactpages (2014).

2.3 Glacial history

During the Neogene, temperatures started to fall, ice accumulated around the poles and the global sea-level dropped (Martinsen & Nøttvedt, 2006). The glaciation in Scandinavia started slowly around 12.6 Ma but accelerated in Pleistocene 2.6 - 2.7 Ma. This is indicated by sediments derived from ice-rafted debris (IRD) and oxygen isotopes from fossil organisms (Figure 2.7) (Vorren & Mangerud, 2008; Mangerud et al., 2011).
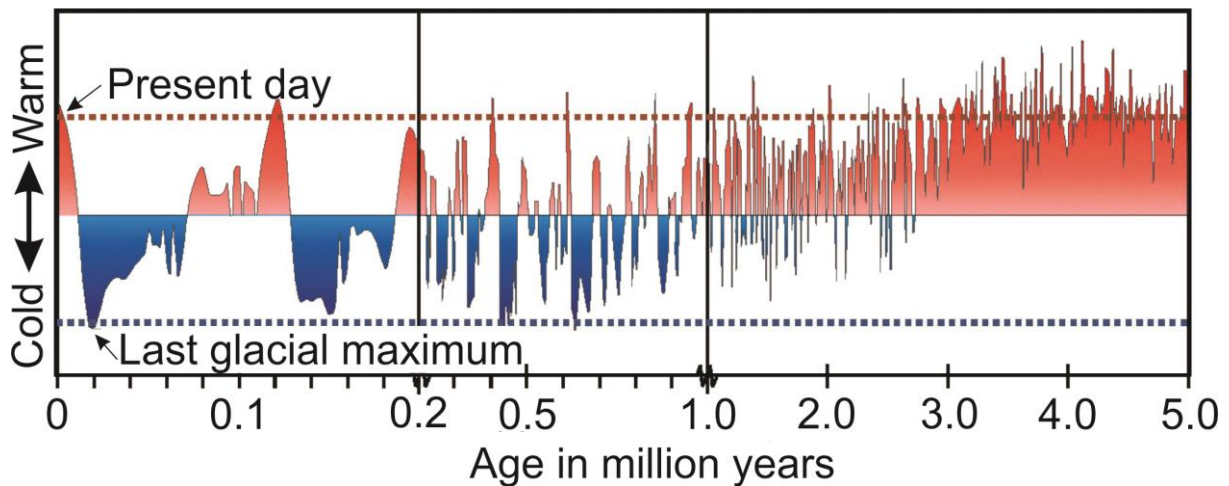

Figure 2.7: Variations in isotope content during the last 2.7 Ma measured in deep marine sediments. The content can be an indication of the total global volume of glaciers at a specific time span. 2.6-0.9 Ma were dominated by cyclic variations of 41 ka and 23 ka, changing between glacial accumulation and ablation. The past million years have been dominated by cycles of 100 ka and the global volume of glaciers increased. Note the change in timescale from 0.2-1.0 Ma. Modified from Vorren and Mangerud (2008).

The glacial history through the Quaternary (the last 2.6 Ma) is often divided into three scenarios. The conditions of the first and second scenarios appeared throughout the entire period and have been calculated to be lasting for approximately 1.2 and 1.3 Ma in total. Moreover, the third scenario started ~ 0.9 Ma and only lasted for 0.2 Ma in total. The glaciation is composed of a series of stadials and interstadials which means that ice ages come and go (Vorren & Mangerud, 2008).

The first scenario is the interstadials characterized by local glaciers and cirques in the mountain areas. In this period the Scandinavian mountains were exposed for climatic cycles of 41 ka or 23 ka which altered between glacial accumulation and ablation. These climatic cycles were a consequence of the variations in the earth's axial tilt and precession and dominated from 2.6-2 Ma, before the second scenario took place.

The second scenario is the coastal phase which is characterized by the Scandinavian Ice Sheet expanding and reaching the coastline (Mangerud et al., 1996).

The third and final scenario was when the Scandinavian Ice Sheet covered the entire mainland of Norway, Sweden and Finland and reached its maximum extension in the southern part of Germany. This occurred periodically over the past million years with a dominating cycle of 100 ka and was caused by variations in the earth's orbital path. The older cycles also still affected the climate. This period is often referred to as Mid Pleistocene Revolution and the climatic changes can be seen in the intensity of the IRD deposits (Mangerud et al., 1996; Mangerud et al., 2011).

In the Late Pliocene–Pleistocene age, glacial sediments were transported and deposited on the continental slope. Over time, substantial sedimentation formed a sedimentary wedge where the stratigraphy often is referred to as the Naust Formation (Dahlgren et al., 2005).This made it possible for the glaciers to move even further west. The present-day morphology on the mid-Norwegian continental shelf, with banks and troughs, indicates the earlier presence of glaciers and their movement (Vorren & Mangerud, 2008).

2.3.1 The Last Glacial Maximum (LGM) and deglaciation

The Last Glacial Maximum occurred around 25-18 ka in the Late Weichselian (Vorren & Mangerud, 2008). During this period, the Scandinavian Ice-sheet advanced to the shelf break area (Svendsen et al., 2004; Rydningen et al., 2013) and the mid-Norwegian margin was characterized by a high sedimentation rate (Dowdeswell et al., 2010).

Fast-flowing ice-streams drained the Scandinavian Ice Sheet during the LGM and earlier glaciations and the ice-streams have been important for the development of the present-day shelf morphology. In between the ice streams, a more slow-flowing ice mass was present, preserving the banks (Figure 2.8) (Ottesen et al., 2005a; Rise et al., 2005; Dowdeswell et al., 2006; Ottesen et al., 2008; Rydningen et al., 2013). Mega-scale glacial lineations (MSGLs) are formed subglacially by fast flowing ice-streams and commonly occur within troughs (Clark, 1993).

Trænadjupet is an extension of Vestfjorden embayment predominantly formed by ice-streams from Vestfjorden but also other smaller ice-streams coming from east and southeast of Trænadjupet. Vestfjorden and Trænadjupet have played an important role draining the Fennoscandian Ice Sheet during the Late Weichselian (Ottesen et al., 2005b). The Lofoten Islands acted as a barrier and therefore the Fennoscandian Ice Sheet was drained through Trænadjupet – Vestfjorden – Ofotfjorden troughs in the south and Andfjorden in the north (Laberg et al., 2001).

The LGM of the Vøring margin was characterized by substantial offshore sedimentation and the sedimentation was highly controlled by periodically oscillations of the ice-sheet (Ottesen et al., 2002; Dowdeswell et al., 2010). On the mid-Norwegian margin, this can be indicated by terminal moraines deposited during the LGM where the largest one is the Skjoldsryggen (Figure 2.8) (Sejrup et al., 2005).

The recession of the ice-sheet happened rapidly from 15 ^{14}C ka BP (Laberg et al., 2007) and large amounts of sediments were deposited on the shelf by melt-water rivers and icebergs, especially in the troughs. Due to the glacial influence, the uppermost sedimentary layers on the continental shelf are defined as diamictons (Vorren & Mangerud, 2008).
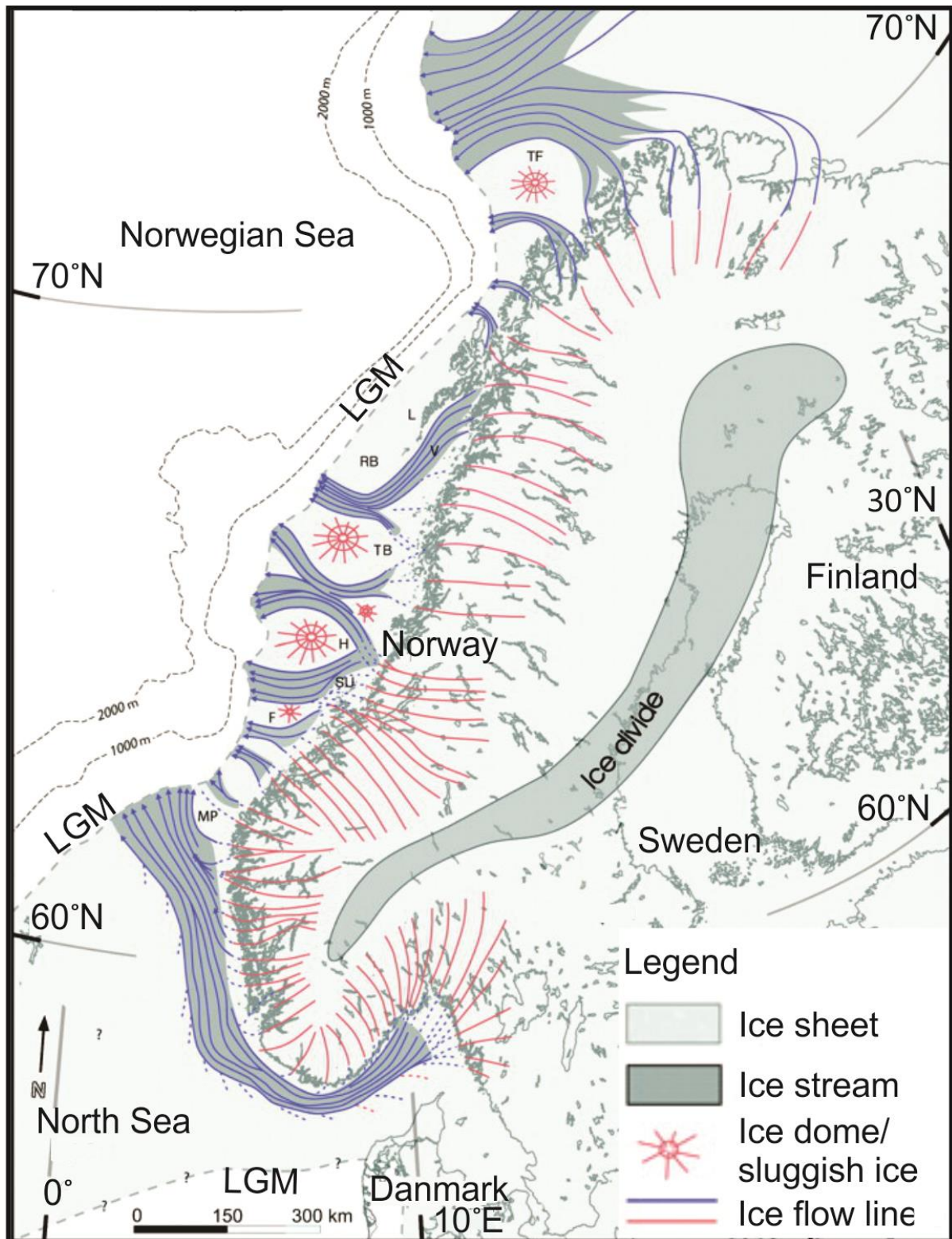
Figure 2.8: Reconstruction of the ice sheet during the Last Glacial Maximum (LGM) along the Norwegian margin. The reconstruction of the ice-sheet regime is indicated. Modified from Ottesen et al. (2005a).

2.4 Sedimentary processes on a glaciated margin

2.4.1 The mid-Norwegian prograding wedge

The prograding wedge of the mid-Norwegian margin is comprised of partly merged depocenters coming from Trænadjupet, Sklinnadjupet and Suladjupet (Dahlgren et al., 2005). Initially, the wedge was deposited west of the late Neogene deltaic Molo Formation and prograded westward (Olsen et al., 2013).

The wedge is up to 1000 m thick (Olsen et al., 2013), predominantly build-up of debris flows with a glacigenic origin during the last 3 Ma. Uplift of the mainland has probably contributed to more erosion (Dowdeswell et al., 2010). Glacigenic debris flows can occur in different shapes and sizes, e.g. as delineated singular lobes or homogeneous stacked. The shape of the debris deposit is influenced by the morphology of the surrounding environment, water content of the sediments and mineralogy (Figure 2.9) (Dahlgren et al., 2002a).

Debris flows with a glacigenic origin are commonly interbedded with contourite deposits and hemipelagic sediments. The Fennoscandian Ice Sheet deposited such glacigenic diamictons in front of its grounding-line while it was grounded near the shelf break. These sediments were later transported downslope and deposited there (Dahlgren et al., 2002a).

Sediments transported downslope due to gravity are considered downslope processes and a trigger-mechanism is often required to initiate these failures. Downslope processes can be divided into several subdivisions, e.g. slides, turbidity currents and debris flows (Figure 2.9 & 2.10) (Dahlgren et al., 2005). A high rate of sedimentation or the presence of shallow gas, may lead to an unstable soil and the risk of slope failure (Vorren et al., 1998). Slope sediments can reveal information about geological events such as extent and timing and can therefore make it easier to reconstruct the geological history (Dahlgren et al., 2002a).

Turbidity currents have had a low contribution to sediment transport on the slope of Vøring margin. This assumption is based on lack of evidences of morphological features such as for instance channels and associated levees (Dahlgren et al., 2002a).
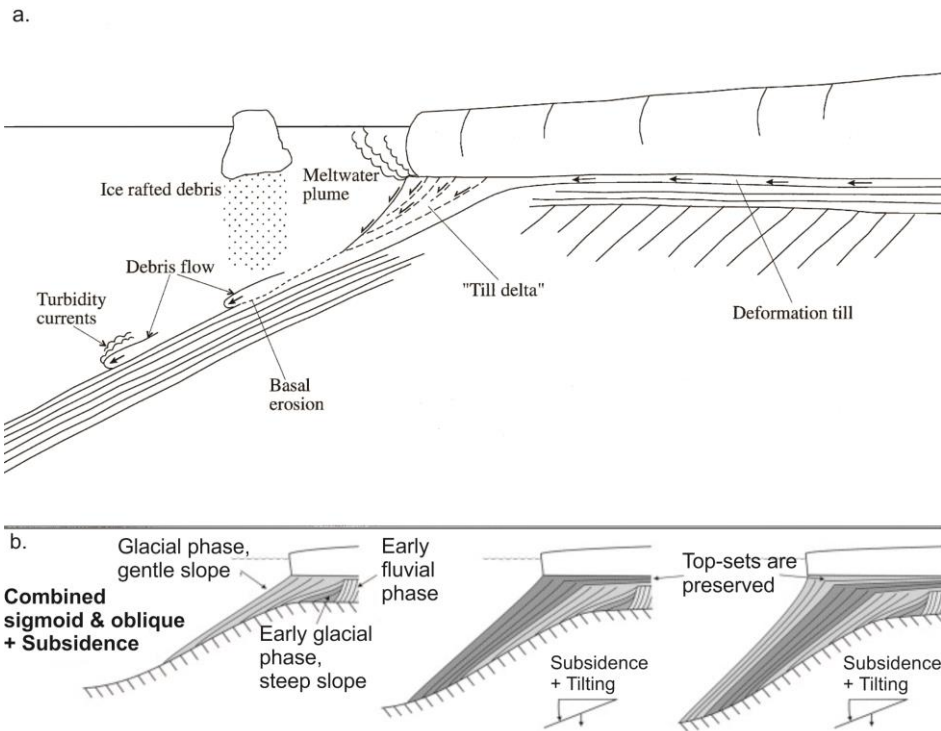
Figure 2.9: **a.** A schematic model showing a prograding glaciated shelf and sedimentary processes working on the slope. **b.** Conceptual model indicating the prograding wedge of the mid-Norwegian margin and its geometry and subsidence. The prograding wedge gets a stratal stacking pattern. Due to the subsidence, a thick top-set package is preserved. Modified from Laberg and Vorren (1995), Vorren et al. (1998), Laberg et al. (2005b).

Figure 2.10: Schematic illustration of the continental margin and the different downslope and alongslope processes that may be present. Modified from Dahlgren et al. (2005).

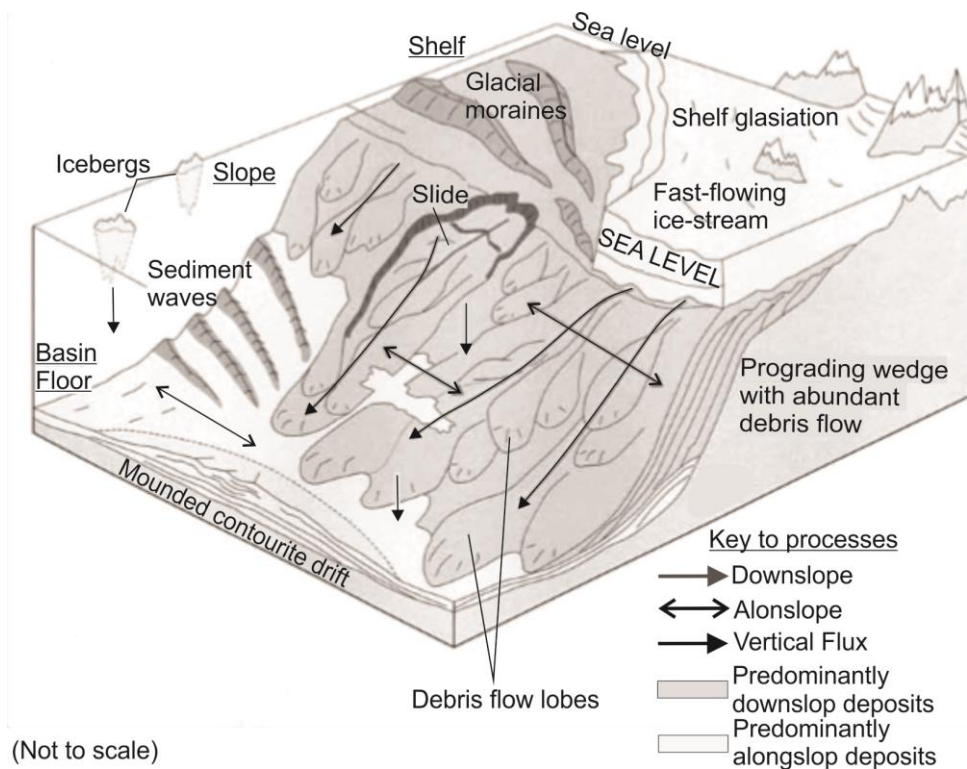### 2.4.2 The upper regional unconformity (URU)

The upper regional unconformity (URU) indicates the transition from inclined wedge-shaped sedimentary units to more flat-lying units on the continental shelf. It occurs within the prograding wedge where it indicates the base of Naust T (Ottesen et al., 2009). All the underlying prograding units (Naust units N, A, U, and S) are being truncated by this boundary. The overlying sedimentary unit is composed of glacial till deposited over multiple glacial advances. This sedimentary unit can also indicate the first till deposition from the Last Glacial Maximum in some areas (Dahlgren et al., 2005). URU has a regional extent but is often best developed in the mid and inner part of the continental shelf. It is considered a complex surface due to different timing of erosion of different locations (Dahlgren et al., 2005; Ottesen et al., 2009). Dahlgren et al. (2005) estimated the age of URU of mid-Norway to be about 0.35 Ma and Ottesen et al. (2009) suggest it formed by the Elsterian ice-sheet, which took place in the same period. The boundary can also be linked to GU located NW of Britain. GU represent the glacial unconformity and is a distinct and regional intra-Pleistocene erosional surface (Dahlgren et al., 2005).

2.4.3 Contourites on the Norwegian margin

Oceanography has a high influence on alongslope processes, sedimentation, and climate. During the last 200.000 years, the meridional ocean current system has been similar to the one that occurs today (Hebbeln et al., 1998).Today, the west coast of Norway is influenced by three different water masses transported by different currents. The Norwegian Atlantic Current is an extension of the Gulf Stream and is considered most essential. It transports warm and saline water northwards along mid- and north of Norway before it separates in the Barents Sea. One branch bifurcates east into the Barents Sea and the other continues further north into the Arctic (Laberg et al., 2005b). The Atlantic surface water sinks in the Norwegian - Greenland Sea due to cooling and increasing density. Further, the Norwegian Sea Arctic Intermediate waters returns to the North Atlantic as a deep-water current at a depth of approximately 1000 m (Laberg et al., 2001).

Close to the Norwegian mainland, the Norwegian Coastal current transports low salinity water from the Baltic Sea northward. This current is affected by the run-off of fresh water

from the Norwegian continent and therefore this current may have seasonal variations in temperature. The water masses of the current mixes with the North Sea Waters and the Norwegian Atlantic Water mass. It flows above the Norwegian Atlantic Current and ends up in the Barents Sea (Figure 2.11) (Sætre, 1999; Gascard et al., 2004).
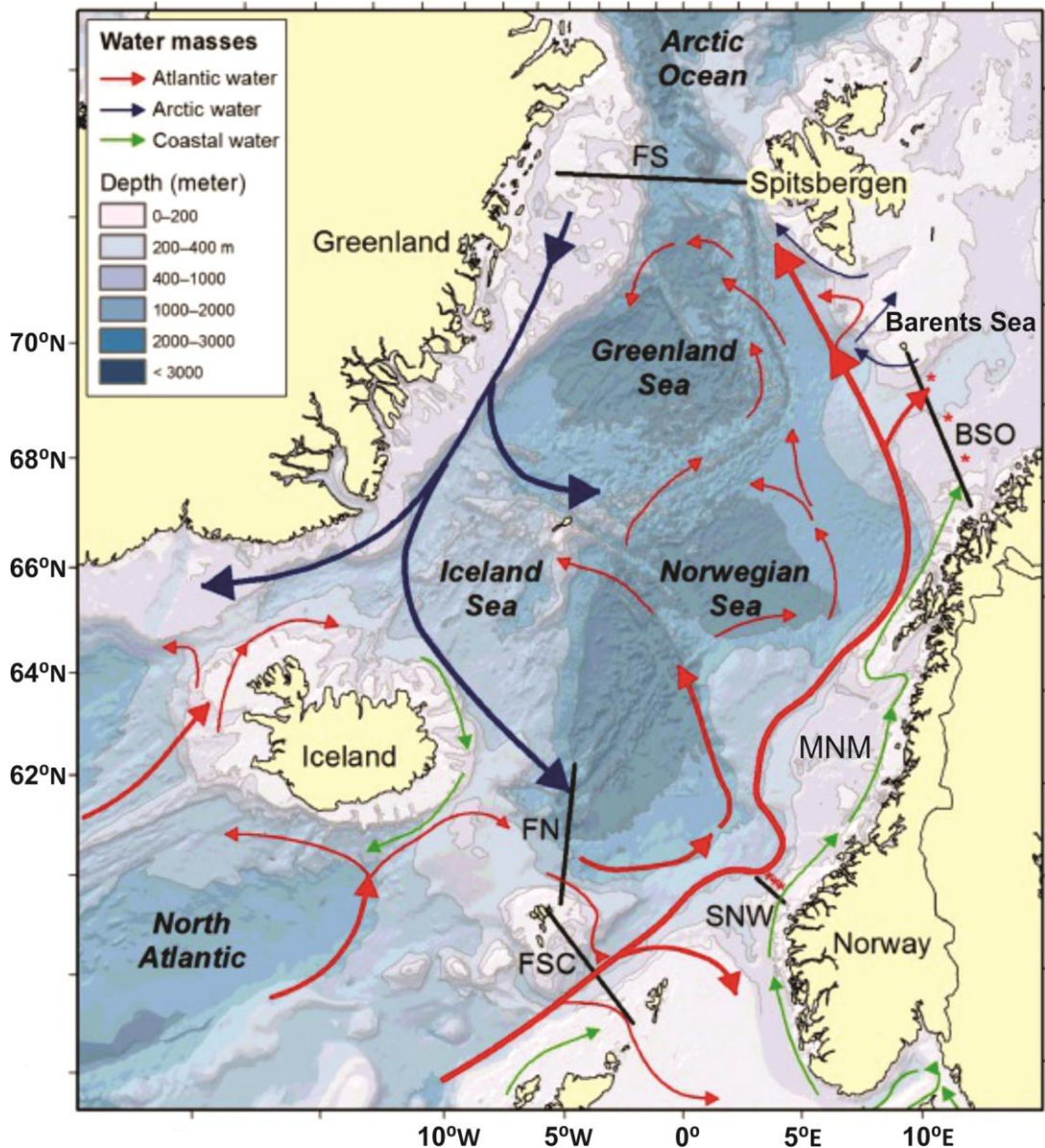

Figure 2.11: Present-day ocean circulation pattern in the North Atlantic. FSC - Færøy-Shetland Channel; SNW – Svinøy Northwest; MNM – Mid-Norwegian Margin; BSO – Barents Sea Opening; FS – Fram Strait. Modified from Lien et al. (2016).

Alongslope sedimentary processes are processes caused by ocean currents concerning erosion, transport, and deposition of sediments along a continental margin. Ocean currents can be formed as a result of atmospheric influence such as wind stress, pressure gradient, evaporation and heat changes. In addition, the Coriolis effect, basin shape, tidal currents, internal waves and benthic storms are other important factors forming the ocean circulations. Alongslope currents can lead to both destructive and constructive sediment effects. The erosional effects can be seen as seismic unconformities, while depositional effects may be observed as formation of contourite, sediment drift and/or plumites (Laberg et al., 2005b).

A contourite is a sedimentary deposition derived from a bottom-currents and can be formed at varying depths (Faugères & Mulder, 2011). They are distinguishable and described based on their geometry and seismic character (Figure 2.12) (Laberg et al., 2001). Contourites have been observed in deep water sediments outside the mid-Norwegian margin since the early Miocene. During this epoch, there was an expansion in sediment drift (Faleide et al., 2008). From the Late Plio-Pleistocene, younger contourites are found on the continental slope of the Naust Formation. Drift growth of the Naust Formation has been observed as mounded elongated drifts surrounded by debris flow units with a glacigenic origin (Laberg et al., 2005b).

Along the slope of the mid-Norwegian margin, four major drift accumulations have been identified, i.e. the Vesterålen Drift, the Lofoten Drift, the Nyk Drift, and the Sklinnadjupet Drift. The Vesterålen and Lofoten drifts are located north of the study area, the Nyk Drift is partially inside, and the Sklinnadjupet Drift is located south of the study area (Figure 2.13). The Nyk Drift is situated in between the glacigenic depocenters of the Sklinnadjupet and Trænadjupet slides. Among the mentioned drifts, the 130 m thick Nyk Drift have had the highest average sedimentation rate where the sediment rich Vøring margin has been the main source of sediments. It is defined as a mounded, elongated upslope accretion drift and was deposited during the Late Saalian to the late Weichelian. The north – eastern part of the drift is lost due to two major slope failures (Trænadjupet- and Nyk Slide) (Laberg et al., 2001; Laberg et al., 2005b). The seismic signature of the Nyk Drift is characterized by high amplitude upper and lower reflectors with a layered, continuous, parallel or slightly divergent, medium amplitude internal seismic signature (Figure 2.14) (Laberg et al., 2001)
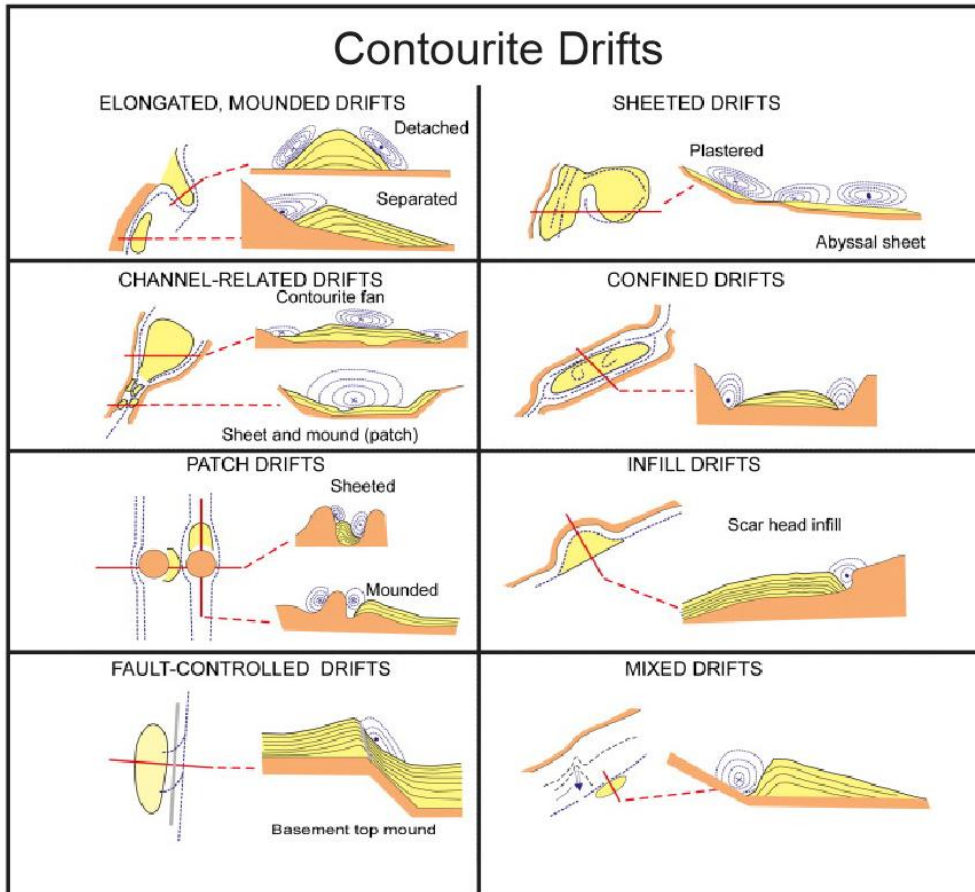
Figure 2.12: Classification of contourite drifts with the inferred bottom-current path. Modified from Rebesco et al. (2014).

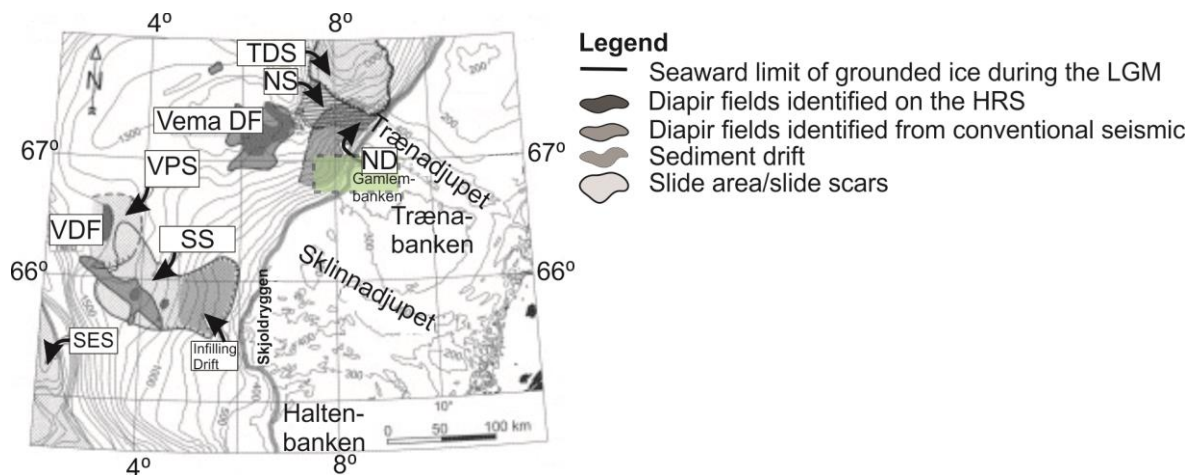*Figure 0.13: Late Quaternary morphology of Vøring margin which indicates slides and drifts along the continental slope and margin. The study area is indicated as a green rectangle. SES – Storegga Slide; VDF – Vigrid Diapir field; SS – Sklinnadjupet Slide; VPS – Vøring Plateau Slide; Vema DF – Vema diapir field; NS – Nyk slide; TDS – Trænadjupet Slide; ND – Nyk Drift. Modified from Dahlgren et al. (2002a).*
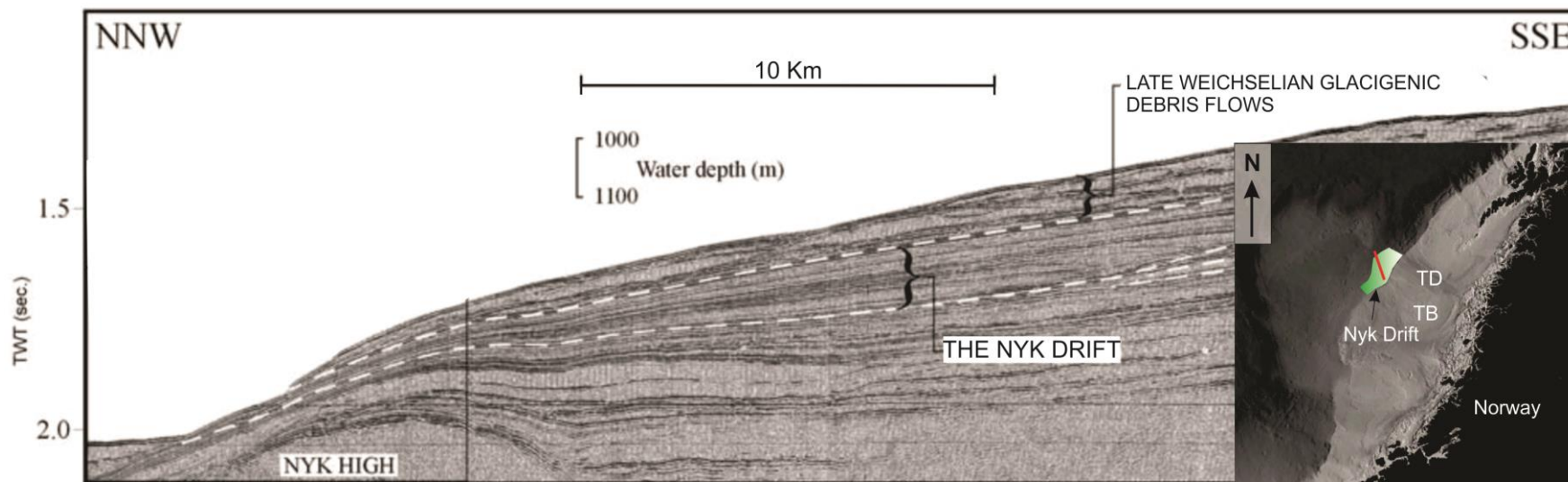
22

Figure 1.14: Seismic section of the Nyk Drift west of Trænabanken and Trænadjupet Trough. The extent of the drift is indicated in green where the location of the cross-profile is indicated as a red line in the inset map in the right corner. TD – Trænadjupet; TB - Trænabanken. Modified from Laberg et al. (2001)

2.5 Cenozoic stratigraphy

From oldest to youngest, the Cenozoic stratigraphy of the mid-Norwegian margin can be separated into three sedimentary formations, i.e. Brygge, Kai/Molo and Naust (Figure 2.16).

The Brygge Formation, which is part of the Hordaland group, was deposited between 55-18 Ma in the Early Eocene – Early Miocene. It is predominantly comprised of claystone on the continental shelf and mudstone in the deeper Møre and Vøring basins. The thickness of Brygge Formation is largest in the Møre Basin, however, the Vøring Basin had a thickness of 500 - 700 m (Laberg et al., 2005a; Eidvin et al., 2007).

During the mid-Miocene, the uplift and compression of the Norwegian mainland led to the deposition of the Molo Formation and the deep marine Kai Formation in the mid-Miocene to Early Pleistocene (Eidvin et al., 2007). Due to this tectonic episode, an unconformity represents the base of these formations. They can be observed on the innermost part of the mid-Norwegian continental shelf, underneath the Naust Formation, and extends parallel to the coast from Møre to Lofoten.

The Molo Formation is likely deposited by coastal progradation in a wave dominated environment. It is described as a sandy deltaic deposition, influence by extensive long-shore drifts (Eidvin et al., 2007).

The Kai Formation consists of deep marine sediments with high content of siliceous ooze in the Vøring Basin and clay-, silt and sandstone on the shelf. Syn-sedimentary faulting occur in this formation where some of the faults are affecting overlying sediments all the way to the seafloor (Dahlgren et al., 2002a).

2.5.1 The Naust Formation

The Naust Formation is the uppermost and youngest formation of the mid-Norwegian continental margin and is comprised of a thick succession of low angle sediment wedges and sheet-like units with a west-thinning trend (Figure 2.17). The Naust Formation overlays the Molo Formation in the east (Figure 2.15) with a down-lap termination onto the Kai Formation (Dahlgren et al., 2002a; Ottesen et al., 2009).

The deposition of the Naust Formation occurred during the Late Pliocene-Pleistocene epoch as a consequence of substantial erosion due to the formation of ice-sheets and uplift in the late Neogene. Fluctuating ice-sheets on the shelf transported and deposited substantial amounts of glacigenic sediments which accumulated along the margin. Most of the sediments were first deposited on the shelf and later transported by downslope processes onto the slope. The Naust Formation is composed of approximately 100,000 Km^3 of glacigenic sediments derived from the Fennoscandian Ice Sheet. The substantial deposition of the Naust Formation led to subsidence and therefore the dip of the seismic Naust reflectors increase with depth (Dahlgren et al., 2005; Rise et al., 2005; Dowdeswell et al., 2010).

Difficulties defining the base Naust unconformity (BNU) has led to problems estimating the thickness and age of the Naust Formation. However, current estimates specifies a couple of hundred meters in the area of Trænabanken (Dahlgren et al., 2002a; Rise et al., 2005).

The Naust Formation is predominantly comprised of fine sediments, i.e. interbedded claystone, siltstone and sand, but more coarse sediments occur in the upper part (NPDfactpage, n.d.-a). Basically, the formation is organized in two different facies: Acoustic massive sediment units and mass transport depositions, with the former being comprised of flat lying moraines deposited on the shelf (Rise et al., 2010).

Several frameworks of the Naust Formation have been established. From oldest to youngest, Dahlgren et al. (2002a) divided the Naust Formation into five sequences, i.e. E, D, C, B and A. Rise et al. (2006) also divided the Naust Formation into five sequences but noted them N, A, U, S and T and Rise et al. (2010) revised the age estimates (Figure 2.16). Both frameworks will further be used in this thesis (Table 2.1), however, the age estimation and sequences of Rise et al. (2010) will mainly be utilized.
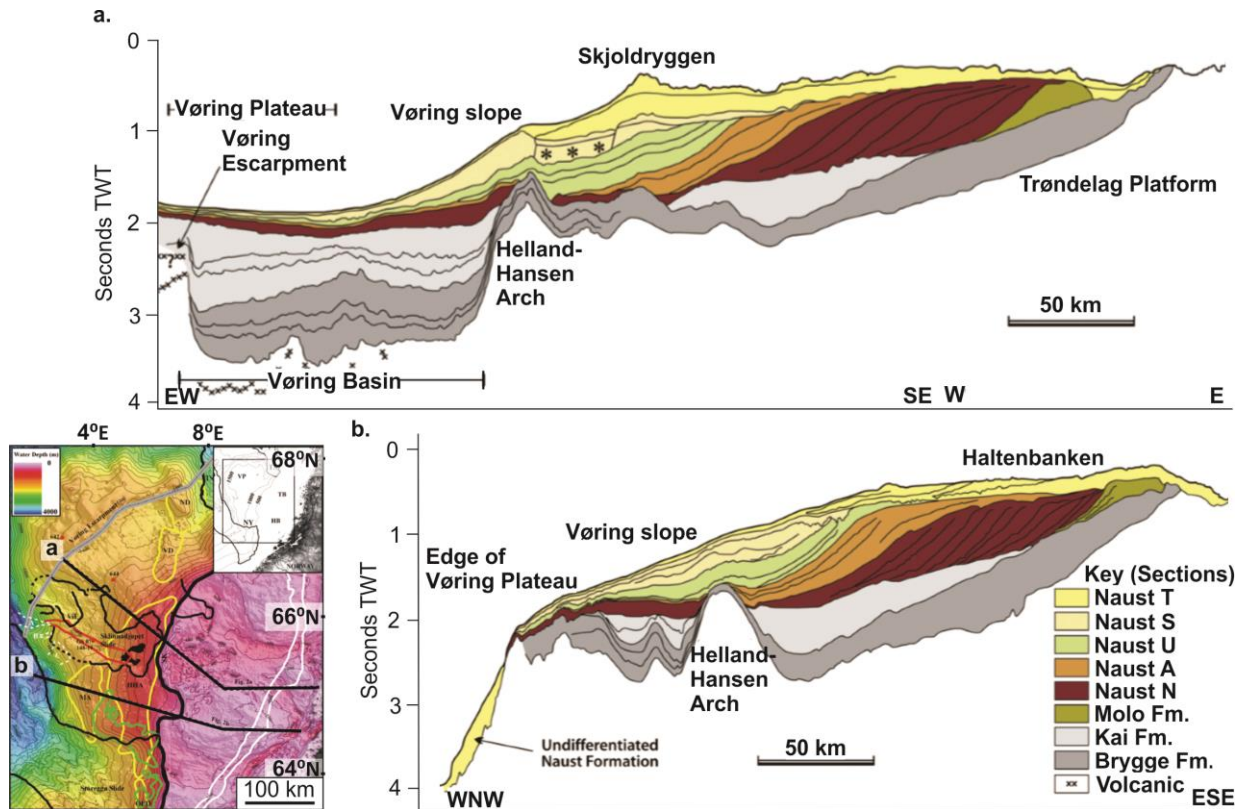
Figure 2.16: Stratigraphic profiles from the mid-Norwegian margin indicating the Cenozoic sedimentary formations in this area. The locations of the profiles are indicated in the inset map in the lower left corner. Modified from Rise et al. (2010).

Table 2.1 Frameworks and age estimates of the Naust Formation on the mid-Norwegian margin (Dahlgren et al., 2002a; Ottesen et al., 2009; Rise et al., 2010). From Laberg (pers.com.).

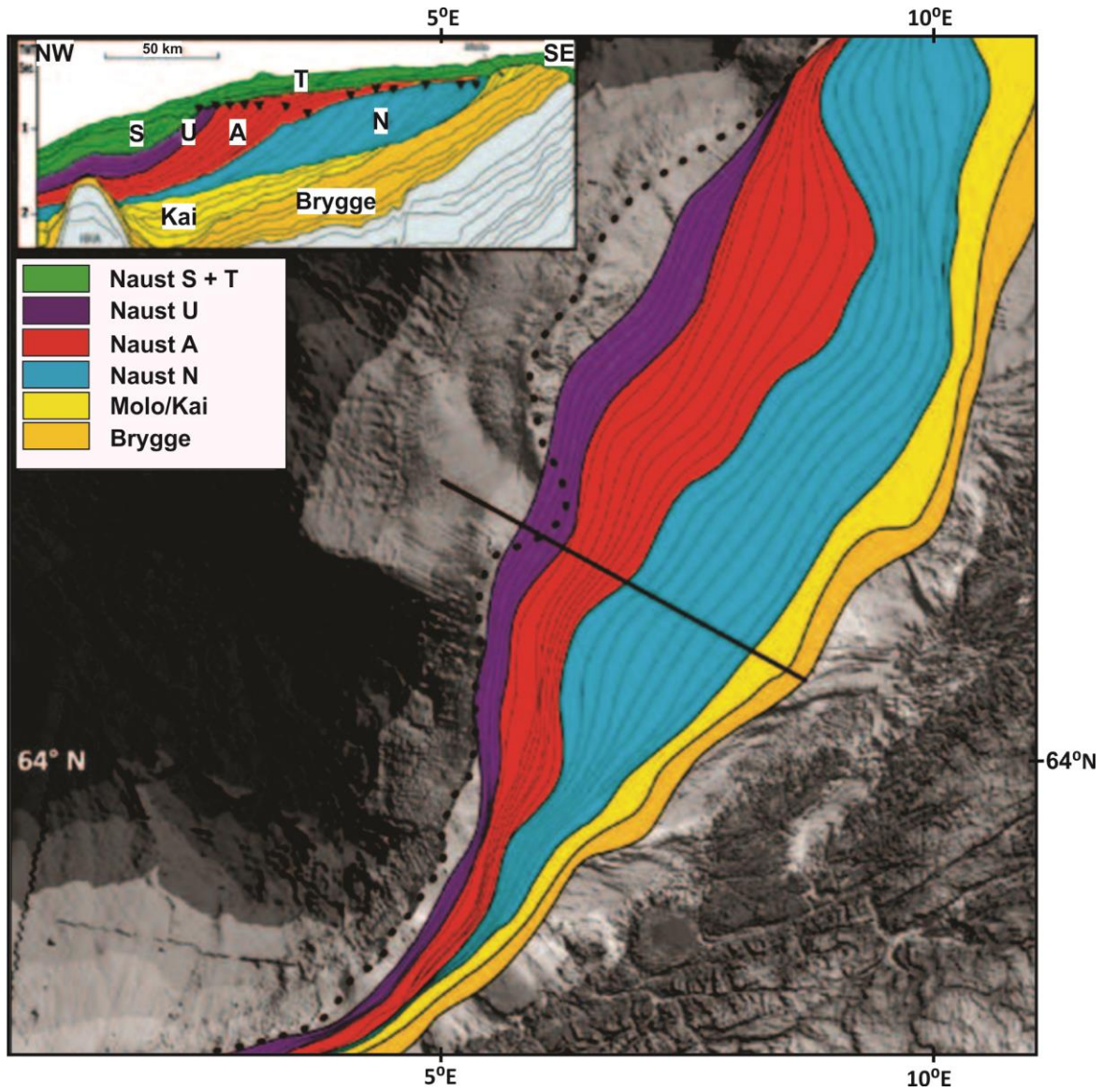| Dahlgren et al. (2002)		Ottesen et al. (2009) Rise et al. (2010)	
Units	Ma	Units	Ma
A1/A2		T	
	0.3		0.2
B		S	
	0.4		0.4
C		U	
	0.5		0.8
D		A	
	0.9-1.1		1.5
		N	
	2.7		2.8

Figure 2.17: Sediment catchment area of the prograding wedge (Naust N, A, U, S and T) of the mid-Norwegian continental margin with different units indicated. The geoseismic profile in the left corner is indicated by a black line crossing the wedge. The dotted line indicates the present shelf break. Modified from Ottesen et al. (2009).

Naust N and A were deposited in the period of 2.8-0.8 Ma and are the oldest sub-sequences of the Naust Formation (Rise et al., 2010). They marked a great increase in the sedimentation rate and are described as wedge-shaped sediment packages prograding from the continental margin with a northwest orientation. Their deposition indicate the onset of the glaciation of Scandinavia (Ottesen et al., 2009). Indications of fast-flowing ice-streams on the paleo-shelf occur from Naust A (Rise et al., 2005; Rise et al., 2006).

Naust U was deposited from 0.8-0.4 Ma by several slope-building events which may indicate glacial oscillations during this period (Ottesen et al., 2009; Rise et al., 2010). This sequence is characterized by substantial deposition of glaciganic debris flows (Rise et al., 2006) and may have had the greatest sediment delivery among the Naust sequences (Dowdeswell et al., 2010).

The deposition of **Naust S** occurred from 0.4-0.2 Ma (Rise et al., 2010) and is often characterized by generally coarser and less sorted sediments than Naust U (Plaza-Faverola et al., 2011). The Elsterian Ice-sheet have probably influence the deposition of Naust S (Ottesen et al., 2009). Debris flows sediments are often interbedded with contourites in this sequence and contourites are often well preserved as climbing internal reflectors on the palaeo-slops. (Plaza-Faverola et al., 2011).

The deposition of **Naust T** started 0.2 Ma and continued throughout the Saalian and Weichselian. It is the youngest sequence of the Naust Formation and is mainly comprised of flat-lying units of massive till and debris flows (Ottesen et al., 2009; Rise et al., 2010). Further in this thesis, the main focus will be the upper part of the Naust Formation (Naust A, U, S and T).

3 Data and methods

3.1 Seismic data

This study is mainly based on 3D seismic data acquired by PGS Geophysical AS in 2012. The dataset (RD1202) is covering an area of ~1200 km^2 (Figure 3.1) and the data quality is considered to be very good in the Naust Formation. The inline and crossline intervals are 18.75 m and 12.5 m, respectively.

The acoustic impedance (AI) contrast at the seafloor was used to determine the phase and polarity of the seismic data (Figure 3.2). According to the SEG (Society and Exploration Geophysicists) polarity standard of Sheriff (1985), this dataset is characterized as zero-phase normal polarity. Using the convention of Badley (1985), the dataset has a zero-phase reverse polarity.
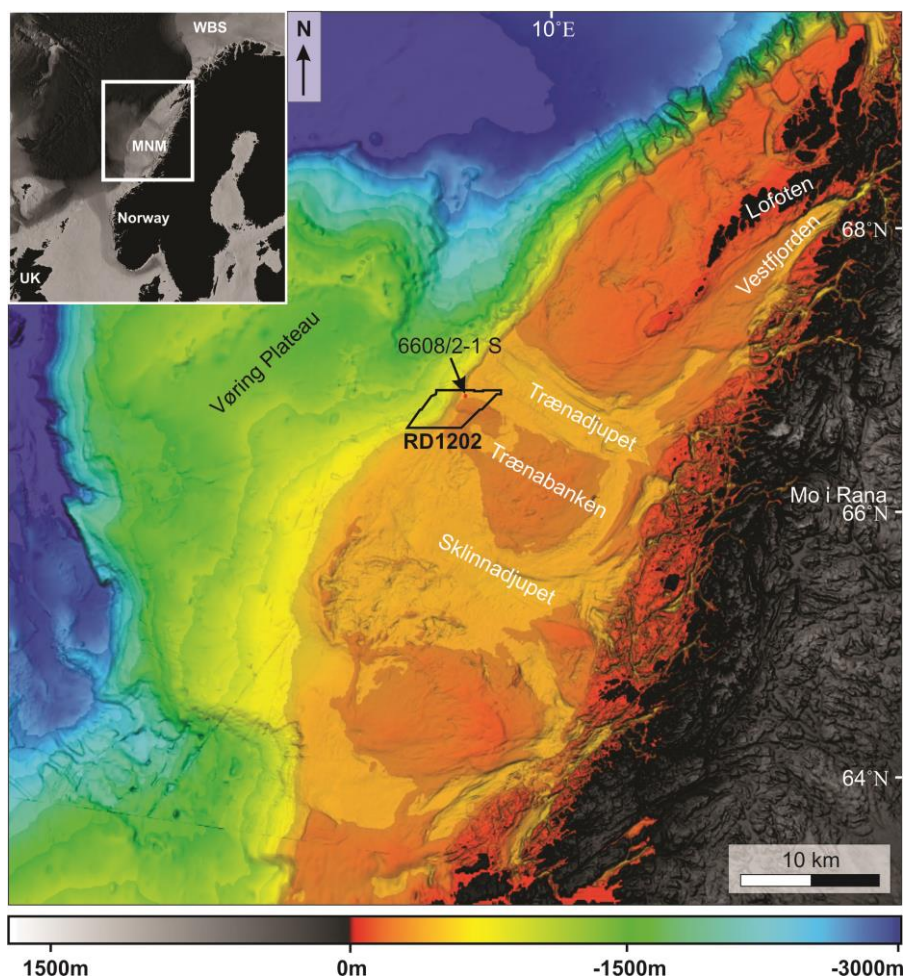

Figure 3.1: Bathymetric map of the mid-Norwegian margin with the 3D seismic dataset (RD1202) of this study indicated by a black polygon. Well 6608/2-1 S is indicated by a red dot within the study area.

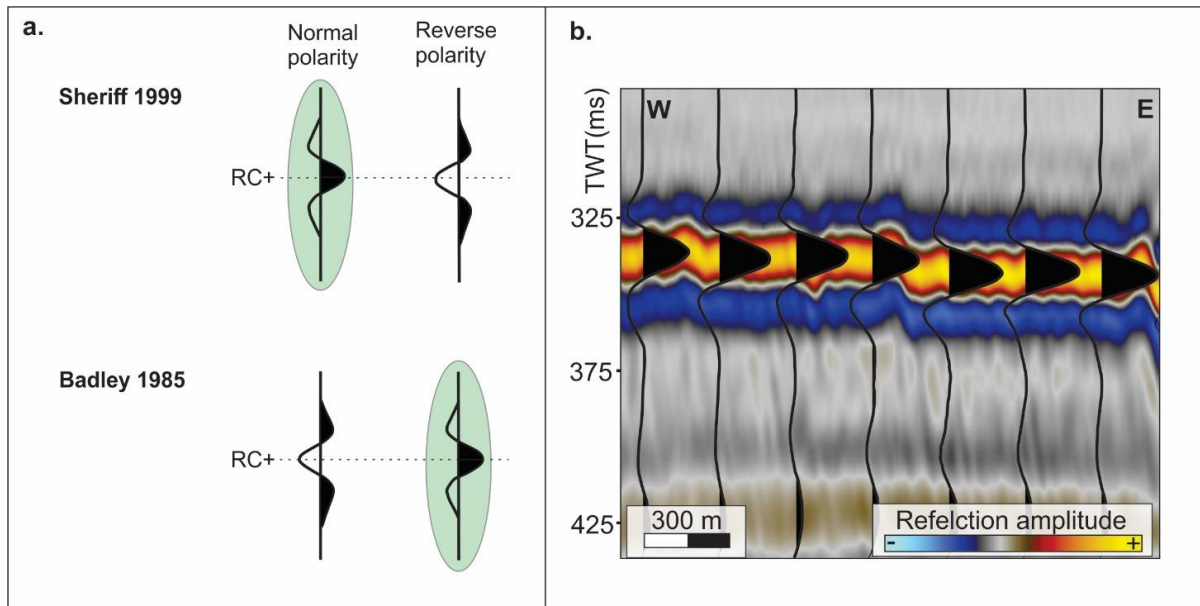*Figure 3.1: **a.** Normal and reverse polarity of the SEG and Badley polarity convention for plotting seismic signals. The polarity of the seismic data used in this study is highlighted in green. **b.** The seafloor reflection indicated by wiggles displayed from the dataset RD1202. The central peak of the seafloor reflector indicates a positive acoustic impedance contrast. Modified from Badley (1985) and Sheriff (2002)*

3.2 Correlation

Data from well 6608/2-1 S was used to correlate the stratigraphic velocity with the seismic data to get a better understanding of the stratigraphy. Well tops were absent within the Naust Formation, and therefore, checkshots were utilized to calculate an average velocity of the formation. This velocity was further used to calculate the resolution of the dataset and time-depth convert for example negative and positive relief of landforms. Additionally, 2D seismic lines were used to correlate the interpreted stratigraphy in RD1202 to the established stratigraphy (Table 3.1).

Tabell 3.1: 2D seismic lines were used to correlate the framework of this study to the established stratigraphy.

2D seismic data	
GMNR-94-1071	N2N3T96R005-106
GMNR-94-107	N2N3T96R005-212
GMNR-94-107A	

3.3 Seismic resolution

Seismic resolution is defined as a measurement of how small an object can be in order to be visible in seismic (Sheriff, 2002). Normally, each seismic survey is customized to provide a specific penetration depth and resolution of geological features in the area (Kearey et al., 2013). Seismic resolution can be divided into vertical and horizontal resolution. Both dimensions are highly dependent on the frequency (F) and wavelength (λ) of the seismic signal (Schlumberger, n.d) (Equation 3.1). In most cases, these features are being affected by the propagation depth. With increasing depth, the sound signal will lose energy to the environment due to quickly attenuation of the higher frequencies and therefore decreasing the frequency of the signal. This will further lead to a gradual increase in wavelength and finally resulting in a poorer resolution with depth (Figure 3.3). The rate of compaction of rocks will also increase with depth and this will boost the sound velocities (Badley, 1985; Brown, 1999; Rafaelsen, 2006).

The eastern part of the Vøring margin is an exception. According to Reemst et al. (1996) there is an velocity inversion in this area which is an anomaly with respect to the theory regarding velocity and depth. They suggest the inversion to be a result of high pore fluid pressures from pre-Pliocene sediments and the rapid deposition of the sedimentary wedge from Plio-Pleistocene.

Equation 3.1 - Wavelength

$$\lambda = \frac{V}{F}$$

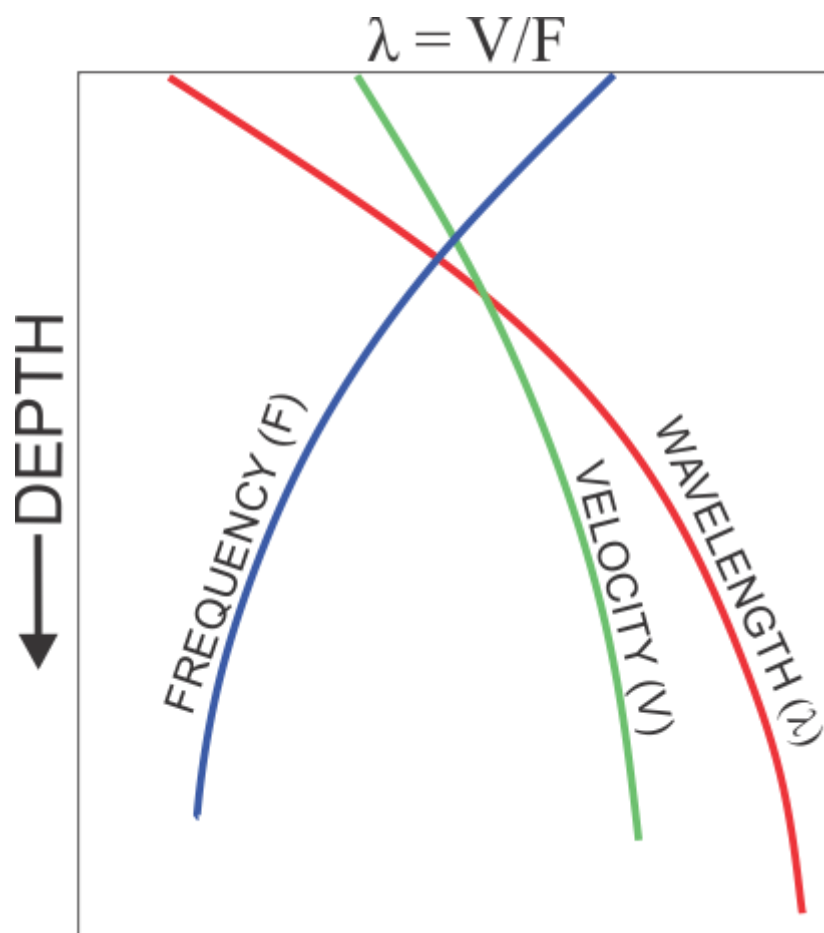λ= Wavelength, V= Seismic velocity and F= Seismic frequency

Figure 3.3: *The relationship between frequency, velocity, and wavelength of a signal as it is affected by propagation depth. Seismic resolution will generally decrease with depth. Modified from Brown (1999).*

3.3.1 Vertical resolution

The vertical resolution is a measurement of how closely two seismic reflectors can be spaced in order to be noticeable (Badley, 1985). This is determined by the wavelength of the seismic signal and the distance between the reflectors. Interaction between wavelets (Figure 3.4) encountering closely spaces interfaces lead to two different limits of vertical resolution. If the distance between the reflectors are below ¼ of the wavelength, wavelets start interfering with each other. One-quarter of a wavelength (or half a period) is therefore named the limit of separability and the wavelets will from this point on start to constructively interfere. This interference will give a seismic visualization of only one interface/reflector instead of two with a stronger amplitude than expected (Brown, 1999; Rafaelsen, 2006). Vertical resolution can be calculated by using Equation 3.2.

When the spacing between two reflectors become thinner than one-quarter of a wavelength, progressively destructive interference occur until one-thirtieth of a wavelength. At this point, both reflectors are absent and it is therefore called the limit of visibility (Sheriff, 1985; Brown, 1999; Rafaelsen, 2006). Deconvolution is a process that can improve the vertical resolution in the data processing stage (Kearey et al., 2013).
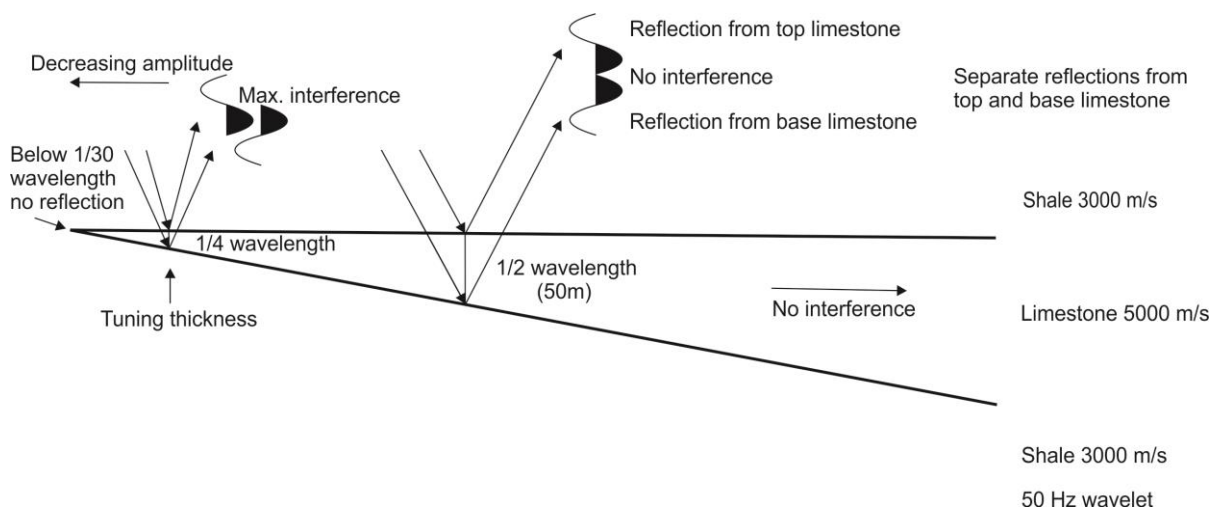

Figure 3.4: Vertical resolution illustrated by wave interference on a wedge with high acoustic impedance. Modified from Badley (1985).

Equation 3.2 – Vertical resolution

$$Vr = \frac{\lambda}{4}$$

$$Vr = vertical\ resolution, \lambda = wavelength$$

3.3.2 Horizontal resolution

Horizontal resolution is described in terms of the Fresnel zone. Seismic waves are spreading out from the source in three dimensions where the spreading increases by distance. By using the principal technique migration, it is possible to concentrate the energy in the Fresnel zone (Figure 3.5). The principle of the process is to improve the horizontal resolution. This can for example be done through re-arranging misplaced reflectors due to dip and to change the reflection pattern when it comes to points and edges. If 2-D migration is utilized, it is only possible to reduce the Fresnel zone to an elliptic shape, however, 3-D migration may decrease it to a small circle. The Fresnel zone increases with depth and this is due to the general depth velocity increase. Calculation of the Fresnel Zone radius can be done by Equation 3.3 (Brown, 1999; Rafaelsen, 2006).

Both vertical and horizontal resolutions have been calculated in the center of the 3D-cube based on equation 3.2 and equation 3.3 (Table 3.2). In Petrel, the frequency spectral analyzing tool and inspector tool were used in combination, to find the dominating frequency of the seafloor and the lowermost horizon in this study. The dominating frequency of these horizons ranged from 30-50 Hz. 1500 m/s was used to calculate the resolution of the seafloor, which is commonly used as a standard velocity of brine. Based on three checkshots from the interval between the seafloor and the lowermost horizon of this study, the average velocity of the stratigraphy was calculated to be 1962.5 m/s. Both Dahlgren et al. (2002a) and Ottesen et al. (2009) used ~ 2000 m/s to time-depth convert the velocities of Naust Formation. The vertical resolution is better on the slope than on the shelf in this study. This may be a result of A greater overburden on the shelf compared to on the slope.

Equation 3.3 – Horizontal Resolution

$$rf = \frac{v}{2}\sqrt{\frac{t}{f}}$$

$rf = the\ radius\ of\ Fresnel\ zone, v = average\ seismic\ velocity\ \left(\frac{m}{s}\right),$

$t = Two - way\ travel\ time\ (s)\ and\ f = dominant\ frequency\ (Hz)$

Fresnel zone before migration

○ 2D migrated Fresnel migration
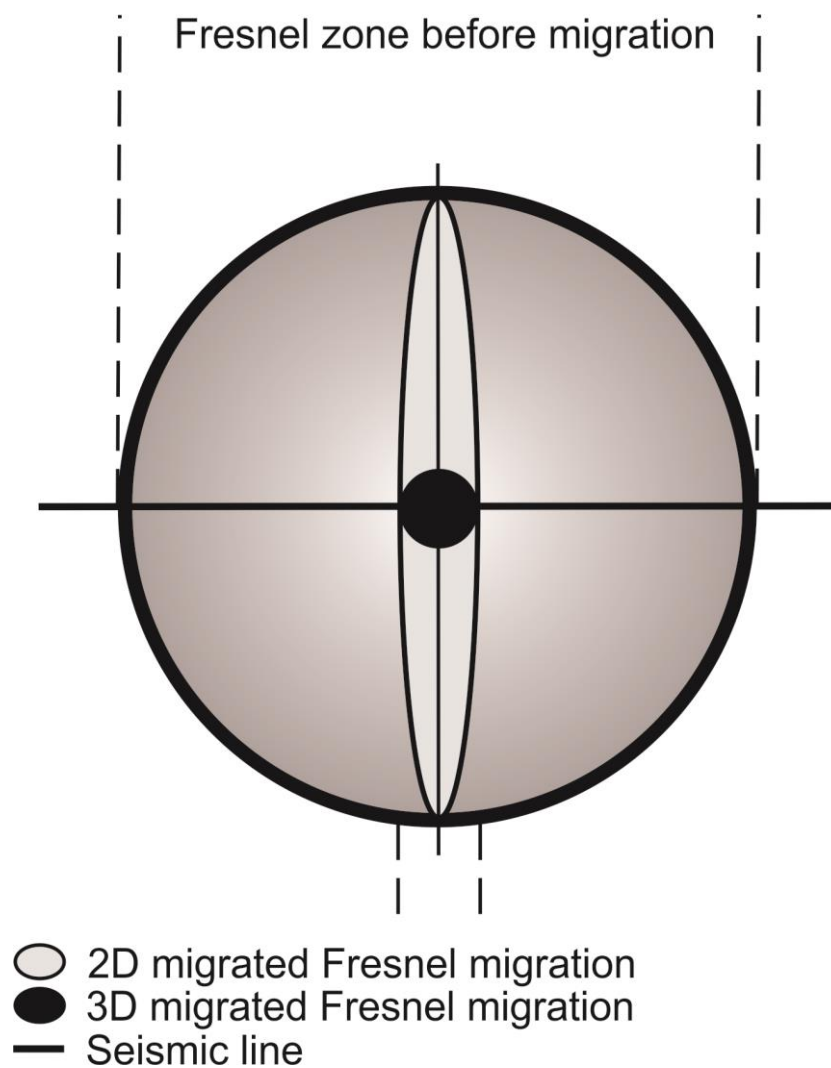● 3D migrated Fresnel migration
— Seismic line

Figure 3.5: The Fresnel zone and how the size and shape differ with 2D and 3D migration. Modified from Brown (1999).

35

Tabell 3.2: Resolution calculation of different parts of the stratigraphy in the study area. The table indicates how the resolution is affected by the variations in velocity, frequency, and propagation depth.

Dataset	Location	Measured interval	Average interval velocity (v)	Depth in TWTT (t)	Frequency (f)	Wavelength (λ)	Vertical resolution (Vr)	First Fresnel zone (rf)
RD1202	Shelf	Seafloor	1500 m/s	0.437 s	~ 30 Hz	50 m	~ 13 m	~ 91 m
		Horizon 1	1962.5 m/s	0.706 s	~ 40 Hz	49 m	~ 12 m	~ 130 m
	Mid - Slope	Seafloor	1500 m/s	0.950 s	~ 42 Hz	35.7 m	~ 9 m	~ 113 m
		Horizon 1	1962.5 m/s	1.460 s	~ 46 Hz	43 m	~ 11 m	~ 181 m

36

3.4 Artefacts and noise

Seismic data is often characterized by the influence of artefacts and noise. Artifacts and noise may cause misinterpretations of the seismic data and is therefore important to ignore. A geophysical waveform is comprised of signal and noise where the signal is the geological information and the noise is all other components. By processing the seismic data, it is possible to remove noise and thus be able to only look at geological information. Noise can be deviated into two subdivisions, i.e. random and coherent noise. Random noise is caused by everything but the source, e.g. seismic pulses coming from ship probs, other exploration and production activity, or wind and tidal waves. Coherent noise is created by the source or geophysical experiments but are of no interest. Surface waves produced by the source can be one example. These waves reach the receivers and may obscure the pulses with geological information coming from underneath (Kearey et al., 2013). In this seismic dataset, artefacts, and noise such as for example acquisition footprints, diffractions and multiples have been identified. They are described in the next sections.

A linear spatial grid pattern may occur on shallow 3D seismic horizons, surfaces, or time slices after processing the data. Such features tend to reflect parts of the acquisition geometry and is therefore defined as acquisition footprints (Figure 3.6) (Marfurt et al., 1998; Chopra & Larsen, 2000).

Diffractions are radial scattering of incident seismic energy and is caused by energy encountering an abrupt discontinuity with a radius shorter than the wavelength of the incident signal (Kearey et al., 2013). They occur as weak parabolic reflections on the seafloor but could also be observed in deeper parts of the stratigraphy (Figure 3.7).
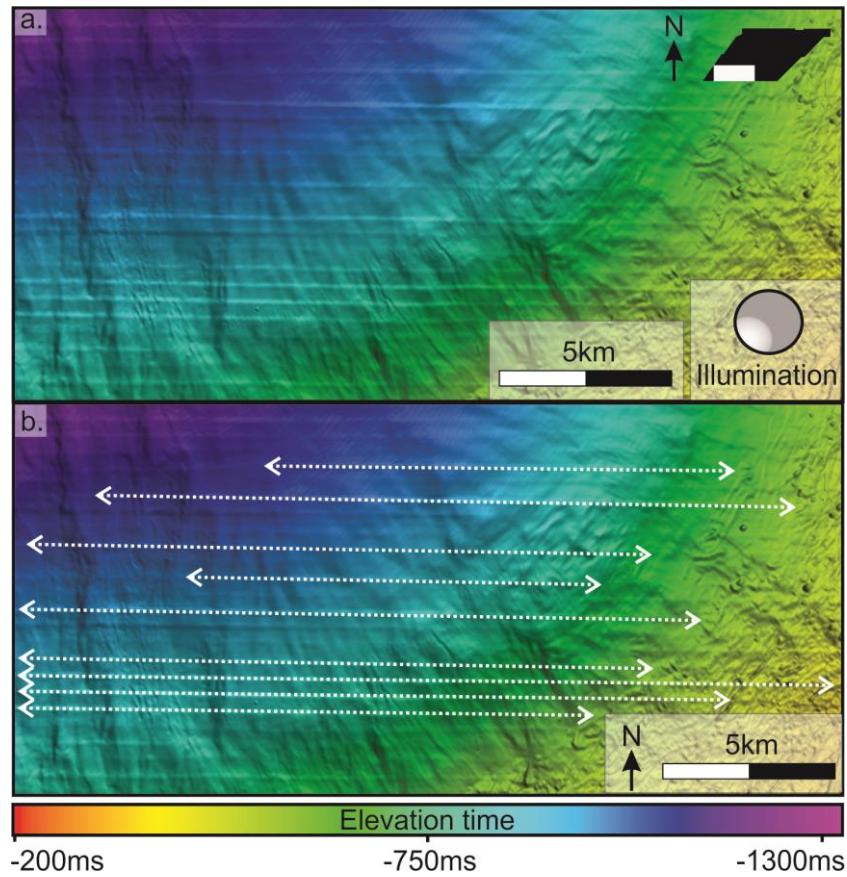
Figure 3.6: *a. Acquisition footprints without interpretation and b. acquisition footprints with interpretation (white stippled arrows). The location of the profile is indicated (white line) in the inset map in the right corner of a. Vertical exaggeration is 25.*
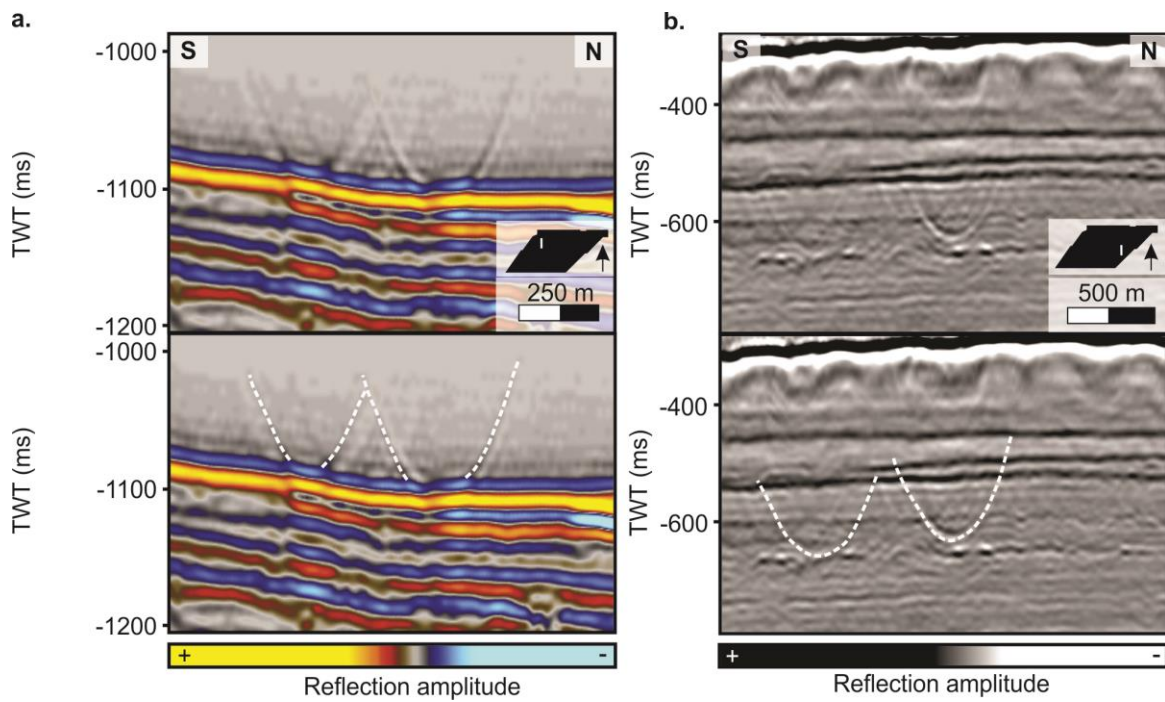

Figure 3.7: *a. Diffractions on the seafloor with and without interpretation and b. diffractions seen in greyscale located in the deeper parts of the stratigraphy with and without interpretation. Locations of the profiles are indicated (white line) in the inset maps.*

Multiples are seismic signals reflected at several interfaces before they return to the surface. Compared to primary reflections, multiples are characterized by a time delay and a lower amplitude due to energy loss. However, surfaces with a high reflection coefficient (for example the seafloor) may produce multiples with similar reflection amplitude as the primary reflection. This may cause confusion and lead to interpretation errors (Kearey et al., 2013). By creating a fictive seafloor horizon in Petrel (2 times the original depth of the seafloor), the seafloor multiple was detected in this thesis (Figure 3.8).

Sub-vertical areas with low seismic reflectivity and highly distorted reflections (acoustic masking) can be observed within the study area. Such features can be associated with focused fluid flows and are often referred to as acoustic "pipes" or "chimneys". The acoustic pipes in this study gently twist their way through the seismic profile (Figure 3.9) (Løseth et al., 2001; Løseth et al., 2009).
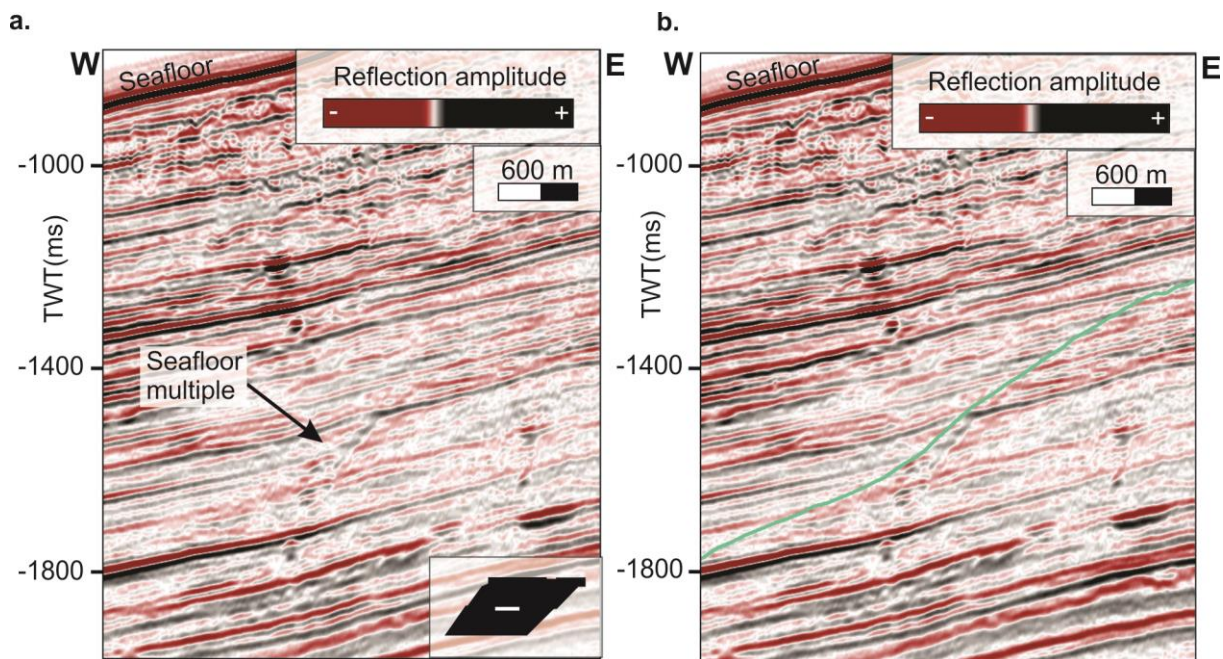

*Figure 3.8: **a**. Seafloor multiple observed as a crosscutting reflector at 1600 ms. **b**. same section with a fictive seafloor multiple indicated in green. The location of the profile is indicated (white line) in the inset map in the right corner of a.*
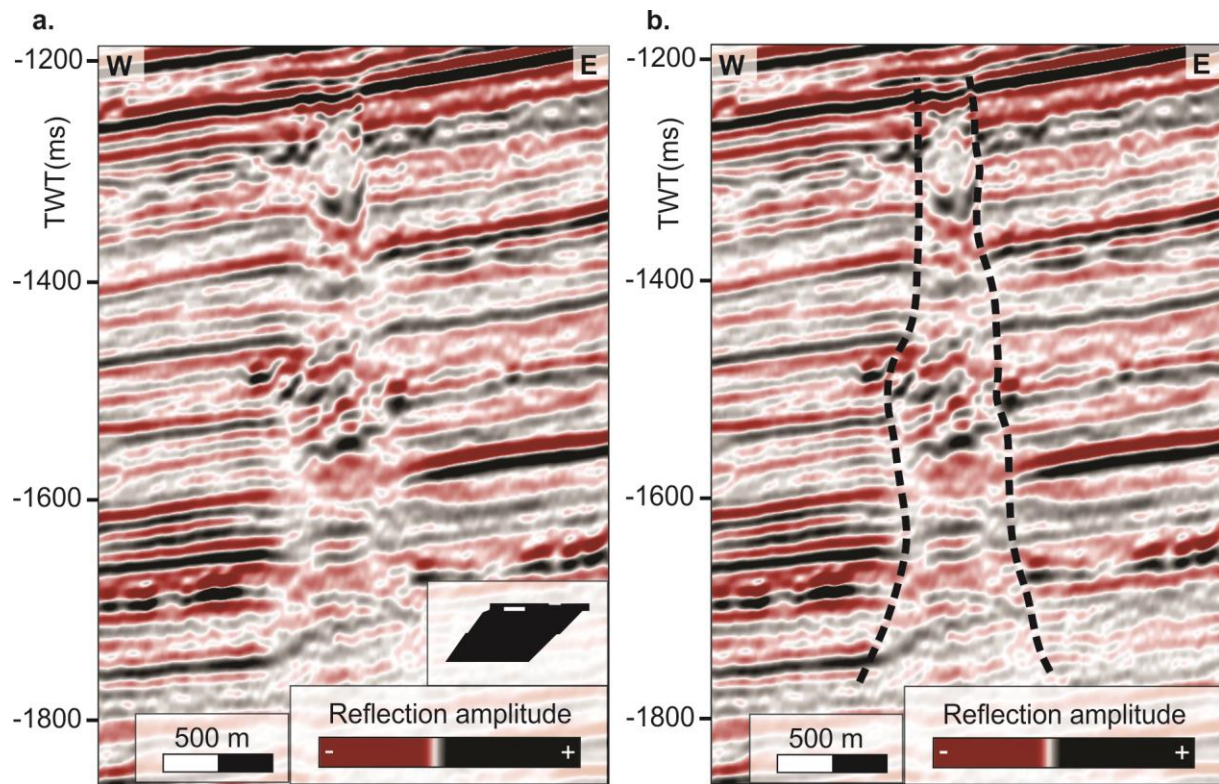
*Figure 3.9: **a.** Acoustic pipe influencing the stratigraphy in the study area. **b.** same pipe with interpretation. The location of the profile is indicated (white line) in the inset map in the right corner of a.*

3.5 Software

3.5.1 Petrel

Petrel E&P 2018 software developed by Sclumberger has been utilized in this thesis to interpret and visualize the seismic dataset. It was used to interpret seismic horizons, generate surfaces, and attribute maps. Smoothing was applied to some of the final maps.

Seismic attributes are used to increase and highlight information regarding geological features or trends to get a better visualization and understanding of the seismic data (Sheriff, 2002). RMS, thickness, and variance attributes were utilized in this study. However, variance attribute did not give desired results and was therefore less utilized. In addition, the dip angle attribute was occasionally used on surfaces to get an overview of the dipping trend.

RMS (Root Mean Square) is an averaging technique which highlights strong amplitudes in a seismic volume. These amplitudes can both be positive or negative and the attribute can be used to easier recognize amplitude anomalies (Brown, 1999; Veeken, 2007). In this study, this attribute was useful to recognize different downslope processes, furrows, lineations and shallow gas accumulations.

Thickness attributes calculate the thickness in two-way travel time between two surfaces. In this study, this attribute was used to determine the thickness trends of units and some morphological features. This can reveal information about larger and smaller depositional trends in the study area.

3.6 Seismic interpretation method

According to Mitchum et al. (1977), seismic stratigraphic analysis can be defined as the study of stratigraphy and depositional facies interpreted from seismic data. It is used to recognize and correlate different depositional sequences, interpret the depositional environment and to estimate lithofacies of sequences. The definition of a depositional sequence is a delimited stratigraphic unit composed of genetically related strata which is bordered at its top and base by unconformities and their correlative conformities (Vail, 1977). In this study, the seismic interpretation method has been useful to establish the stratigraphic framework of the Naust Formation.

A seismic stratigraphic analysis can be divided into a two-step process, i.e. (1) Seismic sequence analysis and (2) Seismic facies analysis. The first step is to subdivide a seismic section into packages of concordant reflections. These reflections are separated by discontinuous surfaces and interpreted as depositional sequences. The second step is to analyze and map the different seismic facies units within a seismic sequence (Mitchum et al., 1977). Further description follows in the next sections.

3.6.1 First step: seismic sequence analysis

Reflection terminations are the boundaries of seismic sequences (Figure 3.10) and can be divided into top- and base-discordant seismic reflections (Mitchum et al., 1977).

Top-discordant reflections can further be sub-divided into erosional truncation and toplap. Erosional truncations are defined as strata against an overlying eroded surface and can be formed by subsequent removal of strata, with following deposition of sediments. A toplap can be recognized as strata terminating against an overlying surface and are formed by sedimentary bypassing or non-deposition, with a low rate of erosion. Toplaps commonly occur locally but are difficult to correlate regionally. Erosional truncations are the most reliable top-discordant criterion for a sequence boundary (Mitchum et al., 1977). Such erosive boundaries may represent an important time break (Veeken, 2007; Veeken, 2013)

Onlaps and downlaps are examples of base-discordant reflections. An onlap can be recognized in two different relations. One relation may be where seismic reflections of

initially horizontal strata terminating gradually against an initially inclined surface. Another relation is when initially inclined strata gradually terminating up-dip against a surface of greater inclination. Downlap is recognized as the termination where initially inclined strata downdip and encounter initially inclined or horizontal strata. The general term baselap is used when trouble differentiating between onlap and downlap occur (Mitchum et al., 1977).

Internal convergence and offlap are terminations which are related to internal boundaries within a sequence. The term 'internal convergence' is commonly used to describe that strata is thinning out to below seismic resolution (Mitchum et al., 1977).
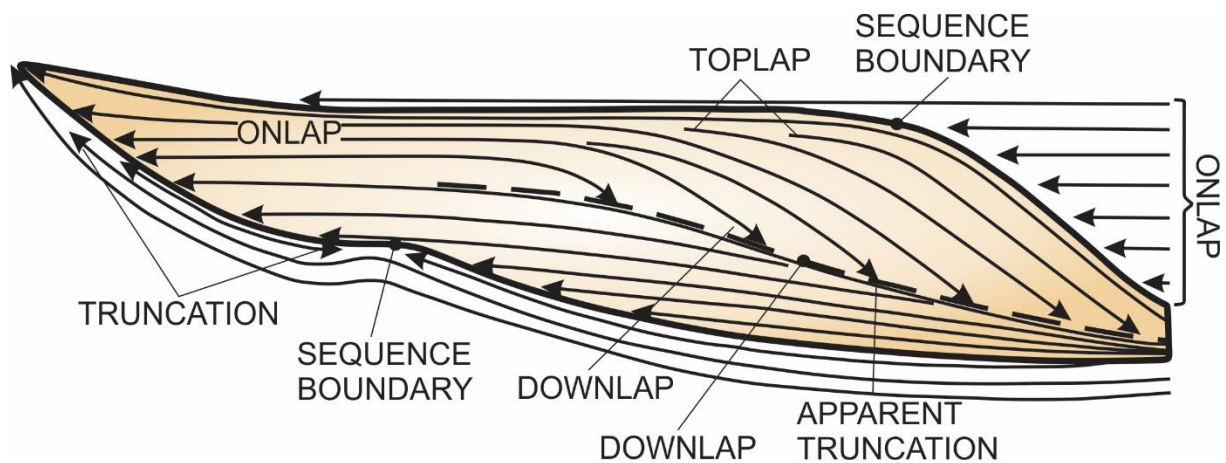

Figure 3.10: Reflection terminations within or in contact with a seismic sequence. Modified from Mitchum et al. (1977) and Vail (1987).

3.6.1 Second step: seismic facies analysis

After a seismic sequence is defined, the second step is to interpret the environment and lithosfacies within the sequence. This is part of the seismic facies analysis and is done by describing and interpreting different seismic reflection parameters, i.e. reflection configuration, continuity, amplitude, frequency and interval velocity (Table 3.3 & Table 3.4) Each parameter provides important geological information about the subsurface (Mitchum et al., 1977; Veeken, 2013).

Information regarding the gross sedimentation pattern, depositional processes and erosion, in addition to palaeotopegraphy, can be revealed by reflection configuration. Reflection continuity is characterized as continuity of strata, which means uniformly stratified deposits over larger areas. Thus, fluid contact reflections are often easily detectable in reflection configuration. Reflection amplitude can reveal information about the velocity and density contrasts of the individual interfaces and their spacing. For instance, changes in reflection amplitude may be used to anticipate lateral bedding changes. The frequency contains information about the distance between reflectors and lateral differences in interval velocities, i.e. often associated with the presence of gas. By grouping of all the seismic reflection parameters it is possible to interpret the depositional environment, sediment source and geological setting of the facies units (Table 3.3) (Mitchum et al., 1977).

It is an important link between the description of seismic facies and the external reflection configuration of the unit. This relation (Table 3.5) often gives an understanding of their geometric interrelation and depositional setting (Mitchum et al., 1977).

Table 3.3: Reflection parameters used in seismic stratigraphy and their geological significance. Modified from Mitchum et al. (1977).

Reflection parameters	Geological interpretation
Reflection configuration	❖ Bedding patterns ❖ Depositional processes ❖ Erosion and palaeotopography ❖ Fluid contacts
Reflection continuity	❖ Bedding continuity ❖ Depositional processes
Reflection amplitude	❖ Velocity-density contrast ❖ Bed spacing ❖ Fluid content
Reflection frequency	❖ Bed thickness ❖ Fluid content
Interval velocity	❖ Estimation of lithology and porosity ❖ Fluid content
External form and areal association of seismic facies units	❖ Gross depositional environment ❖ Sediment source ❖ Geological setting

Table 3.4: *Five different common seismic facies units dependent on amplitude, frequency, continuity, and configuration. Modified from Veeken (2007).*
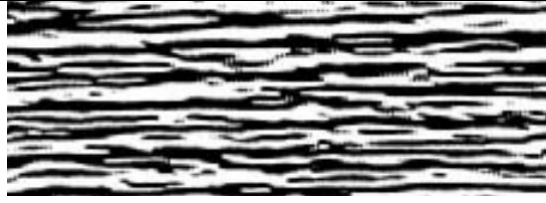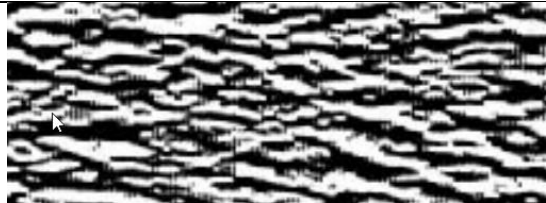
Seismic facies	Reflection configuration	Reflection amplitude	Seismic facies after Veeken (2007)
A	Parallel continuous	Medium amplitude	
B	Parallel continuous	High amplitude	
C	Parallel continuous	High amplitude	
D	Subparallel discontinuous	High amplitude	
E	Chaotic	Medium amplitude	

Table 3.5: Geological interpretation of seismic facies parameters. Modified from Mitchum et al. (1977).

Reflection configurations *(within sequences)*	***External forms (of sequences and seismic facies units)***

Principal stratal configuration
 	
❖ <u>Parallel</u>
❖ <u>Subparallel</u>
❖ <u>Divergent</u>
❖ <u>Prograding clinoforms</u>
   - Sigmoid
   - Oblique
   - Complex sigmoid-oblique
   - Hummocky clinoform
❖ <u>Chaotic</u>
❖ <u>Reflection-free</u>
 	
Modifying terms
 	
❖ Even   ❖ Hummocky
❖ Wavy   ❖ Lenticular
❖ Regular   ❖ Disrupted
❖ Irregular   ❖ Contorted
❖ Uniform
   variable
	❖ <u>Sheet</u>
	❖ <u>Sheet drape</u>
	❖ <u>Wedge</u>
	❖ <u>Bank</u>
	❖ <u>Lens</u>
	❖ <u>Mound</u>
	❖ <u>Fill</u>

3.6.2.1 Internal reflection configuration

Prograding clinoforms

In a standing body of water, a prograding slope system is comprised of clinoforms or foresetted reflection configurations. The morphology of clinoforms can be influenced by several factors, i.e. sedimentation rate and quantity of sediment input, water depth, energy level of the environment of deposition, etc. Ideally, a clinoform is comprised of a topset, foreset and a bottomset. Topsets are highly dependent on the sea-level conditions where a rising relative sea-level allow the sediments to be stacked and preserved on the shelf. If the relative sea-level drops, accumulated shelf sediments are removed and an erosional truncation is formed (Veeken, 2007).

Three types of foresets were recognized in this study: Oblique, sigmoidal and complex sigmoid / oblique (Figure 3.11). Oblique clinoforms represent a high-energy slope system, suggesting a composition of coarser sediments. Topsets are absent as a result of sediment bypassing and bottomsets are commonly poorly developed. A toplap geometry occur and this can indicate a rapid fall in relative sea-level before deposition of the overlying strata. Sigmoidal clinoforms represent a low-energy slope system, suggesting a relatively rise in sea-level and/or substantially deposition from suspension. Complex sigmoid /oblique is a combination of sigmoid and oblique clinoforms (Veeken, 2007).
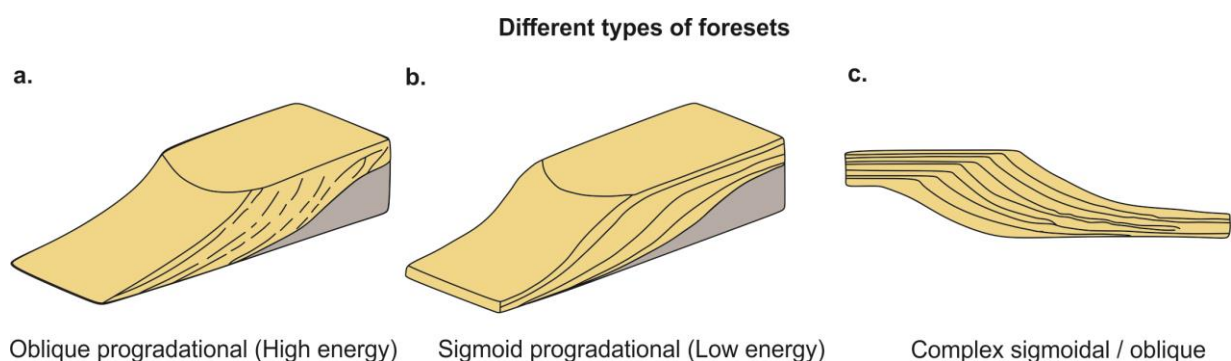

*Figure 3.11: Different types of forests **a.** Oblique progradational (high energy). **b.** sigmoid progradational (low energy). **c.** Complex sigmoidal / oblique. Modified from Veeken (2007).*

3.6.2.2 External geometry

The shape of the external geometry of seismic units in a three dimensional sense, can be described as followed (Mitchum et al., 1977; Veeken, 2007) (Table 3.5):

- A sheeted external geometry can imply a uniform sedimentation in the area often related to hemipelagic deposition.
- A wedge-shaped external geometry indicates a sudden break in sedimentation pattern. This is often caused by lateral variations in sediment distribution.
- Banks have an elongated shape and can imply substantial differences in the sedimentation pattern. This may indicate local variation in energy conditions.
- Mounds are interpreted to be related to submarine fan complexes or contourite deposits and their internal reflection configuration variates.

3.6.3 Seismic signature of contourite drifts

As a standard method today, contourites have been studied with the use of reflection seismic to be able to identify and map these sedimentary deposits. The identification of contourites through seismic data has contributed to reconstruct the geological and palaeo-oceanographic history in an area, although, reflection seismic data should always be supported by additional evidence. 3-D seismic data give the ability to visualize the extent of contourites in three dimensions (Rebesco & Stow, 2001; Nielsen et al., 2008).

The seismic characterization of contourites are often divided into three different orders of seismic elements related to the amount of details revealed. However, the vertical resolution of this dataset and the thickness of the Nyk Drift, limits the study to the first order of seismic elements. The first order of seismic elements compromises information regarding the overall drift geometry (Nielsen et al., 2008).

To be able to study a thick contourite drift in seismic properly, it is necessary to use different types of seismic systems. Ultra-high-resolution seismic favors high resolution of the shallower parts but are not able to image the deeper parts of the drift with a satisfying

resolution. Therefore, it is necessary to use a signal with a lower frequency, for example high-resolution seismic, which provides good penetration and resolution of the deeper parts (Figure 3.12) (Nielsen et al., 2008).
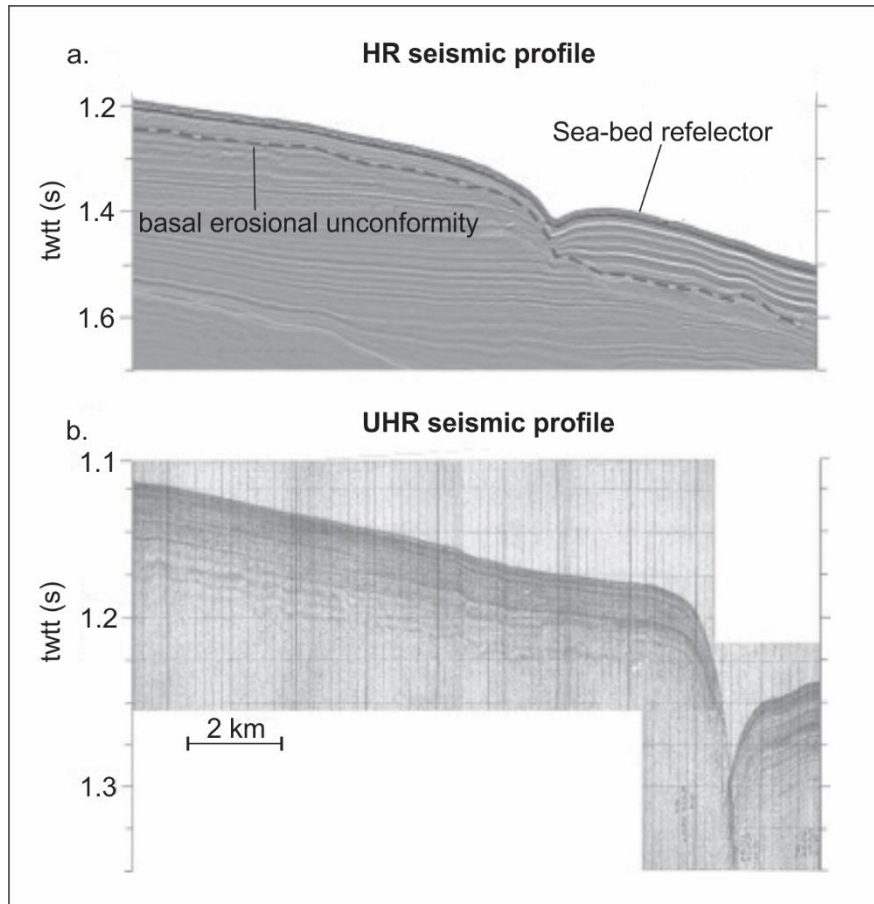

Figure 3.12: Comparison of two different seismic profiles displaying examples of contourite drift systems. These examples illustrate the advantage and disadvantage of using different seismic systems. ***a.*** *A high-resolution (HR) seismic system with the use of a relatively low frequency allows deep penetration but lower resolution.* ***b.*** *Ultra high resolution (UHR) seismic system with the use of a high frequency allows a high resolution of the shallow parts of the drift, but the base is not recognized. Modified from Nielsen et al. (2008).*

3.6.3.1 First-order seismic elements: large scale

A large scale contourite deposit has a seismic identification which is based on the general architecture of the drift depositional system, for instance the external geometry, the upper and lower boundaries delimiting the drift, in addition to the shape of large internal seismic units (Figure 3.13). The external geometry of a contourite deposit is commonly classified based on the overall morphology as either sheeted or mounded. By looking at the different geological and oceanographic settings, the sheeted and mounded drifts can be subdivided further into five main type drift systems: (1) Sheeted drifts, (2) Giant elongated drifts, (3) Channel-related drifts, (4) Confined drifts and (5) Mixed drift systems. Some difficulties regarding distinguishing contourites from other deep-sea deposits may occur, but the key characteristics are that contourites create elongated along-slope geometries deposited in the direction of the geostrophic bottom current. On the other hand, turbidity-fan systems are gravity-driven mass transport which can be seen as elongated down-slope geometries. In some cases these two end-member processes form complex sediment pattern on the continental slope as a result of interaction with each other (Nielsen et al., 2008).

The bounding reflectors of a contourite drift are normally recorded by the unconformities caused by a change in the depositional style. The depositional style often changes between a non-current-dominated to a current-dominated regime depending on the upper and lower boundary. These upper and lower reflectors can be seen as regional unconformities. The basal unconformity is normally characterized by a semi-regional to regional boundary with a high amplitude reflector which often extent beyond the limits of the drift system. Internal reflectors can often be observed as low-angle reflectors downlaping onto the basal unconformity. The upper boundary reflector of a contourite can be seen as either a continuous high amplitude reflector if the deposit is buried or as the seafloor if the drift is still active (Nielsen et al., 2008).

The configuration of a large internal seismic unit of a contourite is characterized by a continuous pattern with low-to medium-amplitude reflectors normally with a gross drift morphology direction. To be able to form large contourite drifts, it is required long-lasting, stable conditions, and this is something that can be reflected by the internal seismic pattern. Large temporary changes in the intensity of the ocean current may determine whether the drift is erosional or depositional (Nielsen et al., 2008).
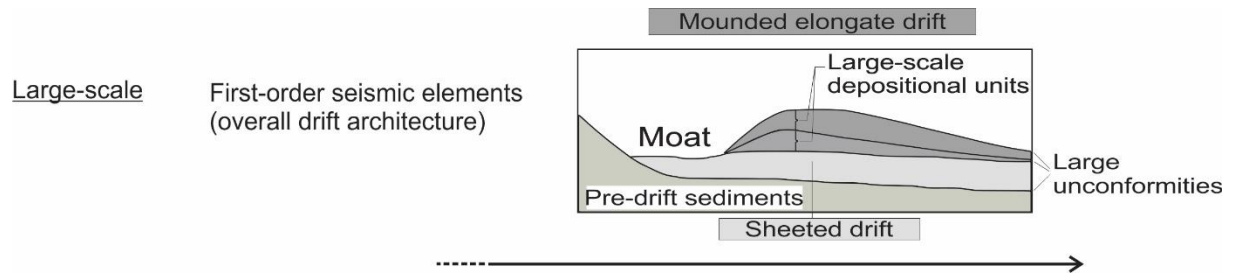
Figure 3.13: Seismic characteristics of contourites illustrated by large-scale geometry. Modified from (Nielsen et al., 2008)

4 Results

The seismic stratigraphic framework for the Cenozoic sediments on the Vøring margin is here described in chronological order. The framework comprises seismic boundaries and adjacent seismic units mainly represented by horizons and thickness maps. In addition, geomorphological features on different surfaces are described and interpreted.

Seismic units, seismic unit boundaries and geomorphological features are described and interpreted from east to west, i.e. generally starting on the shelf and continuing onto the slope. Color codes of unit boundaries and associated units are summarized in figure 4.1.

The seismic stratigraphic framework in this study has been correlated with the established stratigraphic framework in the area from (Ottesen et al., 2009) (Figure 4.2 and 4.3). From oldest to youngest, they divided the Naust Formation into five sequences named N, A, U, S and T by utilizing both 2D and 3D seismic data. Their nomenclature was revised from Bugge et al. (2004) and Rise et al. (2006). Naust U base correspond to seismic horizon 3 and Naust S+T base correspond to seismic horizon 6. However, in this study, unit A is interpreted to represents Naust A, unit B and C represent Naust U, and - unit D represents Naust S and T. A further correlation to previous work will be done in the discussion part.

Five main horizons defining four main units, in addition two internal horizons have been mapped within the 3D-cube (Figure 4.4-4.9). Six seismic facies were identified based on the configuration, amplitude, continuity, frequency and interval velocity of the reflections (Mitchum et al., 1977) (Figure 4.10).
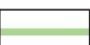
Figure 4.1: Symbols assigned for units and color codes assigned for the associated unit boundaries interpreted in the seismic 3D-cube, in addition to correlations with the established framework of Ottesen et al. (2009).
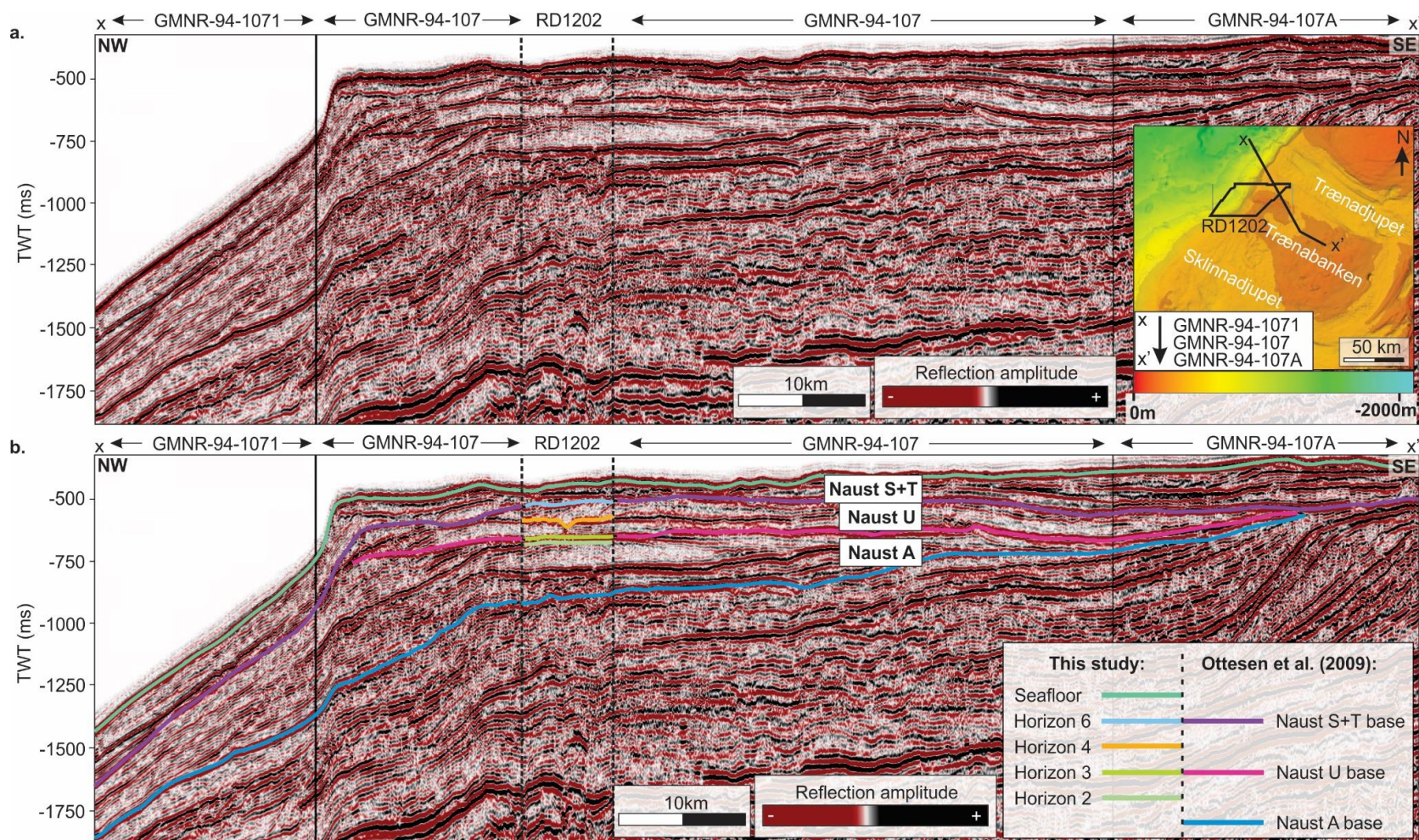
Figure 4.2: 3D-sismic data of this study (RD1202) correlated to 2D seismic data interpreted and used by Ottesen et al. (2009). **a.** Regional seismic profile along the shelf and slope crossing the study area in NE. The location of the profile is indicated in the inset map in the right corner. It is composed of three 2D-lines listed in the lower part of the inset map. **b.** The same profile as in a. with interpretations from this study compared to interpretation from Ottesen et al. (2009).
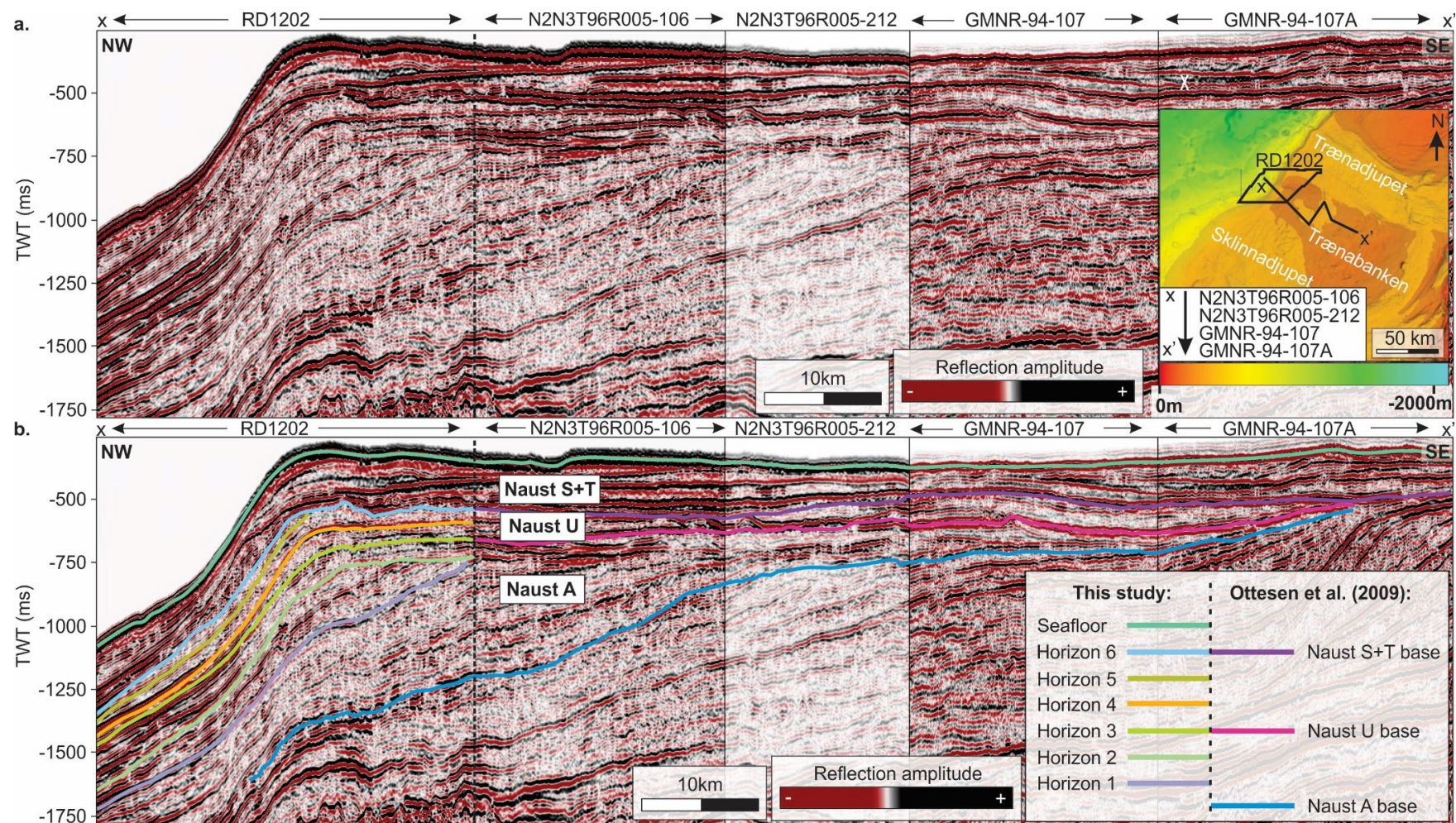
Figure 4.3: 3D-sismic data of this study (RD1202) correlated to 2D seismic data interpreted and used by Ottesen et al. (2009). *a.* Regional seismic profile along the shelf and slope crossing the study area in NE. The location of the profile is indicated in the inset map in the right corner. It is composed of four 2D-lines listed in the lower part of the inset map. *b.* The same profile as in a. with interpretations from this study compared to interpretation from Ottesen et al. (2009).
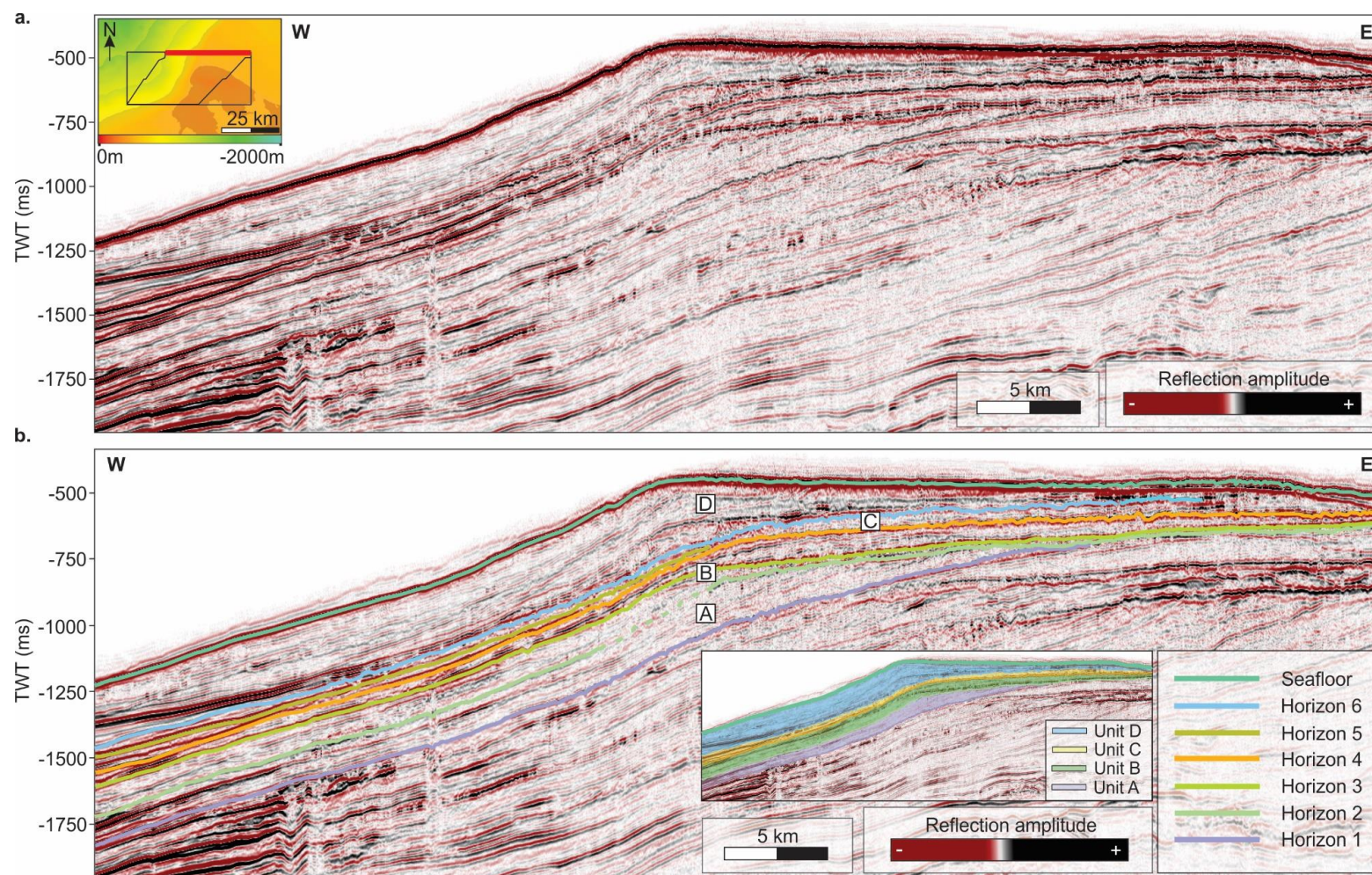
Figure 4.4: **a**. Regional seismic profile along the shelf and slope in the northernmost part of the study area. The location of the profile is marked as a red line on the inset map in the left corner. **b**. Seismic profile where the interpreted seismic units and unit boundaries are indicated.
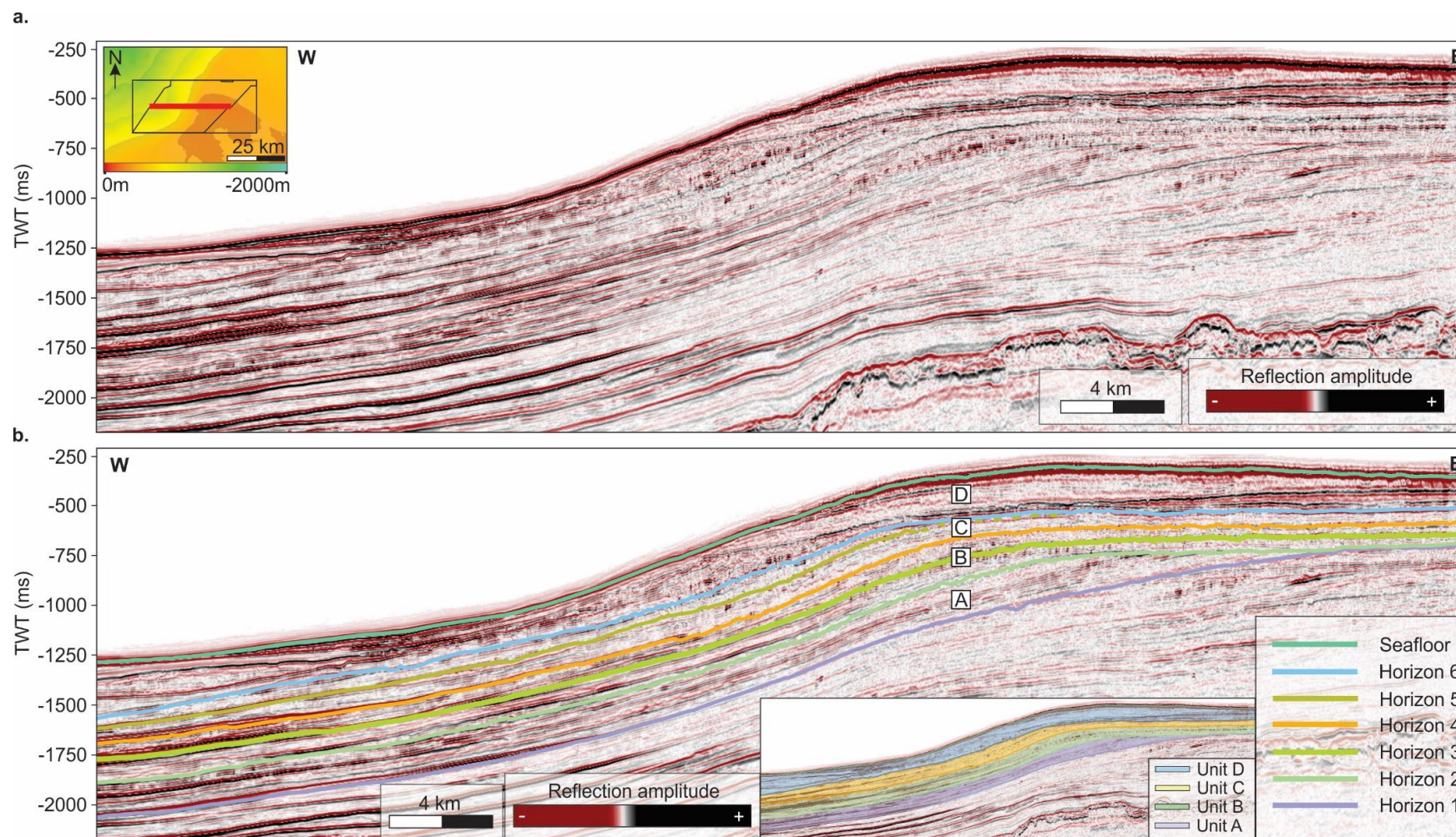
Figure 4.5: *a*. Regional seismic profile along the shelf and slope in center of the study area. The location of the profile is marked as a red line on the inset map in the left corner.
b. Seismic profile where the interpreted seismic units and unit boundaries are indicated.
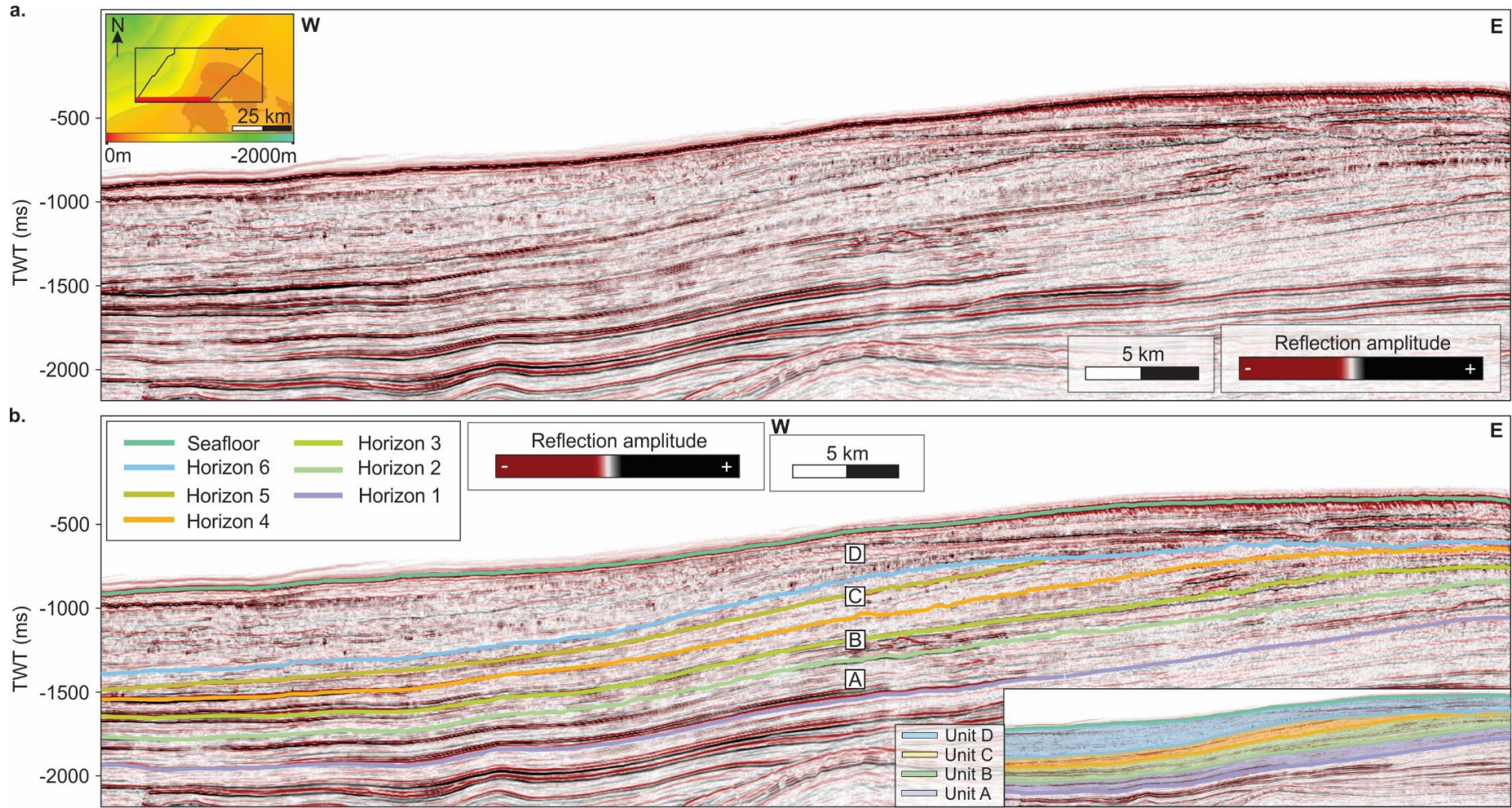
Figure 4.6: *a*. Regional seismic profile along the shelf and slope in the southern part of the study area. The location of the profile is marked as a red line on the inset map in the left corner. *b*. Seismic profile where the interpreted seismic units and unit boundaries are indicated.
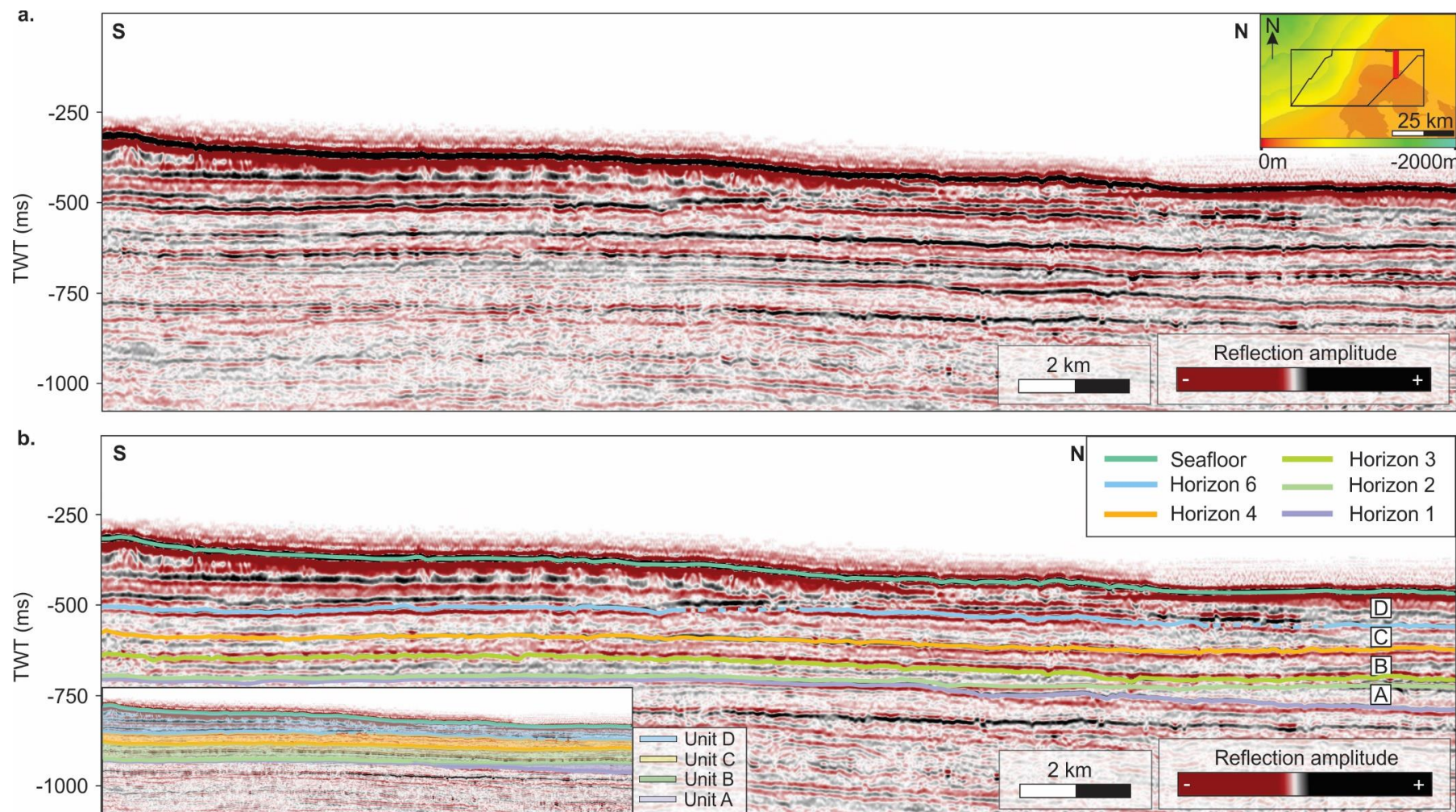
*Figure 4.7: **a**. Regional seismic profile across the shelf in the eastern part of the study area. The location of the profile is marked as a red line on the inset map in the right corner. **b**. Seismic profile where the interpreted seismic units and unit boundaries are indicated.*
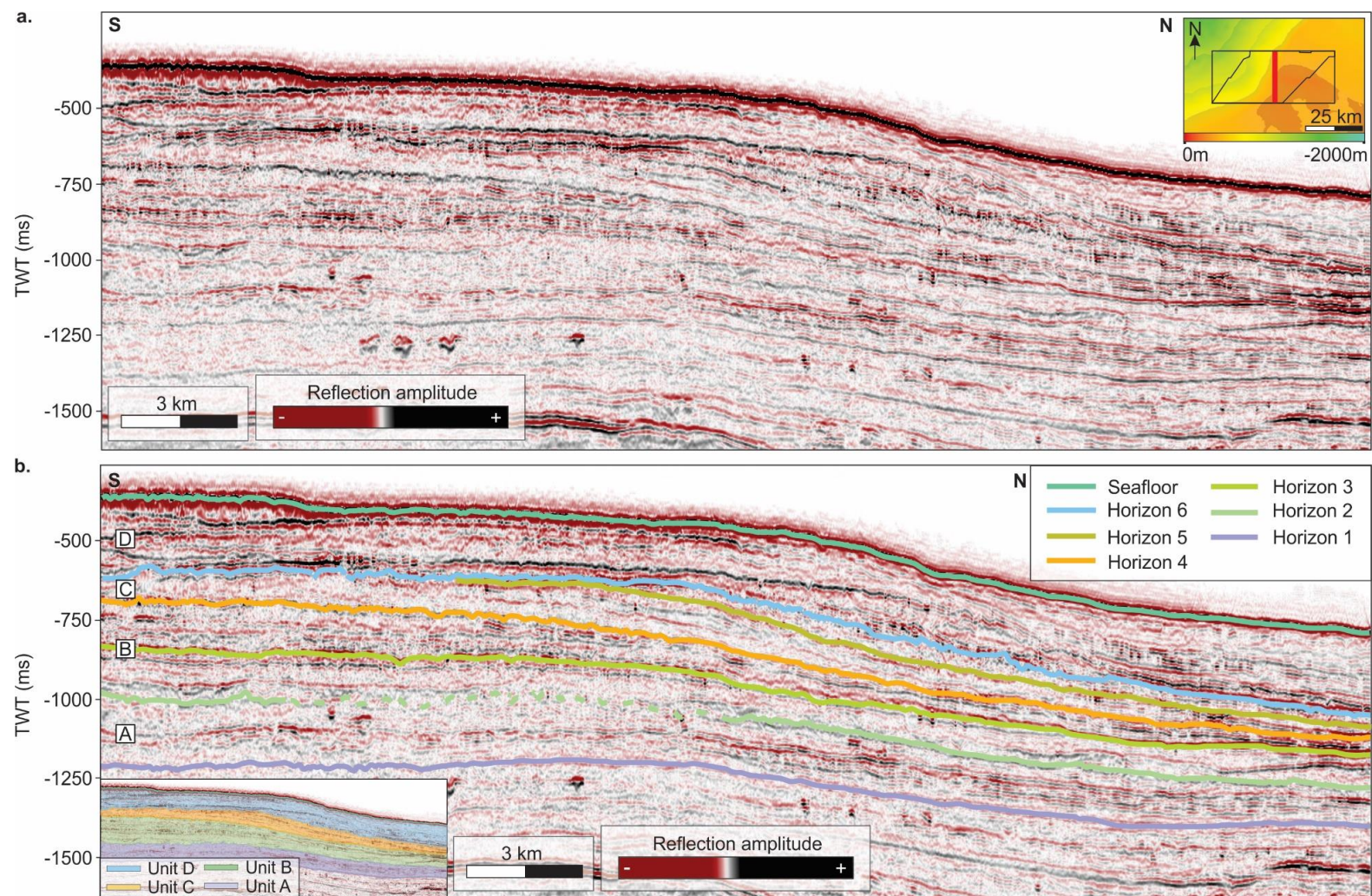
Figure 4.8: **a**. *Regional seismic profile across the slope in the center of the study area. The location of the profile is marked as a red line on the inset map in the right corner.* **b**. *Seismic profile where the interpreted seismic units and unit boundaries are indicated.*
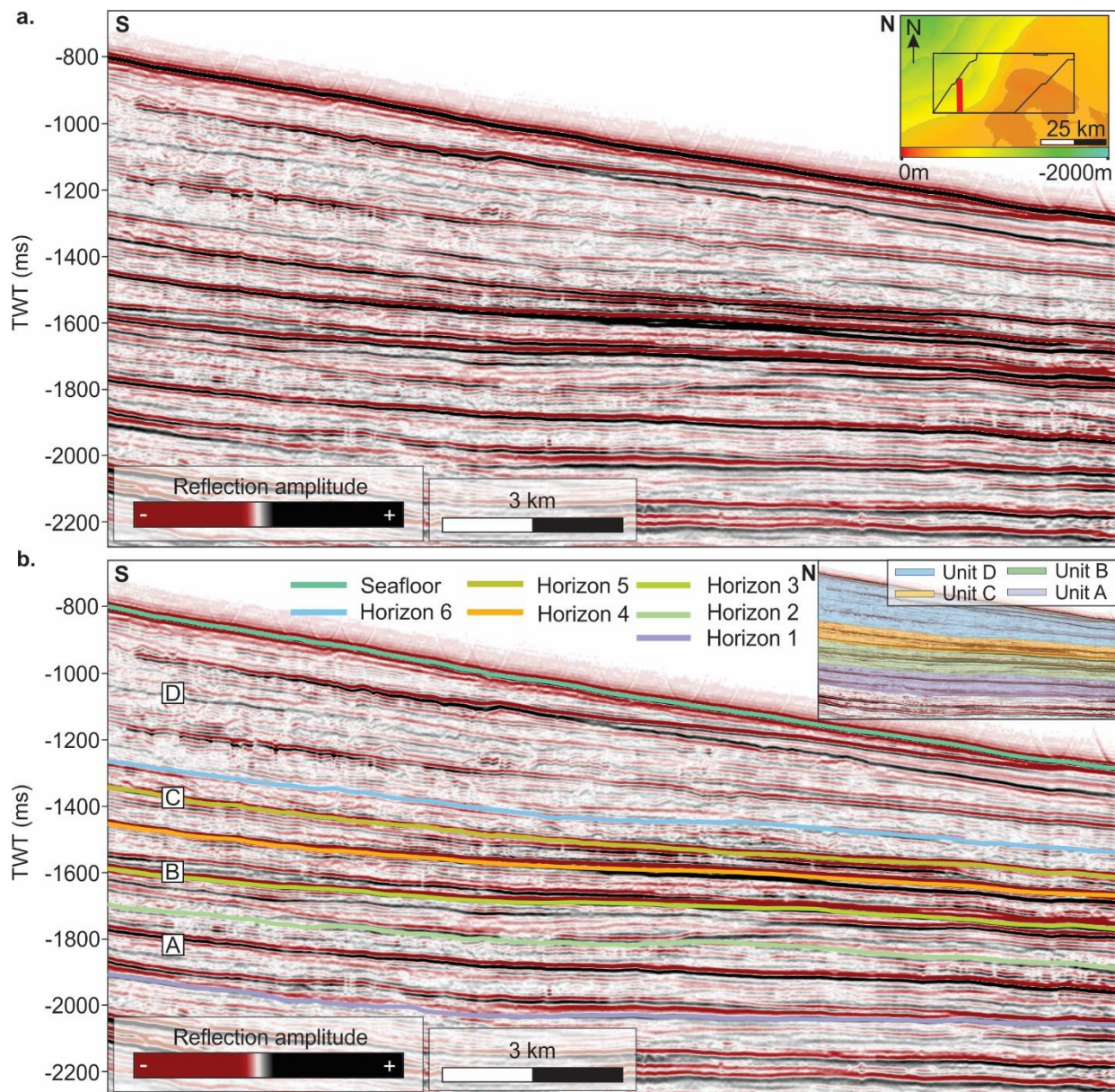
Figure 4.9: *a*. Regional seismic profile across the lower part of the slope in the western part of the study area. The location of the profile is marked as a red line on the inset map in the right corner. *b*. Seismic profile where the interpreted seismic units and unit boundaries are indicated.
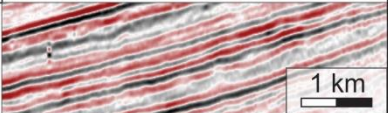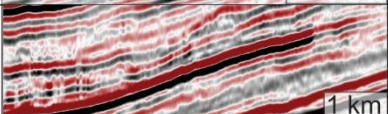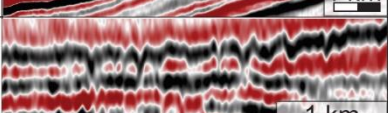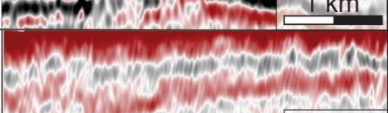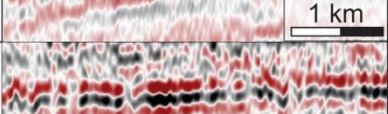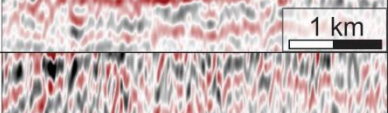
	Example	Discription	Interpretation	Shelf	Slope
Facies 1	1 km	Continuous, parallel clinoforms Medium frequency Low-medium amplitude	Hemipelagic-deposits	●	●
Facies 2	1 km	Semi-continuous, sub-parallel clinoforms Low frequency Low-to high-amplitude	Slide debrites		●
Facies 3	1 km	Acoustically semi-transparent seperated by high amplitude reflectors	Basal till	●	
Facies 4	1 km	Acoustically transparent seperated by reflectors with a weak amplitude	Basal till	●	●
Facies 5	1 km	Semi-continuous to discontinuous Parallel, Planar Medium frequency Low-to high-amplitude	Hemipelagic/ basal till deposits	●	●
Facies 6	1 km	Discontinuous to chaotic Low-to high-amplitude	Slide debrites	●	●

Figure 4.10: Seismic facies identified on the continental shelf and slope of the Vøring margin including geological interpretation and geographic distribution. These facies are based on Mitchum et al. (1977).

4.1 Seismic horizon 1

Horizon 1 is an oblique clinoform comprising a palaeo-shelf and palaeo-slope. It is the lowermost surface in this study and extends from the shelf in the east to the lower part of the slope in the west.

Horizon 1 has a medium strong, positive reflection amplitude on the shelf, a weaker amplitude on the upper part of the slope, and a strong amplitude on the lower part of the slope (Figure 4.4-4.6). The reflection amplitude is generally strongest in the north (Figure 4.5 – 4.7). Horizon 1 is continuous, and it separates the more chaotic, low-amplitude reflections underneath from the mainly parallel reflections above. Thus, it clearly separates two different seismic facies, and was therefore chosen as the lower boundary in this study. This is less evident in the southern part of the study area.

The horizon represents a positive reflection coefficient. On the upper part of the slope in the southern part of the study area (Figure 4.4), the reflector is discontinuous with a low reflection amplitude and the interpretation is therefore tentative here.

Horizon 1 is relatively flat on the shelf, and dips gently westwards on the slope. The apparent dip angle of the slope ranges from 2.5-4.5º and is generally higher in north (Figure 4.11). A very gentle north-dipping trend also occurs (Figure 4.6- 4.7). Several smaller geomorphological landforms occur on horizon 1. These are detailed below (Figure 4.12).
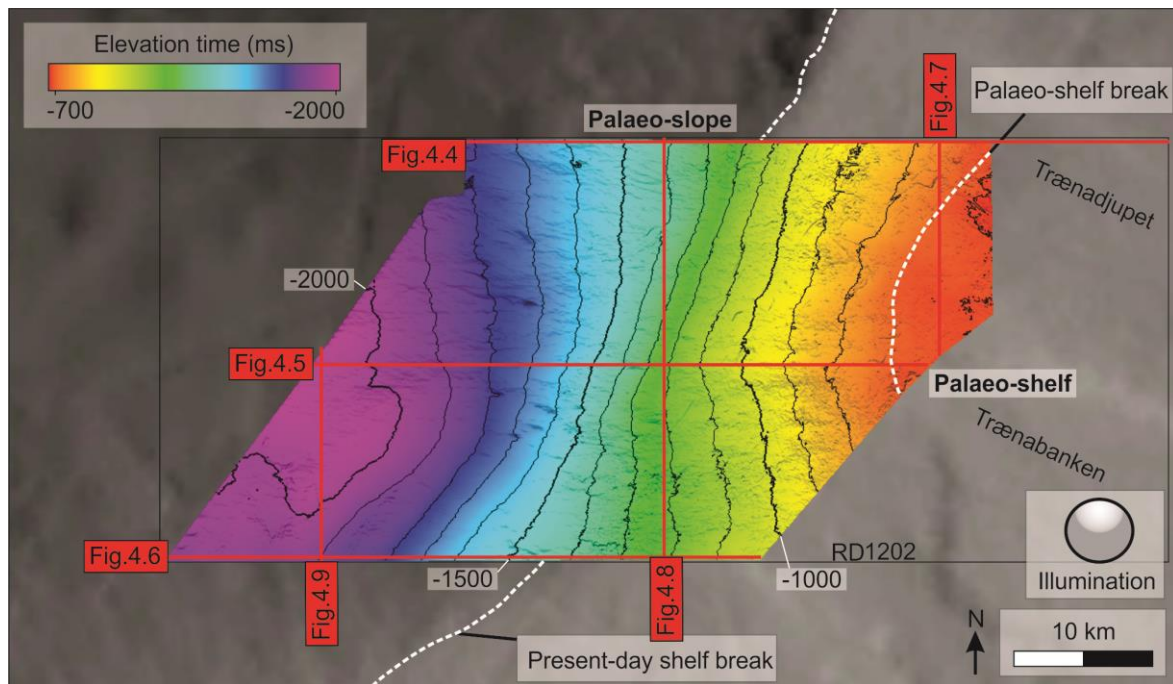
Figure 4.11: Horizon 1 situated on the continental shelf and slope within RD1202. Depths are in ms two-way travel time and the contour lines are indicated every 100 ms (bold every 500 ms). Vertical exaggeration is 10.
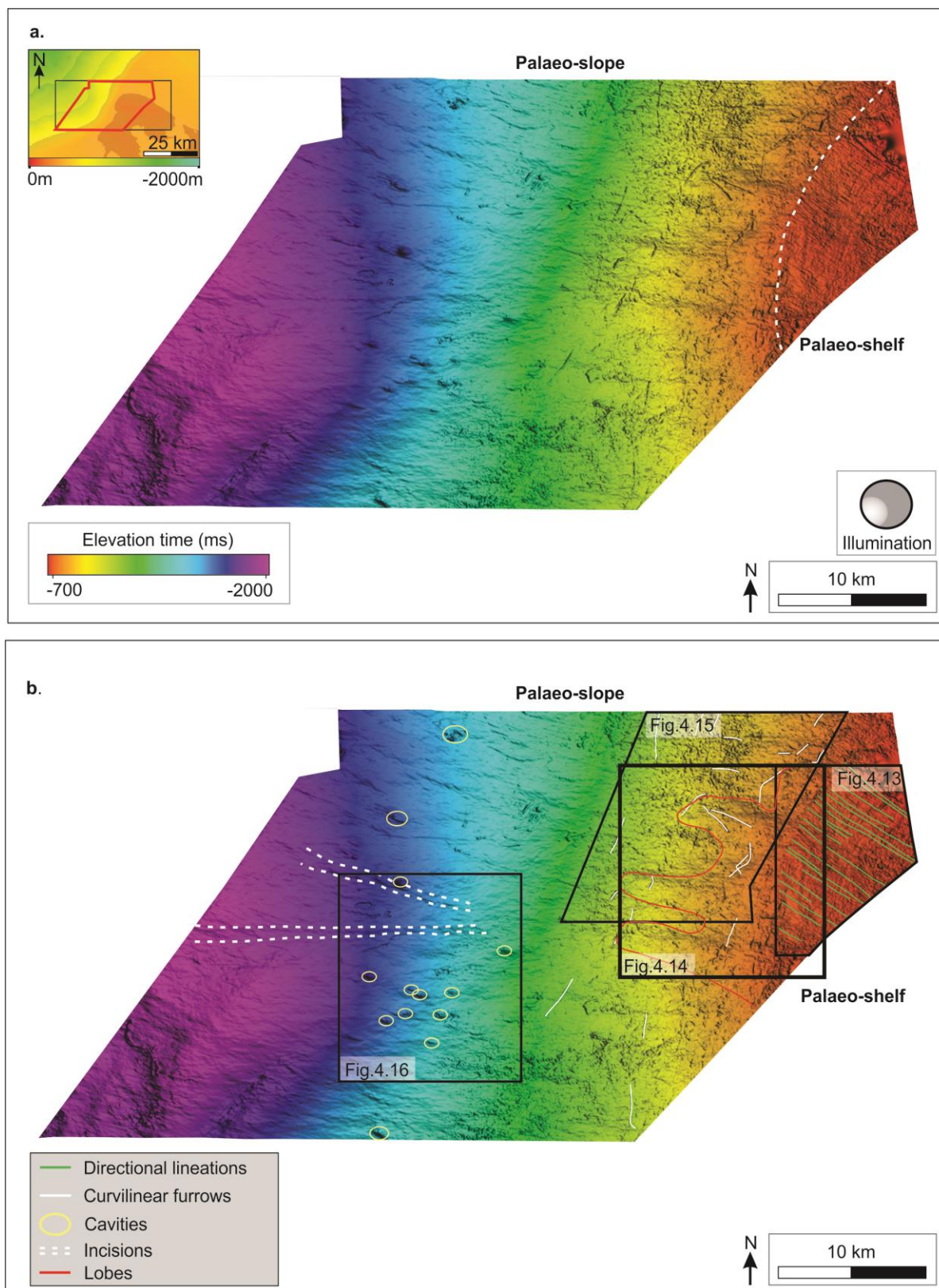
Figure 4.12: **a.** Overview of the morphology of horizon 1 divided into palaeo-shelf and palaeo-slope (indicated by dotted white line). The location of the horizon is indicated by a red polygon on the inset map in the left corner. **b.** Horizon 1 with interpreted morphology. Figure 4.13-4.16 are indicated by black polygons. Vertical exaggeration is 25.

Directional lineations

A set of NW-SE trending linear ridges and furrows occur on the horizontal part of horizon 1, i.e. on the palaeo-shelf. The lineations extend from the eastern part of the shelf to the palaeo shelf break, where they terminate abruptly (Figure 4.13). These are up to 8.5 km long, 120-200 m wide and with a relief up to 9 m. The widest one, which occurs on the northern part of the shelf, has a width of 300 m. The lineations are densely spaced, and it is therefore hard to distinguish whether they are negative or positive landforms.

Interpretation:

The lineations are located on a palaeo-shelf, they have a high length-to-width ratio, and their orientation is consistent and parallel to the modern Trænadjupet Trough. They are therefore interpreted to have formed subglacially from fast-flowing ice that was moving from SE to NW. Similar subglacial bedforms from other troughs and palaeo-troughs are often referred to as mega-scale glacial lineations (MSGL) (Clark, 1993). The abrupt ending of these lineations indicate that the grounded and fast-flowing glacier extended all the way to the palaeo-shelf break. Dowdeswell et al. (2004) described similar features on Antarctica and Rydningen et al. (2013) in cross-shelf troughs outside Troms County, Northern Norway.

Slide-lobes

Several lobe-shaped features with a W to WNW orientation occur below the shelf break. They are widely spaced with lengths between 7-14 km and widths up to 3 km. The lobes have a medium reflection amplitude with an acoustically transparent internal signature. They have a positive relief up to 17 m (Figure 4.14).

Interpretation:

Situated below the shelf break with evidence of a fast-flowing ice-stream on the shelf, these lobes can be seen in context with deposition of glacigenic sediments from a grounded ice-sheet on the shelf. The internal seismic signature of the lobes lead to the interpretation that sediments were deposited from debris flows. The sediments were either deposited directly on the upper part of the slope or in the shelf break area before they were transported downslope.
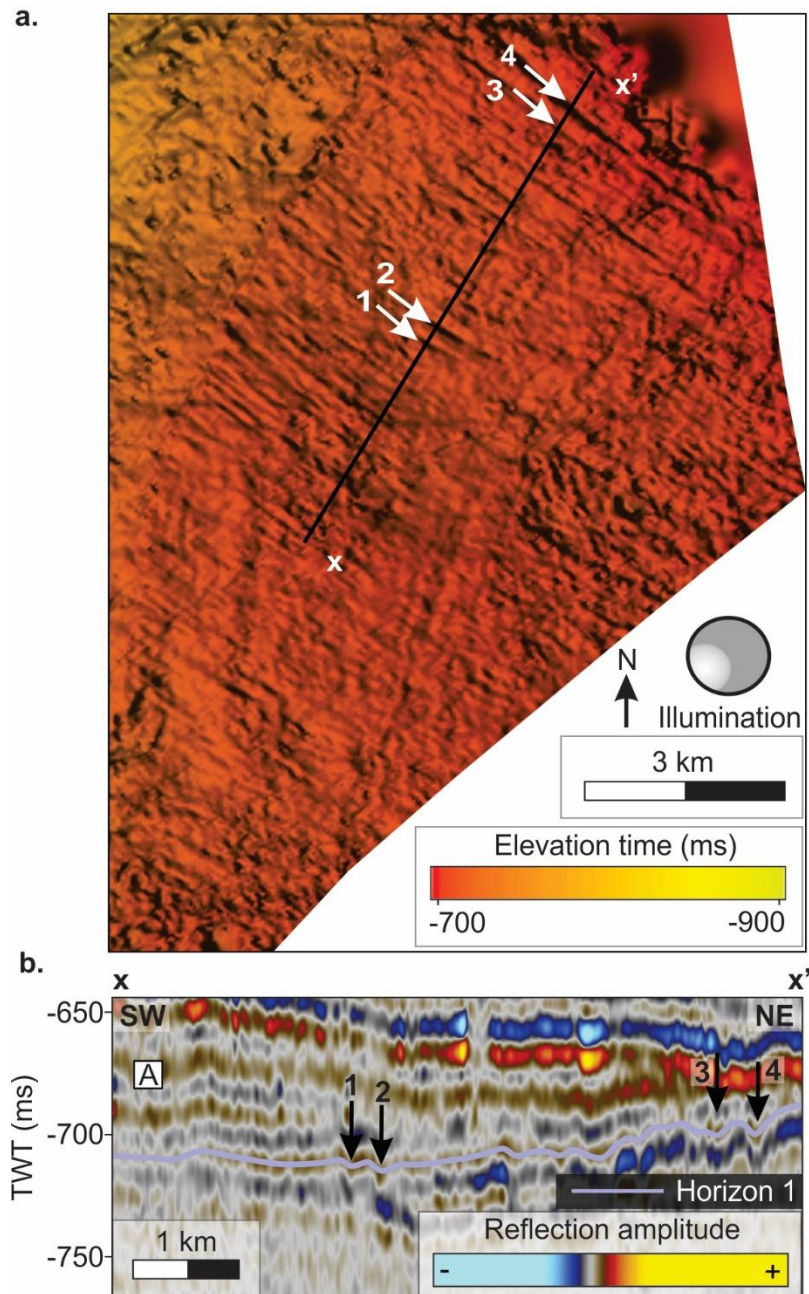
Figure 4.13: *a.* The palaeo-shelf of the NE part of horizon 1 featuring directional lineations. The black line indicates the location of the seismic profile in b (x-x'). Vertical exaggeration is 25. *b*. Seismic profile across the directional lineations. Some of the most distinct lineations are indicated by arrow 1-4. The location of the figure is indicated in figure 4.12.
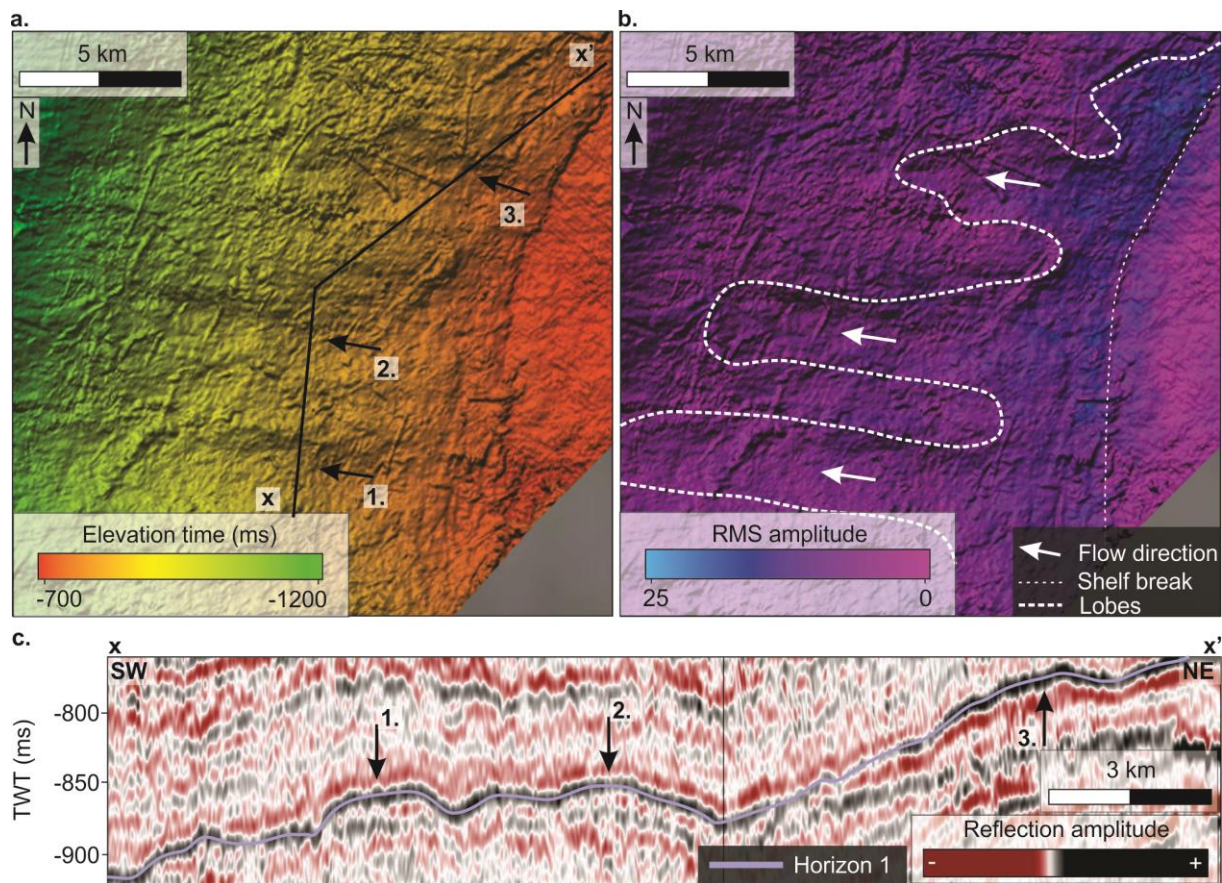
Figure 4.14: ***a.*** *The upper part of the slope of horizon 1 featuring lobe-shaped features. The black line indicates locations of the profile in c (x-x'). Arrows with numbers indicate some of the lobes.* ***b.*** *RMS map of the same area as in a. with interpretation. Vertical exaggeration is 25. The location of the figure is indicated in figure 4.12.* ***c.*** *Seismic profile with interpretation across lobe-shaped features with arrows corresponding to arrows in a.*

Curvilinear furrows

On the upper part of the slope, furrows with varying dimension, orientation and extent occur (Figure 4.15). They are present from the palaeo-shelf and down to 1450 ms depth on the palaeo-slope. Near the shelf break, the furrows have a crisscrossing orientation pattern. Generally, the orientation becomes sub-parallel to the shelf break on the deeper parts of the slope further west. In cross-profile, they are V-shaped with a negative relief ranging between 5 and 11 m. The shallow lying furrows are up to 3 km long, with widths up to 250 m. The deeper lying furrows are up to 7 km long and tens of meters wide. Some of the furrows have associated ridges along their flanks.

Interpretation:

Based on the geomorphology, the limited depth interval and their sub-parallel orientation to the slope, these furrows are interpreted to have formed from iceberg ploughing on the upper parts of the slope. This have formed ridges on the elongated flanks of the plough marks which are interpreted to be levees. The NE-SW orientation trend on the deeper parts is likely resulting from the oceanographic circulation pattern at that time. Similar features were described by Rydningen et al. (2013) on the continental shelf and in the cross-shelf troughs further north of the study area, and by Montelli et al. (2018) on the mid-Norwegian continental slope.
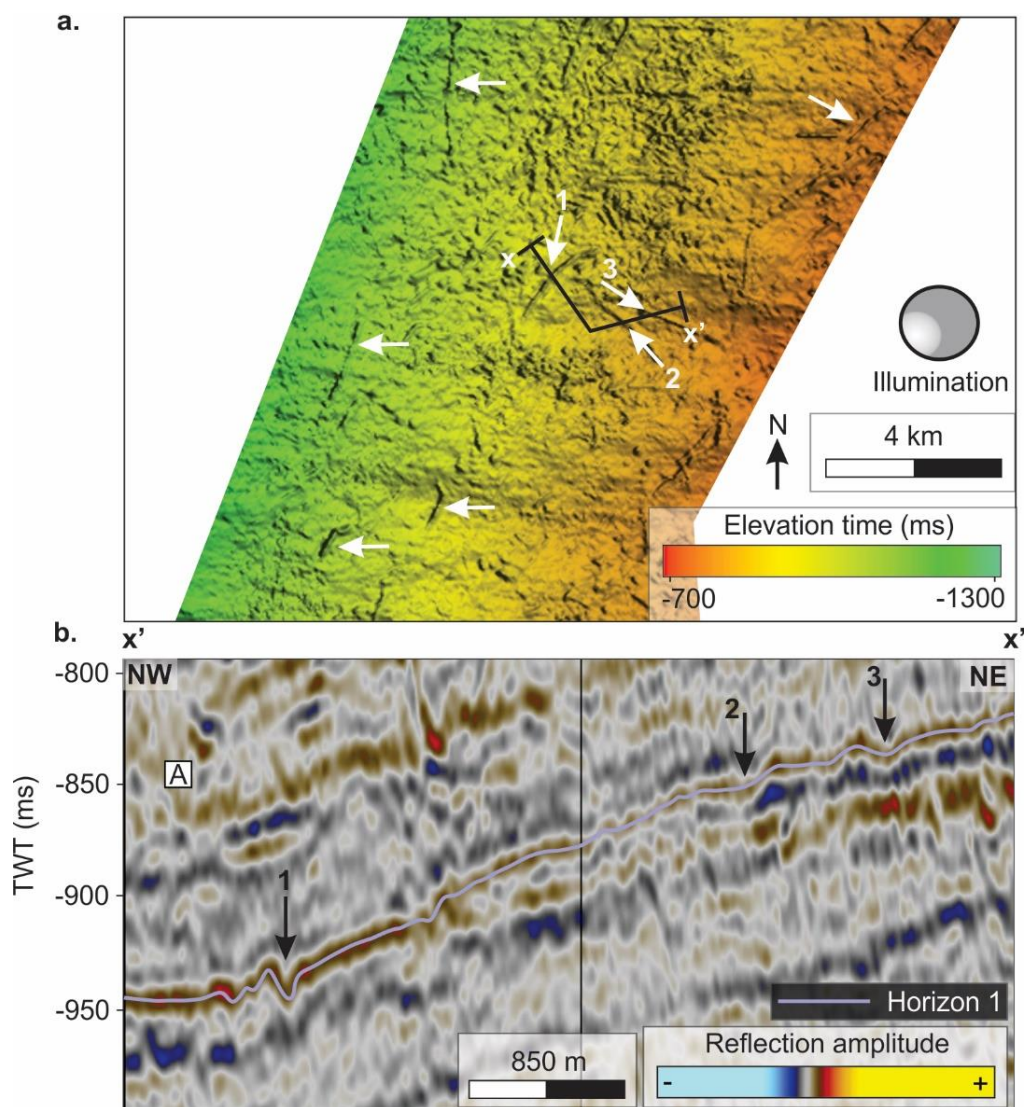
Figure 4.15: **a.** The upper part of the palaeo-slope of horizon 1 featuring curvilinear furrows. Arrows indicate the most distinct furrows and the black line indicates the location of the seismic profile in b (x-x'). Vertical exaggeration is 25. **b.** Seismic profile across three curvilinear furrows, indicated by numbers. The location of the figure is indicated in figure 4.12.

Depressions

A number of depressions with diameters up to 850 m occur on the lower part of the slope (Figure 4.16). They can be described as circular to elliptical in shape, widest in the middle, becoming narrower as they shallow. Their appearance is either as single depressions or in clusters. In cross-profile, they are concave with a negative relief ranging between 10 and 50 m. Above and below the depressions, the section is characterized by a vertical degraded seismic signal (acoustic masking) (Figure 4.17) where the internal reflectors are depressed in the same manner as on horizon 1. The strongest amplitudes occur on the uppermost part of this section (Figure 4.16b).

Interpretation:

Due to their seismic expression and presence of strong amplitudes in the upper part of the seismic section, these depressions are interpreted to be a result of a velocity "pushdown" effect. The velocity pushdown effect may be caused by shallow gas expressed as strong amplitude reflections in the upper part of the section. Shallow gas accumulations may originate from in situ decomposition of organic material, biogenic gas, or rapid migration of hydrocarbon fluids from deeper sediments, thermogenic gas. Similar features have been described by Løseth et al. (2009) below a hydrocarbon filled trap and by Andreassen et al. (2007) in the SW Barents Sea. The origin of the shallow gas is discussed shortly in chapter 5.
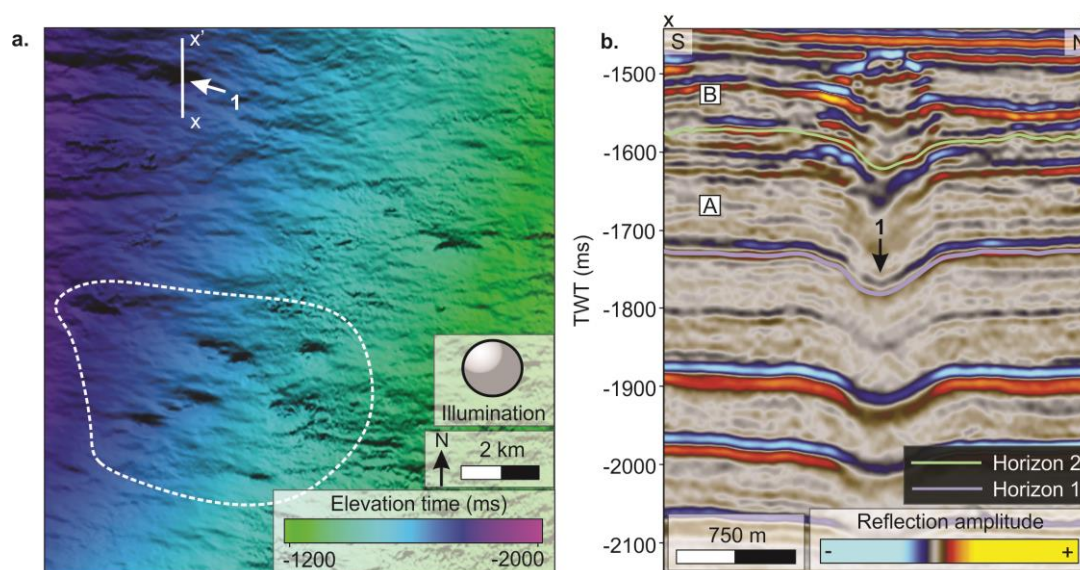
*Figure 4.16: **a**. Southwestern part of horizon 1 featuring depressions. The dotted white circle indicates a cluster of depressions and the white line indicates the location of the seismic profile in b (x-x'). Vertical exaggeration is 25. **b**. Seismic profile across one of the largest cavities, indicated by arrow 1. The location of the figure is indicated in figure 4.12.*
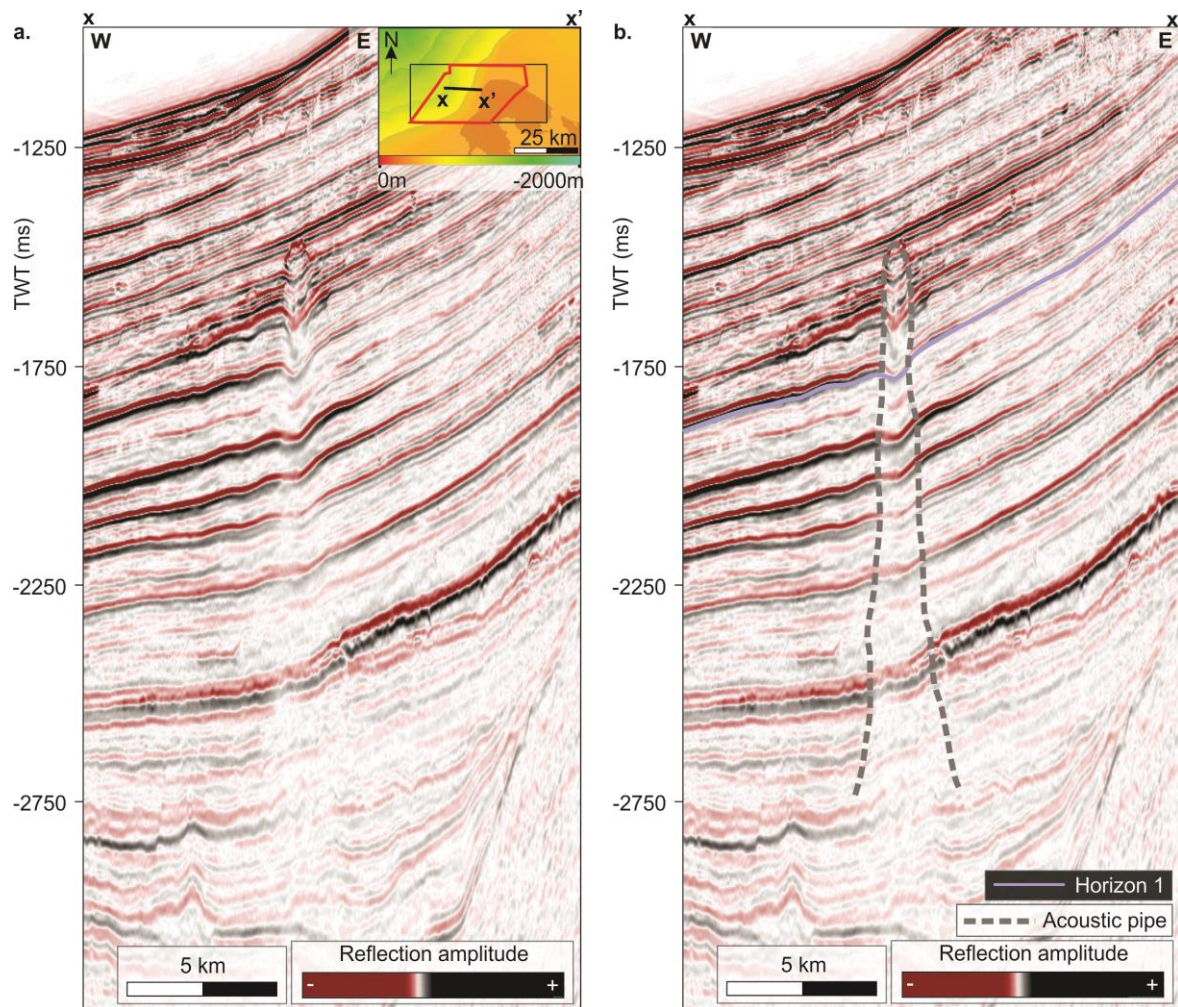
Figure 4.17: **a.** Overview of the vertical degraded seismic signal shown in figure 4.16. The location of the profile is indicated in the inset map in the right corner. **b.** Same profile as in a. with interpretation.

4.2 Seismic unit A

Seismic unit A is the stratigraphic interval bounded by the underlying horizon 1 and the overlying horizon 2. Unit A is comprised of oblique clinoforms prograding from east to west and the unit has an overall wedge-shaped external form (Figure 4.4-4.9 & Figure 4.18).

On the shelf, the topset of unit A is truncated by seismic horizon 2, i.e. the unit is pinching out eastwards (Figure 4.19). Unit A consists of continuous, parallel, medium frequency reflections with a low to medium amplitude on the shelf (Facies 1; Figure 4.10). Some high amplitudes and chaotic reflections (Facies 6; Figure 4.10) occur on the upper part of the slope (Figure 4.20).

The internal seismic signature of the lower part of the slope is semi-continuous, sub-parallel, low frequency reflections with a low to high amplitude (Facies 2; Figure 4.10). An internal high amplitude reflector can be followed along the lower part of the slope from north to south (Figure 4.9).

A 200-250 ms thick accumulation of sediments with an N-S orientation is preserved along the upper part of the slope. The greatest sediment thickness (225-275 ms) occurs in the southern part of the study area, and the unit gradually thins toward northeast (Figure 4.18).
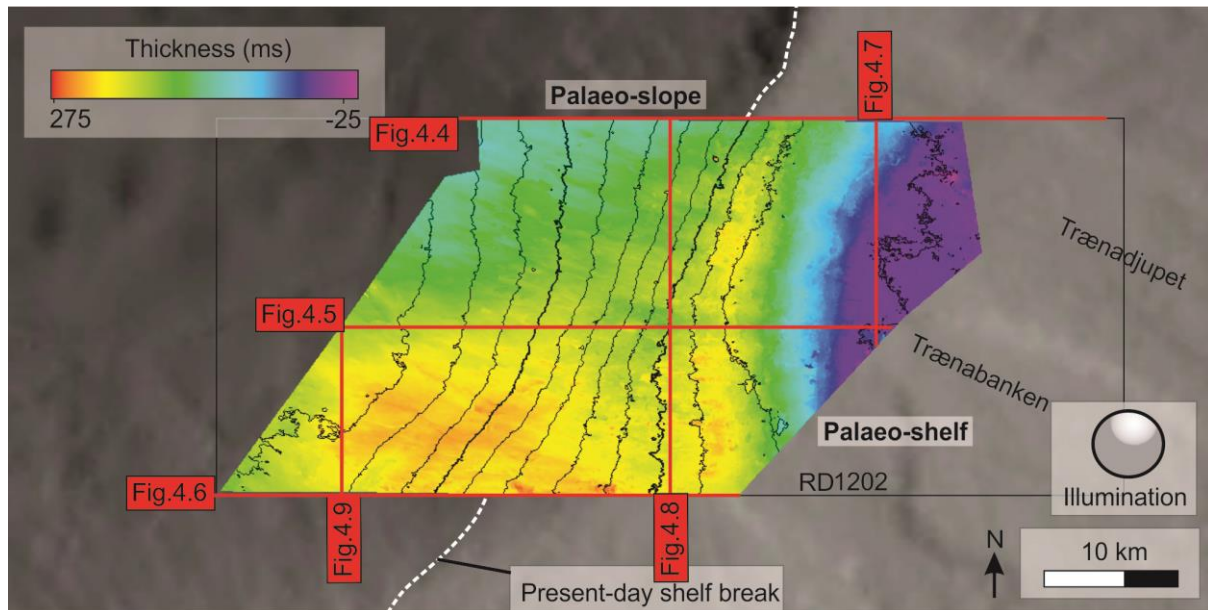
Figure 4.18: Thickness map of seismic unit A situated on the continental shelf and slope within RD1202. The map was defined between horizon 1 and horizon 2. Contour intervals are 100 ms (bold every 500 ms).
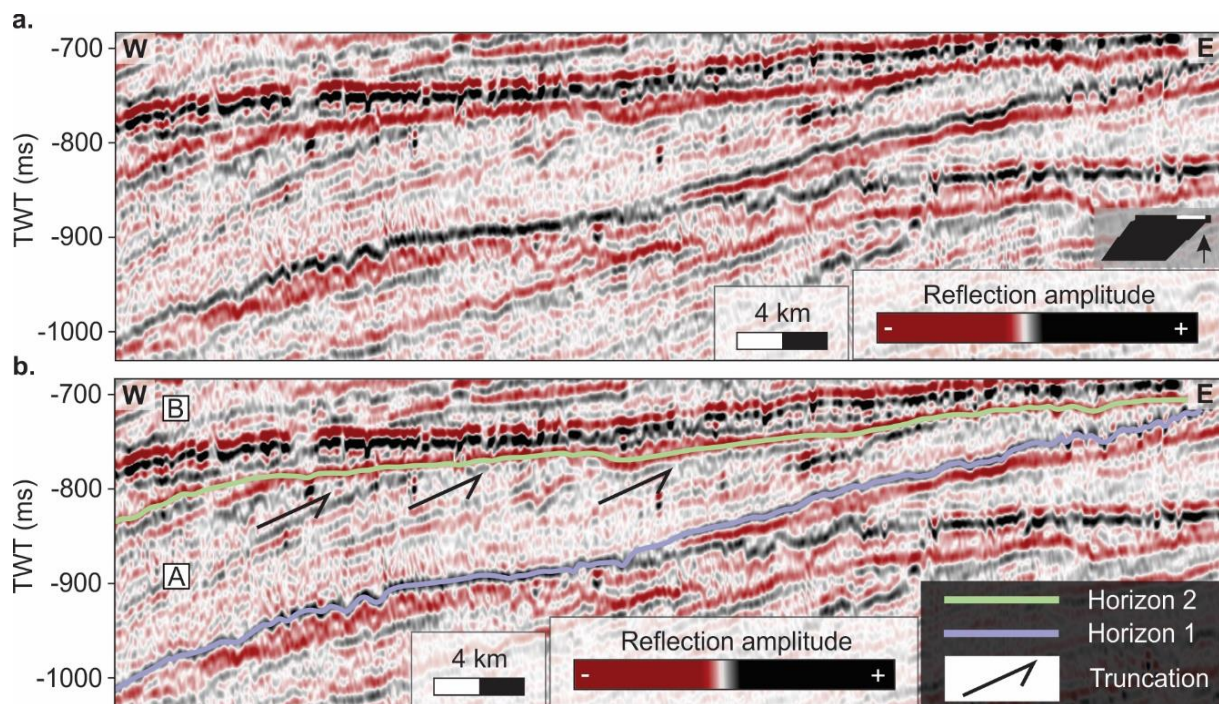
Figure 4.19: **a.** Seismic profile from the eastern most part of the seismic unit A with a pinching out trend. The location of the profile is marked as a white line on the inset map in the right corner. **b.** Seismic profile where the interpreted seismic units and unit boundaries are indicated.

75
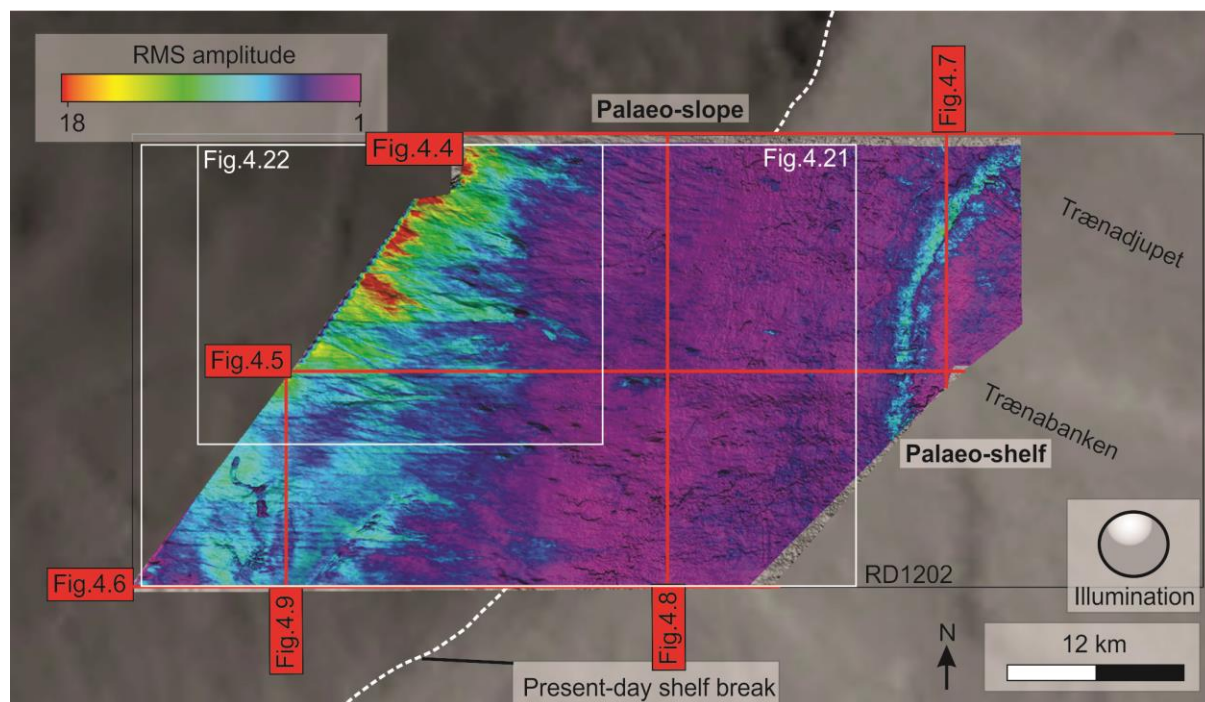
Figure 4.20: RMS seismic amplitude map of unit A situated on the continental shelf and slope within RD1202. The map was defined between horizon 1 and horizon 2. Figure 4.21 and 4.22 are indicated by white polygons. Vertical exaggeration is 25.

Bifurcating channel systems

Several systems comprised of bifurcating; sinuous-shaped channels extend from the shelf break to the lower part of the slope (Figure 4.21). They occur in the southern part of the study area where three of them are overlapping. These systems are defined by high amplitudes and are generally best developed on the lower part of the slope. (Figure 4.21b).

System 1 can be followed up to 21 km from the middle (1200 ms) to the lower part of the slope. It is NW-SE orientated, and up to 4 km wide. The strongest amplitude anomalies of system 1 occur on the upper most part with an abrupt border to lower amplitude anomalies of system 2 in the southeast.

System 2 is oriented E-W, 4.5-5.5 km wide, and can be followed 37 km from the shelf break to the lower part of the slope. The largest amplitude anomalies of system 2 occur below the shelf break and in the lower part of the slope where they meet another system with crossing amplitude anomalies. However, amplitude anomalies of system 2 are generally weaker than in system 1.

The third system are present in the southwestern part of the study area with a NW-SE orientation. System 3 has a 13 km length and up to 7 km width. It has a slightly higher amplitude anomaly than system 2 and similar orientation as system 1.

In center of the lower part of the slope (1400 ms), system 4 can be followed up to 16 km with a NW-SE orientation. System 4 has the strongest reflection amplitude (Figure 4.21c).

Wedge-shaped amplitude anomalies

On the lower part of the slope, overlapping wedge-shaped amplitude anomalies with an E-W orientation occur within a greater time interval (Figure 4.22). Along slope, they are best developed in the north. They are initiated at 1500 ms depth, ranging between 8-16 km length downslope and their maximum detected width are 6 km. These features are well defined by a strong amplitude anomaly. The strongest amplitudes occur in the north on the lower part of the wedge-shaped features
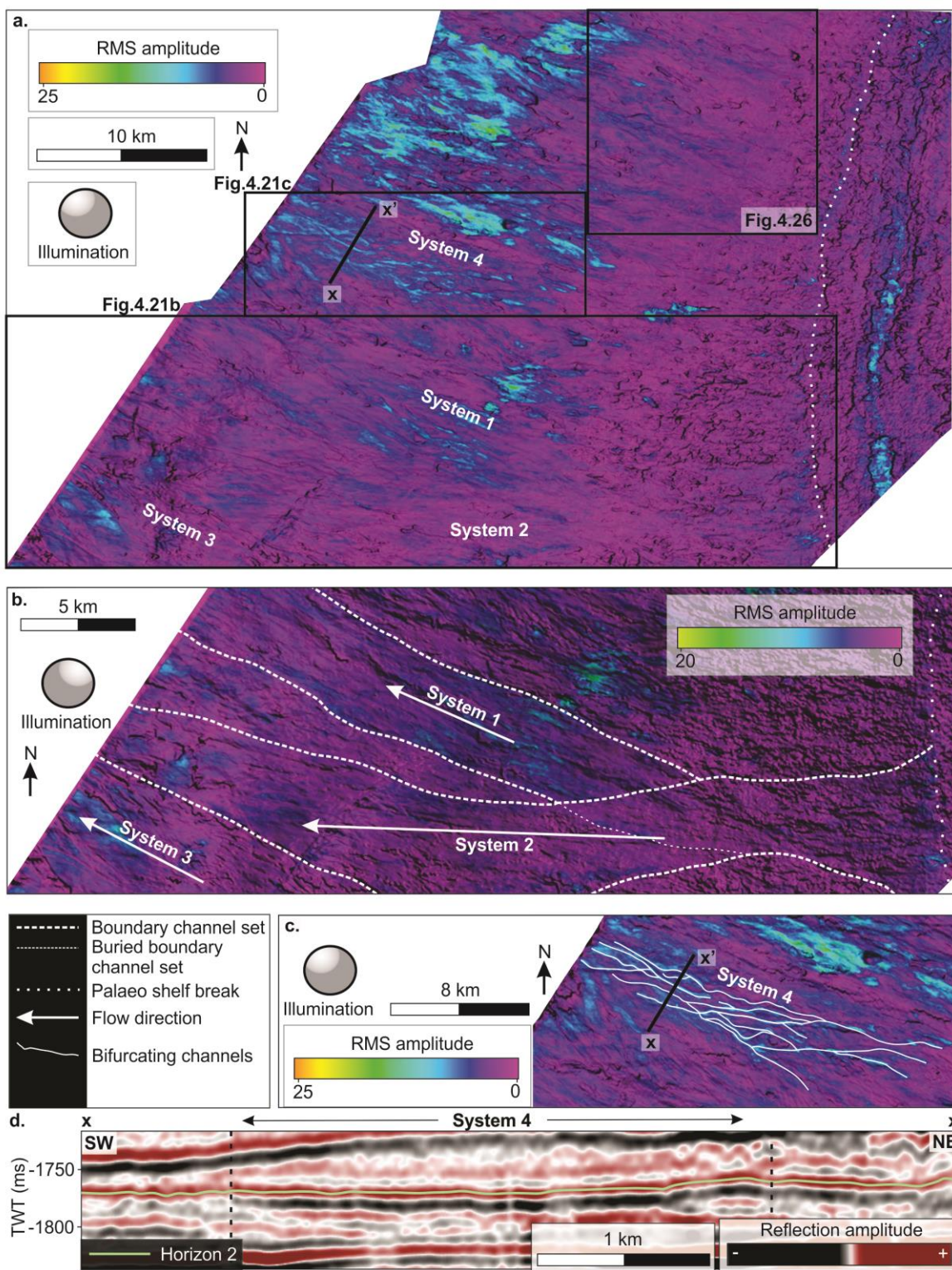
*Figure 4.21: RMS seismic amplitude map for the volume between horizon 2 and 20 ms below. **a.** An overview of the shelf break and slope. Location of b and c are indicated by black polygons. **b.** Southern part of the slope with interpretation of three channel systems (1-3). **c.** Channel system 4 with interpretation. **d.** Cross-profile of channel system 4. Dotted black lines indicate the width of the set. The location of the figure is indicated in figure 4.20.*
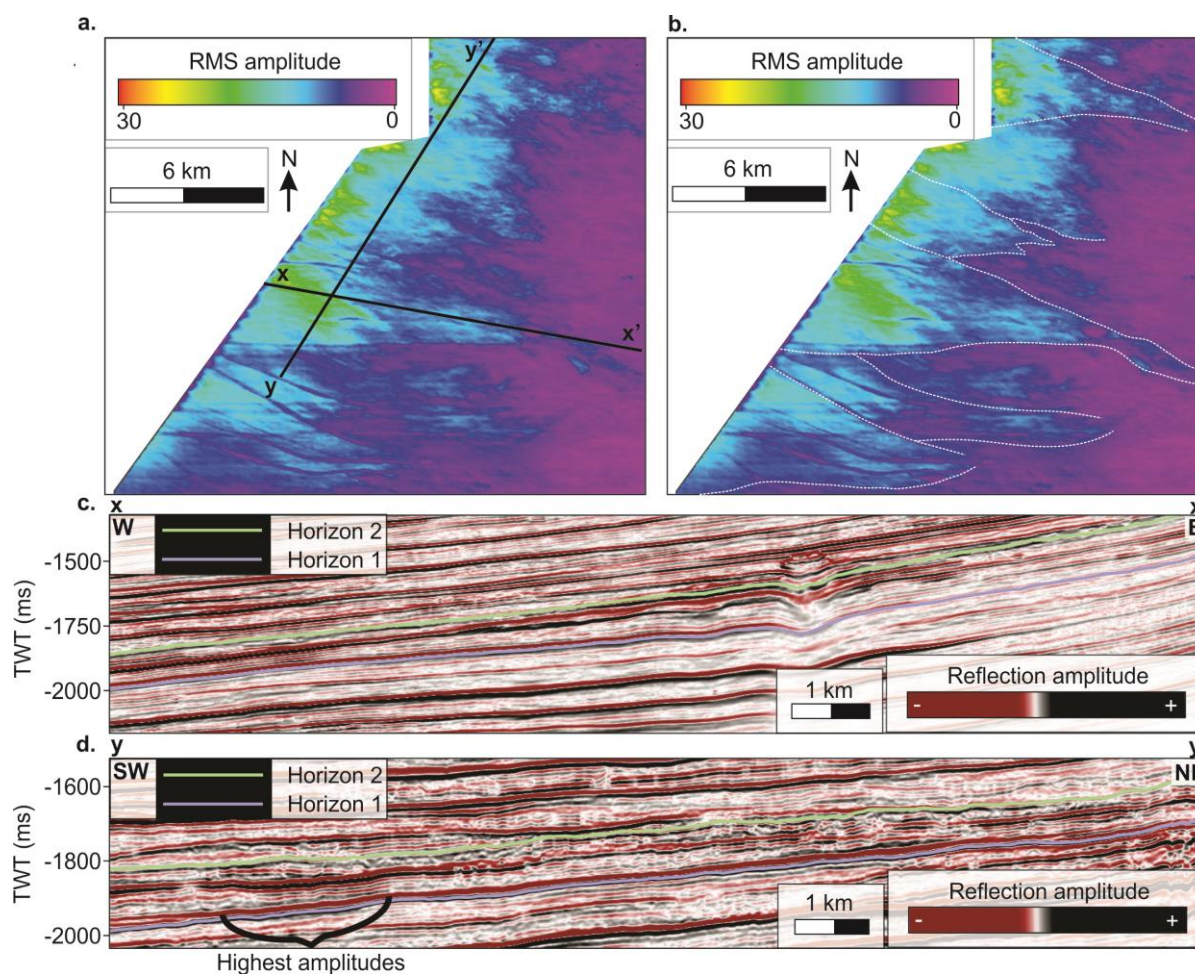
*Figure 4.22. **a.** RMS seismic amplitude map for the volume between horizon 1 and horizon 2 in c and d, showing the lower part of the slope of unit A. Lines indicate seismic profiles of c and d. **b.** Lower part of the slope of unit A outlining fan-shaped accumulations (dotted white line). The location of the figure is indicated in figure 4.20. **c.** Cross-profile (x-x') showing the RMS volume and the internal seismic signature of the fans. **d.** Cross-profile (y-y') showing the RMS volume and the internal seismic signature of the fans.*

79

Interpretation:

The large wedge-shaped external form, the oblique reflection configuration, and continuous internal horizons, indicate an outbuilding of a high-energy slope-system from east to west (Veeken, 2007). This and the observation of glacial lineations on horizon 1, suggest a prograding margin formed by glacial processes. The wedge-shaped external form and location of the greatest sediment accumulation of unit A, indicate that substantial amounts of sediments have been sourced from south with declining deposition further north.

The internal low to medium amplitude reflections of the shelf generally imply little variation in lithologies. Amplitude anomalies from the upper slope related to the systems, imply that glacimarine processes have been influencing the slope. The internal reflection signature and amplitude of the lower part of the slope, points to larger lithological differences. Such differences may be a result of deposition of coarse-grained sediments, commonly deposited by downslope processes.

The bifurcating sinuous-shaped systems indicate several crisscrossing channels formed by masses with a low viscosity behavior. According to Weaver et al. (2000) such features often occur in front of fast flowing ice-streams crossing the shelf in troughs. The channel systems have different orientation and they are crosscutting each other, which would imply a different relative age. Therefore, they probably occurred as separated events where the channel system 1 is the oldest and channel system 3 is the youngest. It is hard to distinguish the relative age of system 4. It may have been active in the same period as system 1 and 3 due to similar orientation.

The wedge-shaped amplitude anomalies on the lower part of the slope may indicate a larger and more continuous flow of sediments with a higher viscosity compared to the channel systems. It also suggests that these are fans overlapping each other (Figure 4.22). Channel systems and fans suggest that the slope of unit A is predominantly comprised of two different downslope processes, i.e. turbidity currents and debris flows.

The abrupt ending of strata on the shelf and the belt of unsorted sediments below the shelf break indicate erosion over a large area and accumulation derived from a grounded ice-sheet.

4.3 Seismic horizon 2

Horizon 2 is a sigmoidal clinoform comprising a palaeo-shelf and palaeo-slope, and marks the boundary between units A and B (Figure 4.23). It has a low to medium strong, negative reflection amplitude on the shelf, generally with a stronger reflection amplitude in the north. The reflection amplitude of the slope change from low on the upper part to medium on the lower part (Figure 4.4-4.9).

The horizon is continuous, except from parts of the upper slope below the shelf break. Therefore, the interpretation in the north (Figure 4.4) and in the center (Figure 4.8) are tentative.

The shelf represents a flat but rough horizon, truncating clinoforms below (horizon 1 and unit A). Below the shelf break, the slope gently dips toward the northwest. The lowest gradient occurs in the south and becomes steeper in the center of the study area (Figure 4.23). Geomorphological landforms are detailed below (Figure 4.24).
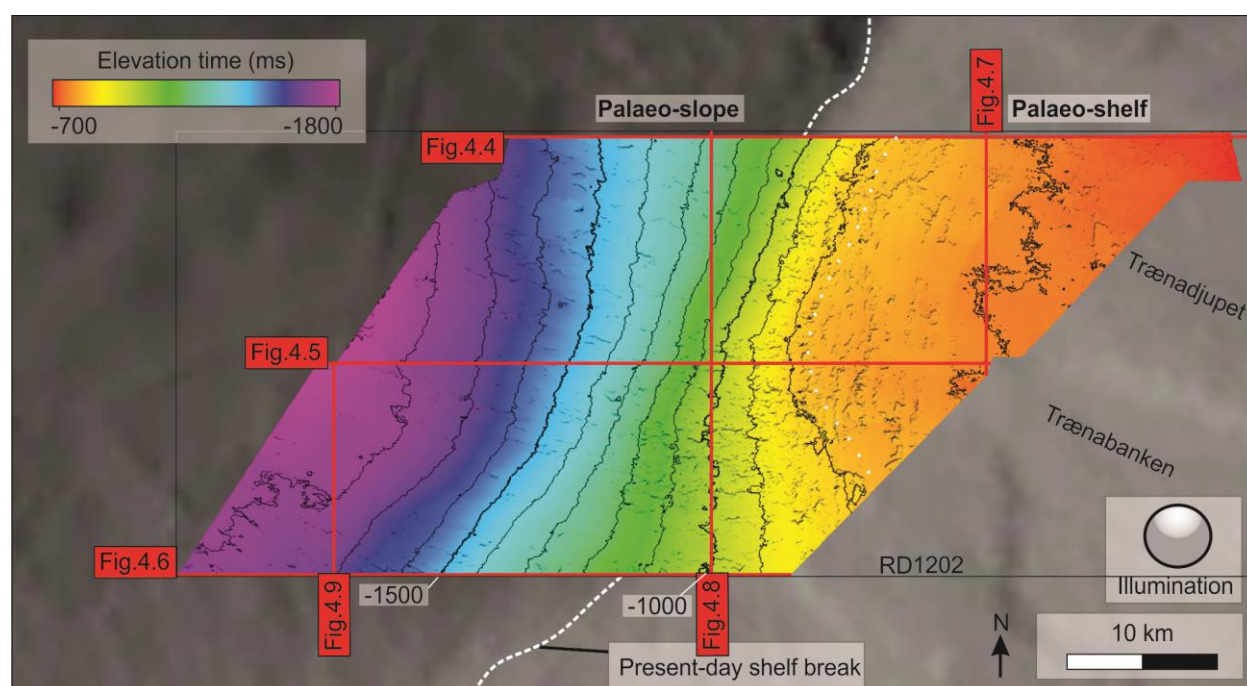
Figure 4.23: Horizon 2 situated on the continental shelf and slope within RD1202. Depths are in ms two-way travel time and the contour lines are indicated every 100 ms (bold every 500 ms). Vertical exaggeration is 10.
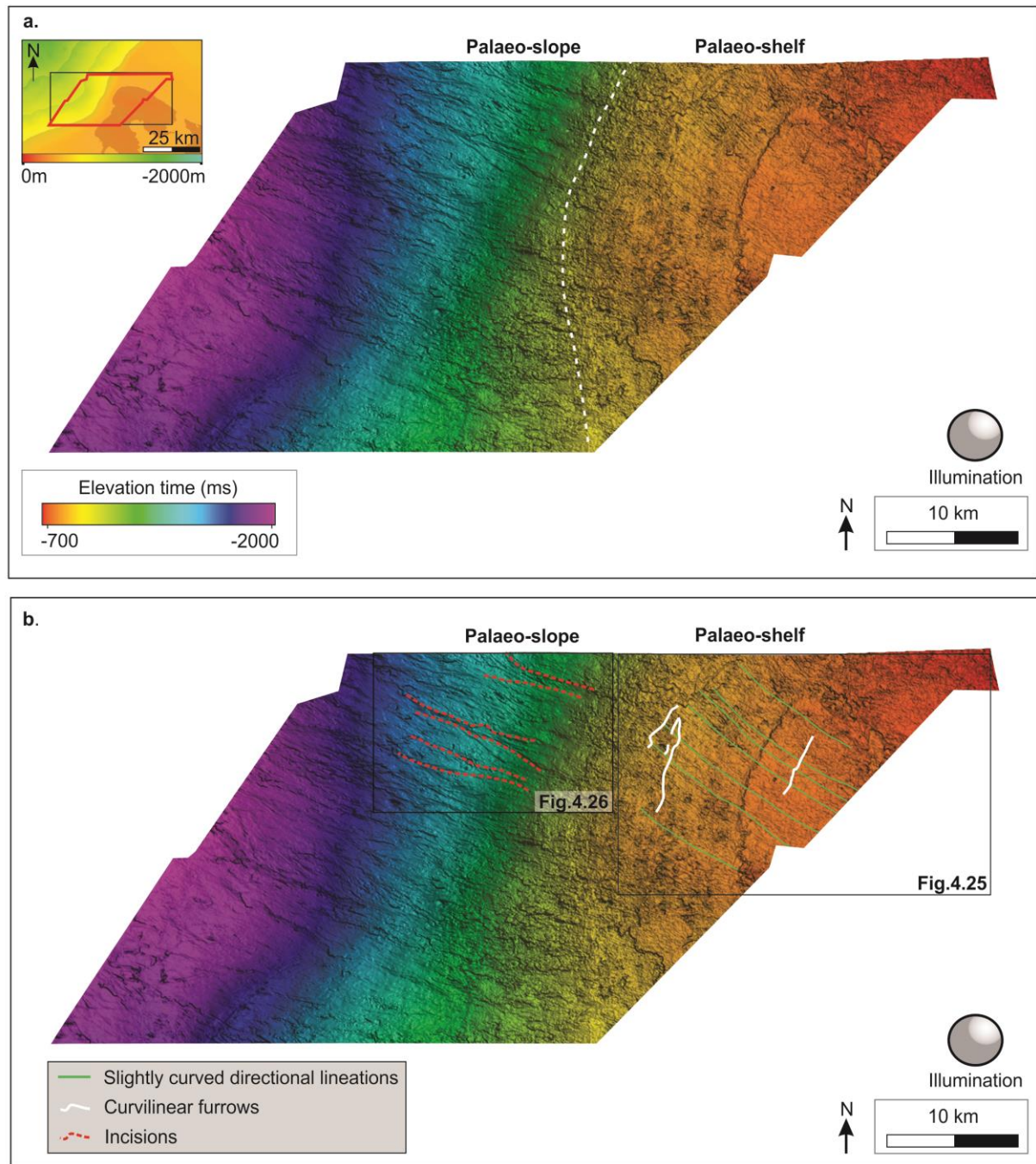
Figure 4.24: **a.** *Overview of the morphology of horizon 2 divided into palaeo-shelf and palaeo-slope (indicated by dotted white line). The location of the horizon is indicated by a red polygon on the inset map in the left corner.* **b.** *Horizon 2 with interpreted morphology. Figure 4.25-4.26 are indicated by black polygons. Vertical exaggeration is 25.*

Slightly curved directional lineations and curvilinear furrows

A set of NW-SE trending linear to slightly curved ridges and furrows occur on the palaeo-shelf (Figure 4.25). These features are similar to the directional lineations described on the palaeo-shelf of horizon 1, slightly bending toward north. They extend up to 15 km from the eastern part of the shelf to the shelf break, before they gradually disappear. The lineations are densely spaced with widths varying between 100-160 m. They are most distinct on the outer part of the shelf with a relief up to 12 m.

In the same area, crosscutting curvilinear furrows orientated sub-parallel to the shelf break occur (Figure 4.25). They are present on the eastern part of the shelf until 800 ms depth. These furrows are up to 8 km long with widths ranging between 70 and 100 m. In cross-profile, they are V-shaped with a negative relief ranging between 10 and 12 m.

Interpretation:

These slightly curved directional lineations have a similar geomorphology, position, and the same orientation trend as those described on horizon 1, i.e. orientated parallel to the modern Trænadjupet Trough. Therefore, they are interpreted to be mega-scale glacial lineations formed in a subglacial environment. Their orientation and extent imply the palaeo-ice flow direction and minimum extent of the palaeo-shelf at that time.

The morphology, limited depth interval and orientation of the curvilinear furrows suggest that these are iceberg plough marks, similar as described in horizon 1. The curvilinear furrows crosscut the directional lineations, which imply that they are younger. They are most likely formed during a withdrawal and calving of a grounded glacier in a glacimarine environment. Their sub-parallel orientation may indicate the oceanographic pattern along the shelf at that time.
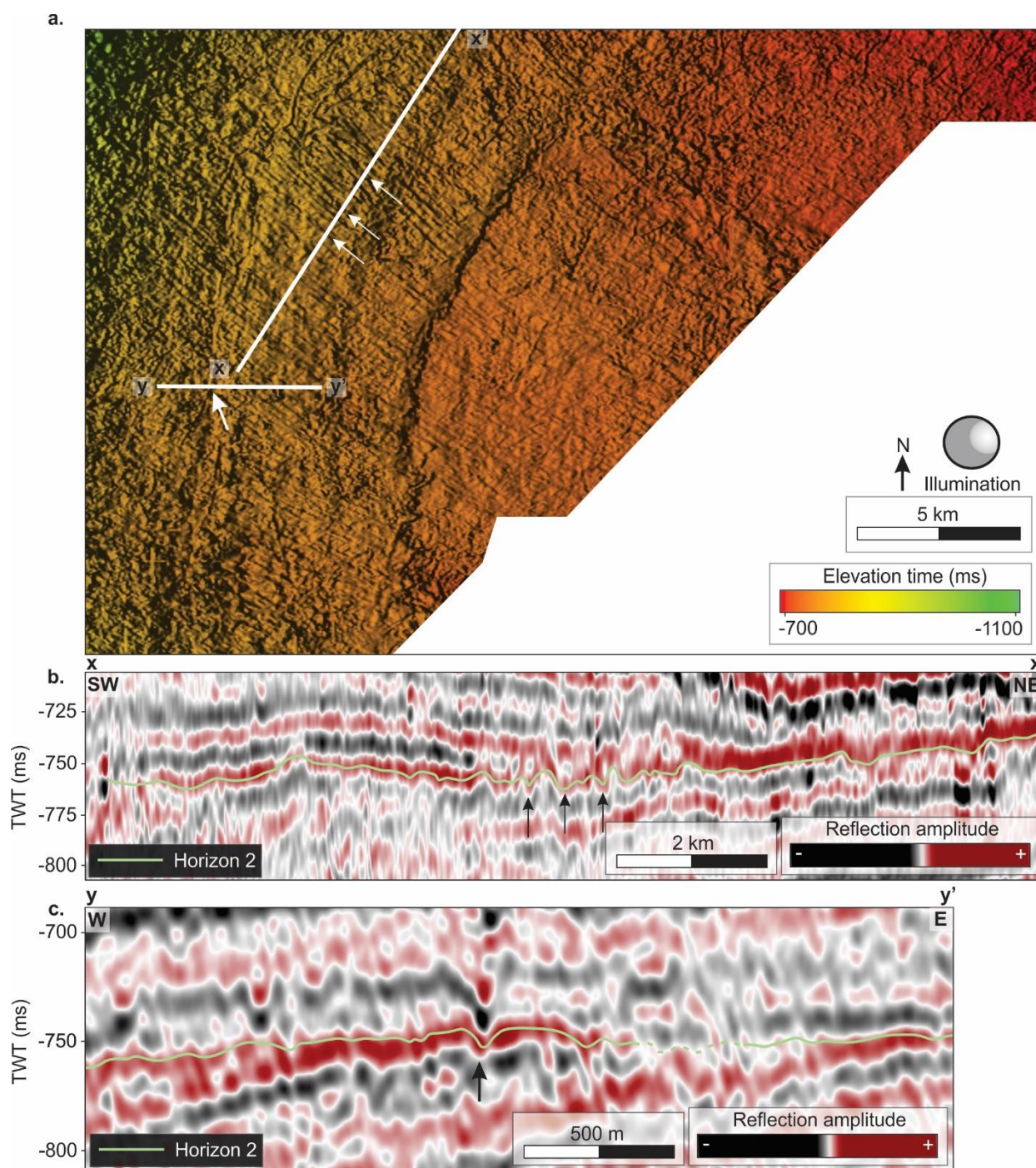
Figure 4.25: **a.** The palaeo-shelf of the NE part of horizon 2 featuring directional lineations. The white lines indicate the location of the seismic profiles in b (x-x') and c (y-y'). Arrows indicate some of the most distinct lineations. Vertical exaggeration is 25.**b.** Seismic profile across the slightly curved directional lineations (indicated by arrows) with interpretation. **c.** Seismic profile across a curvilinear furrow (indicated by an arrow) with interpretation. The location of the figure is indicated in figure 4.24.

Incisions

Three incisions are initiated 400 ms below the shelf break in the area where the horizon has greatest dip angle. They have a NW-SE orientation with a low sinuosity and hourglass-shaped morphology defined by a high amplitude. These amplitude anomalies merge in NW. The incisions have a mean length of 12 km, widths ranging between 700 – 2500 m and their spacing vary between 3-4 km. They are U-shaped in cross-profile and can be up to 20 m deep (Figure 4.24 & 4.26).

Interpretation:

The configuration, negative relief and location of these incisions indicate erosion initiated below the shelf break. Gravity-driven processes can occur and cause erosion in areas with a higher gradient. The amplitude anomaly of the incisions can be a result of coarser sediments deposited in this area. Debris flows may deposit coarse sediments and therefore these incisions are interpreted to be channels formed by gravity-driven processes, possibly by debris flows.
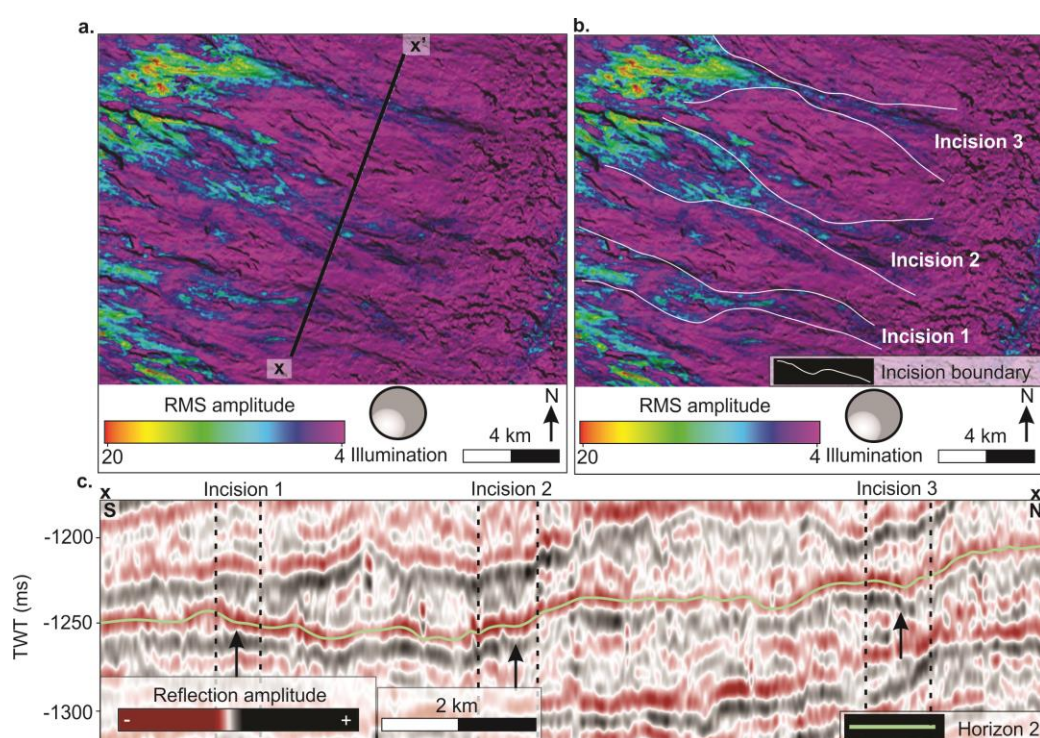
Figure 4.26: *a.* RMS seismic amplitude map of the upper part of the slope of horizon 2 featuring incisions. The black line indicates the seismic profile of c. *b.* Upper part of the slope featuring incisions with interpretation. The location of the figure is indicated in figure 4.21 and 4.24. Vertical exaggeration is 25. *c.* Seismic profile across the incisions shown in a. and b. The amplitude anomalies of the incisions are indicated with black arrows and dotted black lines.

4.4 Seismic unit B

Seismic unit B is the stratigraphic interval bounded by the underlying horizon 2 and the overlying horizon 4. Unit B is comprised of sigmoidal clinoforms prograding from east to west and the unit has an overall wedge-shaped external form (Figure 4.4-4.9 & Figure 4.27).

The lowest sediment thickness occurs on the shelf, generally lowest in the northeast (50-75 ms). Unit B nearly pinches out in this area. The greatest sediment thickness (250-325 ms) occurs on the southern part of the upper slope, more concentrated than in unit A. It gradually thins toward N-NW.

The internal seismic signature of the shelf is dominated by semi-continuous to discontinuous, parallel, low to medium frequency reflections with a medium to high amplitude (Facies 5; Figure 4.10). From north to south, it changes from an acoustically transparent signature separated by reflectors with medium to high amplitude (Facies 4; Figure 4.10), to a medium frequency signature (Facies 5; Figure 4.10).

The internal seismic signature of the slope is continuous to semi-continuous, medium frequency, sub-parallel, inclined reflections with a low to high amplitude (Facies 1 & 2; Figure 4.10). Medium high-elongated amplitudes on the middle part of the slope lead down to high reflection amplitudes on the lower part of the slope. The strongest amplitudes generally occur from the center to the southern part of the unit (Figure 4.4, 4.5, 4.8 & Figure 4.28).
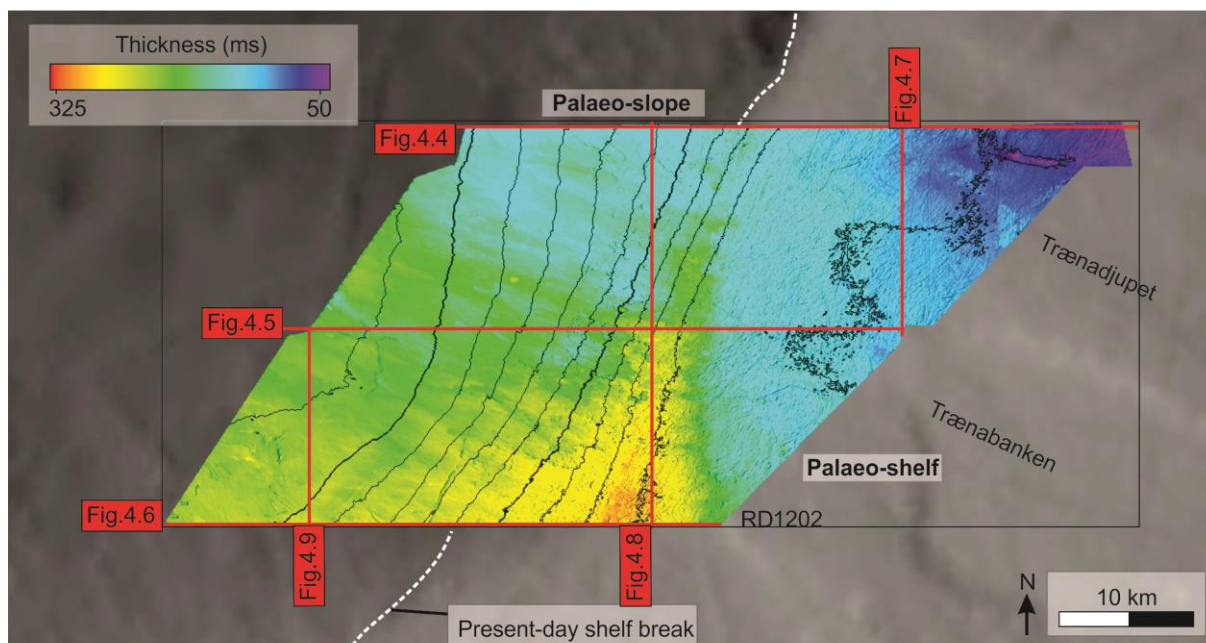
Figure 4.27: Thickness map of seismic unit B situated on the continental shelf and slope within RD1202. The map was defined between horizon 2 and horizon 4. Contour intervals are 100 ms (bold every 500 ms). Vertical exaggeration is 10.
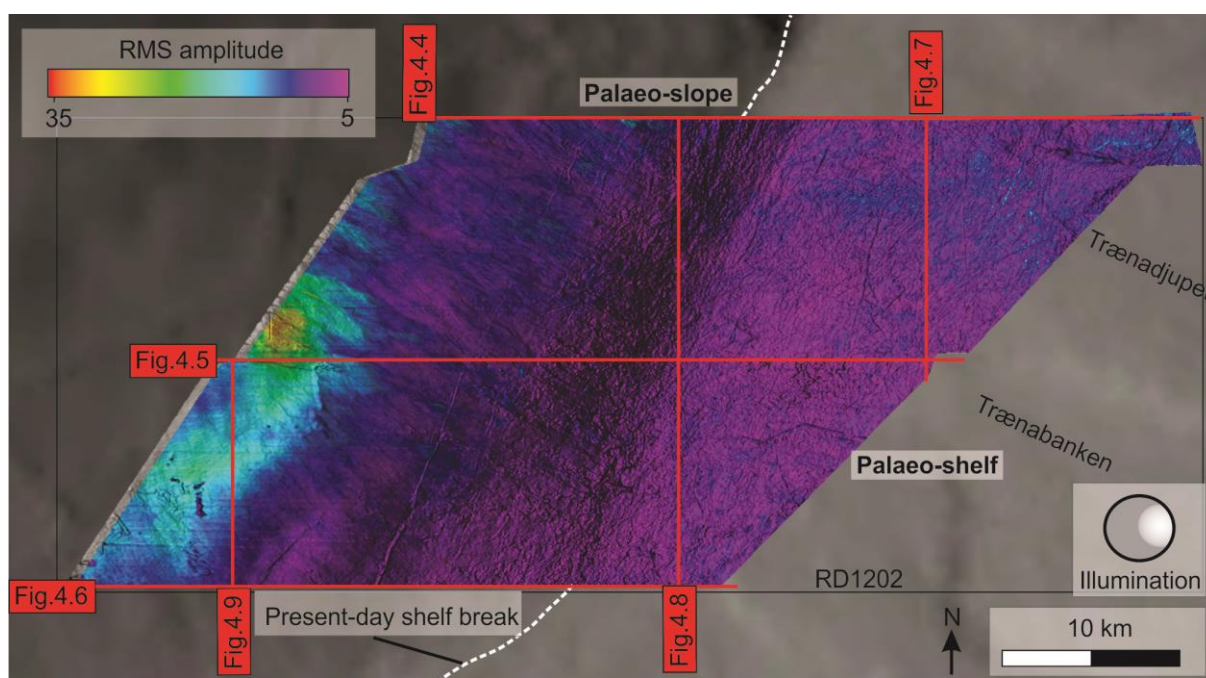
Figure 4.28: RMS seismic amplitude map of unit B situated on the continental shelf and slope within RD1202. The map was defined between horizon 2 and horizon 4. Vertical exaggeration is 25.

Interpretation:

The truncation of unit A by horizon 2 indicates erosion over a larger area. Changes in stratal architecture occur from unit A to B.

The wedge-shaped external form and the sigmodal reflection configuration of unit B imply a lower energy slope-system building a sediment-wedge from the south (Veeken, 2007). The wedge-shaped depocenter indicates a more concentrated sediment accumulation in the south with sparse accumulation in the north.

The internal seismic signature of the slope indicates successive variations between well sorted and more chaotic sediments. This and the amplitude variations suggest successive variation between hemipelagic deposits and slide debrites.

Incisions with adjacent sediment accumulations

Along intra unit B above horizon 2 on the lower part of the slope, several rectilinear incisions separated by sediment accumulations (mounds) occur (Figure 4.29). They have a NW-SE orientation and can downslope be up to 18 km long. The slope has a mean apparent dip angle of 2.5º.

The incisions have widths varying from 2-6 km and have a concave relief with a high reflection amplitude in cross-profile. The mounds have elongated, convex relief (lenticular geometry), low reflection amplitude and thickness varying between 40-60 ms. Their internal seismic signature is acoustically transparent with discontinuous, low amplitude reflectors (Facies 4; Figure 4.10) (Figure 4.29b).

Interpretation:

The linear, wide section of the incisions and the high amplitudes indicate transportation of heavy load sediments by downslope processes. These incisions also have a concave relief and reflection amplitude, which leads to the interpretation that these are erosional channels. Such channels may be formed by debris flows.

The lenticular geometry of the mounds imply that they are depositional features. Due to the internal seismic signature, geomorphology and location on the slope, they are interpreted to be basal till reworked and deposited by downslope processes. Laberg and Vorren (1995) and Cofaigh et al. (2003) describe similar features on the Bear Island Trough Mouth Fan.
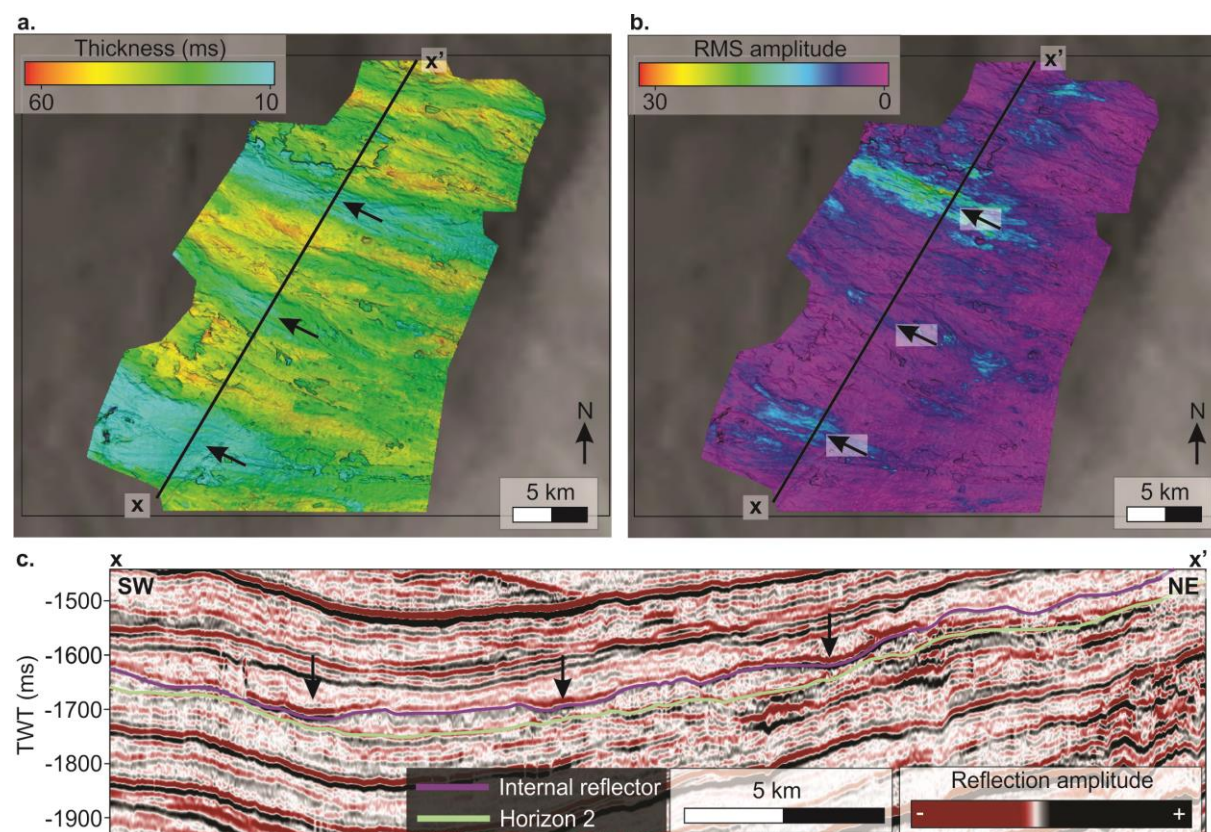
*Figure 4.29. Lower part of the slope defined between horizon 2 and an internal reflector above. Black arrows indicate the incisions with mounds in between. Vertical exaggeration is 25. **a.** Thickness map of intra unit B located on the lower part of the slope. **b.** RMS seismic amplitude map of intra unit B located on the lower part of the slope. The black line indicates the seismic profile of c. **c.** Seismic profile crosscutting the intra unit B with interpretation.*

4.4.1 Seismic horizon 3

Horizon 3 is a sigmoidal clinoform comprised of palaeo-shelf and palaeo-slope (Figure 4.30) and represents an internal boundary in unit B. The horizon is generally continuous on the shelf, with some discontinuity in the center of the study area. It has a medium to high, positive reflection amplitude. The shelf break area of the horizon is predominantly discontinuous (Figure 4.4-4.7).

The upper part of the slope has a low to medium strong, positive reflection amplitude (Figure 4.4 & 4.6) where the lower part of the slope has a continuous, high, positive reflection amplitude (Figure 4.7).

Horizon 3 can be described as a smooth reflector with a gently NW dipping trend on the slope. The apparent dip angle of the slope is 3-5°, generally higher on the upper part in the north (Figure 4.30). Some smaller geomorphological landforms are detailed below (Figure 4.31).
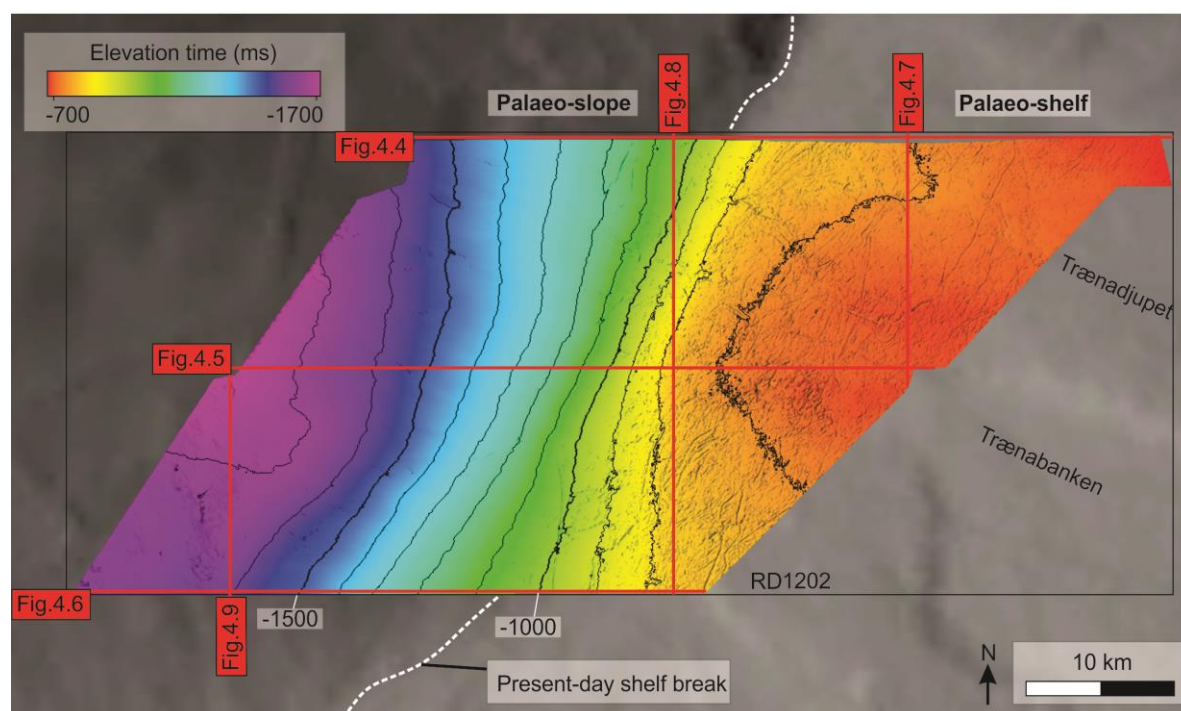
Figure 4.30: Horizon 3 situated on the continental shelf and slope within RD1202. Depths are in ms two-way travel time and the contour lines are indicated every 100 ms (bold every 500 ms). Vertical exaggeration is 10.
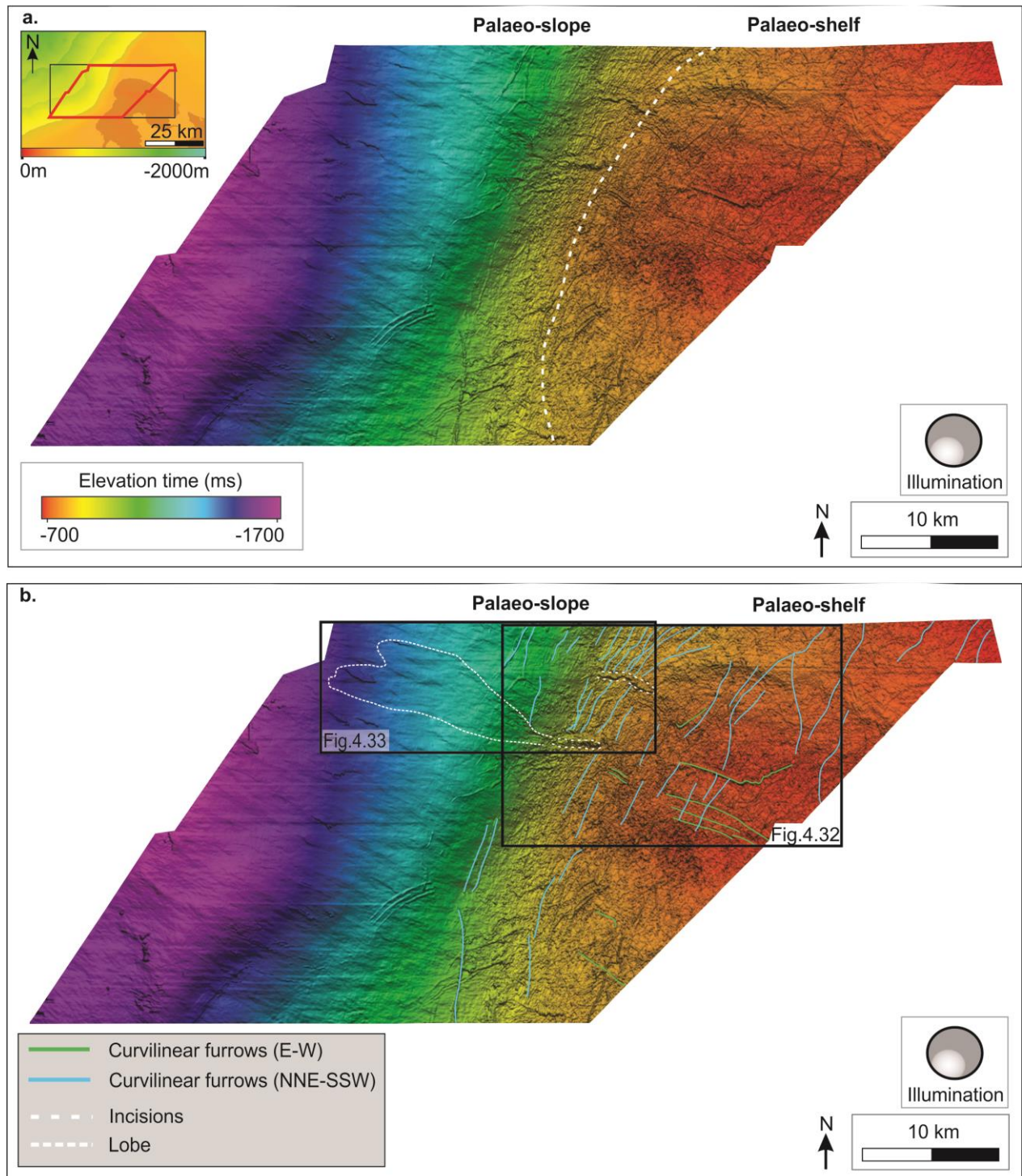
Figure 4.31: **a.** Overview of the morphology of horizon 3 divided into palaeo-shelf and palaeo-slope (indicated by dotted white line). The location of the horizon is indicated by a red polygon on the inset map in the left corner. **b.** Horizon 3 with interpreted morphology. Figure 4.32-4.33 are indicated by black polygons. Vertical exaggeration is 25.

Curvilinear furrows:

A large number of curvilinear furrows occur on the shelf and upper part of the slope with NNE-SSW parallel orientation (Figure 4.32). They can be followed up to 15 km and are ~150 m wide. The furrows are densely spaced, especially on the upper part of the slope where they are present down to 1200 ms depth. They have a V-shaped relief up to 6 m.

Several curvilinear furrows with an approximately E-W orientation crosscut the curvilinear furrows described above. They can be followed up to 11 km and their width are ranging from 150-350 m. In cross-profile, they have a negative relief up to 13 m (Figure 4.32).

Interpretation:

The large number of curvilinear furrows on the shelf and upper slope have similar geomorphology as the plough marks described on horizon 1 and 2, and therefore interpreted to be iceberg plough marks. They differ from the curvilinear furrows previously described when it comes to consistency in orientation and their parallel densely spacing. This may imply a high concentration of drifting icebergs and a strong NNE-SSW orientated ocean current in this period. Crosscutting plough marks have a relative younger age and large plough marks can indicate formation by larger icebergs.
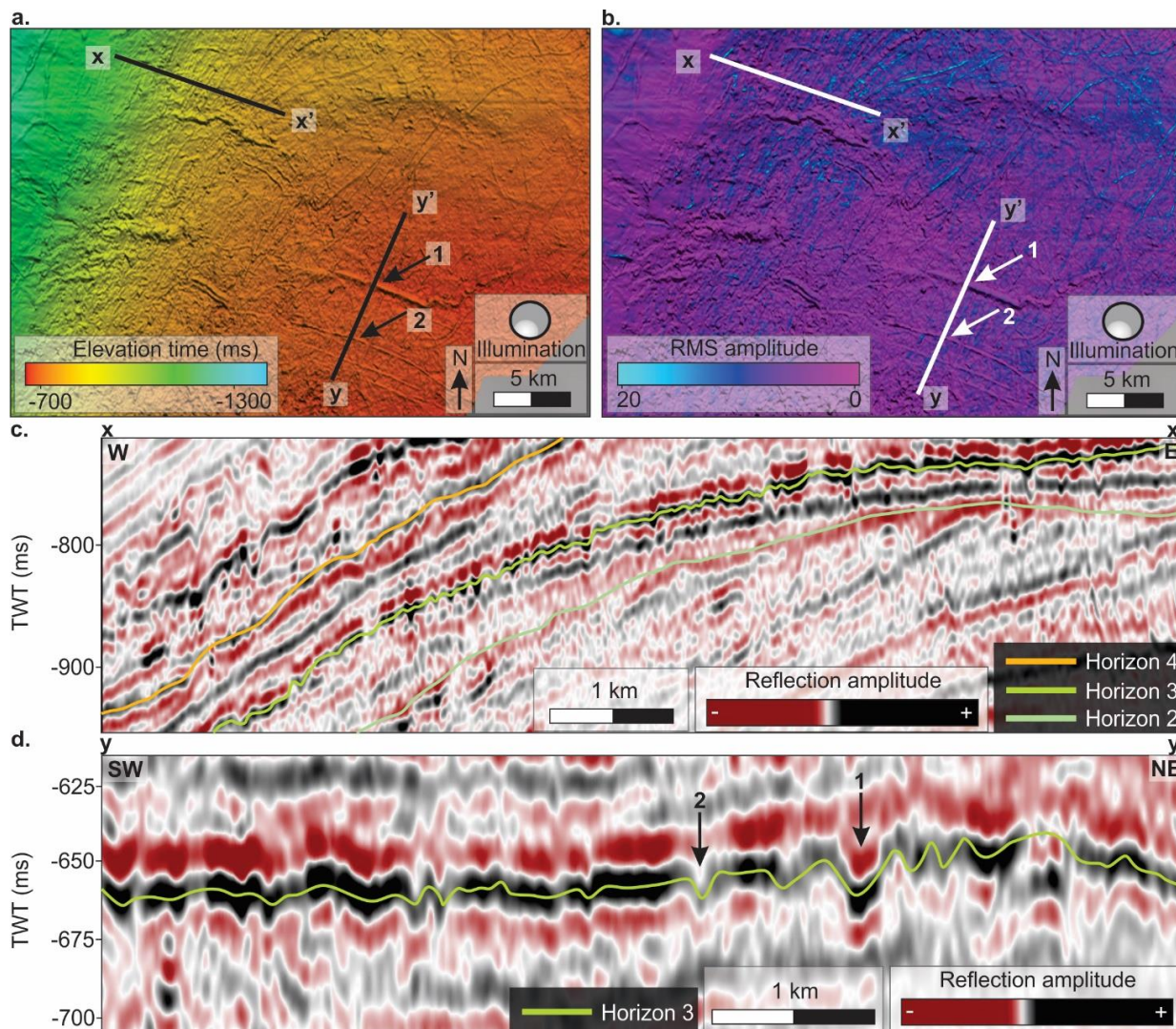
Figure 4.32: ***a.*** *Shelf and upper part of the slope of the seafloor horizon featuring curvilinear furrows. The black lines indicate locations of the profiles in c and d (x-x', y-y').* ***b.*** *RMS map of the same area as in a. featuring curvilinear furrows. The white lines indicate locations of the profiles in c and d (x-x', y-y'). Vertical exaggeration is 10. The location of the figure is indicated in figure 4.31.* ***c.*** *Seismic profile with interpretation across curvilinear furrows with NNE-SSW orientation.* ***d.*** *Seismic profile with interpretation across curvilinear furrows with E-W orientation. Arrows indicates some of the most distinct curvilinear furrows*

Buried incisions with lobe-shaped feature

Two sinuous-shaped incisions with an ESE-WNW orientation occur on the outer shelf and upper slope (Figure 4.33). They can be followed up to 7 km and have widths ranging from 700-1000 m. They are U- and V-shaped, with depths up to 40 m (Figure 4.33a and c).

The southern incision can be described as a headwall. Downslope of the headwall, an elongated lobe-shaped feature occurs on the lower part of the slope. The lobe is 16 km long, up to 6 km wide and consist of low amplitude reflections bounded by moderate-to high amplitude reflections. In cross-profile, it has a semi-transparent body with a relief of up to tens of meters (Figure 4.33b, d and e).

Interpretation:

The negative relief of the incisions indicate that they are a result of erosion, probably caused by gravity-driven processes. The northern incision may be formed by cold and dense meltwater released beneath an ice-sheet on the shelf. If the sediment content is high enough, a turbidity current may form and potentially erode gullies. Gullies have been described from Arctic and Antarctic by Gales et al. (2013) and by Montelli et al. (2018) on the mid-Norwegian continental slope.

A headwall indicate that sediments have been removed from the area and probably transported downslope. The lobe-shaped features below the southern incision may be a result of slope failure causing downslope deposition of a debris flow. Laberg and Vorren (1995) describes similar features on the Bear Island Trough Mouth Fan.
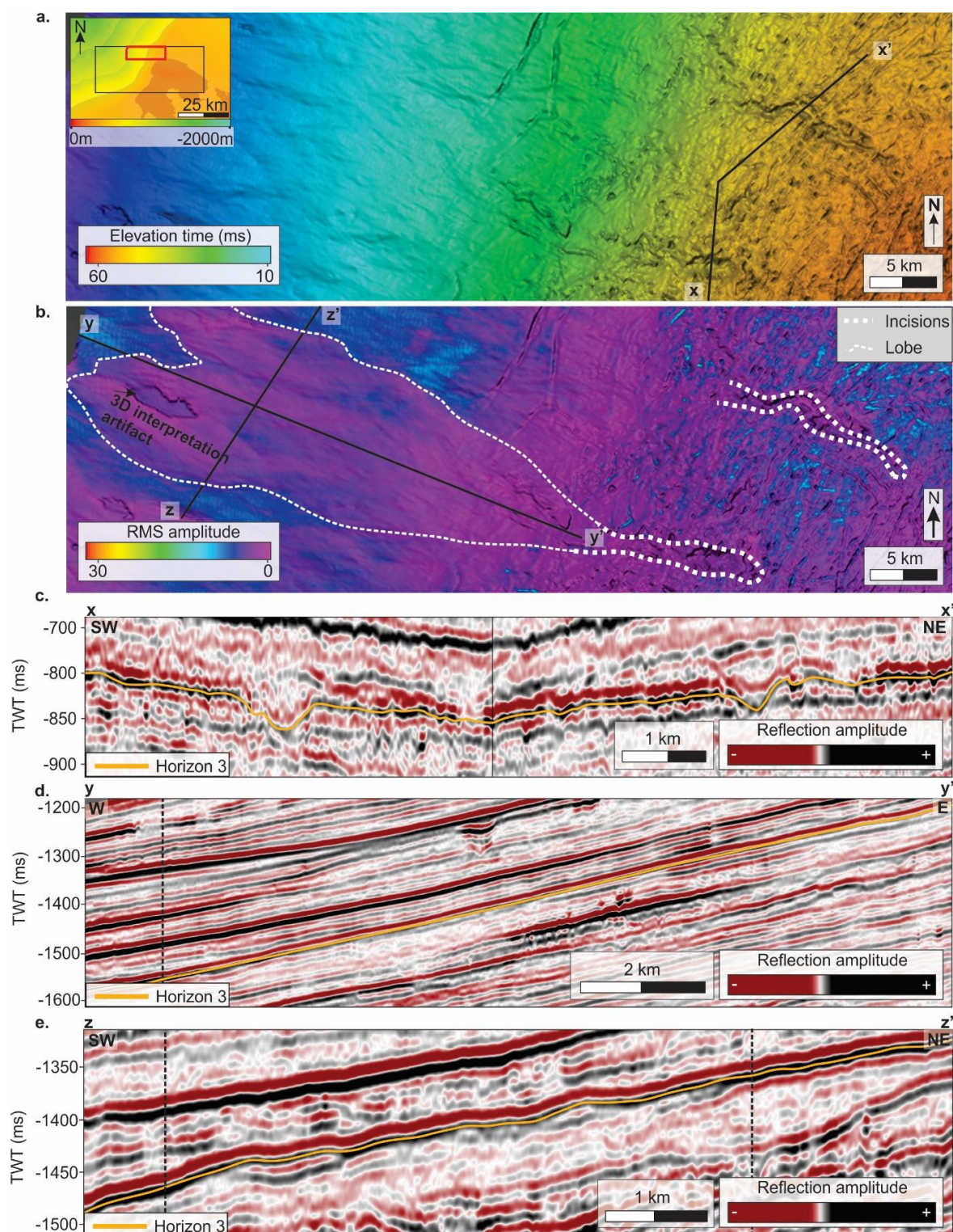
Figure 4.33: **a.** *Below the shelf break in the northern part of horizon 3 featuring two sinious-shaped incisions. The black line indicates the seismic profile in c (x-x')* **b.** *RMS seismic amplitude map of horizon 3 featuring two sinuous-shaped incisions and a lobe-shaped feature below with interpretation. The black lines crosscut the lobe and indicate the location of the seismic profiles in d (y-y'). The location of a. and b. are indicated by a red polygon on the inset map in the left corner and in figure 4.31. Vertical exaggeration is 25.* **c.** *Seismic profile across the sinuous-shaped incisions in a.* **d.** *Seismic profile along the lobe in b.* **e.** *Seismic profile across the lobe-shaped feature in b. The lobes are delimited by black dotted lines in d. and e.*

95

4.5 Seismic horizon 4

Horizon 4 is a sigmoidal clinoform comprised of a palaeo-shelf and a palaeo-slope (Figure 4.34). It is the upper boundary of unit C and lower boundary of unit D. The shelf is continuous with a medium to high, positive reflection amplitude. Generally, the strongest amplitudes occur in the north. Below the shelf break and parts of the upper slope, the horizon is discontinuous with low to medium, positive reflection amplitude. From this point on, it is continuous and gradually increases to a high amplitude on the lower part of the slope (Figure 4.4-4.9).

Horizon 4 can be described as a smooth reflector with a gently NW dipping trend on the slope. The dip angle is generally higher on the upper part of the slope, north of the center. Some smaller geomorphological landforms situated on the horizon are detailed below (Figure 4.35).
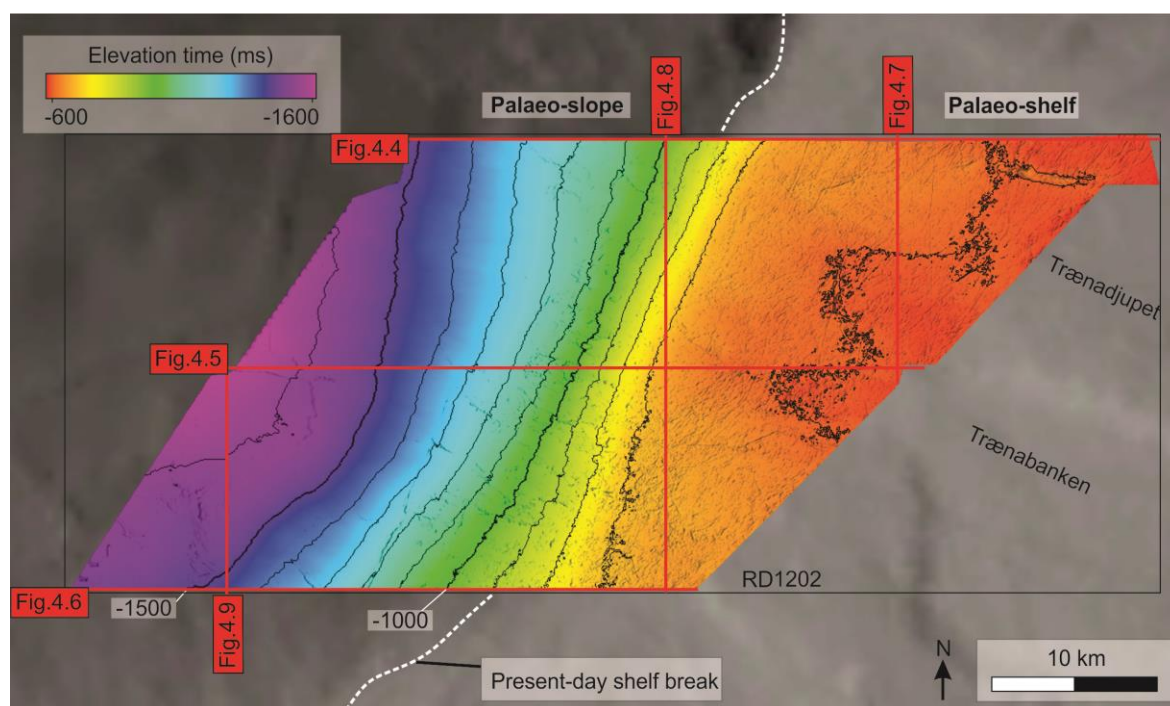
Figure 4.34: Horizon 4 situated on the continental shelf and slope within RD1202. Depths are in ms two-way travel time and the contour lines are indicated every 100 ms (bold every 500 ms). Vertical exaggeration is 10.
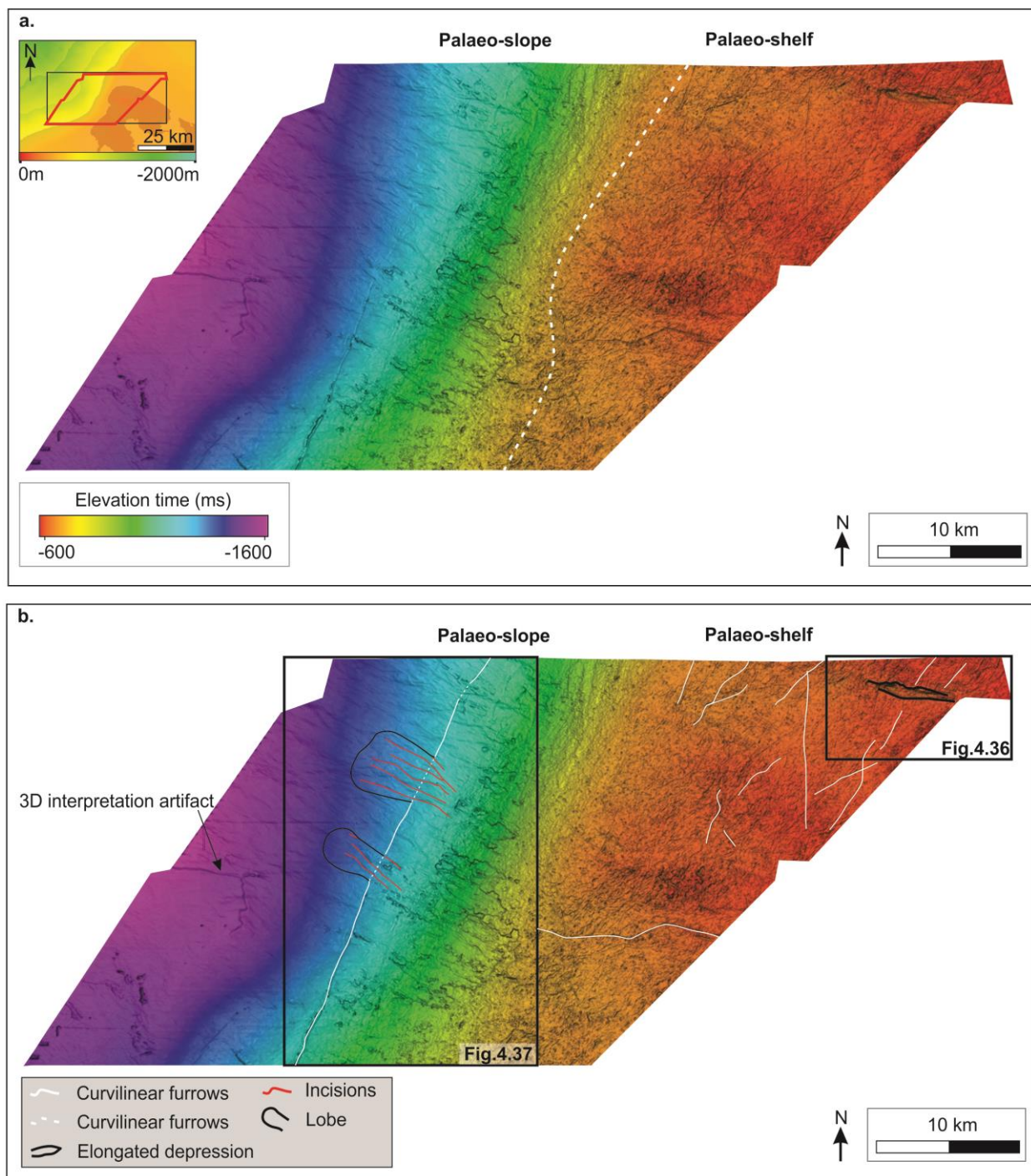
*Figure 4.35 **a.** Overview of the morphology of horizon 4 divided into palaeo-shelf and palaeo-slope (indicated by dotted white line). The location of the horizon is indicated by a red polygon on the inset map in the left corner. **b.** Horizon 4 with interpreted morphology. Figure 4.36 and 4.37 are indicated by black polygons. Vertical exaggeration is 25.*

Elongated depression

An elongated depression with E-W orientation occurs on the northeastern part of the shelf (Figure 4.36). It is 6 km long and up to 1 km wide. Generally, the depression has a V-shaped relief cutting off the adjacent seismic reflectors. It is separated into two sections by an internal, asymmetric elevation. The relief is up to 22 m in the east and 37 m in the west. In cross-profile, the elevation has an elongated, low gradient side in the west and a short, high gradient side in the east. The internal seismic signature is acoustically transparent separated by weak amplitude reflectors (Facies 4; Figure 4.10). Curvilinear furrows surround the depression.

Interpretation:

The V-shaped relief cutting off the adjacent seismic reflectors and internal seismic signature imply erosion of basal till. Unlithified moraines can be eroded in an elongated way by concentrated water currents. Such currents may occur under subglacial conditions and the erosional landform is therefore interpreted to be caused by a meltwater-channel.

The surrounding curvilinear furrows are most likely plough marks formed by floating icebergs. This implies that no grounded ice-sheet was present in the shelf area at that time, but icebergs were drifting around. In that case, the erosional depression was formed and well preserved prior to the formation of plough marks.
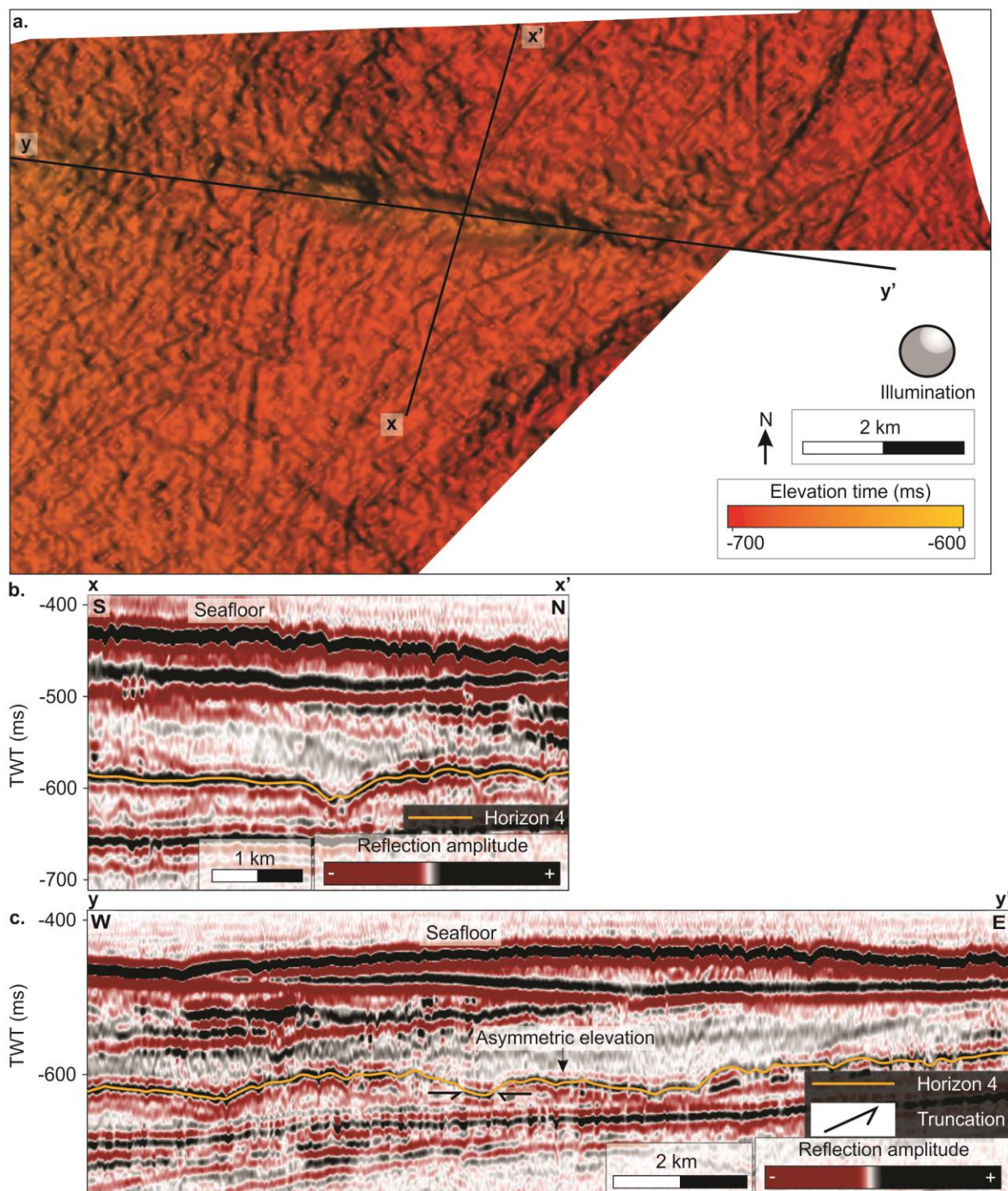
Figure 4.36: ***a.*** *The palaeo-shelf of the NE part of horizon 4 featuring an elongated depression. The black lines indicate the location of the seismic profiles in b (x-x') and c (y-y'). Vertical exaggeration is 25 and the location of the figure is indicated in figure 4.35.* ***b.*** *Seismic profile across the elongated depression with N-S orientation.* ***c.*** *Seismic profile across the elongated depression with E-W orientation.*

A curvilinear furrow and crosscutting incisions

A curvilinear furrow with an NNE-SSW orientation occurs on the middle part of the slope (Figure 4.37). It has a 33 km length across the slope with a width ranging between 50-300 m. The furrow is most prominent in the south and is present at a depth of ~ 1250 ms. It has a negative V-shaped relief up to 18 m (Figure 4.37d).

Semi-linear incisions superpose the curvilinear furrow, and lobe-shaped features occur downslope of these. Their orientation is WNW-ESE, almost perpendicular to the contours and they are initiated at a depth of 900 ms. They reach the lower part of the slope with lengths ranging between 13-16 km and widths up to 3 km. In cross-profile, they are U to V-shaped with a negative relief ranging between 6 - 8 m and are defined by a low amplitude area (Figure 4.37b, e)

Interpretation:

The geomorphology of the curvilinear furrow and parallel orientation to the shelf break leads to the interpretation that this is an iceberg plough mark. This plough mark is similar to the curvilinear furrows observed on lower lying horizons, although, it is longer and preserved at a deeper depth than previously described. Orientation and length of the plough mark may imply an NNE-SSW intensive and continuous ocean current at this time.

An almost perpendicular orientation to the contours and a negative relief indicate that the semi-linear incisions are a result of erosion caused by gravity-driven processes. Gravity-flows such as debris flows may form lobes. Therefore, these features are interpreted to be incisions with remnants below formed by debris flows. The lobes crosscut the plough mark, suggesting a younger relative age. Similar features were described on Andfjorden and Malangsdjupet TMFs by Rydningen et al. (2015).
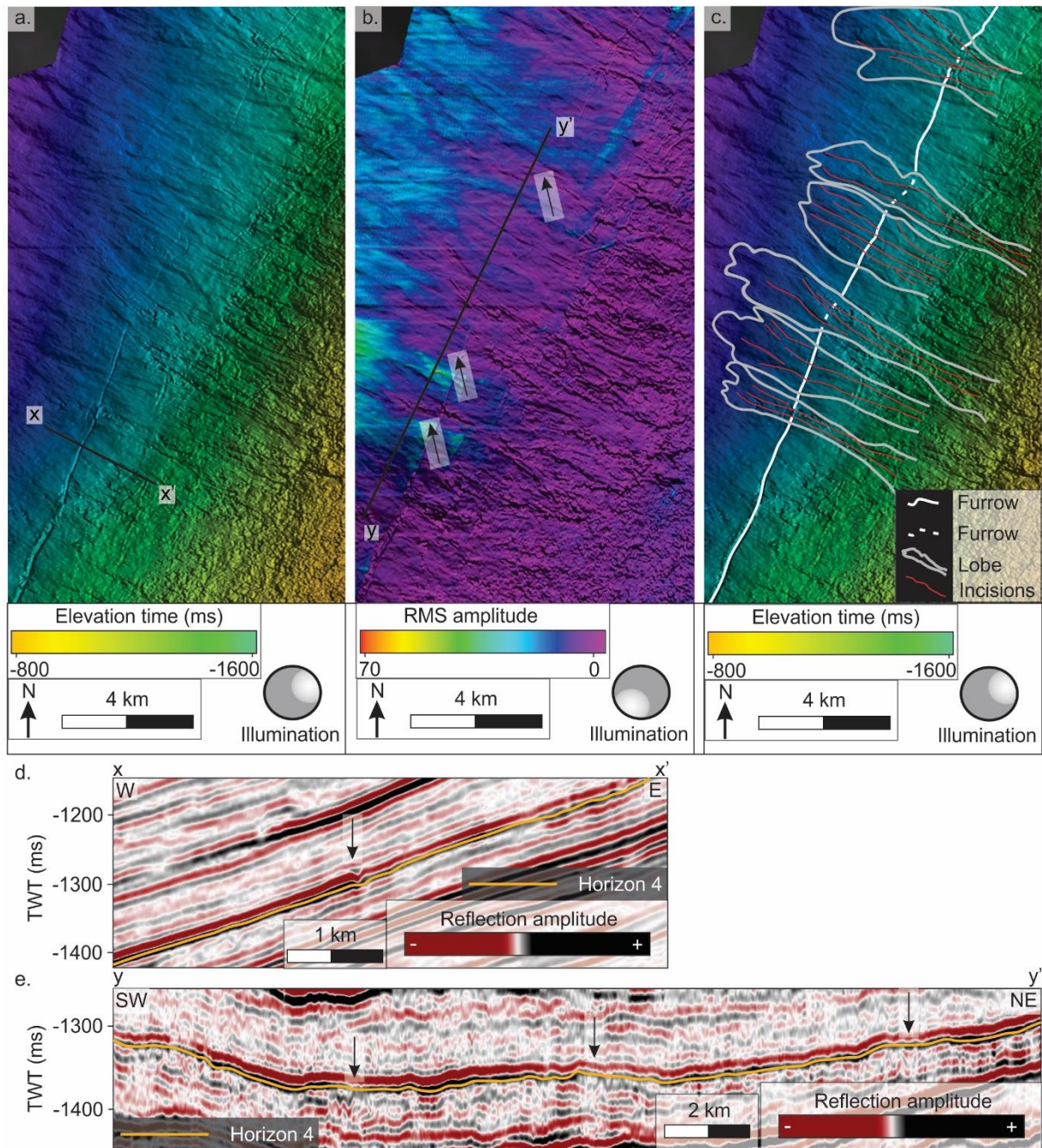
Figure 4.37: *a. Lower part of the slope of horizon 4 featuring a curvilinear furrow and crosscutting incisions. b. RMS map of the lower part of the slope of horizon 4 featuring an elongated furrow and crossing lobe-shaped features. The black line indicates the location of the seismic profile in d (x-x'). Arrows indicate some of the lobe-shaped features. c. Lower part of the slope of horizon 4 featuring an elongated furrow and crossing lobe-shaped features. Vertical exaggeration is 25 and the location of the figures is indicated in figure 4.35. d. Seismic profile across the elongated furrow with interpretation. The arrow indicates the furrow. e. Seismic profile across the lobe-shaped features with interpretation. Arrows indicate some of the lobe-shaped features*

4.6 Seismic unit C

Seismic unit C is the stratigraphic interval bounded by the underlying horizon 4 and the overlying horizon 6. Unit C changes vertically from sigmoidal to oblique clinoforms prograding from east to west (Figure 4.4-4.9 & Figure 4.38). The overall external form of the unit is sheet-shaped in the east and wedge-shaped in the west. In the southern part of the wedge, the greatest sediment thickness (200-250 ms) occurs, i.e. on the slope west of Trænabanken. The wedge gradually thins towards the north (Figure 4.38).

The internal seismic signature of the shelf varies from semi-continuous to discontinuous, parallel reflectors with weak amplitudes (Facies 5; Figure 4.10). This seismic signature continues on the upper slope with a gradually increase in amplitude further west. The slope sediments of unit C are separated by the internal reflector horizon 5. On the lower part of the slope, horizon 5 separates the semi-continuous, sub-parallel, low frequency reflections with a low amplitude (Facies 2; Figure 4.10). Strong reflection amplitudes occur on the lower part of the slope, generally strongest in the southern part of the study area (Figure 4.39).

Interpretation:

The change from sigmoidal to oblique reflection configuration indicates a prograding margin changing from a low-energy slope-system to a high-energy slope-system (Veeken, 2007). This may lead to a greater sediment supply caused by glacial processes.

The sigmoidal reflection configuration, large sheet-shaped external form in the east and the internal seismic signature indicate a uniform sedimentation, often caused by sediments deposited out of suspension. In the west, the wedge implies a change in depositional environment and sedimentation rate along the upper part of the slope. The sedimentary wedge is sourced from the south with declining sedimentation further north (Veeken, 2007). On the lower part of the slope, the internal seismic signature reveals slide debrites.
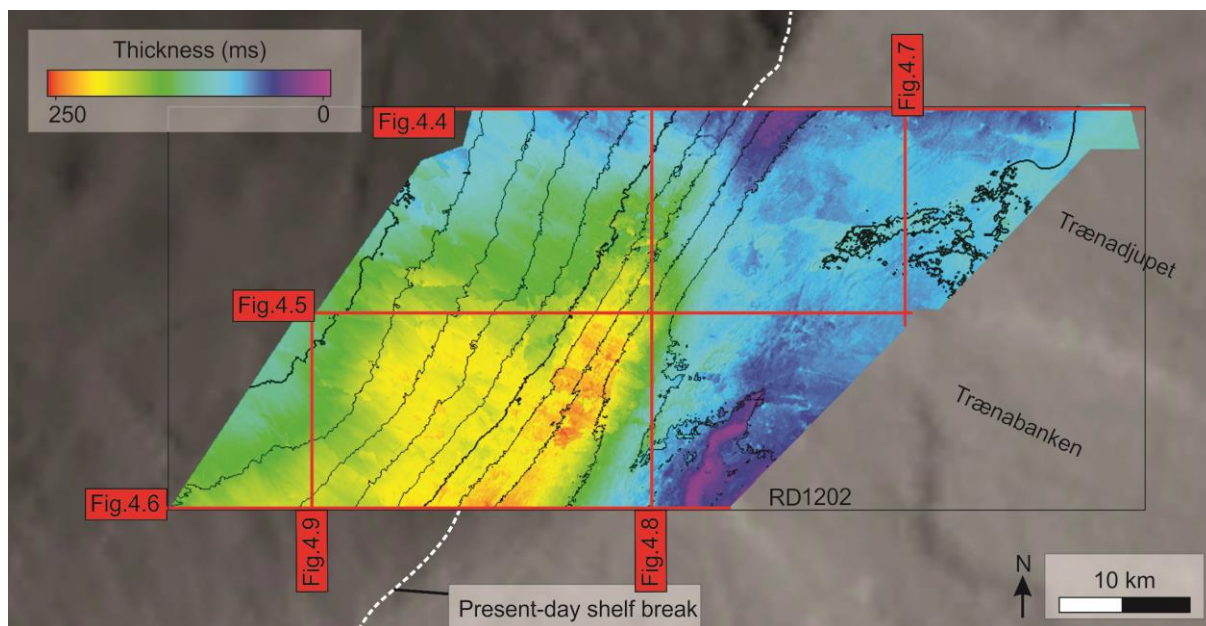
Figure 4.38: Thickness map of seismic unit C situated on the continental shelf and slope within RD1202. The map was defined between horizon 4 and horizon 6. Contour intervals are 100 ms (bold every 500 ms).
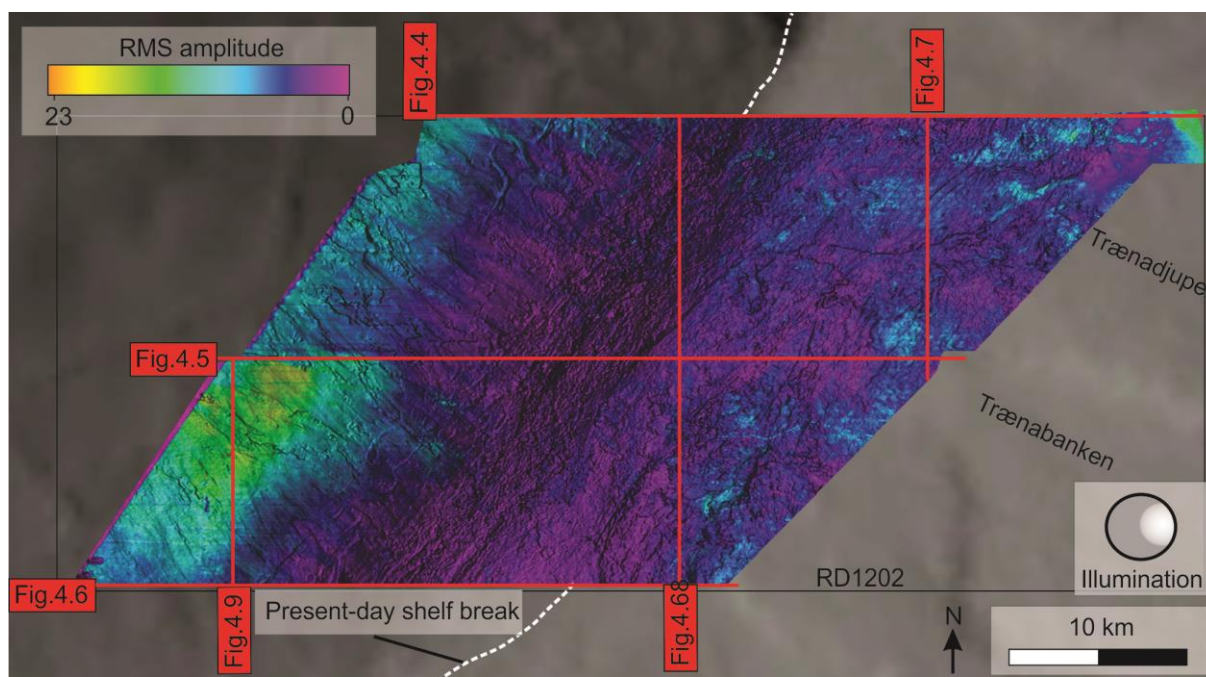
Figure 4.39: RMS seismic amplitude map of unit C situated on the continental shelf and slope within RD1202. The map was defined between horizon 4 and horizon 6. Vertical exaggeration is 25.

103

4.6.1 Seismic horizon 5

Horizon 5 is an oblique clinoform, which is truncated by horizon 6 in the east (Figure 4.40). It is an internal boundary in unit C and extends from the shelf break to the lower part of the slope. Horizon 5 has a medium to high, positive reflection amplitude, generally strongest to the west (Figure 4.4-4.6 & 4.9).

The horizon is continuous, except from parts of the upper slope in the center of the study area (Figure 4.5). Further, it represents a smooth, gently northwest dipping palaeo-slope. One of the geomorphological landforms situated on horizon 5 is detailed below (Figure 4.40).
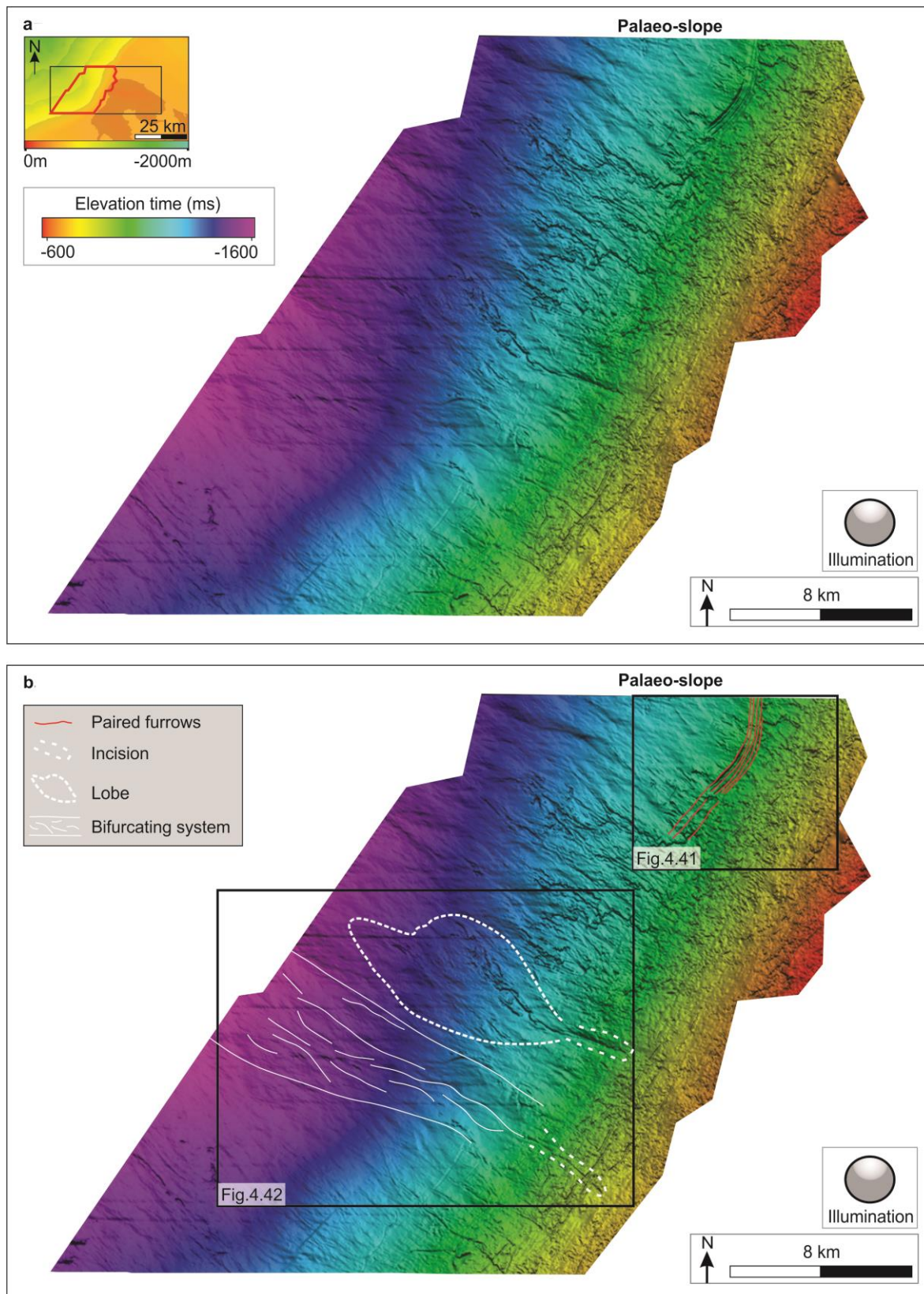
Figure 4.40: **a**. *Overview of the morphology of horizon 5 within RD1202. The location of the horizon is indicated by a red polygon on the inset map in the left corner. **b**. Horizon 5 with interpreted morphology. Figure 4.41 and 4.42 are indicated by a black polygon. Vertical exaggeration is 25.*

105

Paired furrows

On the upper part of the slope, a number of curved, parallel furrows with an NNE-SSW orientation occur (Figure 4.41). They are 5 km long, 600-800 m wide and are present at a depth of 1050 ms. In cross profile, they are U- to V-shaped with a negative relief of up to 25 m.

Interpretation:

The curvilinear furrows have similar morphology and setting as the curvilinear furrows described earlier - except for the width and parallel orientation to each other. Therefore, they are interpreted to be paired plough marks. An iceberg forms paired plough marks if it has multiple protruding keels (3-4) scraping the seafloor sediments. Such phenomenon have been described previously by Longva and Bakkejord (1990) in southeast Norway and by Rafaelsen et al. (2002) in the Barents Sea.
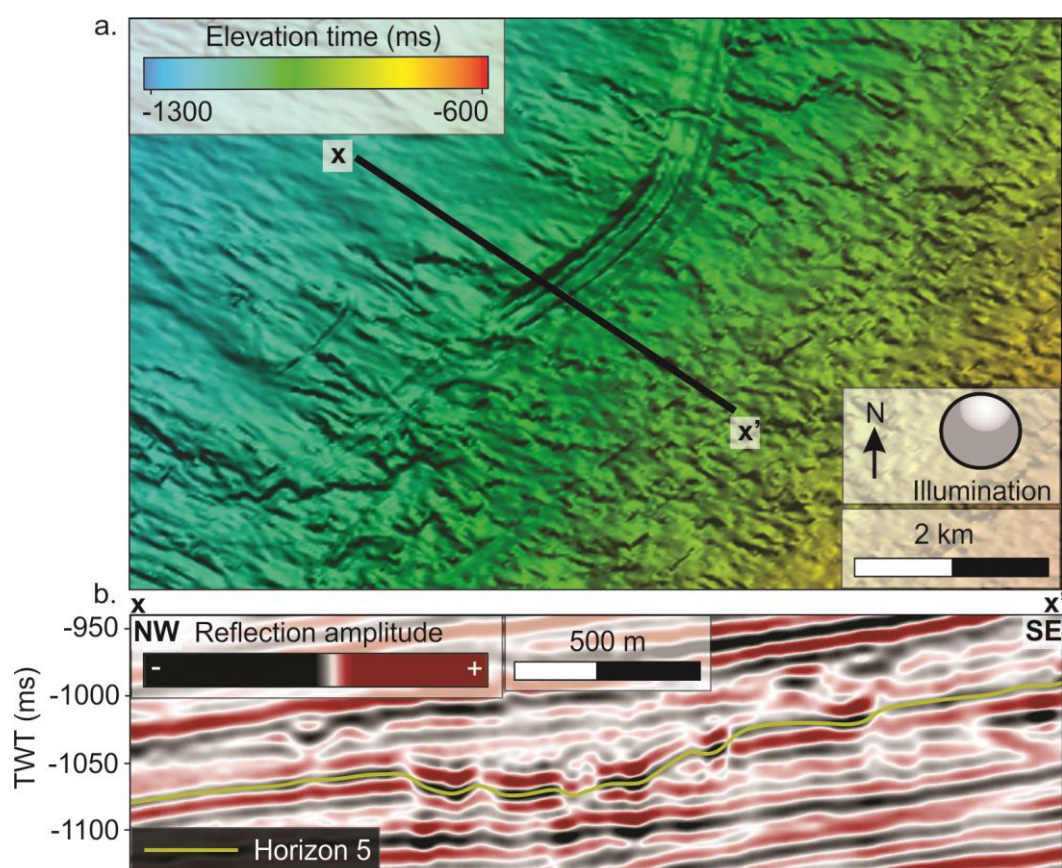
Figure 4.41: *a. The slope of the NE part of horizon 5 featuring paired furrows. The black line indicates the location of the seismic profile in b (x-x'). Vertical exaggeration is 25. b. Seismic profile across the paired furrows. The location of the figure is indicated in figure 4.40.*

Buried incisions with slope system

Two slope incisions with an E-W orientation occur on the upper part of horizon 5 (Figure 4.42). The northern incision can be followed up to 13 km downslope, is ~300 m wide and has a V-shaped relief up to 12 m. Further south, the other incision is 10 km long and up to 150 m wide. It has a V-shaped relief up to 7 m defined by a high amplitude.

An elongated, lobe-shaped feature occurs on the lower part of the slope, downslope of the northern incision. It is defined by a low amplitude reflection with surrounding moderate-to-high amplitude reflections. The lobe`s longest axis is 13 km while the lobe is up to 4 km wide. In cross-profile, it has a semi-transparent body (Figure 4.42).

Downslope of the southern incision, a system of smaller braiding high-amplitude incisions occurs. It is hard to establish whether all the high amplitude reflections are related to the incisions or not. The system is 16 km long and on average 3 km wide (Figure 4.42).

Interpretation:

The negative relief of the incisions indicate that they are a result of erosion. Similar incisions were observed on horizon 3, interpreted to have been formed by two different processes, i.e. turbidity currents and a debris flow. Amplitude variance points to larger lithological differences. Such differences suggest depositional process, type of sediment and depositional environment. The configuration and amplitude differences of the features below the incisions indicate two different systems.

Based on the seismic character and similarities to the lobe described on horizon 3, the lobe-shaped feature is interpreted to be formed by a glacigenic debris flow. Similar features have been widely studied from the Norwegian margin, for instance by Vorren and Laberg (1997).

The braiding amplitudes may indicate deposition of coarser (sandier) sediments commonly deposited by downslope processes. Therefore, a system of braiding amplitudes suggests several crisscrossing channels caused by downslope processes. A channel system like this indicate sediments with low viscosity in a lower energy environment. Similarities from the channel system in unit A occur, however, those channels are better preserved.
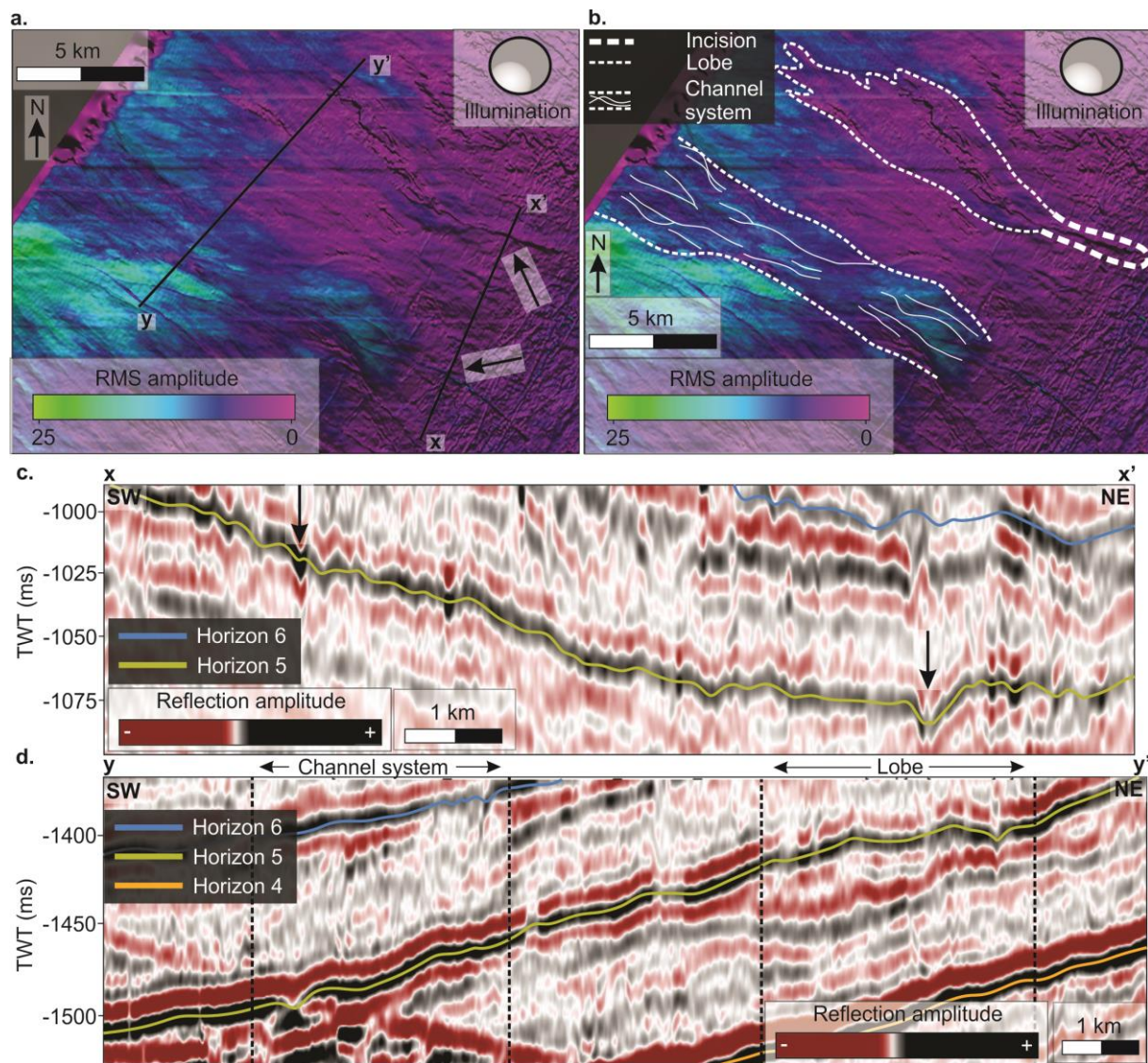
*Figure 4.42: **a.** RMS seismic amplitude map of horizon 5 showing parts of the slope. Black lines indicate seismic profiles in c. and d. Arrows correspond with arrows in c. and indicate incisions. **b.** RMS seismic amplitude map of horizon 5 with interpretation. The location of the figure is indicated in figure 4.40. **c.** Seismic profile across the incisions (indicated by arrows) on the upper part of the slope. **d.** Seismic profile across amplitude variations on the lower part of the slope. The extent of the channel system and the lobe is indicated by black dotted lines.*

4.7 Seismic horizon 6

Horizon 6 is a sigmoidal clinoform comprised of a palaeo-shelf and palaeo-slope (Figure 4.43). It marks the boundary between units C and D. The shelf of horizon 6 has a medium to high, positive reflection amplitude, where the slope has a generally low reflection amplitude. A medium amplitude occurs in the north on the upper part of the slope (Figure 4.4).

The horizon is continuous, except from two local areas on the shelf, i.e. north and north of the center (Figure 4.7). This is probably due to seismic interference and makes the interpretation tentative.

The palaeo-shelf represents a flat horizon except for the northern part where it slightly dips toward WNW. It appears as an irregular reflector, cutting off inclined reflections from horizon 5 and unit C (Figure 4.43). Some of the geomorphological landforms situated on the palaeo-shelf are detailed below (Figure 4.44).
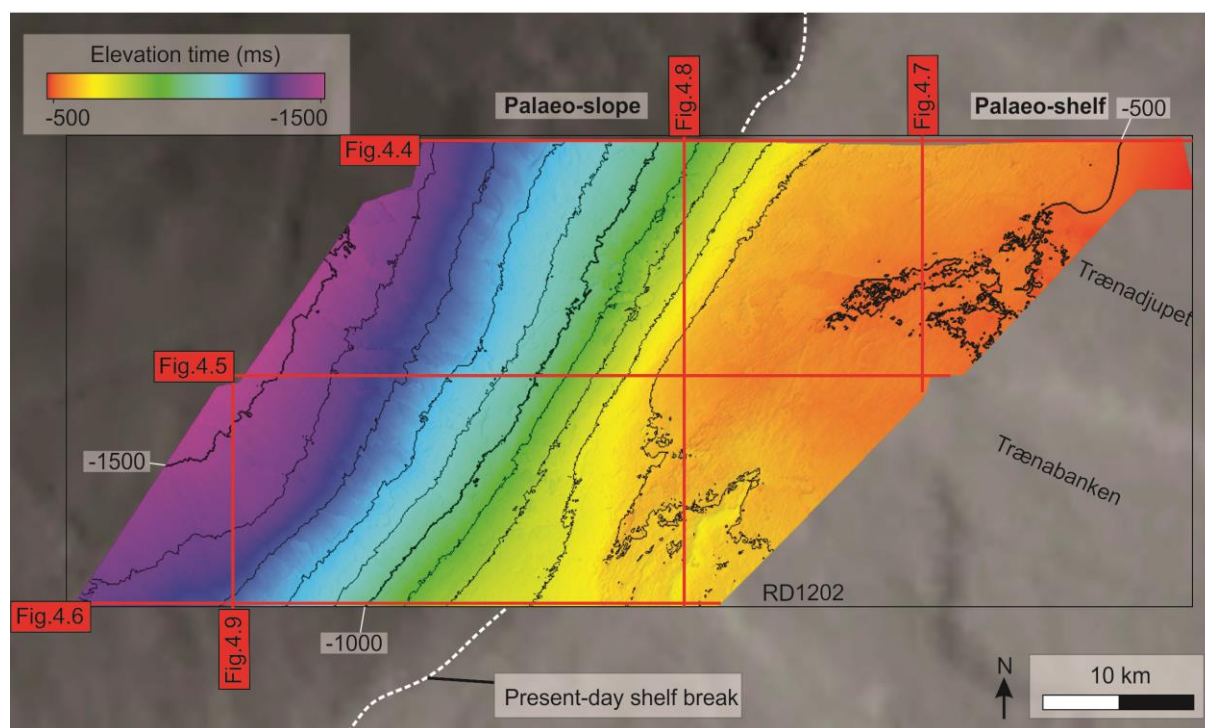
Figure 4.43: Horizon 6 situated on the continental shelf and slope within RD1202. Depths are in ms two-way travel time and the contour lines are indicated every 100 ms (bold every 500 ms).

Palaeo-shelf

On the southeastern part of the palaeo-shelf, directional lineations with a WNW-ESE orientation occur (Figure 4.44). They extend up to 3.3 km, are ~300 m wide and have a negative relief of 6 m.

Further west, an elongated depression with a NE-SW orientation occurs. It is most distinct on the southern part of the palaeo-shelf (Figure 4.44). The depression has an asymmetric negative relief where the walls vary with a gentle dip in the east to a high angel in the west. It is 10 km long, ~ 1500 m wide and on average 30 m deep. Above and below the depression, the seismic signature is acoustically transparent to chaotic separated by reflectors with weak amplitudes (Facies 4 & 6; Figure 4.10). The depression truncates underlying strata (Figure 4.45).

In front of the depression, a parabolic-shaped ridge with a series of densely spaced ridges and furrows on top occur. It is 15 ms high, can be followed up to 30 km and is ~ 5 km wide. The internal seismic signature is chaotic to acoustically transparent, separated by reflectors with a weak amplitude (Facies 4 & 5; Figure 4.10).

NW of the ridge, curvilinear furrows with a NE-SW orientation are present. They are up to 7 km long and 70 m wide.

Interpretation:

As the directional lineations previously described, these features are suggested to be formed by a fast-flowing grounded glacier on the shelf. Therefore, they are interpreted to be mega-scale glacial lineations formed in a subglacial environment. Their presence indicates an active ice stream and its flow direction.

The asymmetric negative relief of the depression implies that this is an erosional landform. Based on the geomorphology and the presence of MSGLs in the east, the depression represents a point where the glacier terminated. The glacier was stationary, and a high rate of erosion occurred. Such depressions may be reworked by meltwater which is smoothing the depression.

The positive relief and an acoustically transparent to chaotic seismic signature of the ridge, implies a depositional landform comprised of basal till. Based on its location in front of MSGLs and the erosional depression, it is interpreted to be a large terminal moraine. The series of ridges and furrows may imply seasonal variations in deposition from a glacier in a marine environment. Such moraines are often referred to as De-Geer moraines. The composition of moraines are commonly unsorted sediments and therefore possess an acoustically transparent to chaotic seismic signature. Larsen et al. (1991) describe similar features below the marine limit in the Møre area, western Norway.

Due to their morphology, the curvilinear furrows are interpreted to be plough marks similar as described earlier. Their appearance in front of the moraine supports a grounded ice-sheet where calving occurs in front.
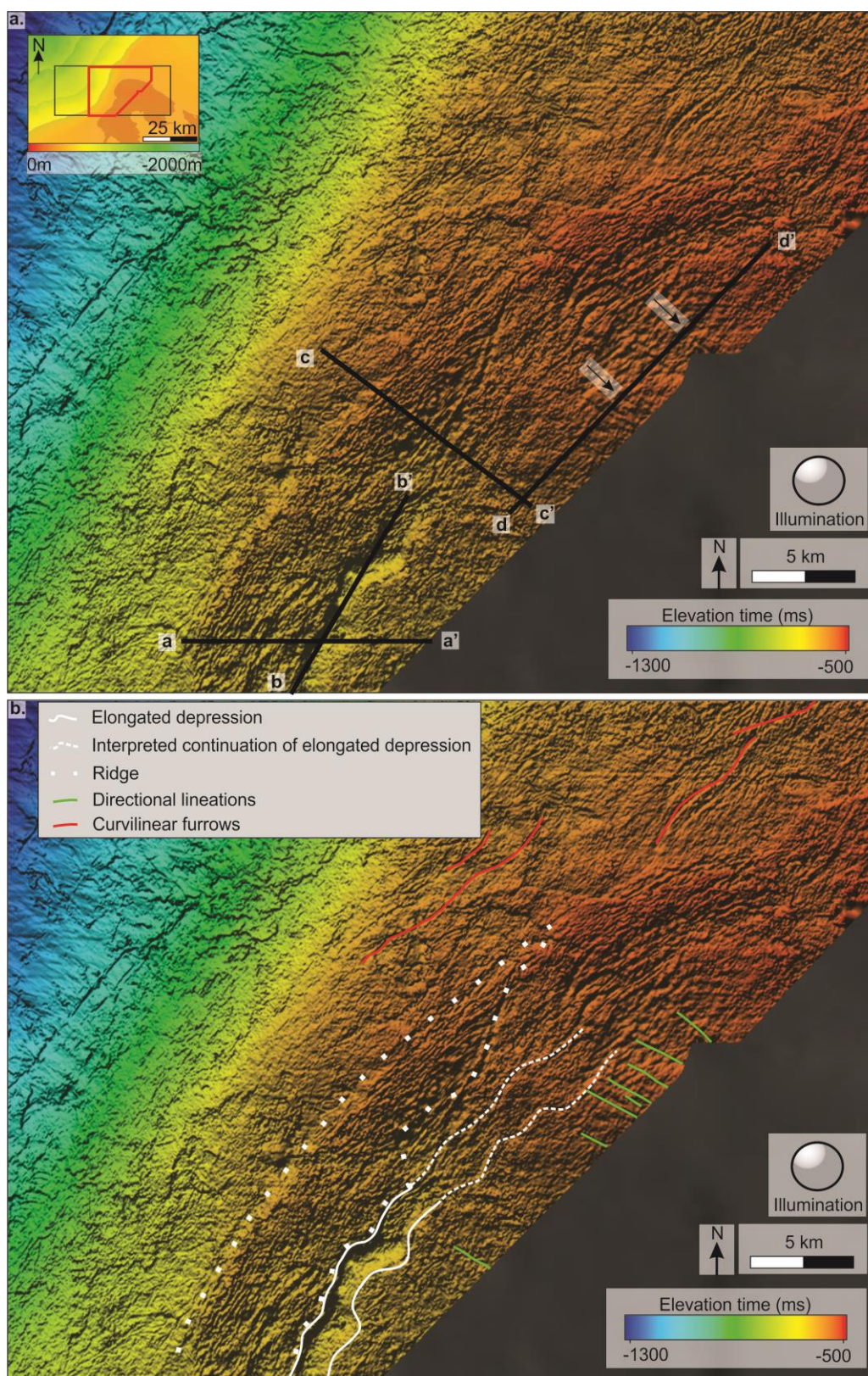
*Figure 4.44: **a.** Overview of the morphology of the shelf of horizon 6. The location of the figure is indicated by a red polygon on the inset map in the left corner and the black lines indicate the location of the seismic profiles in figure 4.45. **b.** Overview of the morphology of the shelf of horizon 6 with interpretation. Vertical exaggeration is 25.*
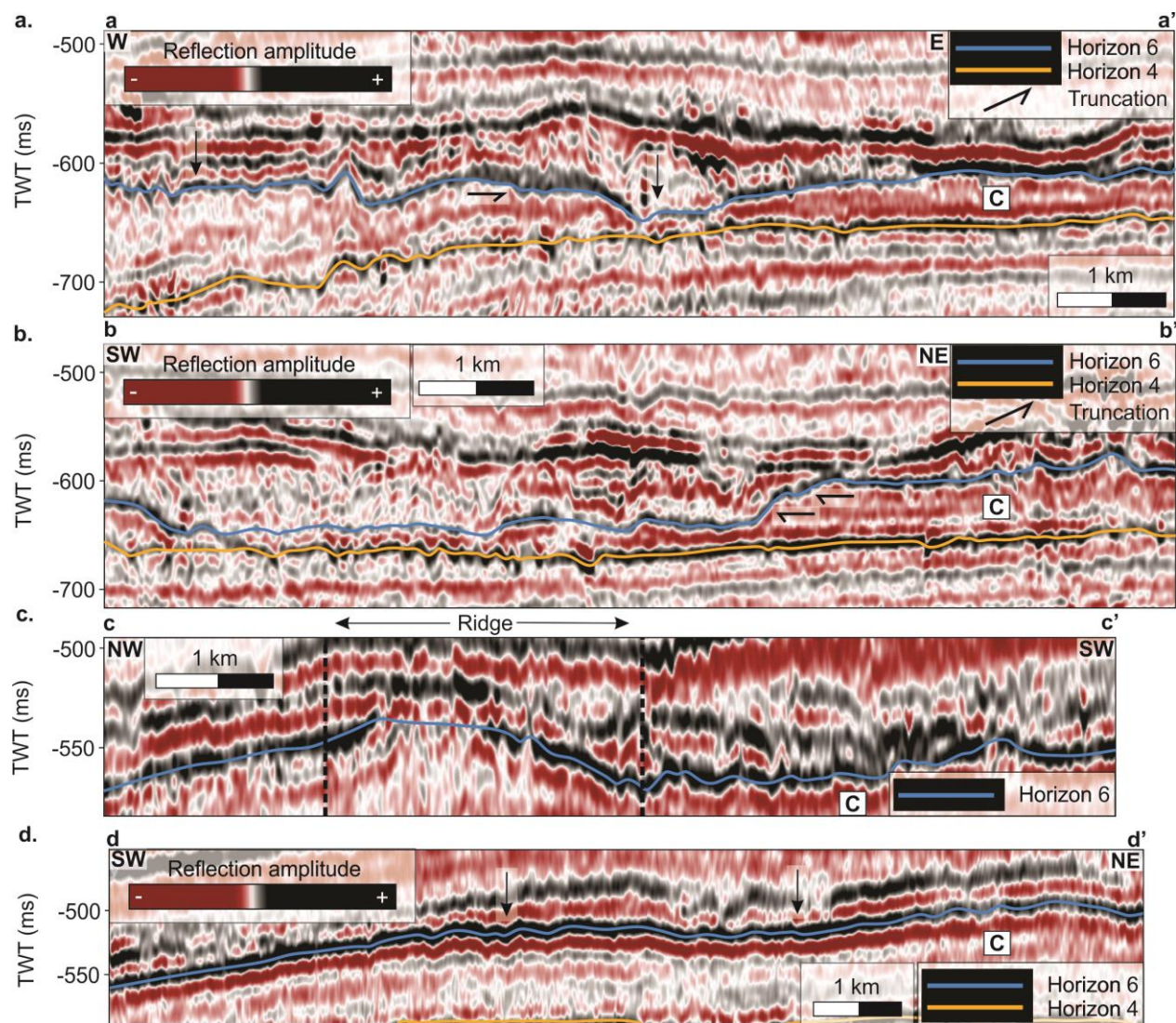
Figure 4.45: **a.** Seismic profile (a-a') across the elongated depression and ridge with interpretation. **b.** Seismic profile (b-b') along the elongated depression and ridge with interpretation. **c.** Seismic profile (c-c') across the northern part of the ridge with interpretation. **d.** Seismic profile (d-d') across the directional lineations. The ridge is delimited by black dotted lines. Location of the profiles is indicated in figure 4.44.

4.8 Seismic unit D

Seismic unit D is comprised of complex sigmoid-oblique clinoforms prograding from east to west (Figure 4.46). It is the youngest stratigraphic interval bounded by the underlying horizon 6 and the overlying seafloor horizon. The shelf has an overall sheet-shaped external form with a non-erosive mound in the center. The overall external form of the slope is comprised of two wedges, one coming from north and the other from south.

Trænadjupet Trough on the northern part of the shelf has the lowest sediment thickness. An elongated sediment accumulation is preserved on the southern part of the shelf with a NE-SW orientation. The greatest sediment thickness occurs in the south as part of the southern wedge, west of Trænabanken and Sklinnadjupet Trough (400-500 ms), where the northern wedge occurs west of Trænadjupet Trough (Figure 4.46).

The seismic signature of the shelf can be separated in two sections. On the lower part of the shelf it is acoustically, semi-transparent separated by continuous, low frequency, high amplitude reflections (Facies 3; Figure 4.10). On the upper part, it is acoustically transparent separated by low frequency reflectors with a weak to nearly absent amplitude (Facies 4; Figure 4.10). The highest amplitudes appear in the northeastern part of the shelf, i.e. the area of Trænadjupet Trough (Figure 4.47).

Unit D consists of continuous, inclined, parallel, medium frequency reflections with a generally low amplitude on the slope (Facies 1; Figure 4.10). Some chaotic and high amplitude reflections (Facies 6; Figure 4.10) occur locally at the center of the unit.

Interpretation:

With an east-west orientation, the complex sigmoid-oblique clinoforms indicate a prograding, alternating slope system. The sheet-shaped external form of the shelf indicates a uniform sedimentation, often caused by sediments deposited out of suspension (Veeken, 2007). The low sedimentation and high reflection amplitude of Trænadjupet Trough imply erosion over a large area. Directional lineations on horizon 6 and the seafloor in the same area suggest that this is caused by a fast-flowing ice-stream. One possible interpretation is that the internal

seismic signature of the shelf is basal till deposited as a combination of material from suspension and subglacial processes.

The wedge-shaped external forms on the slope indicate a lateral change in sedimentation rate along the slope. These accumulations occur due to high cross-shelf sediment transport by fast-flowing ice-streams. The greatest sediment accumulation of the unit is sourced from the south. This may imply a more active Sklinnadjupet Trough than Trænadjupet Trough during that period. The sediment accumulated ridge on the southern part of the shelf, supports the interpretation made earlier of deposition of a terminal moraine. On the slope, the internal seismic signature suggests a combination of hemipelagic sediments and slide debrites.

The non-erosive mound in the center of the shelf can be a result of less or absent erosion compared to adjacent areas. This may be caused by slow-flowing ice covering the area, i.e. today's Trænabanken.
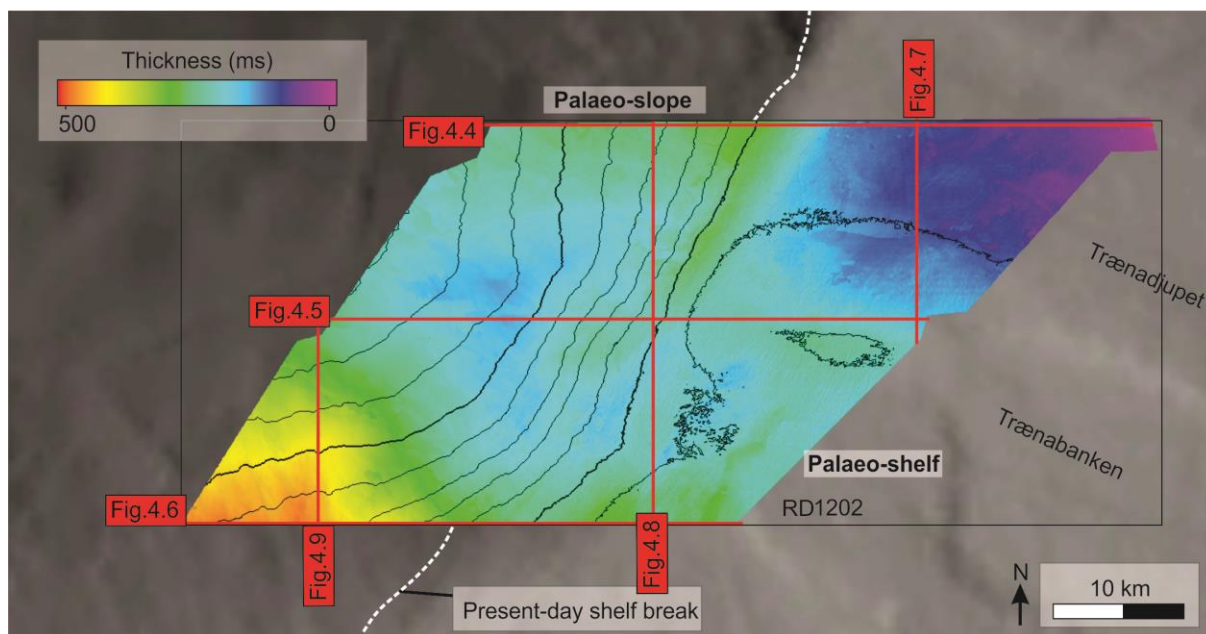
Figure 4.46: Thickness map of seismic unit D situated on the continental shelf and slope within RD1202. The map was defined between horizon 6 and seafloor horizons. Contour intervals are 100 ms (bold every 500 ms) and vertical exaggeration is 10.
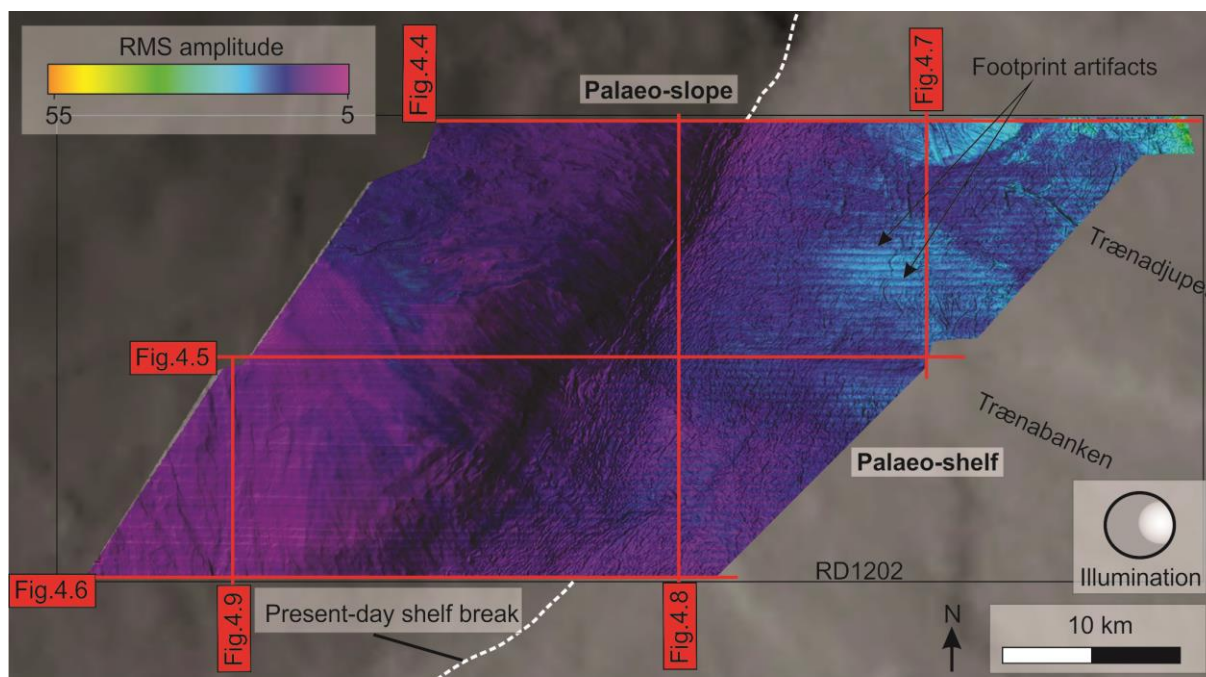
Figure 4.47: RMS seismic amplitude map of unit D situated on the continental shelf and slope within RD1202. The map was defined between horizon 6 and the seafloor horizon. Vertical exaggeration is 25.

4.8.1 Wedge on the lower slope

A wedge-shaped feature on the western part of the study area is delimited by two intra unit boundaries, covering an area of ~180 km^2. It is initiated at 1100 ms on the lower part of the slope with a NW-SE orientation (Figure 4.48).

The lower boundary is 15 km long in NW-SE direction and present from the south of the study area up to 30 km in NE direction. It has a NW-SE dipping trend, with the highest dip in the SE, flattening toward NW. The reflector is slightly irregular, continuous with a medium to high reflection amplitude. Curvilinear furrows occur on the lower boundary, where the majority have a NW-SE orientation along the slope. They are up to 15 km long and 1.3 km wide. A paired furrow with a NW-SE orientation crosses one of them.

The upper boundary is up to 14 km long and 26 km wide with an NNW-SSE dipping trend. It is an irregular, convex, and continuous reflector with a strong, positive reflection amplitude. Some local interference may occur, and this has caused difficulties regarding the interpretation of the southeastern part of the wedge. The upper boundary is covered by incisions and small lobes with the same orientation as the dipping trend of the boundary.

On the southwestern part of the wedge, the greatest sediment thickness (200-225 ms) occurs, gradually thinning toward NE (0-25 ms), where the accumulation pinches out. The internal seismic reflection is predominantly semi-continuous to discontinuous with a general low reflection amplitude. Locally, some areas are acoustically transparent. Internal reflectors of the wedge onlap the lower boundary in east. NNW-SSE orientated braided channels occur as high amplitudes in the northeastern part of the wedge (Figure 4.48c).

Interpretation:

Based on the NE pinch-out of the wedge and the NW-SE orientation of the incisions and small lobes, the sediments are most likely coming from SE of the study area. Onlapping strata imply an unconformity and a gap in sedimentation. The internal seismic signature suggests that this wedge is composed of gravity-driven sediments. High amplitude can be an indication of where the material is coming from. The high amplitude channels on the northwestern part of the fan are interpreted to be stacked debris flows, thus, this wedge is interpreted to be a sedimentary fan deposited by downslope processes.

117
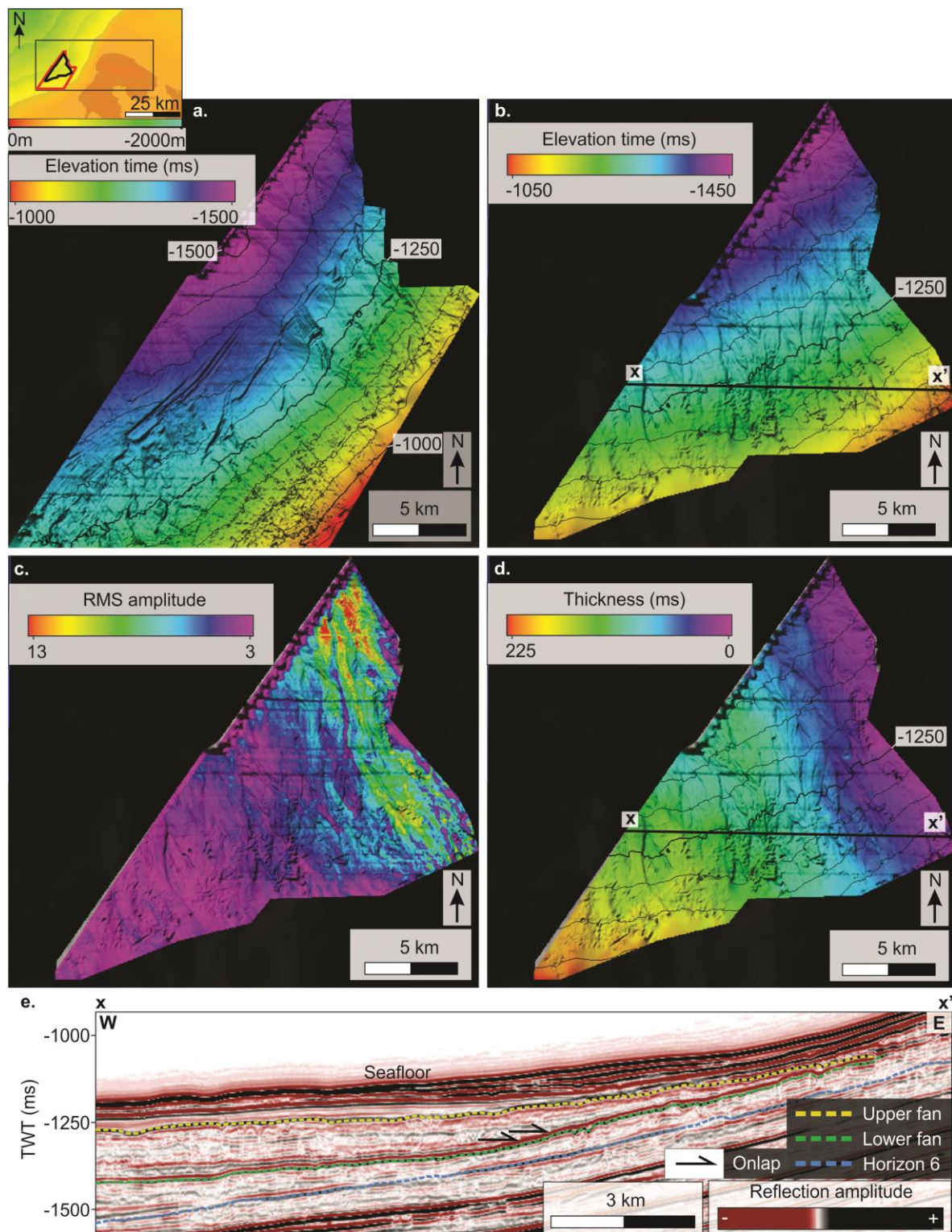
*Figure 4.48: **a.** Lower boundary reflector of the wedge. **b.** Upper boundary reflector of the wedge. The black line indicates the location of the seismic profile in e. (x-x'). **c.** RMS amplitude map of the seismic volume between upper and lower boundary reflectors. **d.** Thickness map of the seismic volume between the upper and lower boundary of the wedge. Depths are in ms two-way travel time and the contour lines are indicated every 50 ms (bold every 250 ms). The location of the lower boundary reflector is indicated as a red polygon and the upper boundary reflector by a black polygon on the inset map in the left corner. Vertical exaggeration is 25. **d.** Seismic profile (x-x') across the wedge with interpretation.*

118

Mounded deposit

Overlying the sediment wedge, a mounded deposit with an NE-SW orientation occurs along the lower part of the slope (Figure 4.49). The extent of the lower boundary of the mounded deposit was limited. The upper boundary is 40 km long and 18 km wide. Its thickness increases from SW to NE and can be up to 110 ms. The internal seismic signature of the mounded deposit is laminated and acoustically transparent to semi-transparent separated by weak reflectors. These reflectors have an onlapping trend on to the underlying slope.

Interpretation:

Based on the internal seismic signature, these sediments are suggested to be composed of hemipelagic sediments with slightly homogeneous composition. This and the extent of the deposit, imply sediments influenced by along-slope currents. The mounded and onlapping configuration of the deposit indicate an unconformity, a gap in sedimentation and a 'climbing deposit'. Finally, the deposit is delimited by medium to strong amplitudes and is therefore interpreted to be part of a contourite drift.
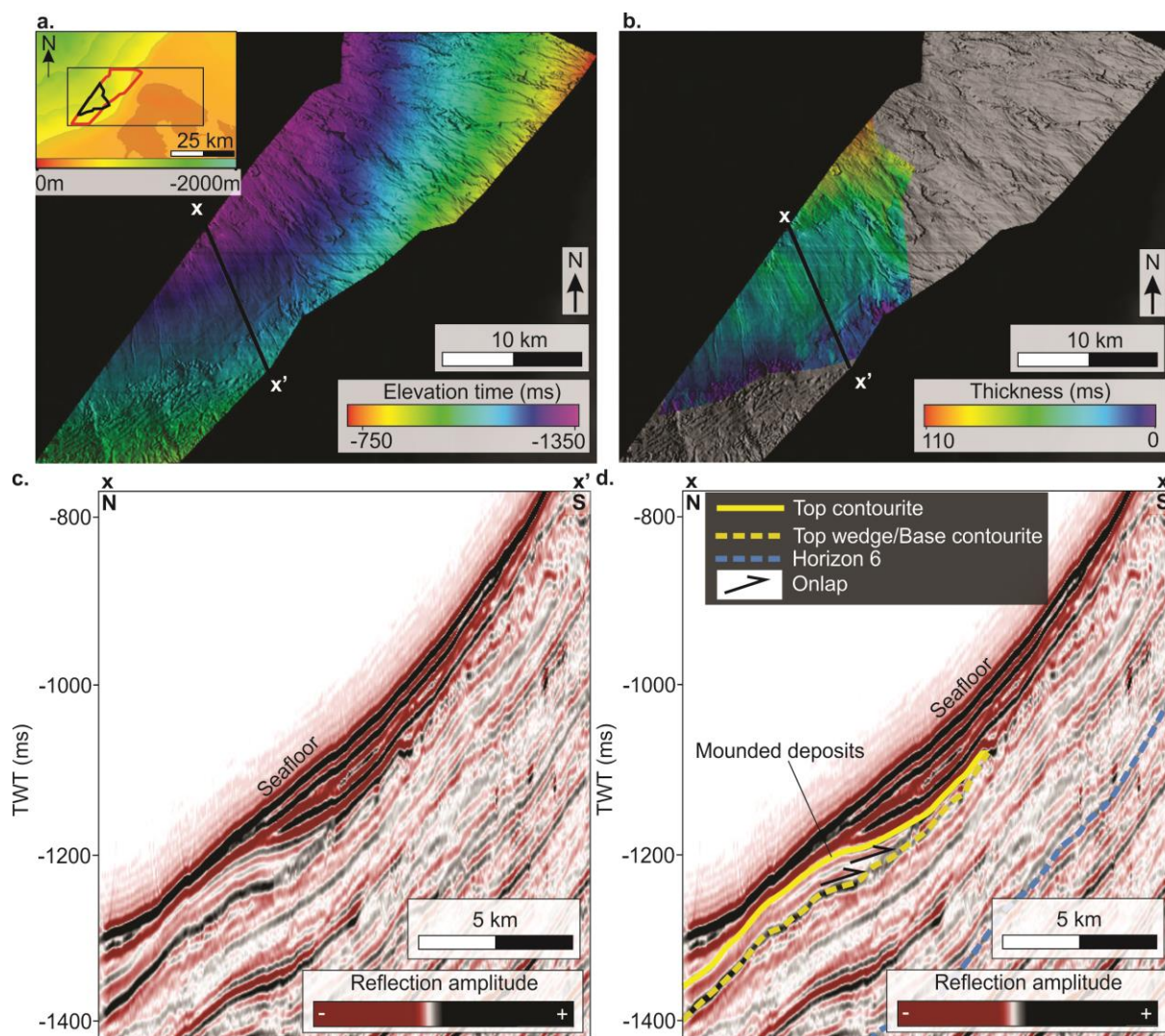
Figure 4.49: **a.** Upper boundary reflector of the mounded deposits. The black line indicates the location of the seismic profile in c. and d. (x-x'). **b.** Thickness map of the seismic volume between the upper and lower boundary of the mounded drift. The lower boundary corresponds to the upper boundary of the wedge in figure 4.48 and the upper reflector to the upper boundary shown in a. In the inset map in the left corner, the location of the lower boundary reflector is indicated as a red polygon and the upper boundary reflector by a black polygon. Vertical exaggeration is 20. **c.** Seismic profile (x-x') across the mounded deposits without interpretation. **d.** Seismic profile (x-x') across the mounded deposits with interpretation.

4.9 Seafloor horizon

The seafloor horizon is a sigmoidal clinoform comprised of shelf and slope (Figure 4.50). It marks the uppermost boundary in this study. The reflector is continuous with a strong, positive reflection amplitude (Figure 4.4-4.9).

Generally, the shelf represents a flat reflector with elevated areas in the south and in the center. The slope has an overall gentle dip toward NW with the greatest dip angle in the center of the upper part (Figure 4.50). Some smaller geomorphological landforms are detailed below (Figure 4.51).
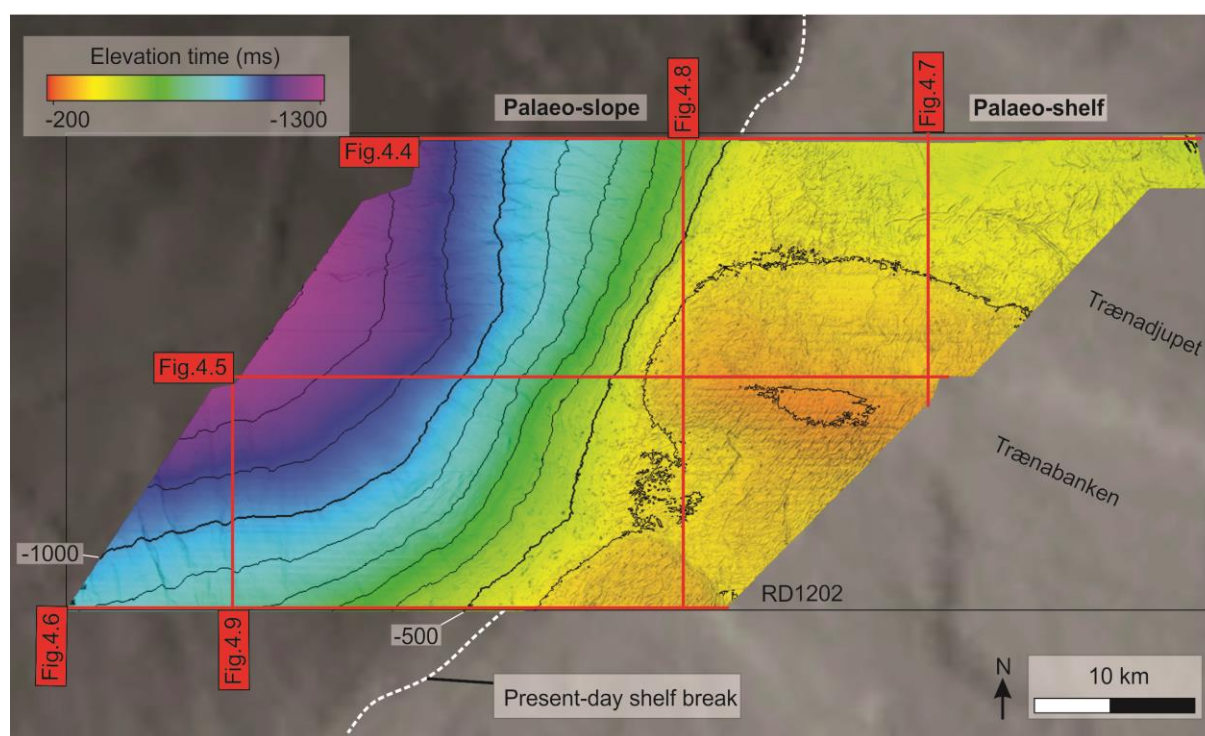
Figure 4.50: The seafloor horizon situated on the continental shelf and slope within RD1202. Depths are in ms two-way travel time and the contour lines are indicated every 100 ms (bold every 500 ms). Vertical exaggeration is 10.
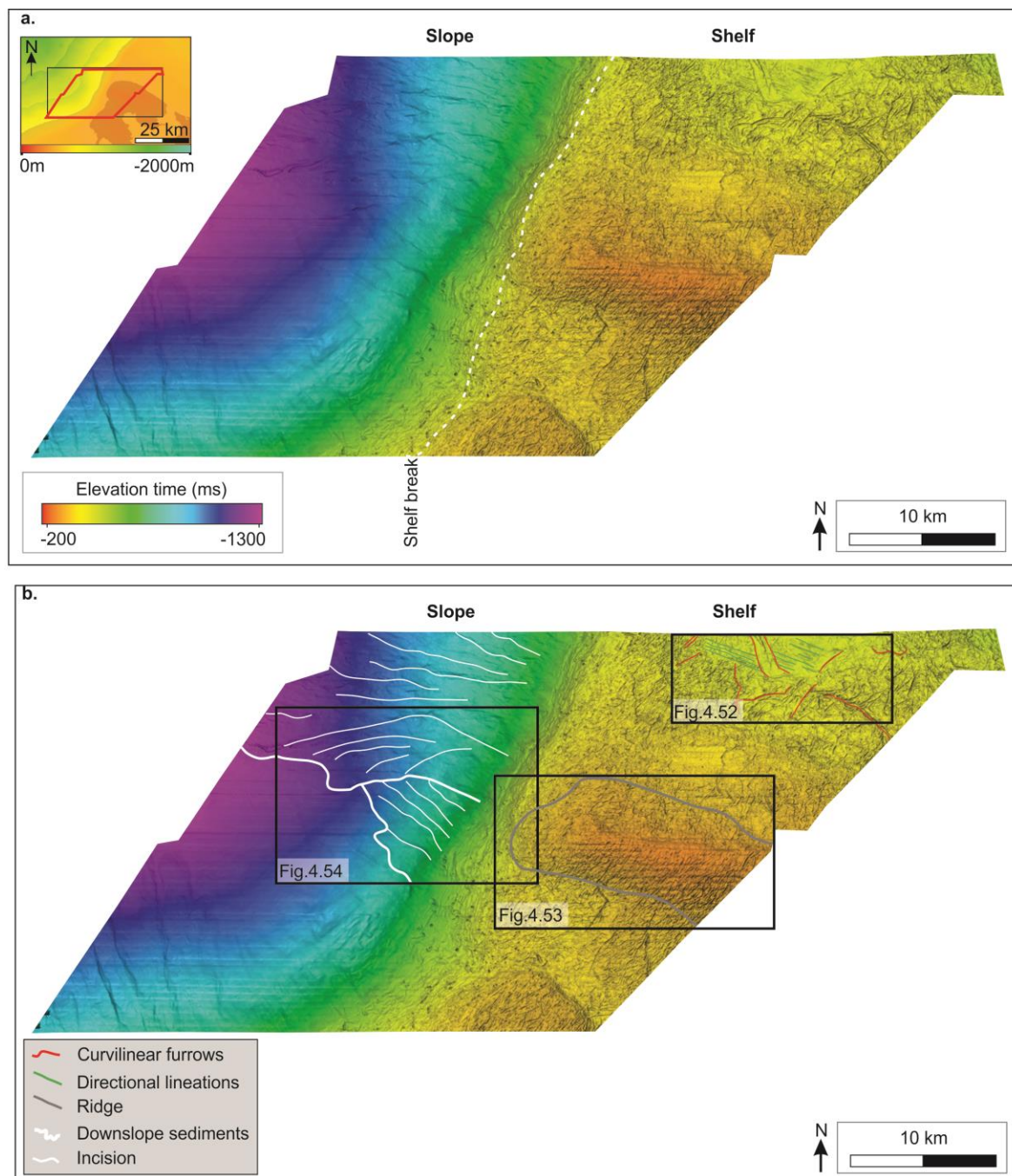
Figure 4.51: **a.** Overview of the morphology of the seafloor horizon within the study area divided into shelf and slope (indicated by dotted white line). The location of the horizon is indicated by a red polygon on the inset map in the left corner. **b.** Seafloor horizon with interpreted morphology. Figure 4.52-4.54 are indicated by black polygons. Vertical exaggeration is 25.

Directional lineations and curvilinear furrows

On the northern part of the shelf, a set of directional lineations with a NW-SE orientation extent with 9 km length and width up to 4 km (Figure 4.52). The spacing between the directional lineations is 150-300 m and it is hard to distinguish whether the relief is negative or positive. These features are similar to the directional lineations described on the palaeo-shelf of horizon 1, but only occur in a small area on the middle part of the shelf. They appear as an amplitude anomaly delineating the feature. Curvilinear furrows surround the directional lineations and some are crosscutting them (Figure 4.52).

The curvilinear furrows are crisscrossing each other and do not have a general orientation trend. They are up to 7 km long with widths up to 600 m. Variance attribute illustrates the curvilinear furrows and make them easier to distinguish from the directional lineations (Figure 4.52b). In a cross-profile, they have a negative U- to V-shaped relief ranging between 6-30 m (Figure 4.52d).

Interpretation:

Similar to the directional lineations previously described, these features are interpreted to be formed by a fast-flowing grounded glacier on the shelf. Hence, they would be mega-scale glacial lineations preserved in a subglacial environment. Their orientation and extent imply the palaeo-ice flow direction.

The morphology of the curvilinear furrows suggests that these are iceberg plough marks, similar as described earlier. Some of the curvilinear furrows crosscut the directional lineations, which imply a younger relative age. This may also indicate that few icebergs were large enough to plough the seafloor where the MSGLs are preserved. No general orientation pattern of the plough marks may indicate little or no influence by ocean currents on the iceberg drift.
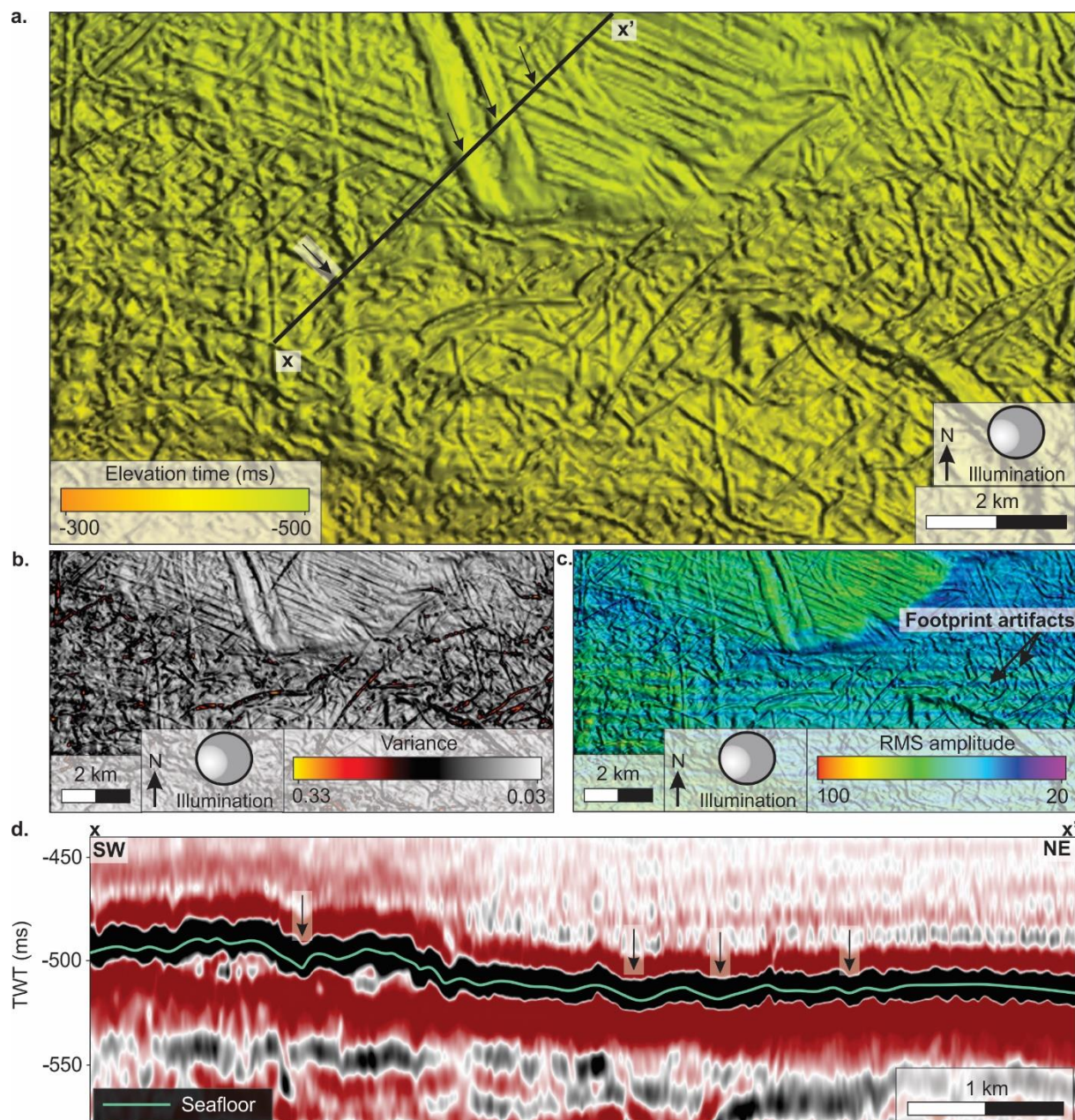
Figure 4.52: *a.* The shelf of the northern part of the seafloor horizon featuring directional lineations and curvilinear furrows. The black line indicates the location of the seismic profile in d. (x-x'). *b.* Variance map of the same area as in a. featuring directional lineations and curvilinear furrows. *c.* RMS amplitude map of the same area as in a. featuring directional lineations and curvilinear furrows. Vertical exaggeration is 25. The location of the figure is indicated in figure 4.51. *d.* Seismic profile with interpretation across the directional lineations and some of the curvilinear furrows. Arrows indicate some of the most distinct curvilinear furrows.

Large-scale ridge

A large-scale ridge with a WNW-ESE orientation occurs on the shelf in the center of the study area (Figure 4.53). It is 16 km long and 8 km wide with a positive relief of up to 90 m. The ridge appears as a boundary between Trænadjupet in the north and part of Sklinnadjupet in the south. In cross-profile, it is acoustically transparent separated by weak amplitude reflectors (Facies 4; Figure 4.10).

Interpretation:

The geomorphology and internal seismic signature of the ridge leads to the interpretation that this is a lateral moraine comprised of basal till. Based on the geographical position it is interpreted to be Gamlembanken.
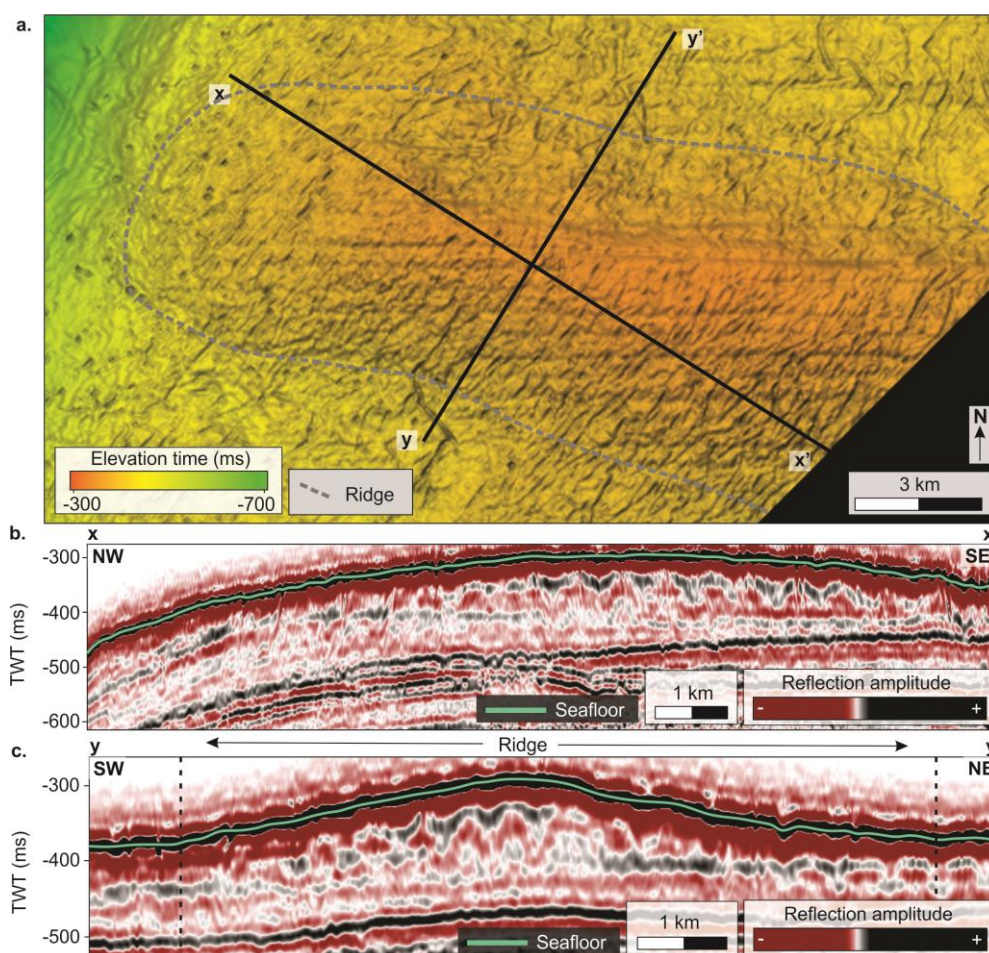
*Figure 4.53: **a.** The shelf of the seafloor horizon featuring a ridge in the center of the study area. The black lines indicate the location of the seismic profiles in b (x-x') and c (y-y'). Vertical exaggeration is 25. **b.** Seismic profile along the ridge. **c.** Seismic profile across the ridge. The ridge is delimited by black, dotted lines. The location of the figure is indicated in figure 4.51.*

Wedges on the slope

Two different sized wedge-shaped features occur on the northern part of the slope (Figure 4.54). They are defined by a high amplitude positive relief. The southern wedge is comprised of two fronts and has a NW-SE orientation. It is 7 km long and wide with an up to 45 m relief. Several incisions occur on top of the wedge orientated in the same manner as the wedge.

The northern wedge occurs west of Trænadjupet Trough with a WSW-ENE orientation. It has a relief of up to 83 m with an increasing trend toward NE. A number of incisions occur on top, leading into small lobes on the western part of the wedge. The wedge is up to 21 km long and can be followed up to 8 km in the northern direction. It overlaps the northern part of the smaller wedge (Figure 4.54).

Interpretation:

The orientation of the wedges imply that they are sourced from two different parts of the shelf. The greatest sediment input occurs in the north, i.e. the wedge in front of Trænadjupet Trough. Both wedges are comprised of several incisions and lobes which indicates that they are built by downslope processes over time. Such sedimentary build-ups are commonly referred to as fans. The overlapping wedges indicate that the northern wedge was active after the deposition of the southern wedge. Based on these implications, these wedges are interpreted to be trough mouth fans (TMFs) of different scales.
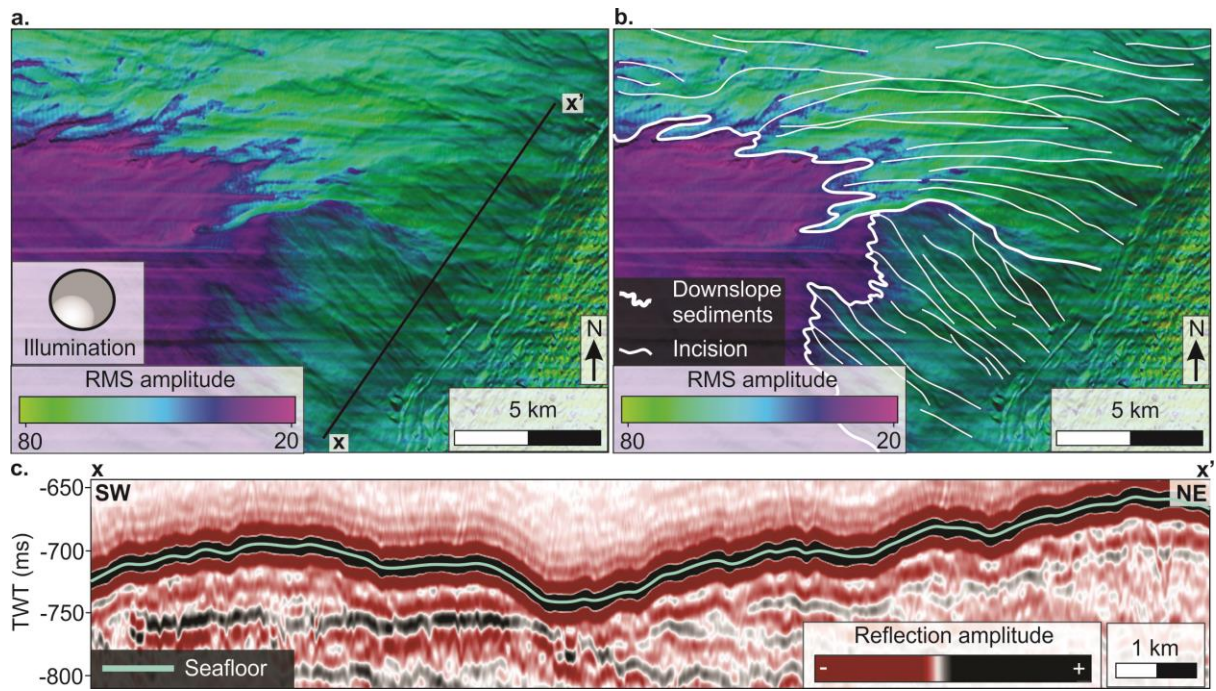
*Figure 4.54: **a**. RMS seismic amplitude map of seafloor horizon showing parts of the slope. Black line indicates the seismic profile in c. **b**. RMS seismic amplitude map of seafloor horizon with interpretation. The location of the figure is indicated in figure 4.51. **c**. Seismic profile across the incisions on the upper part of the slope.*

4.10 Summary

The sediment distribution and geomorphological features found, described, and interpreted in this study can be used to reconstruct the glacial history of the area (Table 4.1) (Figure 4.55). Generally, the shelf and slope in the study area are part of a prograding margin formed by glacial processes, predominantly sourced from Sklinnadjupet Trough. An increase in deposition of sediments from Trænadjupet Trough occurs in the youngest unit.
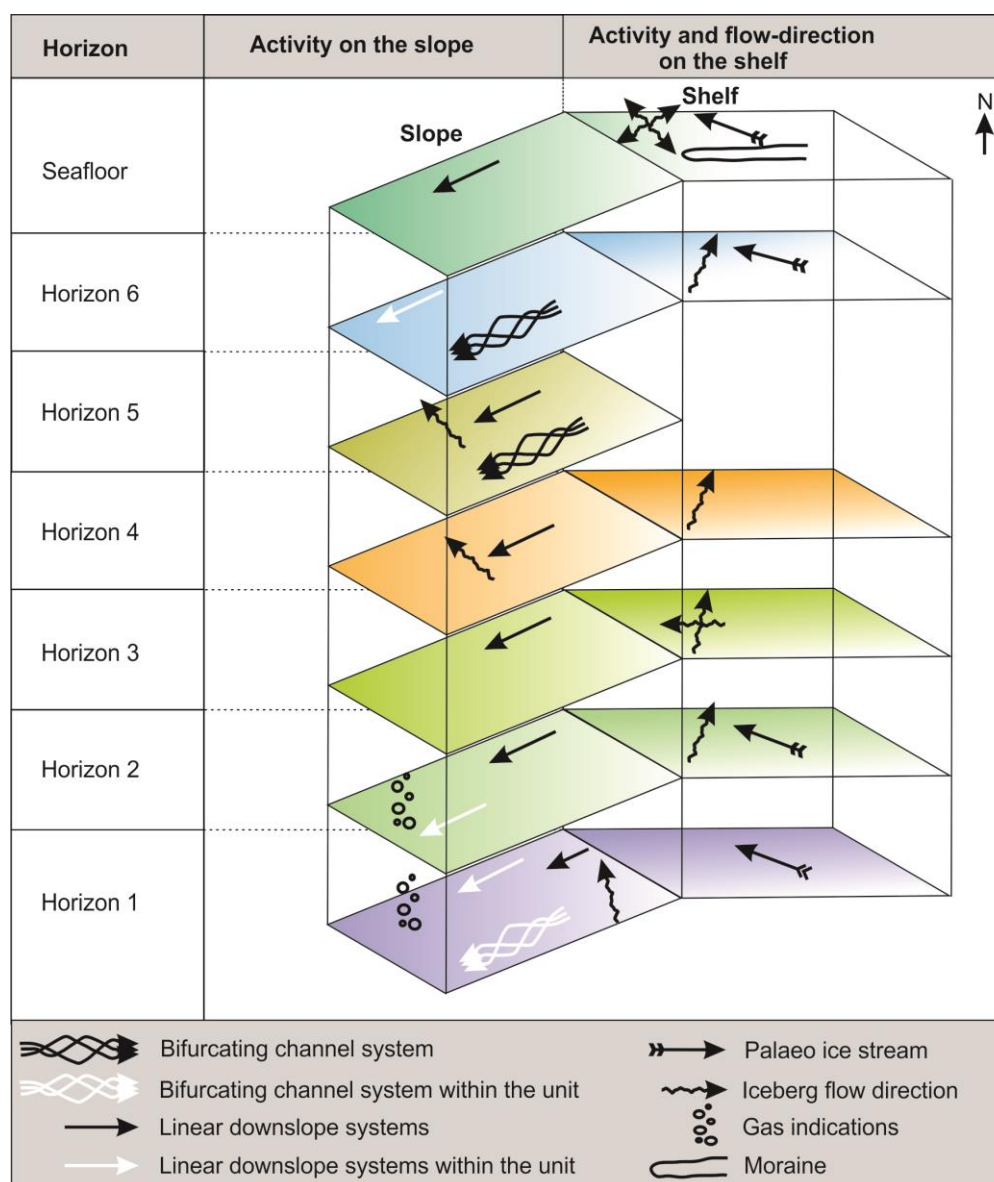
Figure 4.55: Sketch of the buried horizons and seafloor where flow directions of palaeo-ice-flow, ocean currents and different types of slope activity are indicated

128

Table 4.1: Dimensions and orientations of geomorphological features in this study. MSGLs - mega scale glacial lineations; TMFs - trough mouth fans.

	Length	Width	Relief (+/-)	Orientation
Horizon 1				
MSGLs	8.5 km	120-200 m (up to 300 m)	Up to 9 m	NW-SE
Slide -lobes	7-14 km	3 km	(+) Up to 17 m	W to WNW
Plough marks	3-7 km	250 m	(-)5-11 m	Crisscrossing to sub-parallel to the shelf break
Depressions	850 m	850 m	(-)10-50 m	
Unit A				
Channel system 1	Up to 21 km	Up to 4 km		NW-SE
Channel system 2	37 km	4.5-5.5 km		E-W
Channel system 3	13	7 km		NW-SE
Channel system 4	16 km	3 km		NW-SE
Fans	8-16 km	6 km		E-W
Horizon 2				
MSGLs	15 km	100-160 m	Up to 12 m	NW-SE
Plough marks	8 km	70-100 m	(-) 10-12 m	Sub-parallel to the shelf break
Channels	12 km	700-2500 m	(-) up to 20 m	NW-SE

Horizon 3				
Plough marks	15 km	150 m	(-) 6 m	NNE-SSW
Plough marks	11 km	150-350 m	(-) 13 m	E-W
Buried incisions	7 km	700-1000 m	(-) up to 40 m	ESE-WNW
Fan	16 km	6 km	(+) tens of meters	ESE-WNW
Unit B				
Channels	18 km	2-6 km	(-)	NW-SE
Horizon 4				
Depression	6 km	1 km	(-) Up to 37 m	E-W
Plough mark	33 km	50 – 300 m	(-) 18 m	NNE-SSW
Channels	13-16 km	Up to 3 km	(-) 6-8 m	WNW-ESW
Horizon 5				
Paired plough mark	5 km	600-800 m	(-) 25 m	NNE-SSW
Buried incisions	10-13 km	150-300m	(-) 7-12 m	E-W
Fan	13 km	4 km		E-W
Channel system	16 km	3 km		E-W
Unit C				
Horizon 6				
MSGLs	3.3 km	300m	6 m	WNW-ESE
Depression	10 km	1500 m	(-) up to 33 m	NE-SW

Terminal moraine	30 km	5 km	(+)	NE-SW
Plough marks	7 km	70 m	(-)	NE-SW
Unit D				
Lower wedge	15 km	30 km (NE-SW)		NW-SE
Upper wedge	14 km	26 km		NW-SE
Mounded deposit	40 km	18 km	(+) 110 ms	
Seafloor				
MSGLs	9 km	150-300 m	4 m	NW-SE
Plough marks	Up to 7 km	Up to 600 m	(-) 6-30 m	None
Gamlembanken	16 km	8 km	90 m	WNW-ESE
TMF S	7 km	7 km	(+) 45 m	NW-SE
TMF N	21 km	8 km	(+) 83 m	WSW-WNE

5 Discussion

In the first part of this chapter, the established seismic stratigraphy is correlated to previous work in the area. In the second part, the late Cenozoic evolution and glacial history of the study area are reconstructed in three stages. The evolution is discussed in chronological order, i.e. from oldest to youngest. Finally, shallow gas accumulations from the area are shortly discussed.

5.1 Correlation of seismic stratigraphy to previous work

In addition to correlation with Ottesen et al. (2009), the seismic stratigraphic framework in this study has been correlated with Dahlgren et al. (2002a) (Figure 5.1 & Figure 5.2). Dahlgren et al. (2002a) shows a regional profile located slightly SW of the study area and therefore correlations are done predominantly based on table 2.1 but also similarities from the buried seismic signature.

Dahlgren et al. (2002a) has achieved a chronological/lithological framework based on correlation of seismic data to scientific boreholes and short gravity cores. Based on high-resolution seismic data, they divided the stratigraphy of the Naust Formation on the mid-Norwegian margin into units A, B, C, D and E with sub-units (e.g A1 and A2, and B1, B2, B3 and B4, and C1 and C2).

Unit A and the lower part of unit B in this thesis is correlated to what Dahlgren et al. (2002a) defines as Naust D, and Naust C are correlates to the upper part of unit B as well as unit C in this study. Unit D is correlated to comprise Naust B and Naust A. Dahlgren et al. (2002) describe URU as the boundary between Naust A2 and B4 (Figure 5.3).
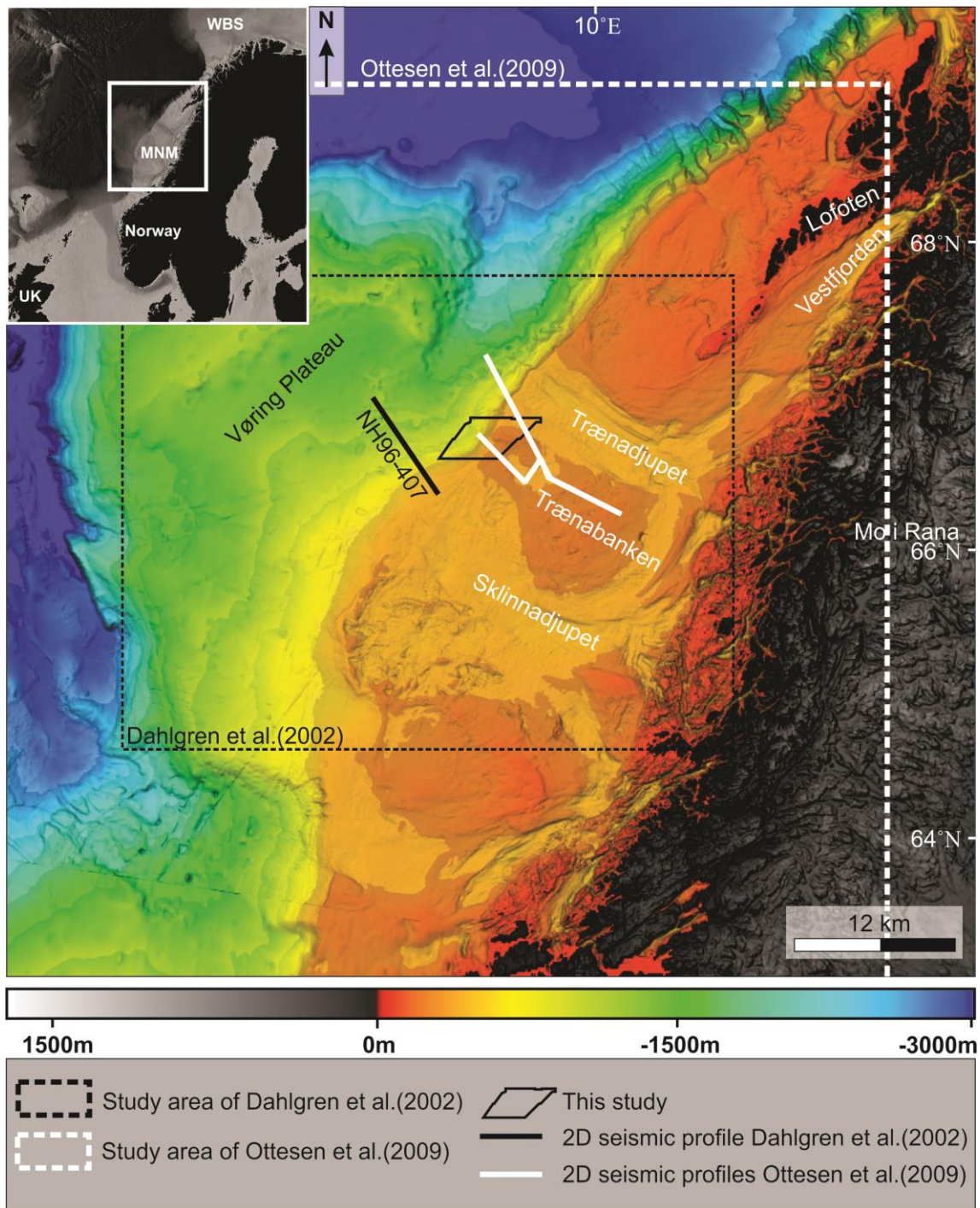
Figure 5.1: Regional bathymetric map of the mid-Norwegian continental shelf with compilation of previous work in the area. Study area of Ottesen et al. (2009) reaches Sognefjorden in the south but this is not indicated in the figure.

133

Stratigraphic legend

This study			Ottesen et al. (2009) / Rise et al. (2010)		Dahlgren et al. (2002)	
UNITS	MAIN UNIT BOUNDARY	INTERNAL UNIT BOUNDARY	AGE	UNITS	UNITS	AGE
	Seafloor					
D				Naust S+T	Naust B+A	
	Horizon 6		0.4 Ma		· · · · · ·	·0.4 Ma· ·
C		Horizon 5		Naust U	Naust C	
	Horizon 4					
B		Horizon 3	0.8 Ma		· · · · · ·	·0.5 Ma· ·
	Horizon 2			Naust A	Naust D	
A						
	Horizon 1					
			1.5 Ma ↓			0.9-1.1 Ma ↓

Figure 5.2: Correlations of seismic unit and horizons from studies done on mid-Norwegian continental shelf and slope. The arrows indicate age estimates of Naust A and Naust D base which are not included in this study.
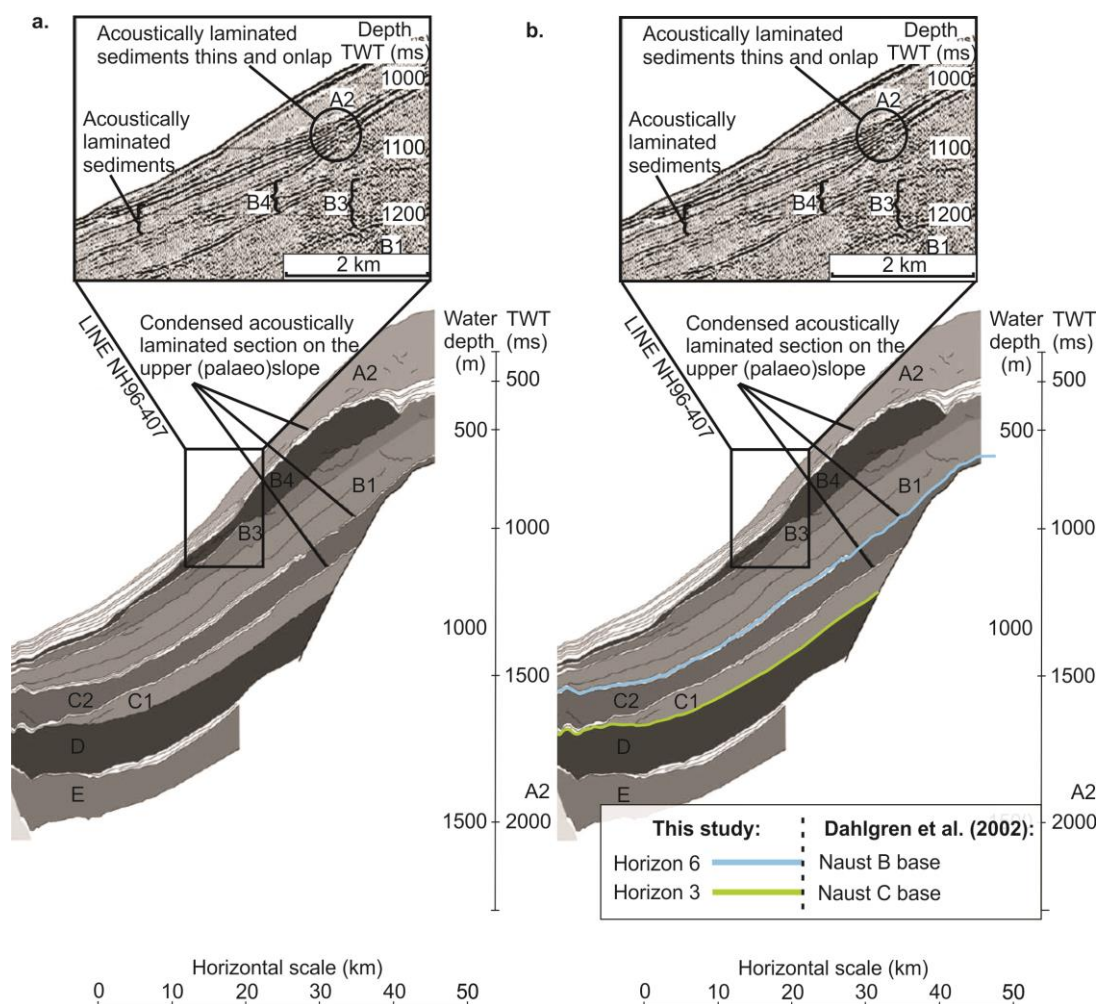
Figure 5.3: **a.** 2D-seismic profile NH96-407 interpreted and used by Dahlgren et al. (2002a). **b.** Profile NH96-407 correlated to horizons interpreted in this study. The location of the profile is indicated in figure 5.1. Modified from Dahlgren et al. (2002a).

134

5.2 Reconstruction of the ice-sheet dynamics and sedimentary processes in the outer area of Trænadjupet Trough and Trænabanken

5.2.1 Depositional stage 1 (unit A)

The large sediment volumes of the early stages of the Naust Formation is interpreted to represent deposition from an ice-sheet on the continental shelf, as previously also indicated by Dahlgren et al. (2002a) and Ottesen et al. (2009). During depositional stage 1, a grounded glacier reached the palaeo-shelf break and the palaeo-slope prograded westwards as downslope processes build out the margin (Figure 5.4).

A fast-flowing ice-stream traversed the shelf in this period, as evidenced by MSGLs on the continental shelf of horizon 1 (Figure 4.13). Ice masses were drained from the Scandinavian mainland, advancing across the shelf in an NW-SE direction within Trænadjupet Trough. The abrupt ending of these lineations indicate that the grounded and fast-flowing ice-stream extended all the way to the palaeo-shelf break. Evidence of a grounded fast-flowing ice-stream occupying palaeo-Trænadjupet and reaching the shelf break, suggests that large amount of glacial till was subglacially transported and deposited on the outer shelf and upper slope. The main depocenter occurs as a wedge on the southern part of the slope (Figure 4.18), indicating a substantial sediment transport to this area, which suggests that active ice-streams also were present on the continental shelf south of the study area, i.e. in the Sklinnadjupet Trough.

Landforms caused by gravity-driven processes on the continental slope provide information, which can support observations on the shelf. However, morphological landforms from the palaeo-slope on the mid-Norwegian margin are less studied than the morphology of the shelf. The configuration of the slope sediments suggests two main downslope processes: debris flows and turbidity currents, where evidence of turbidity currents only occur in the south.

Slide-lobes interpreted to be deposited by debris flows occur below the shelf break (Figure 4.14). Based on the morphology of these lobes, sediments have most likely accumulated in front of the glacier, become unstable and slumped onto the upper slope. It is likely that such debris flows also reached deeper parts of the slope, as similar deposits are observed on the

lower part of the slope (Figure 4.22). The internal seismic signature and reflection amplitude of these remobilized sediments has a different composition than surrounding sediments, and they are interpreted to be debris flow deposits. Well-defined fan-shapes occur in the north, but these become less evident on the southern part of the slope. Alternatively, these fans may have been deposited by sandy turbidity currents. Turbidity currents can cause erosion and form channels with fan-shaped accumulations in the end. There are, however, no observed gullies or levees in the northern part of the study area, so this alternative is less likely. Evidence of bifurcating channel systems are found on the slope south in the study area (Figure 4.21). They are likely formed by turbidity currents initiated on the outer shelf or upper slope. Their channelized, downslope movement bypassing the study area favors this alternative. This indicate that both debris flows and turbidity currents have contributed to deposit the great sediment accumulation in the southern part of the study area.

Plough marks orientated sub-parallel to the shelf break (Figure 4.15) indicate a glacimarine environment in front of the fast-flowing ice-stream with icebergs drifting along the shelf. Plough marks were absent on the shelf, suggesting that the shelf was covered by ice during this period. Icebergs originate from calving glaciers, meaning that the glacier fronts terminated in the marine environment. Thus, these icebergs most likely originated from local shelf break-terminating glaciers. The sub-parallel orientation of the plough marks implies that a persistent ocean current prevailed along the shelf, drifting toward NE. Plough marks orientated sub-parallel to the shelf break is reported from the Naust Formation already from Naust N (Ottesen et al., 2009).

Dahlgren et al. (2002a) suggest that Naust A-D are mainly composed of glacigenic diamicton. Such sediments were deposited at the grounding-line of the Fennoscandian Ice Sheet and redeposited by gravity flows onto the continental slope. Moreover, Dahlgren et al. (2002a) describes Naust D (unit A and the lower part of unit B in this thesis) as a unit with a relatively uniform thickness across the slope with an acoustically homogeneous internal seismic signature. Thus, they suggest that Naust D was deposited during a single ice-sheet maximum event, meaning that a fast-flowing ice-stream was present in the palaeo-shelf break area during this period. Both palaeo-Trænadjupet and Sklinnadjupet troughs were active in this stage, however the Sklinnadjupet Trough south of the study area was the main sediment source during this period.

Rydningen et al. (2016) suggest that deposition of coarse-grained sediments from gravity flows may be observed as high-amplitude reflections found in the base of channels or incisions. The observed bifurcating sinuous shaped channel systems have similar characteristics with submarine channels described by Montelli et al. (2018) from the mid-Norwegian continental margin during the Quaternary. Montelli et al. (2018) suggest that their origin may be controlled by local slope morphology and high episodic melt-water discharge.

According to Weaver et al. (2000) turbidity currents can be initiated in the shelf break area and funneled downslope forming channels. They suggest that meandering channels often occur as a result of a low slope gradient and transport of fine-grained sediments. The lowest slope gradient of the study area occurs in the south. Generally, the palaeo-channels on the mid-Norwegian slope have a low sinuosity and length. This suggest that they were formed by a high velocity flow over a short time period (Montelli et al., 2018).
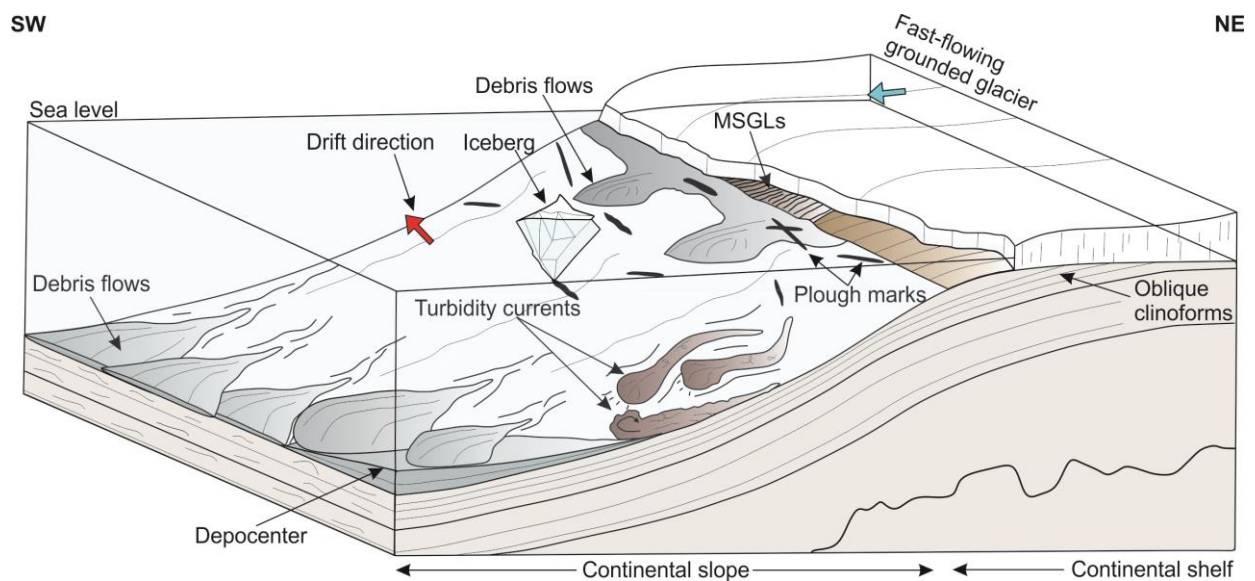
Figure 5.4: Conceptual model showing the sedimentary processes of depositional stage 1 (unit A) on the margin offshore Trænadjupet and Trænabanken (not drawn to scale). MSGLs - Mega scale glacial lineations; Depocenter - the greatest sediment thickness of the area, mainly comprised of glacigenic sediments.

5.2.2 Depositional stage 2 (units B and C)

Changes in stratal architecture from unit A to B is indicated by a truncational boundary. This, and preserved MSGLs of horizon 2 (Figure 4.25), suggest large-scale erosion of the shelf strata by a fast-flowing ice-stream. The extent of the MSGLs to the palaeo-shelf break may imply that erosion occurred during full-glacial conditions. MSGLs were only observed on horizon 2, so fast-flowing ice streams can be reconstructed with confidence on the shelf only in the beginning of depositional stage 2. However, indications of a periodically glaciated shelf and the presence of grounded glaciers are found. This is suggested by large sediment distribution during unit B and C (Figure 4.27 & 4.38) and the elongated depression on horizon 4, interpreted to have been formed by sub-glacial meltwater (Figure 4.36). In addition, the internal boundary reflectors in between the units may represent deposition of hemipelagic sediments on an ice-free shelf. MSGLs that formed throughout this period have probably been overprinted by iceberg plough marks.

Environmental changes occur from unit A to B, suggested by the slope configuration going from oblique to sigmoidal clinoforms. This imply changes from a high-energy slope system to a low-energy slope system (Figure 5.5). The slope angle of the clinoforms decrease and the outflow distance of the slope system increases. Large downslope mounds and associated channels (Figure 4.29) are observed throughout unit B and C, and these mounds are interpreted to be debris flows that originated as basal till on the outer shelf and upper slope. The channels likely developed by basal erosion caused by these downslope flows, transporting sediments to the lower slope. They suggest that a heavy, non-viscous mass have been transported downslope, partly bypassed the area, and deposited west of the study area. This sediment bypass is likely partly responsible for the sigmoid character of the slope, as discussed by Dahlgren et al. (2005).

The primary sediment input of the area is coming from the south as a line source at or near the shelf break. This is indicated by large sediment accumulation in the southern part of the slope suggesting that ice-streams of Sklinnadjupet Trough were more erosive during this depositional stage compared to stage 1.

Iceberg plough marks on the shelf and slope of horizons 3 and horizon 4 can reveal information about the palaeo-environment. The large amount of iceberg ploughing indicates

that the outer shelf was periodically ice-free during this stage. On horizon 3, two different drift directions are indicated by a large amount of plough marks (Figure 4.32). The primary drift follows the shelf break, implying a strong, consistent along slope current, i.e. the Norwegian Atlantic Current. Some plough marks have an E-W orientation, i.e. a similar orientation as the fast-flowing ice-streams of horizon 2. A retreating glacier may produce a substantial amount of cold, dense meltwater, which can cause circulation in the water column. This circulation may have drifted some of the icebergs in the area away from the glacier, and, as such, these iceberg plough marks indicate that a grounded ice was present on the shelf at this time. The dominant orientation of plough marks are suggested to be an indication of the prevailing wind and ocean-current direction (Rafaelsen et al., 2002). Rafaelsen et al. (2002) suggest that katabatic winds and meltwater discharge may influence drift direction of icebergs proximal to a retreating ice. If correct, this may have formed the E-W orientated plough marks.

The gully observed on horizon 3 has been interpreted to be formed by turbidity currents, suggested by the incision and no associated depocenter on the slope (Figure 4.33). This imply that the area was glacially influenced, and sediments bypassed the study area. The seafloor may be eroded by turbidity currents formed by meltwater from underneath an ice-sheet. Debris flows may have a higher viscosity than turbidity currents and therefore the southern slope failure is interpreted to have generated a debris flow. This is suggested by the travel distance before deposition downslope and the elongated morphology of the lobe.

On the lower part of the slope of unit B, the successive variations between hemiplegic deposits and slide debrites reflect suspension settling interbedded with deposition from periodic mass movement processes. Suspension fall-out through the water column may indicate a relatively low-energy environment. Similar periodic glacigenic debris flows are observed through the entire depositional stage and can likely relate to slope failure of weak sedimentary layers on the upper slope. This is indicated by debrites that superimpose a long plough mark across the lower slope (Figure 4.37).

Debris flows are observed on the Bear Island TMF, estimated to have been deposited during the LGM (Laberg & Vorren, 1995, 1996). They were described as glacigenic slope sediments with a mounded geometry, probably generated by oversteepening of the upper slope. Ice-

sheets at the shelf break are interpreted to be the main sediment input of such sediments. These sediments were probably transported on to the shelf and outer slope as subglacial, basal, and deforming till layers. Downslope, sediments were transported mainly as large debris flows reaching the lower fan (Figure 2.11a). The areal distribution and stacked geometry of the slope sediments suggest an episodic sediment delivery. The acoustically transparent internal seismic signature of the mounds is probably caused by deformational homogenization of sediments due to downslope processes. Debris flows can be characterized as sediment flows comprised of heterogeneous sediments, i.e. a low grade of sorting. Laberg and Vorren (1996) suggest that most of these glacigenic sediments are deposited during peak glacials and therefore, the slope progradation is highly controlled by the oscillations of the glacier margin. This imply that large amount of sediments was deposited during short periods. If correct, the deposition of mounded glacigenic debris flows on the slope, may indicate that ice sheets have reached the shelf break during depositional stage 2.

Based on the available data in this thesis, it is difficult to precisely explain the formation of the gully on the upper slope. Three different ways of gully formation on a glaciated margin has been suggested by Montelli et al. (2018). First, an ice-sheet grounded on the shelf break may form turbidity currents from sediment-laden meltwater producing erosional downslope currents. Another possibility is that mass flows initiated by for example gas-hydrates or plough marks may erode and form gullies. Finally, dense saline bottom-water formed as a consequence of sea-ice freezing and brine rejection may produce gullies. The first alternative is supported by high sedimentation and the morphology of the slope. A fluctuating ice-sheet produce large amount of meltwater and therefore the first alternative is believed to have formed the gully.

Furthermore, Gales et al. (2013) explain that mechanisms and factors involved in the formation of gullies are highly complex. They suggest that differences in gully morphology may be a result of formation over multiple glacial cycles and environmental controls such as oceanographic regimes. An ice-sheet is known to be dynamic features over time within cross shelf troughs. Therefore, it is possible that the gully formed from a grounded ice-sheet in the shelf break area, producing turbidity currents from sediment-lade meltwater over several glacial advances.

Dahlgren et al. (2002a) divided Naust C (upper part of unit B and unit C in this thesis) into sub-units C1 and C2. C1 was described to have a limited extent deposited at the flanks of the lobes in Naust D, where C2 had wider lobe-shaped depocenter. In contrast to Naust D, this depositional stage was suggested to be deposited during at least two fluctuations in ice-sheet extent to the shelf break. These observations fit well with observations in this thesis, where the upper part of unit B and C may represent the sub-units of Naust C. The wedge-shaped accumulation of unit B has a more limited extent compared to unit C.
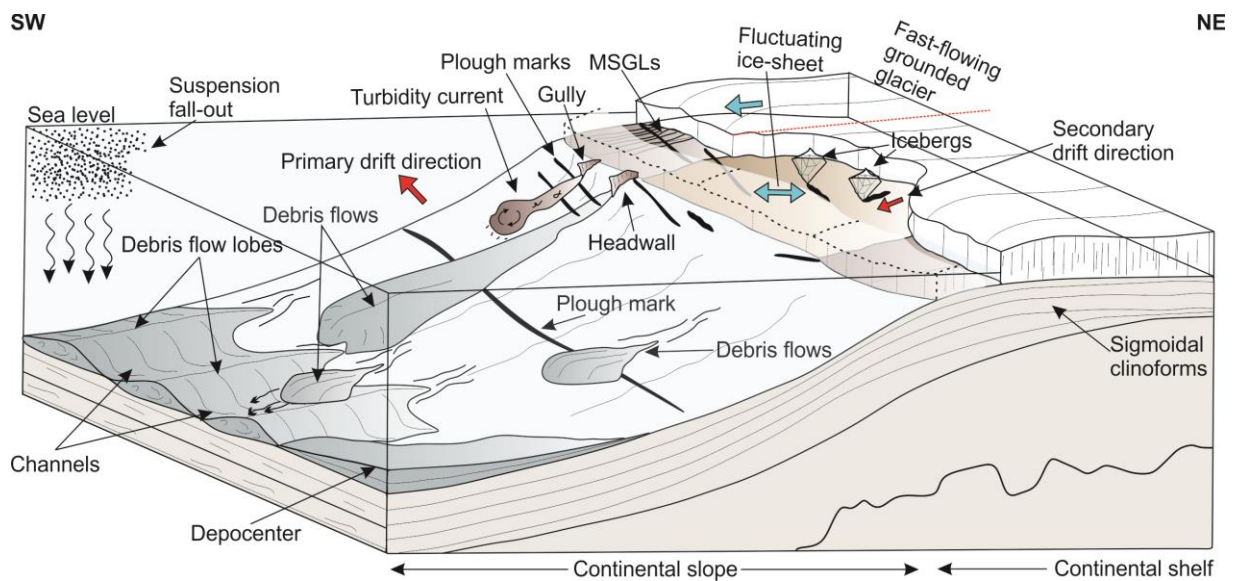

Figure 5.5: Conceptual model showing the sedimentary processes of depositional stage 2 (unit B and C) on the margin offshore Trænadjupet and Trænabanken (not drawn to scale). MSGLs - Mega scale glacial lineations; Depocenter - the greatest sediment thickness of the area, mainly comprised of glacigenic sediments.

5.2.3 Depositional stage 3 (unit D + horizon 5)

A configuration of large-scale morphology such as banks and troughs can be revealed from the thickness map of unit D (Figure 4.46) and the topography of the seafloor (Figure 4.50). The Trænadjupet Trough in the north and the Sklinnadjupet Trough in the south indicate two different pathways of fast-flowing ice-streams in the area during deposition of unit D.

On horizon 6, the terminal moraine of the southern trough indicates that the glacier terminated on the outer part of the shelf (Figure 4.44). It occurs in front of MSGLs, which may indicate that the ridge is formed at a stillstand or an ice retreat by a fast-flowing ice-stream. On the seafloor horizon, MSGLs of Trænadjupet Trough are only preserved with a geographically limited extent in a deeper lying area of the trough (Figure 4.52). An explanation may be that a fast-flowing grounded ice-stream occurred on the shelf forming the MSGLs, and that icebergs later started to drift around in the same area forming plough marks, thereby eroding the MSGLs, except for the deepest part of the trough where the icebergs did not reach down to the seafloor.

The bank south of Trænadjupet, Gamlembanken, separates this trough from Sklinnadjupet. Due to less erosion than adjacent areas, it is likely that the bank was covered by a slow flowing ice-mass in this period. If correct, less sediments were probably glacially transported and deposited onto the slope compared to west of the troughs (Figure 5.6).

Indications from the slope implies frequent deposition from downslope processes. The northern and southern wedge of the slope are predominantly built out by glacigenic debris flows that commonly deposited on the slope in front of fast-flowing ice streams. The sediment thickness of the southern wedge implies a substantial sediments transport to this area, sourced from the south (Figure 4.46). This depocenter suggest that Sklinnadjupet Trough played an important role in the development of the margin during this stage, similar to depositional stage 2. Within this depocenter, a wedge-shaped accumulation occurs, located on the lower part of the slope (Figure 4.48), possible formed by several slope failures during a shorter time period. This is suggested by its composition of braiding channels defined by amplitude anomalies, in addition to a relatively homogeneous internal seismic signature. The wedge-shaped fan may therefore be a result of a failure of the outer shelf/upper slope, following an

ice-sheet maximum event, where substantial amount of sediment was transported and deposited onto the shelf.

A mounded accumulation with an onlapping pattern occurs on top of the sedimentary fan (Figure 4.49). This and the laminated internal seismic signature, suggest that sediments accumulated up-slope, in contrast to the prograding system generally characterizing the units studied in this thesis. This is therefore interpreted to be an ocean current-controlled accumulation. If correct, it implies a possible along-slope current system from south toward north, which transported and deposited sediments. This means that the slope west of Trænadjupet and Trænabanken was influenced by along-slope currents during unit D time.

In an embayment between the depocenters of Sklinnadjupet and Trænadjupet, Laberg et al. (2001) infer a current-controlled sedimentation deposited during the late Saalian to the late Weichelian. It is stratigraphically bounded by glacigenic diamictons above and below, which may be correlated to seismic interval unit D in this thesis. They classified it as a mounded, elongated contourite (Rebesco et al., 2014) named the Nyk Drift. It covers an area of at least 2,000 km^2 where the depocenter of the drift is located on the upper slope at about 67ºN. The thickness of the depocenter gradually decrease toward north and south. This suggest that the depocenter of the drift corresponds to the area where both upper and lower reflector in this thesis were mapped. The sediment distribution and areal extent of the drift may indicate that large amount of glacial sediments was deposited along the Vøring margin and redistributed by along slope ocean currents. Equivalent sediments accumulated up-slope were not observed in deeper parts of the stratigraphy. Suggestions may be that the absence of these sediments can be a result of either slope failures or that the seismic resolution of the data is not satisfactory.

Horizon 6 represent the base of both Naust S and T, where Naust S is predominantly present as slope sediments (Ottesen et al., 2009). Ottesen et al. (2009) interpreted URU to correspond to the base of Naust T which is thus represented by horizon 6 in this study. Ottesen et al. (2009) further suggested that this regional boundary was caused by the Elsterian ice-sheet (300,000-400,000 years ago) which was possibly the largest glaciation in this area during the late Cenozoic. It should be noted that glaciers have reached the shelf break on the mid-Norwegian margin both before and after the formation of URU (Dahlgren et al., 2002a).

143

Dahlgren et al. (2002a) suggested that Naust B represent four fluctuations in ice-sheet all the way to the shelf break. The Pleistocene Naust Formation is thought to be largely composed of glacigenic debris flows interbedded with hemipelagic sediments (Dahlgren et al., 2002a). However, it should be noted that the internal structure of unit D is not studied in detail.

Dahlgren et al. (2002a) infer that Naust A2 was deposited at ca 15-22 ka BP (Marine Isotope Stage 2). The age estimate was also confirmed by radiocarbon dating of foraminifera in glacimarine mud right above the sedimentary interval. A2 is composed of a structurless gray diamicton. In between Sklinnadjupet and Trænadjupet, they describe Naust A2 as a fan-shaped accumulation with several lobes reaching down to the slope. Parts of this accumulation can likely be the southern sedimentary wedge observed, based on its thickness and geographical position. The Trænadjupet Trough has sourced Naust A2 in the northern part of the study area. Dahlgren et al. (2002) further suggest that parts of Naust A was removed from this area due to Trænadjupet Slide and Nyk Slide. Therefore, Naust A1 is only present at the mouth of the large palaeo-Sklinnadjupet Trough and in a small lobe off the Trænadjupet Trough. This implies that A1 is absent in this study area.

Several large-scale troughs occur on the mid-Norwegian margin implying the earlier dynamic ice-flow pattern. These troughs are characterized by MSGLs, which have been regarded as a compelling evidence to indicate former pathway of fast-flowing ice-streams in soft sediments. A hypothesis of their formation mentioned by Ottesen et al. (2009) is so-called keels which are formed in the base of a fast-flowing ice-stream. Ottesen et al. (2009) further suggest that fast-flowing ice-streams often are linked to relatively thick ice and that they are separated by zones of slower moving, thinner ice, commonly frozen to its bed. If correct, thick fast-flowing ice-streams occupied the palaeo-Trænadjupet and Sklinnadjupet troughs, while Gamlembanken was covered by a thinner, cold-based ice during depositional stage 3.
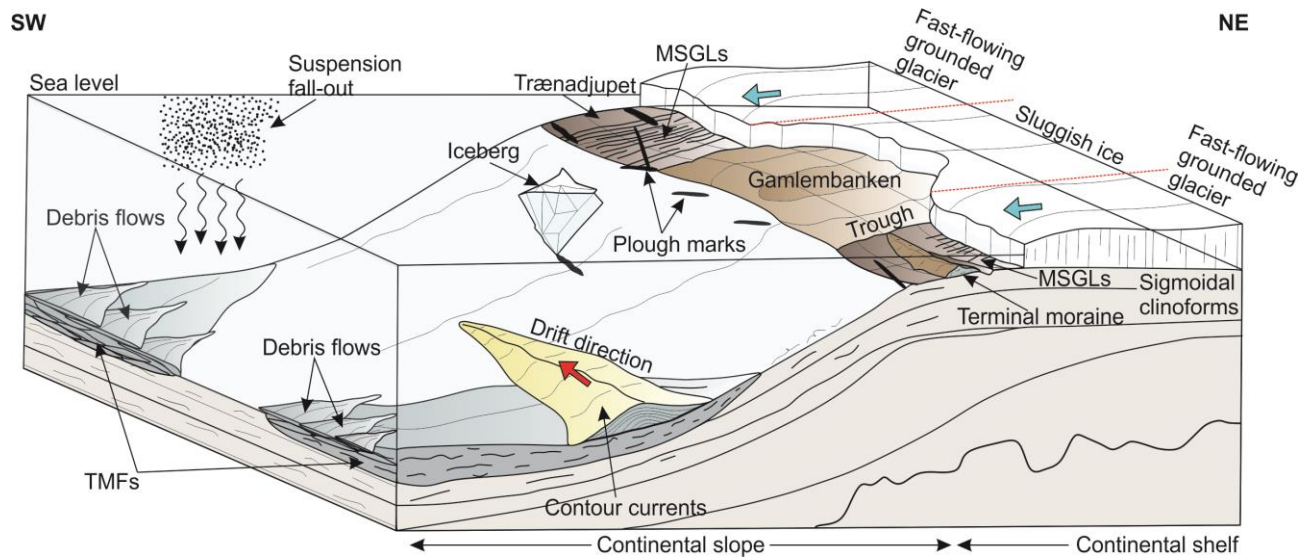
Figure 5.6: Conceptual model showing the sedimentary processes of depositional stage 3 (unit D + horizon 5) on the margin offshore Trænadjupet and Trænabanken (not drawn to scale). MSGLs - Mega scale glacial lineations; TMFs - Trough mouth fans.

5.3 Shallow gas

Evidence of shallow gas occur from both depositional stage 1 and 2 (Figure 4.16). The origin of the shallow gas may either be a result of fluid migration from the deeper strata or in situ production due to decompression of organic material. Fluid migration from the deep may indicate that there is a working source rock buried in the area, while in situ production of gas suggests a high organic content in sediments of depositional stage 2.

It is hard to believe that the high amplitude in the upper part is strong enough to affect the seismic signal to below the Naust Formation. In addition, the acoustic pipe is located above a sedimentary basin (Figure 4.17), which may correspond to the muddy Kai Formation. Such sediments can have source rock potential and therefore suggest fluid migration (Figure 3.9) from this stratigraphic level.

Fluid migration from Kai Formation to the overlying Naust Formation on the mid-Norwegian margin has been reported from earlier studies. Hustoft et al. (2007) suggest that these fluids commonly form cylindrical acoustic pipes, which occur both alone and in clusters. These pathways of fluids are a result of potentially overpressured sediments that may be a consequence of deposition of the early Naust Formation (Figure 5.7). Therefore, fluid migration is the favoured interpretation to the origin of shallow gas accumulations in this thesis.
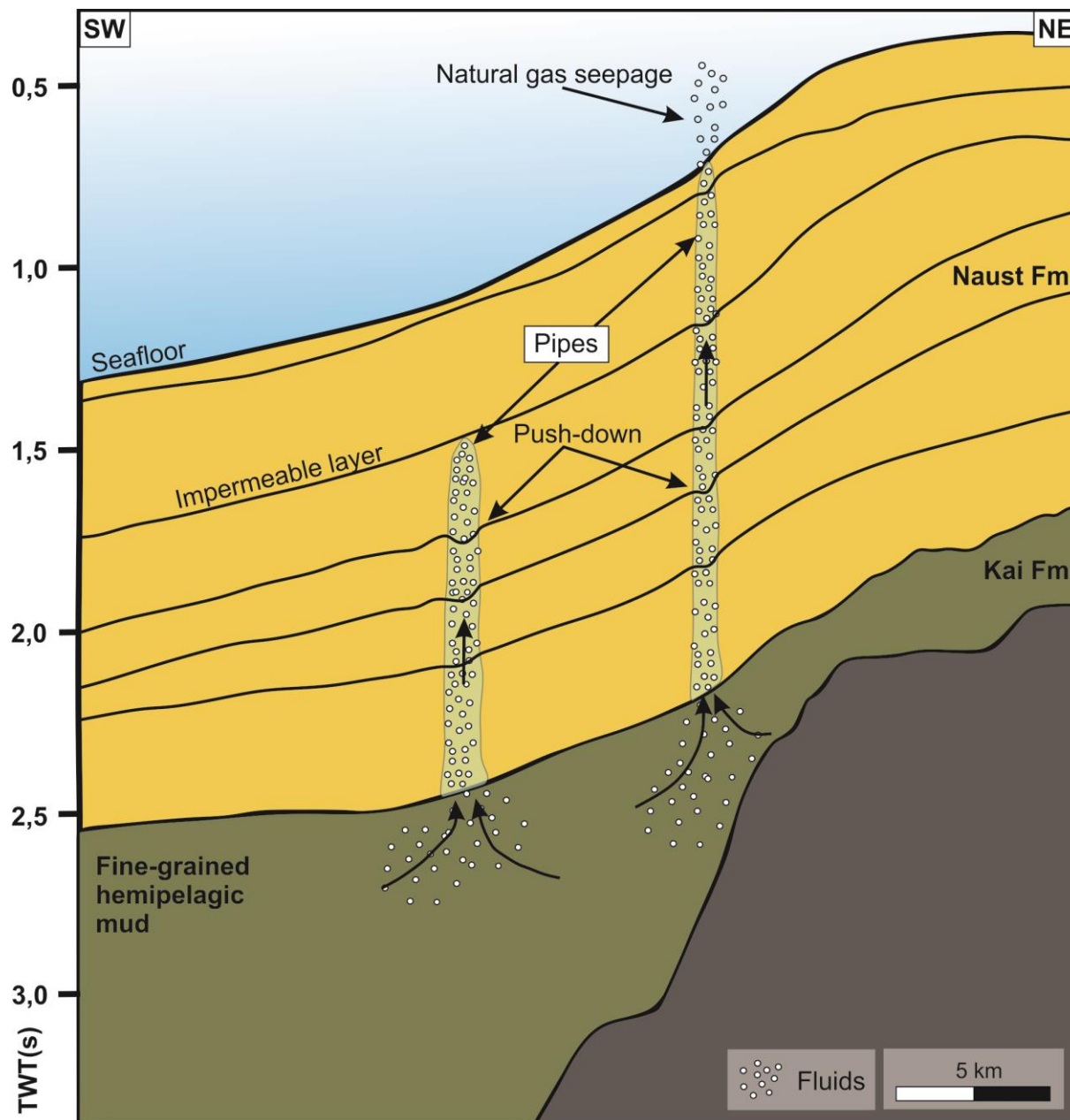
Figure 5.7: Conceptual model of the fluid flow system showing the migration path from deeper lying strata to the seafloor. Modified from Hustoft et al. (2007).

6 Conclusions

Based on 3D-seismic data, the late Cenozoic evolution of the outer shelf and slope on the northern part of the mid-Norwegian margin has been studied, and four seismic units have been defined, i.e. units A, B, C and D. Summarized, the main findings of this study are:

- The seismic stratigraphic framework has been correlated to the established stratigraphic framework of the Naust Formation, where the oldest unit in this study correlates to the upper part of Naust A, unit B and C correlate to Naust U and unit D correlates to Naust S and T. The internal seismic signature of the units and the geomorphology of the unit boundaries have formed the basis for reconstructing the margin evolution.

- The large sediment volumes of Naust A, U, S and T, their external shape, and the geomorphology of the buried surfaces, suggest margin build-out of glacigenic sediments from repeated ice-sheet advances to the palaeo-shelf break.

- In general, the largest depocenters within the units are located in the southern part of the study area, suggesting that repeated ice streams operated in the Sklinnadjupet Trough, and a relatively larger transport of sediments occurred to this area compared to the Trænadjupet Trough.

- The late evolution of Naust A was deposited during a single ice-sheet maximum event by a fast-flowing ice-stream drained from the Scandinavian mainland. It traversed the shelf within the Trænadjupet Trough and reached the shelf break. Large amounts of subglacially transported till were deposited on the outer shelf and upper slope, before they became unstable and moved downslope through gravity driven processes. Consequently, the slope prograded westwards as downslope processes built out the margin, predominantly through the deposition of debris flows, with some turbidity currents. Icebergs were drifting along the shelf, indicating a glacimarine environment in front of the fast-flowing ice-stream.

- Naust U was deposited through several ice-sheet advances reaching the shelf break. The slope morphology indicates episodic deposition of large mounded debris flows as a result of deposition from ice-sheets reaching the shelf break. Most of these glacigenic sediments are deposited during peak glacials and therefore, the slope progradation is controlled by the oscillations of the glacier margin. Large amounts of

148

iceberg plough marks indicate a primary drift direction along slope and a secondary drift direction proximal to a retreating ice-sheet on the shelf.

- During Naust S and T, fast-flowing ice-streams in the Trænadjupet and Sklinnadjupet were separated by a slow-flowing ice mass. This formed the present-day large-scale shelf morphology comprising two troughs and a bank. These fast-flowing ice-streams deposited large amount of sediments in the northern and southern part of the study area, implying a frequent deposition of downslope processes on the slope. The lower part of the slope indicates a contourite drift (the Nyk Drift) which testify to an along slope current system flowing from south to north.

- Shallow gas preserved in the Naust Formation has most likely migrated from the underlying, muddy Kai Formation as a result of overpressured sediments.

7 Research outlook

The results of this study have increased the knowledge on sedimentary processes and the palaeoenvironments on the northern part of mid-Norwegian margin during late Cenozoic. Further research in the area should focus on expanding the regional stratigraphic framework. Some recommendations on further work are therefore:

- Extend the seismic stratigraphic framework west of the study area by using regional 2D-seismic data to get a better understanding of bypassing downslope processes and the deeper marine environment.

- Interpret the deeper parts of the seismic stratigraphy in order to establish a framework of the lower part of Naust A and Naust N.

- Preform a detailed study of unit D by using regional 2D-seismc data in order to investigate Naust B and A north of the Sklinnadjupet Trough.

- Map the Nyk Drift with higher resolution 3D-seismic data in order to investigate the internal signature of the drift and map the extent of the drift by using regional seismic data.

- Further investigate fluid migration in order to detect a potential source rock and to avoid drilling hazards. This could be of a potential interest for the industry.

8 References

Andreassen, K., Nilssen, E. G., & Ødegaard, C. M. (2007). Analysis of shallow gas and fluid migration within the Plio-Pleistocene sedimentary succession of the SW Barents Sea continental margin using 3D seismic data. Geo-Marine Letters, 27(2-4), 155-171.

Badley, M. E. (1985). Practical seismic interpretation.

Blystad, P., Brekke, H., Færseth, R., Larsen, B., Skogseid, J., & Tørudbakken, B. (1995). NPD-BULLETIN No 8, Structural elements of the Norwegian Continental Shelf-Part II: The Norwegian Sea Region. In: The Norwegian Petroleum Directorate (NPD).

Brown, A. (1999). Interpretation of Three‐Dimensional Seismic Data, 541 pp. American Association of Petroleum Geologists, Tulsa.

Bugge, T., Eidvin, T., Smelror, M., Ayers, S., Ottesen, D., Rise, L., Andersen, E., Dahlgren, T., Evans, D., & Henriksen, S. (2004). The Middle and Upper Cenozoic depositional systems on the Mid-Norwegian continental margin. Deep-water sedimentary system of Arctic and North Atlantic margins. NGF Abstract & Proceedings, 3, 14-15.

Chopra, S., & Larsen, G. (2000). Acquisition footprint–Its detection and removal. CSEG Recorder, 25(8), 16-20.

Clark, C. D. (1993). Mega‐scale glacial lineations and cross‐cutting ice‐flow landforms. Earth Surface Processes and Landforms, 18(1), 1-29.

Cofaigh, C. Ó., Taylor, J., Dowdeswell, J. A., & Pudsey, C. J. (2003). Palaeo‐ice streams, trough mouth fans and high‐latitude continental slope sedimentation. Boreas, 32(1), 37-55.

Dahlgren, K. T., Vorren, T. O., & Laberg, J. S. (2002a). Late Quaternary glacial development of the mid-Norwegian margin—65 to 68 N. Marine and Petroleum Geology, 19(9), 1089-1113.

Dahlgren, K. T., Vorren, T. O., & Laberg, J. S. (2002b). The role of grounding-line sediment supply in ice-sheet advances and growth on continental shelves: an example from the mid-Norwegian sector of the Fennoscandian ice sheet during the Saalian and Weichselian. Quaternary International, 95, 25-33.

Dahlgren, K. T., Vorren, T. O., Stoker, M. S., Nielsen, T., Nygård, A., & Sejrup, H. P. (2005). Late Cenozoic prograding wedges on the NW European continental margin: their formation and relationship to tectonics and climate. Marine and Petroleum Geology, 22(9-10), 1089-1110.

Dowdeswell, J., Cofaigh, C. Ó., & Pudsey, C. (2004). Continental slope morphology and sedimentary processes at the mouth of an Antarctic palaeo-ice stream. Marine Geology, 204(1-2), 203-214.

Dowdeswell, J. A., Ottesen, D., & Rise, L. (2006). Flow switching and large-scale deposition by ice streams draining former ice sheets. Geology, 34(4), 313-316.

Dowdeswell, J. A., Ottesen, D., & Rise, L. (2010). Rates of sediment delivery from the Fennoscandian Ice Sheet through an ice age. Geology, 38(1), 3-6.

Eidvin, T., Bugge, T., & Smelror, M. (2007). The Molo Formation, deposited by coastal progradation on the inner Mid-Norwegian continental shelf, coeval with the Kai Formation to the west and the Utsira Formation in the North Sea. Norwegian Journal of Geology/Norsk Geologisk Forening, 87.

Faleide, J. I., Tsikalas, F., Breivik, A. J., Mjelde, R., Ritzmann, O., Engen, O., Wilson, J., & Eldholm, O. (2008). Structure and evolution of the continental margin off Norway and the Barents Sea. Episodes, 31(1), 82-91.

Faleide, J. I., Bjørlykke, K., & Gabrielsen, R. H. (2015). Geology of the Norwegian continental shelf. In Petroleum Geoscience (pp. 603-637): Springer.

Faugères, J.-C., & Mulder, T. (2011). Contour currents and contourite drifts. In Developments in Sedimentology (Vol. 63, pp. 149-214): Elsevier.

Gales, J., Forwick, M., Laberg, J., Vorren, T., Larter, R., Graham, A., Baeten, N., & Amundsen, H. (2013). Arctic and Antarctic submarine gullies—A comparison of high latitude continental margins. Geomorphology, 201, 449-461.

Gascard, J. C., Raisbeck, G., Sequeira, S., Yiou, F., & Mork, K. A. (2004). The Norwegian Atlantic Current in the Lofoten basin inferred from hydrological and tracer data (129I) and its interaction with the Norwegian Coastal Current. Geophysical Research Letters, 31(1).

Hebbeln, D., Henrich, R., & Baumann, K.-H. (1998). Paleoceanography of the last interglacial/glacial cycle in the Polar North Atlantic. Quaternary Science Reviews, 17(1-3), 125-153.

Hjelstuen, B. O., Sejrup, H. P., Haflidason, H., Nygård, A., Berstad, I. M., & Knorr, G. (2004). Late Quaternary seismic stratigraphy and geological development of the south Vøring margin, Norwegian Sea. Quaternary Science Reviews, 23(16-17), 1847-1865.

Hustoft, S., Mienert, J., Bünz, S., & Nouzé, H. (2007). High-resolution 3D-seismic data indicate focussed fluid migration pathways above polygonal fault systems of the mid-Norwegian margin. Marine Geology, 245(1-4), 89-106.

Kearey, P., Brooks, M., & Hill, I. (2013). An introduction to geophysical exploration: John Wiley & Sons.

Laberg, J., & Vorren, T. (1995). Late Weichselian submarine debris flow deposits on the Bear Island Trough mouth fan. Marine Geology, 127(1-4), 45-72.

Laberg, J., & Vorren, T. (1996). The middle and late Pleistocence evolution and the Bear Island trough mouth fan. Global and Planetary Change, 12(1-4), 309-330.

Laberg, J., & Vorren, T. (2000). The Trænadjupet Slide, offshore Norway—morphology, evacuation and triggering mechanisms. Marine Geology, 171(1-4), 95-114.

Laberg, J., Dahlgren, K., & Vorren, T. (2005a). The Eocene–late Pliocene paleoenvironment in the Vøring Plateau area, Norwegian Sea—paleoceanographic implications. Marine Geology, 214(1-3), 269-285.

Laberg, J., Eilertsen, R., Salomonsen, G., & Vorren, T. (2007). Submarine push moraine formation during the early Fennoscandian Ice Sheet deglaciation. Quaternary Research, 67(3), 453-462.

Laberg, J. S., Dahlgren, T., Vorren, T. O., Haflidason, H., & Bryn, P. (2001). Seismic analyses of Cenozoic contourite drift development in the Northern Norwegian Sea. Marine Geophysical Researches, 22(5-6), 401-416.

Laberg, J. S., Stoker, M. S., Dahlgren, K. T., de Haas, H., Haflidason, H., Hjelstuen, B. O., Nielsen, T., Shannon, P. M., Vorren, T. O., & van Weering, T. C. (2005b). Cenozoic alongslope processes and sedimentation on the NW European Atlantic margin. Marine and Petroleum Geology, 22(9-10), 1069-1088.

Larsen, E., Longva, O., & Follestad, B. A. (1991). Formation of De Geer moraines and implications for deglaciation dynamics. Journal of Quaternary Science, 6(4), 263-277.

Lien, V. S., Hjøllo, S. S., Skogen, M. D., Svendsen, E., Wehde, H., Bertino, L., Counillon, F., Chevallier, M., & Garric, G. (2016). An assessment of the added value from data assimilation on modelled Nordic Seas hydrography and ocean transports. Ocean Modelling, 99, 43-59.

Longva, O., & Bakkejord, K. J. (1990). Iceberg deformation and erosion in soft sediments, southeast Norway. Marine Geology, 92(1-2), 87-104.

Løseth, H., Wensaas, L., Arntsen, B., Hanken, N., Basire, C., & Graue, K. (2001). 1000 m long gas blow-out pipes. Paper presented at the 63rd EAGE Conference & Exhibition.

Løseth, H., Gading, M., & Wensaas, L. (2009). Hydrocarbon leakage interpreted on seismic data. Marine and Petroleum Geology, 26(7), 1304-1319.

Mangerud, J., Jansen, E., & Landvik, J. Y. (1996). Late Cenozoic history of the Scandinavian and Barents Sea ice sheets. Global and Planetary Change, 12(1-4), 11-26.

Mangerud, J., Gyllencreutz, R., Lohne, Ø., & Svendsen, J. I. (2011). Glacial history of Norway. In Developments in Quaternary Sciences (Vol. 15, pp. 279-298): Elsevier.

Marfurt, K. J., Scheet, R. M., Sharp, J. A., & Harper, M. G. (1998). Suppression of the acquisition footprint for seismic sequence attribute mapping. Geophysics, 63(3), 1024-1035.

Martinsen, O., & Nøttvedt, A. (2006). Av hav stiger landet. Landet Bliver til, Norges Geologi, Ramberg, IB, Bryhni, I. & Nøttvedt, A. eds., Norsk Geologisk Forening, Trondheim, 440-477.

Martinsen, O., & Nøttvedt, A. (2008). Norway rises from the sea. Palaeogene and Neogene (Cenozoic)—The modern continents take shape: 66-2.6 million years ago. The making of a land—Geology of Norway: The Norwegian Geological Association, 442, 479.

Mitchum, R. M., Vail, P. R., & Sangree, J. B. (1977). Seismic stratigraphy and global changes of sea level: Part 6. Stratigraphic interpretation of seismic reflection patterns in depositional sequences: Section 2. Application of seismic reflection configuration to stratigraphic interpretation.

Montelli, A., Dowdeswell, J., Ottesen, D., & Johansen, S. (2018). Architecture and sedimentary processes on the mid-Norwegian continental slope: A 2.7 Myr record from extensive seismic evidence. Quaternary Science Reviews, 192, 185-207.

Nielsen, T., Knutz, P., & Kuijpers, A. (2008). Seismic expression of contourite depositional systems. Developments in Sedimentology, 60, 301-321.

NPDfactmaps. (n.d). Retrieved from http://gis.npd.no/factmaps/html_21/

NPDfactpage. (n.d.-a). Stratigraphy Naust Fm. Retrieved from http://factpages.npd.no/ReportServer?/FactPages/PageView/strat_Litho_level1_group_formation&rs:Command=Render&rc:Toolbar=false&rc:Parameters=f&NpdId=109&IpAddress=129.242.45.242&CultureCode=en

NPDfactpages. (2014). Litostratigrafisk Diagram Norskehavet In.

Olsen, L., Sveian, H., Ottesen, D., & Rise, L. (2013). Quaternary glacial, interglacial and interstadial deposits of Norway and adjacent onshore and offshore areas. Quaternary Geology of Norway, Geological Survey of Norway Special Publication, 13, 79-144.

Ottesen, D., Dowdeswell, J., Rise, L., Rokoengen, K., & Henriksen, S. (2002). Large-scale morphological evidence for past ice-stream flow on the mid-Norwegian continental margin. Geological Society, London, Special Publications, 203(1), 245-258.

Ottesen, D., Dowdeswell, J., & Rise, L. (2005a). Submarine landforms and the reconstruction of fast-flowing ice streams within a large Quaternary ice sheet: the 2500-km-long Norwegian-Svalbard margin (57–80 N). Geological Society of America Bulletin, 117(7-8), 1033-1050.

Ottesen, D., Rise, L., Knies, J., Olsen, L., & Henriksen, S. (2005b). The Vestfjorden-Trænadjupet palaeo-ice stream drainage system, mid-Norwegian continental shelf. Marine Geology, 218(1-4), 175-189.

Ottesen, D., Stokes, C. R., Rise, L., & Olsen, L. (2008). Ice-sheet dynamics and ice streaming along the coastal parts of northern Norway. Quaternary Science Reviews, 27(9-10), 922-940.

Ottesen, D., Rise, L., Andersen, E. S., Bugge, T., & Eidvin, T. (2009). Geological evolution of the Norwegian continental shelf between 61 degrees N and 68 degrees N during the last 3 million years. Norwegian Journal of Geology, 89(4), 251-265.

Plaza-Faverola, A., Bünz, S., & Mienert, J. (2011). Repeated fluid expulsion through sub-seabed chimneys offshore Norway in response to glacial cycles. Earth and Planetary Science Letters, 305(3-4), 297-308.

Rafaelsen, B., Andreassen, K., Kuilman, L., Lebesbye, E., Hogstad, K., & Midtbø, M. (2002). Geomorphology of buried glacigenic horizons in the Barents Sea from three-dimensional seismic data. Geological Society, London, Special Publications, 203(1), 259-276.

Rafaelsen, B. (2006). Seismic resolution and frequency filtering. Univ. Tromso Lecture Series, Tromso, Norway.

Rebesco, M., & Stow, D. (2001). Seismic expression of contourites and related deposits: a preface. Marine Geophysical Researches, 22(5-6), 303-308.

Rebesco, M., Hernández-Molina, F. J., Van Rooij, D., & Wåhlin, A. (2014). Contourites and associated sediments controlled by deep-water circulation processes: state-of-the-art and future considerations. Marine Geology, 352, 111-154.

Reemst, P., Skogseid, J., & Larsen, B. (1996). Base Pliocene velocity inversion on the eastern Vøring margin—causes and implications. Global and Planetary Change, 12(1-4), 201-211.

Rise, L., Ottesen, D., Berg, K., & Lundin, E. (2005). Large-scale development of the mid-Norwegian margin during the last 3 million years. In Ormen Lange–an Integrated Study for Safe Field Development in the Storegga Submarine Area (pp. 33-44): Elsevier.

Rise, L., Ottesen, D., Longva, O., Solheim, A., Andersen, E., & Ayers, S. (2006). The Sklinnadjupet slide and its relation to the Elsterian glaciation on the mid-Norwegian margin. Marine and Petroleum Geology, 23(5), 569-583.

Rise, L., Chand, S., Hjelstuen, B., Haflidason, H., & Bøe, R. (2010). Late Cenozoic geological development of the south Vøring margin, mid-Norway. Marine and Petroleum Geology, 27(9), 1789-1803.

Rydningen, T., Laberg, J., & Kolstad, V. (2016). Evolution of Andfjorden Trough-Mouth Fan, Norwegian Sea: buried glacigenic debris-flows and mega-scale glacial lineations. Geological Society, London, Memoirs, 46(1), 365-366.

Rydningen, T. A., Vorren, T. O., Laberg, J. S., & Kolstad, V. (2013). The marine-based NW Fennoscandian ice sheet: glacial and deglacial dynamics as reconstructed from submarine landforms. Quaternary Science Reviews, 68, 126-141.

Rydningen, T. A., Laberg, J. S., & Kolstad, V. (2015). Seabed morphology and sedimentary processes on high-gradient trough mouth fans offshore Troms, northern Norway. Geomorphology, 246, 205-219.

Sætre, R. (1999). Features of the central Norwegian shelf circulation. Continental Shelf Research, 19(14), 1809-1831.

Schlumberger. (n.d). Resolution. Retrieved from https://www.glossary.oilfield.slb.com/en/Terms/r/resolution.aspx

Sejrup, H. P., Hjelstuen, B. O., Dahlgren, K. T., Haflidason, H., Kuijpers, A., Nygård, A., Praeg, D., Stoker, M. S., & Vorren, T. O. (2005). Pleistocene glacial history of the NW European continental margin. Marine and Petroleum Geology, 22(9-10), 1111-1129.

Sheriff, R. (1985). Aspects of seismic resolution: Chapter 1.

Sheriff, R. E. (2002). Encyclopedic dictionary of applied geophysics: Society of exploration geophysicists.

Stoker, M., Hoult, R., Nielsen, T., Hjelstuen, B., Laberg, J., Shannon, P., Praeg, D., Mathiesen, A., Van Weering, T., & McDonnell, A. (2005). Sedimentary and oceanographic responses to early Neogene compression on the NW European margin. Marine and Petroleum Geology, 22(9-10), 1031-1044.

Vail, P. R. (1977). Seismic stratigraphy and global changes of sea level. Bull. Am. Assoc. Petrol. Geol., Mem., 26, 49-212.

Vail, P. R. (1987). Seismic stratigraphy interpretation using sequence stratigraphy: Part 1: Seismic stratigraphy interpretation procedure.

Veeken, P. (2007). H. 2007. Seismic Stratigraphy, Basin Analysis and Reservoir Characterisation. Handbook of Geophysical Exploration. Oxford: Elsevier Science.

Veeken, P. C. (2013). Seismic stratigraphy and depositional facies models: Academic Press.

Vorren, T., & Mangerud, J. (2008). Glaciations come and go. The making of land: geology of Norway. Geological Society of Norway, Trondheim, 481-533.

Vorren, T. O., & Laberg, J. S. (1997). Trough mouth fans—palaeoclimate and ice-sheet monitors. Quaternary Science Reviews, 16(8), 865-881.

Vorren, T. O., Laberg, J. S., Blaume, F., Dowdeswell, J. A., Kenyon, N. H., Mienert, J., Rumohr, J., & Werner, F. (1998). The Norwegian–Greenland Sea continental margins: morphology and late Quaternary sedimentary processes and environment. Quaternary Science Reviews, 17(1-3), 273-302.

Weaver, P. P., Wynn, R. B., Kenyon, N. H., & Evans, J. (2000). Continental margin sedimentation, with special reference to the north‐east Atlantic margin. Sedimentology, 47, 239-256.